To establish the role of mutations in *c-KIT* tyrosine kinase in the pathogenesis and therapy of core-binding factor-related acute myeloid leukaemia (AML)

Steven Paul Tinsley

UCL

A thesis submitted for the degree of Doctor of Philosophy

2014

DECLARATION

I, Steven Tinsley, confirm that the work presented in this thesis is my own. Where information has been derived from other sources, I confirm that this has been indicated in this thesis.

Signed:

Date:

Abstract

Haematopoiesis is controlled by complex signal transduction pathways and transcription regulators which may become dysregulated in acute myeloid leukaemia (AML). Activating mutations in *FLT3* and *c-KIT* receptor tyrosine kinases (RTKs) are commonly found in AML and can impact on prognosis. Different types of *FLT3* mutations are known to have distinct biological activities and prognostic implications. The presence of *c-KIT* mutations has been shown to increase the risk of relapse, but there has been no direct comparison of the biological activity of AML specific *c-KIT* mutations occurring in different receptor domains. In addition to prognostic information, RTKs are attractive potential targets for therapy using small molecule inhibitors.

To evaluate their biological activity and response to targeted therapies, human UT-7 cells were transduced with wild-type and mutant c-KIT isoforms - c-KIT-Δ417-419>Y (extracellular domain [ECD]), c-KIT-L576P (juxtamembrane domain [JMD]), c-KIT-D816V and c-KIT-N822K (both in the activating loop domain [ALD). There were intrinsic differences in signal strength between the mutants examined - only c-KIT-Δ417-419>Y and c-KIT-D816V expressing cells had detectable constitutive c-KIT activation and showed ligand-independent growth. The response of transduced UT-7 cells to c-KIT inhibitors was assessed by treating the cells with dasatinib and masitinib. Cells expressing ALD *c-KIT* mutations were more resistant to dasatinib or masitinib-mediated cell killing in comparison to cells expressing *c-KIT* mutations in the ECD and JMD. Western blotting revealed that although c-KIT phosphorylation was potently inhibited, there was residual mTOR and/or PI3K/AKT activation in these cells. The resistance to dasatinib observed in c-KIT-D816V or c-KIT-N822K expressing cells could be overcome by co-blockade of c-KIT and PI3K/mTOR and blockade of c-KIT and PI3K/mTOR was synergistic in all *c-KIT* mutant cell lines at inducing cell death. Blockade of FLT3 and PI3K/mTOR in *FLT3*-ITD AML cell lines also showed similar results.

During the screening of AML cell lines for *c-KIT* and *FLT3* mutations a novel *FLT3*-T820N point mutation was identified in the ME-1 cell line. Expression of FLT3-T820N in 32D cells constitutively activated FLT3 and conferred ligand-independent growth. 32D FLT3-T820N cells were most sensitive to the FLT3 inhibitor AC220 with regard to growth inhibition, cell killing and decreased phosphorylation of FLT3 compared to FLT3-WT and FLT3-D835Y expressing cells. This work highlights the differences in biological outcomes and TK inhibitor-sensitivity between different RTK mutants found in AML and shows that simultaneous blockade of RTKs and PI3K/mTOR may provide a novel therapeutic approach for specific AML subtypes.

Acknowledgements

The completion of this thesis would not have been possible without the help and support of numerous people including colleagues, friends and family.

I would like to thank Prof. Asim Khwaja and Prof. Rosemary Gale for their support, knowledge and patience throughout the duration of my thesis. I am extremely grateful to several colleagues including: Simon Brooks for answering the endless barrage of questions and whose technical expertise has been invaluable, Koremu Meja for teaching me about drugs and always making me laugh and to Rob Sellar, Glenda Dickson and Maria Virgilio who listened to me ranting when things were challenging but always managed to keep me optimistic.

I am forever grateful to Mark Newton, Pam Dhadda and Kirsty Asquith who provided endless reassurance, encouragement and were always there for a cocktail or three in the more trying moments.

Finally I would like to say a huge thank you to my dad, mum, brother and sister who have always been there and have kept me smiling and laughing from start to finish.

TABLE OF CONTENTS:

Table of Figures:

Chapter 1: Introduction

Chapter 2: Materials and Methods

Chapter 3: Functional consequence of *c-KIT* mutations in the UT-7 AML cell line

<u>Chapter 4:</u> Identification and functional analysis of a novel *FLT3* activating mutation in CBFL

<u>Chapter 5:</u> The impact of dasatinib and other small molecule inhibitors on AML cell lines and primary AML cells

List of Tables:

Chapter 1: Introduction

Chapter 3: Functional consequence of *c-KIT* mutations in the UT-7 AML cell line

<u>Chapter 4:</u> Identification and functional analysis of a novel *FLT3* activating mutation in CBFL

<u>Chapter 5:</u> The impact of dasatinib and other small molecule inhibitors on AML cell lines and primary AML cells

Commonly used abbreviations

ALD	Activating loop domain
ALL	Acute lymphoblastic leukaemia
Allo-SCT	Allogeneic stem cell transplantation
AML	Acute myeloid leukaemia
APL	Acute promyelocytic leukaemia
ATRA	*All-trans*-retinoic acid
Auto-SCT	Autologous stem cell transplantation
BFP2	Blue fluorescent protein 2
BM	Bone marrow
bp	Base pairs
CBF	Core binding factor
CBFL	Core binding factor leukaemia
cDNA	Complementary DNA
CIR	Cumulative incidence of relapse
CLP	Common lymphoid progenitor
CML	Chronic myeloid leukaemia
CMP	Common myeloid progenitor
CN-AML	Cytogenetically normal AML
CR	Complete remission
DFS	Disease-free survival
DNA	Deoxyribonucleic acid
ECD	Extracellular domain
EFS	Event-free survival
FAB	French-American-British
FL	FLT3 ligand
FLT3	Fms-like tyrosine kinase-3
gDNA	Genomic DNA
GM-CSF	Granulocyte macrophage colony-stimulating factor
GMP	Granulocyte/macrophage progenitor
GVHD	Graft-versus-host disease
GVL	Graft-versus-leukaemia
HLA	Human leukocyte antigen
HSC	Haematopoietic stem cell
ITD	Internal tandem duplication
JMD	Juxtamembrane domain

LSC	Leukaemic stem cell
MDR-1	Multi-drug resistant protein
MDS	Myelodysplasia
MEP	Megakaryocyte/erythroid progenitors
mIL3	Murine Interleukin 3
MLL	Myeloid/lymphoid leukaemia
MRC	Medical Research Council
MRD	Minimal Residual Disease
NK	Normal karyotype
OS	Overall survival
PB	Peripheral blood
PCR	Polymerase chain reaction
RFS	Relapse-free survival
RTK	Receptor tyrosine kinase
SCT	Stem cell transplantation
SEM	Standard error of the mean
SNP	Single nucleotide polymorphism
TKD	Tyrosine kinase domain
TMD	Transmembrane domain
TRM	Treatment-related mortality
WBC	White blood cell count
WHO	World Health Organization
WT	Wild-type

1. Introduction

1.1 Haematopoiesis

Within the bone marrow (BM) of an adult human approximately one trillion new cells are generated daily. To maintain this high turnover in cell production, haematopoietic stem cells (HSCs) are required to replenish the system through a process called haematopoiesis. HSCs are rare cells that reside in the BM and form the apex of a cellular hierarchy, with the terminally differentiated cells at the bottom (Figure 1.1). HSCs are pluripotent, giving rise to all cell lineages whilst also possessing the ability to self-renew. The HSCs divide via asymmetric cell division, giving rise to a daughter cell committed to differentiation and a daughter cell that maintains the pool of HSCs. This process is controlled by the BM microenvironment and complex genetic interactions, with some of the key transcription factors and signalling molecules highlighted in Figure 1.1. As the HSCs differentiate they form intermediate progenitor cells, e.g. the common myeloid progenitor (CMP), that gradually commit to a specific cell lineage. Blood cells fall into two main branches, the myeloid lineage comprised of red blood cells (RBCs), megakaryocytes, mast cells, eosinophils, neutrophils, monocytes/macrophages and platelets, and the lymphoid lineage made up of B and T lymphocytes and natural killer cells (Orkin & Zon, 2008;Doulatov *et al.*, 2012). A number of transcriptional regulators and/or signalling molecules are dysregulated in acute myeloid leukaemia (AML). AML is characterised by an expansion of immature myeloid cells (blast cells) within the BM and peripheral blood that have lost their ability to respond to anti-proliferative signals and to differentiate normally.

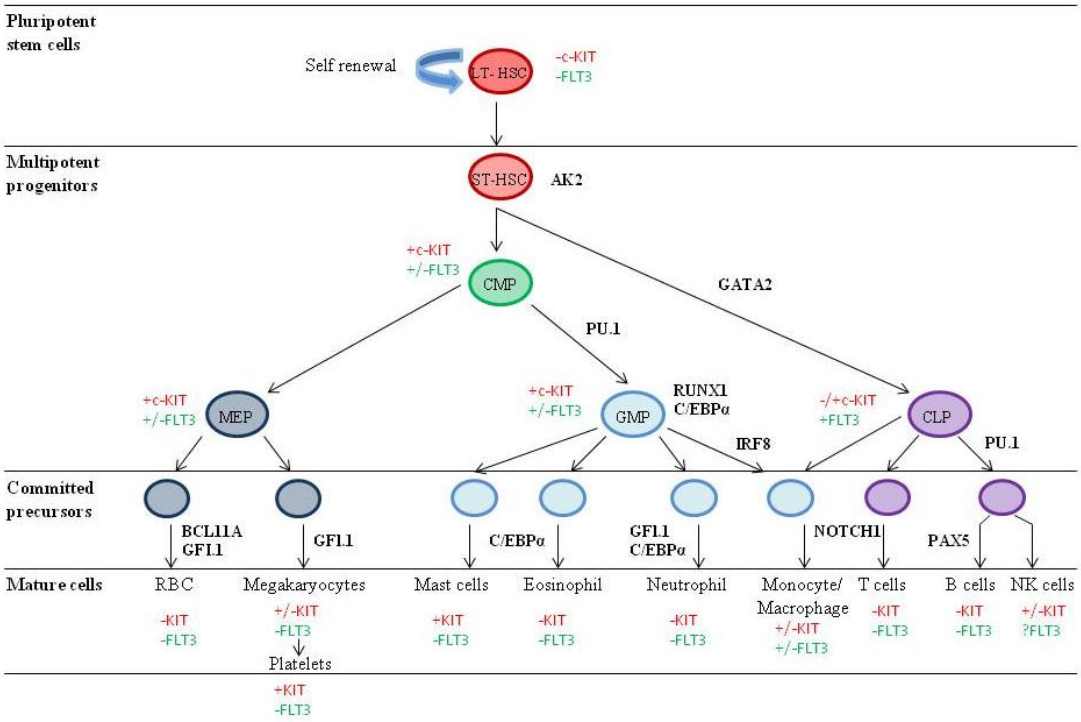

LT-HSC = long term HSCs, ST-HSCs = short term HSCs, CMP = common myeloid progenitor, MEP = megakaryocyte-erythroid progenitor, GMP = granulocyte-macrophage progenitor, CLP = common lymphoid progenitor, AK2 = adenylate kinase 2, GATA2 = GATA binding protein 2, RUNX1 = Runt-related transcription factor 1, PU.1 = ETS domain transcription factor, C/EBPα = CCAAT/enhancer protein alpha, IRFs = interferon regulatory factors, BCL11A = B-cell lymphoma/leukaemia 11A protein, GFI.1 = zinc finger protein, NOTCH1 = Notch homolog 1, translocation-associated (Drosophila) and PAX5 = paired box protein.

Figure 1.1 The current hierarchical model of lineage differentiation from a HSC to mature progenitors, including some of the known transcription factors and key signalling molecules required for haematopoiesis. c-KIT and/or FLT3 expression have been illustrated based on reports of surface expression on specific cell populations or of functional studies. Adapted from Doulatov *et al* (2012) and Orkin & Zon (2008).

1.2 AML Leukaemogenesis

Within AML, a subset of cells known as leukaemic stem cells (LSCs) are thought to be responsible for the initiation, progression and relapse of the disease. The first report of leukaemia-initiating cells was by Dick and colleagues demonstrating that primitive human leukaemic cells characterised by $CD34^+$ $CD38^-$ expression were capable of recapitulating AML within non-obese diabetic mice with severe combined immuno-deficiency disease (NOD/SCID mice) (Bonnet & Dick, 1997). The exact origin and definition of LSCs is, however, widely debated. Subsequent studies have shown that mice with enhanced immunosuppression transplanted with human AML cells from both the $CD34^+$ $CD38^-$ and $CD34^+$ $CD38^+$ cell compartments have leukaemia-initiating properties, highlighting that LSCs are not restricted to one specific cell subset (Taussig *et al.*, 2008;Yoshimoto *et al.*, 2009). A recent report examining BM from patients with $CD34^+$ AML revealed that approximately 80% of patients have two distinct leukaemia progenitor cell populations as characterised by the immunophenotypes $Lin^-CD34^+CD38^-CD90^-CD45RA^+$ (lymphoid-primed multipotential progenitor-like cells (LMPP-like)) and $Lin^-CD34^+CD38^+CD123^+CD45RA^+$ (GMP-like cells). Analysis of these cell populations revealed that both compartments had LSC activity and were more closely related to their normal progenitor cell type than to normal stem cells (Goardon *et al.*, 2011). Interestingly, the LMPP-like cells were able to give rise to the GMP-like population but not the contrary. Mouse models of human AML have demonstrated that murine LSCs are phenotypically downstream of the GMP, which opposes the view of LSCs being equivalent to HSCs in regards to their cellular hierarchy (Huntly *et al.*, 2004;Somervaille & Cleary, 2006). This demonstrates the heterogeneity of LSCs both between and within individual patients.

Although the exact origin of LSCs is debatable, the biological function of LSCs is similar to HSCs as demonstrated by their ability to self renew and reside in a state of quiescence (Bjerkvig *et al.*, 2005). Quiescence may contribute to resistance to cytotoxic chemotherapy as a result the majority of patients with AML relapse. This is supported by emerging data suggesting that patients with AML that express higher levels of stem-cell related genes have a worse prognosis (Eppert *et al.*, 2011). LSCs show a number of features that differ from normal HSCs including constitutive activation of nuclear factor B (NF-κB), active Wnt/β catenin signalling, increased expression of interferon regulatory factor-1 (IRF-1)/death associated protein kinase (DAPK)/Bcl-2, and abnormal cell surface marker expression of CD44, CD47, CD123 and CD96 (Zhang *et al.*, 2013;Lagadinou *et al.*, 2013). Several groups have exploited these differences and shown selective eradication of LSCs and not normal HSCs using the Bcl-2 inhibitor ABT-263, fenretinide (a synthetic retinoid which inactivates

NF-κB) and blocking monoclonal antibodies targeting CD47 (Majeti *et al.*, 2009;Lagadinou *et al.*, 2013;Zhang *et al.*, 2013).

1.3 Clinical presentation

AML is characterised by the accumulation of immature myeloid cells within the BM. This interferes with normal haematopoiesis, leading to a reduction in both red and white blood cells and a decrease in platelets. Symptoms of AML include breathlessness, fatigue, ease of bruising, bleeding and an elevated risk of infection. In 2000-2003 the incidence of AML in younger patients (<65 years of age) was reported to be 1.8 per 100,000 persons which increased to 17 per 100,000 persons in people ≥ 60 years of age (Deschler & Lubbert, 2006).

1.4 AML Classification

1.4.1 French-American-British (FAB) classification and cytogenetics

The first comprehensive classification of AML was using the French-American-British (FAB) sub-type system (Bennett *et al.*, 1976;Bennett *et al.*, 1985). The FAB system stratifies AML according to morphology and histochemistry, with a blast threshold of 30% within the BM. It stratifies AML into nine subtypes, M0-M7, based on the degree of maturity of the leukaemic cells, defined in Table 1.1. Within this classification system specific cytogenetic abnormalities are generally found within particular subgroups, including t(15;17), t(8;21) and inv(16) which fall into the subtypes M3, M2 and M4Eo respectively. In 1998 Grimwade and colleagues showed conclusively that specific cytogenetic abnormalities can impact on clinical outcome in AML and therefore provide a framework for risk-adapted therapy (Grimwade *et al.*, 1998). In 2010 this was refined further to include rarer abnormalities and is illustrated in Table 1.3 (Grimwade *et al.*, 2010). The use of cytogenetics is now considered the gold standard for risk-adapted therapy in AML. However, 40-50% of patients with AML are cytogenetically normal (CN). In recent years somatic mutations have been identified in specific genes in CN-AML, allowing for risk-adapted stratification of patients within this subgroup.

1.4.2 WHO classification

More recently, specific genetic and chromosomal abnormalities within AML have been identified as important prognostic factors. This led the World Health Organisation (WHO) to a more stringent classification system combining cytogenetic, immunophenotypic, morphological, genetic and clinical features (Vardiman *et al.*, 2002). This system identifies

AML using a lowered blast cell threshold of 20% in the BM or peripheral blood (PB). However, AML is still considered if patients present with recurrent genetic abnormalities, even though this blast cell criterion may not be met. Table 1.2 gives the recently revised scheme showing 6 groups: AML with recurrent genetic abnormalities, AML with myelodysplasia-related changes, AML with therapy related neoplasms, AML not otherwise specified, myeloid sarcomas and myeloid proliferations related to Down syndrome. Current revisions have added two provisional AML entities including mutated nucleophosmin 1 (*NPM1*) or mutated CCAAT/enhancer-binding protein alpha (*CEPBA*) (Vardiman *et al.*, 2009). Mutations in *FLT3* are not currently given a distinct classification as they can be associated with other recurrent cytogenetic abnormalities, e.g. t(15;17)(q22;q12) and the t(6;9)(p23;q34). Approximately a third of patients with AML fall into the 'AML not otherwise specified' subgroup. However, the identification of new molecular markers such as *NPM1* and *CEPBA* are likely to allow this group to be stratified further.

FAB subtype	**Description**
M0	Undifferentiated acute myeloblastic leukaemia
M1	Acute myeloblastic leukaemia without maturation
M2	Acute myeloblastic leukaemia with minimal maturation
M3	Acute promyelocytic leukaemia
M4	Acute myelomonocytic leukaemia
M4Eo	Acute myelomonocytic leukaemia with eosinophilia
M5	Acute monocytic leukaemia
M6	Acute erythroleukaemia
M7	Acute megakaryoblastic leukaemia

Table 1.1 The French-American-British classification of AML

AML subgroup	AML characteristics
Recurrent genetic abnormalities	AML with t(8;21)(q22;q22); (*RUNX1T1;RUNX1*)
	AML with inv(16)(p13q22) or t(16;16)(p13;22); (*CBFB;MYH11*)
	Acute promyelocytic leukaemia with t(15;17)(q22;q11-21);(*PML;RARA*)
	AML with t(9;11)(p22;q23); (*MLLT3-MLL*)
	AML with t(6;9)(p23;q34); (*DEK-NUP214*)
	AML with inv(3)(q21q26.2) or t(3;3)(q21;q26.2); (*RPN1-EVI1*)
	AML (megakaryoblastic) with t(1;22)(p13;q13); (*RBM15-MKL1)*
	Provisional entity: AML with mutated *NPM1*
	Provisional entity: AML with mutated *CEBPA*
Acute myeloid leukaemia with myelodysplasia-related changes	
Therapy-related myeloid neoplasms	
Acute myeloid leukaemia, not otherwise specified	AML with minimal differentiation
	AML without maturation
	AML with maturation
	Acute myelomonocytic leukaemia
	Acute monoblastic/monocytic leukaemia
	Acute erythroid leukaemia
	Acute megakaryoblastic leukaemia
	Acute basophilic leukaemia
	Acute panmyelosis with myelofibrosis
Myeloid sarcoma	
Myeloid proliferations related to Down syndrome	Transient abnormal myelopoiesis
	Myeloid leukaemia associated with Down syndrome

Table 1.2 The revised 2008 WHO AML classification system. Adapted from Vardiman *et al* (2009).

1.5 Prognostic factors in AML

1.5.1 Clinical factors

Numerous clinical features in patients with AML have a prognostic impact including age, a high white blood cell count at diagnosis and secondary or therapy-related AML. Increasing age is an independent adverse prognostic factor in AML showing a decrease in overall survival (OS) (Appelbaum *et al.*, 2006;Juliusson *et al.*, 2009). Data from the Medical Research Council (MRC) trials has shown that patients >60 years of age, fit enough for intensive chemotherapy, had an OS of just 14% at 5 years from trial entry (Smith *et al.*, 2011). The poor prognosis of elderly patients is proposed to be the result of a multitude of factors including adverse cytogenetics, increased expression of multidrug resistance protein (MDR-1), prior myelodysplasia (MDS), reduced tolerance to cytotoxic chemotherapy and intrinsic chemoresistance (Slovak *et al.*, 2000;Appelbaum *et al.*, 2006;Erba, 2007;Smith *et al.*, 2011).

In conjunction with the above, the response to induction therapy and the level of minimal residual disease (MRD) are also important prognostic factors. Following treatment complete remission (CR) is defined as a bone marrow aspirate containing <5% leukaemic blasts with evidence of normal maturation of other marrow elements (Grimwade *et al.*, 2010). An MRC study showed that if the BM blast count following the first and second courses of chemotherapy were greater than 15% and 5% respectively then this was associated with a poorer survival and an increased risk of relapse (RR) (Wheatley *et al.*, 1999). Patients falling above these threshold limits should therefore have their therapy re-evaluated. Following induction or consolidation therapy patients may achieve a morphological CR but still retain a proportion of cells with an abnormal karyotype. Such patients have an increased RR and a reduced OS (Marcucci *et al.*, 2004;Balleisen *et al.*, 2009). As MRD is an important prognostic marker, techniques are now used to detect it. Flow cytometry can be used to identify specific aberrant cell immunophenotypes and real-time quantitative polymerase chain reaction (RQ-PCR) can be used to identify leukaemia-specific targets such as fusion proteins or particular mutations associated with AML (Smith *et al.*, 2011).

1.5.2 Cytogenetics

The use of cytogenetic abnormalities has become a powerful prognostic tool for risk-adapted treatment stratification in AML (Mrozek *et al.*, 2004). The MRC recently updated its risk stratification based on these cytogenetic abnormalities using a cohort of 5876 patients with AML aged 16-59 years enrolled on the MRC AML10 (n=1238), AML12 (n=2241) and AML15 trials (n=2397) (Grimwade *et al.*, 2010). Karyotype analysis of these patients showed 55.5% of cases fell into the intermediate risk group of which 41% had a normal karyotype, 25% had recurrent favourable cytogenetic abnormalities including t(15;17)(q22;21)/*PML-RARA*, t(8;21)(q22;q22)/*RUNX1-RUNX1T1* or inv(16)(p13q22)/(t(16;16)(p13;22)/*CBFB-MYH11* and 19.5% cases had adverse risk cytogenetics including -7 del(7q), -5/del(5q), t(9;22) and inv(3)/t(3;3). The survival outcome, 10 years from trial entry, of these patients based on their cytogenetic abnormalities is summarised in Table 1.4, showing 55-81% survival for the favourable risk group, 24-39% for the intermediate and 3-11% for those in the adverse risk group.

1.5.3 Recurrent gene mutations in AML

Cytogenetic abnormalities are established as diagnostic and prognostic markers in AML. However, approximately 50% of leukaemias are CN (Frohling *et al.*, 2005). This has led to targeted sequencing of dysregulated growth factor receptors, signal transduction proteins, transcription factors, chromatin remodelers and apoptosis regulators in patients with AML. Mutations in some of these genes such as *FLT3*, *NPM1* and *CEPBA* have shown an impact on prognosis and are now being used at diagnosis as independent risk factors (Beran *et al.*, 2004;Boissel *et al.*, 2006;Grimwade *et al.*, 2010;Green *et al.*, 2010b). Table 1.5 summarises some of the genes commonly mutated in AML. For some of these genetic lesions the impact on prognosis has not been fully elucidated. Therefore these markers require further study before they can be used for risk-adapted therapy. Two genes not included within the table are *c-KIT* and *FLT3* - the implication of mutations in these genes in AML is discussed individually.

Risk group	Incidence (%)	Cytogenetic abnormalities
Favourable	25	t(15;17) (q22;21)/*PML-RARA*
		t(8;21)(q22;q22)/*RUNX1-RUNX1T1*
		inv(16)(p13q22)/(t(16;16)(p13;22)/*CBFB-MYH11*
Intermediate	41	Normal karyotype
	14.5	Other non-adverse karyotype
Adverse	19.5	inv(3)(q2,1q26)/t(3;3)(q21;q26)
		del(5q), -5, add(5q)
		-7, add(7q)/del(7q) (excluding AML with favourable karyotype)
		t(6;11)(q27;q23)
		t(10;11)(p11~13;q23)
		t(11q23) (excluding t(9;11)(p21_22;q23) and t(11;19)(q23;p13)
		t(9;22)(q34;q11)
		-17/abn(17p) and complex
		abn(3q) (excluding t(3;5)(q21_25;q31_35)
		(≥4 unrelated abnormalities)

Table 1.3. The MRC risk group classification of patients with AML based on cytogenetics. Adapted from Grimwade *et al* (1998) and Grimwade *et al* (2010).

Cytogenetic abnormality	Risk group	10-year overall survival (%)
t(15;17)	Favourable	81
t(8;21)	Favourable	61
inv(16)	Favourable	55
t(9;11)	Intermediate	39
t(3;5)	Intermediate	34
t(6;9)	Intermediate	27
Other t(11q23)	Intermediate	22
AML with other MDS-related	Intermediate	24
t(9;22)	Adverse	11
-7/del(7q)	Adverse	10
-5/del(5q)	Adverse	6
Inv(3)	Adverse	3

Table 1.4 The 10-year survival outcome of patients entered into MRC AML 10, 12 and 15. Adapted from Grimwade *et al* (2010).

Gene	Normal function	Incidence	Type of mutation and importance	Prognostic effect	References
NPM1	NPM1 is a phosphoprotein that shuttles between the nucleus and the cytoplasm. It is involved in ribosome biogenesis and thought to have a tumour suppressive role	42-62% (CN-AML)	Most mutations reside in exon 12. ~75-80% of the mutations are characterised by heterozygous tetranucleotide duplications (TCTG) which result in a frameshift disrupting the C terminus of the protein. This causes aberrant localisation of NPM1 to the cytoplasm	*NPM1* mutations, in the absence of a *FLT3*-ITD, have a favourable outcome in CN-AML. Patients with an *NPM1* mutation are twice as likely to have a *FLT3*-ITD or *FLT3*-TKD mutation when compared to those with WT *NPM1*. The presence of an *NPM1* mutation with a *FLT3*-ITD does not negate the poor outcome of *FLT3*-ITD positive AML. The impact of a *FLT3*-TKD and an *NPM1* mutation is unclear; some groups have reported an association towards a better OS and EFS, others have reported no effect on outcome.	(Schnittger *et al.*, 2005;Mrozek *et al.*, 2007;Schlenk *et al.*, 2008a;Mrozek *et al.*, 2008;Grimwade *et al.*, 2010)
CEBPA	CEBPA functions as a tumour suppressor and is implicated in the regulation of granulocyte development	~7% AML (5-14% CN-AML)	Mutations are heterozygous, primarily residing at the N-terminus (frameshift mutations) or at the C-terminus (in-frame insertion/deletions). N-terminal mutations lead to loss of the full length p42 protein but preserve the p30 isoform which has an inhibitory dominant-negative effect on the remaining wild type p42. Mutations at the C-terminus occur in the leucine zipper region which disrupts DNA binding or dimerisation. ~55% of patients have two mutations usually one N-terminal and one C-terminal mutation.	CN-AML patients with *CEBPA* double mutations, but not *CEBPA* single mutations, are associated with a favourable prognosis. The presence of a *FLT3*-ITD in conjunction with a *CEPBA* double mutation loses its favourable outcome. Coincidence of *CEBPA* double and *NPM1* mutations is infrequent. The presence of a *CEBPA* WT or a *CEBPA* single mutation in conjunction with a *NPM1* mutation does not impact on the favourable prognosis associated with an *NPM1* mutation.	(Pabst *et al.*, 2009;Green *et al.*, 2010b)

Table 1.5 Genes commonly mutated in AML listing their frequency, potential role and prognostic impact.

Gene	Normal function	Incidence	Type of mutation and importance	Prognostic effect	References
TET2	The TET family are a group of enzymes involved in catalysing 5-methylcytosine to hydroxymethylcytosine, implicated in demethylating DNA	8-27 % AML	Mutations are spread throughout the gene. Mutations normally cause loss of function via missense, frameshift or nonsense mutations. The exact effects of *TET* mutations are unknown.	The prognostic impact of *TET2* mutations is unclear. Some studies have reported an unfavourable prognosis for intermediate risk patients with a *TET2* mutation while others have reported no significant prognostic effects.	(Chou *et al.*, 2011;Gaidzik *et al.*, 2012)
DNMT3a	DNMT3a is a methyltransferase enzyme that converts cytosine to 5-methylcytosine and is directly involved in DNA methylation.	18-23 % AML (20-25% CN-AML)	Point mutations are most frequent at residue R882 but frameshift, nonsense and splice-site mutations have been identified across the gene. The consequence of *DNMT3a* mutations remains unclear.	*DNMT3a* mutations are associated with an adverse prognosis in patients with intermediate risk cytogenetics.	(Ley *et al.*, 2010;Thol *et al.*, 2011)
IDH1/2	IDH1/2 are isocitrate dehydrogenase enzymes that convert isocitrate to α-ketoglutarate in an NADP-dependent manner within the TCA cycle.	15-33% AML (primarily CN-AML)	Mutations lead to accumulation of the oncometabolite 2-hydroxglutarate which suppresses TET2 activity and promotes HIF1α expression. This is proposed to be involved in driving leukaemogenesis.	The prognostic impact of *IDH1/2* mutations is unclear. Some studies have reported no difference in outcome in regards to *IDH* mutational status, others have demonstrated that the presence of an *IDH1* mutation in the absence of a *FLT3*-ITD confers an independent adverse prognosis, while mutations in *IDH2* at residue R140 are associated with a favourable prognosis.	(Green *et al.*, 2010a;Green *et al.*, 2011;Naoe & Kiyoi, 2013)
ASXL1	Implicated in activation and silencing of *HOX* genes, which are involved in chromatin remodelling.	3-11% AML	Mutations are commonly found in exon 12. They are often frame-shift, missense or non-sense mutations associated with a loss of function.	Evaluation of prognostic significance is still under review.	(Naoe & Kiyoi, 2013)

Table 1.5 (continued)

Gene	Normal function	Incidence	Type of mutation and importance	Prognostic effect	References
TP53	*TP53* is a tumour suppressor gene involved in cycle arrest, apoptosis and DNA repair.	10-15% AML	Mutations are normally characterised by loss of function. Mutations are predominately found in patients with a complex karyotype.	*TP53* mutations are associated with a poor outcome.	(Marcucci *et al.*, 2011b)
MLL-PTD	Mixed lineage leukaemia protein is a DNA binding protein essential for haematopoiesis.	8% CN-AML	MLL partial tandem duplication (PTD) is an in-frame gain of function mutation that drives proliferation and maintains self renewal.	Patients expressing MLL-PTD have an unfavourable prognosis.	(Whitman *et al.*, 2007)
WT1	Wilms tumour 1 (WT1) is a transcriptional regulator involved in proliferation, apoptosis and differentiation of haematopoietic progenitors.	15% AML	Mutations are predominantly frameshift or nonsense changes resulting in loss of function.	The presence of a *WT1* mutation in CN-AML has an unfavourable outcome compared to patients with WT *WT1*.	(Paschka *et al.*, 2008)
K/N-RAS	K/N-RAS are a family of membrane bound proteins involved in signal transduction.	12-27% AML (most prevalent in CBFL)	*K/N RAS* are usually deregulated by point mutations rendering RAS constitutively active.	*K/N-RAS* mutations do not impact on OS.	(Bowen *et al.*, 2005)

Table 1.5 (continued)

1.5.4 Chemotherapy

Although there have been improvements in therapeutics and supportive care, the majority of patients with AML eventually succumb to the disease. An exception to this is acute promyelocytic leukaemia (APL), which occurs in approximately 10% of patients with AML. The treatment of APL has dramatically improved with >75% of patients achieving a cure when treated with a combination of all-trans retinoic acid (ATRA) with anthracycline-based protocols (Roboz, 2011). The induction treatment for all other subtypes of AML has largely remained unchanged for the last 30 years. Standard induction therapy consists of cytarabine (AraC), a cytotoxic agent, in combination with an anthracycline such as daunorubicin or idarubicin (Tallman, 2005). Overall, 60-80% patients <60 years of age achieve a CR, but only 30-40% of patients are still alive and disease-free after 5 years (Tallman, 2005;Fernandez *et al.*, 2009). It has been reported that 48.5% of patients >60 years of age achieve CR from induction therapy, however elderly patients have a dismal 5 year survival of <10% (Farag *et al.*, 2006). Attempts to improve the induction regime include increasing the dose of AraC, the use of alternative anthracyclines or anthracenediones compounds, or the use of additional drugs such as etoposide, fludarabine or cladribine, however they have all failed to show a significant advantage compared to the standard therapy. In contrast, the addition of gemtuzumab ozogamicin, a monoclonal antibody to CD33, to cytarabine and daunorubicin induction therapy in patients <60 years of age has been shown to significantly improve survival in patients with favourable risk cytogenetics and 70% of patients with intermediate risk cytogenetics (Burnett *et al.*, 2011).

Following induction therapy the optimal treatment choice in AML is still unclear. There are currently three treatment options including intensive chemotherapy for 3-4 cycles, high dose chemotherapy in conjunction with autologous stem-cell transplantation (auto-SCT) or allogeneic stem cell transplantation (allo-SCT). The current consensus following the first CR (CR1) suggests that patients with good-risk cytogenetics should receive chemotherapy or an auto-SCT, while patients with poor-risk cytogenetics should be recommended for a allo-SCT, regardless of response to induction therapy (Koreth *et al.*, 2009;Schmid *et al.*, 2012). For patients with intermediate-risk cytogenetics, the benefit of an allo-SCT over auto-SCT or chemotherapy is highly debated. Allo-SCT administered after CR1 has demonstrated the lowest RR rates and the best anti-leukaemic effect, as a result of the graft-versus-leukaemia (GvL) effect, when compared to auto-SCT or consolidation therapy. However, it is associated with increased treatment-related mortality (TRM) and therefore has shown limited benefit on OS (Burnett *et al.*, 1998;Cassileth *et al.*, 1998). Auto-SCT negates some of the toxicities associated with allo-SCT, and has been shown to reduce the RR in several trials.

However, due to prolonged marrow aplasia and TRM associated with the procedure, there has been no observable improvement in OS (Vellenga *et al.*, 2011). Auto-SCT also does not elicit the immunological response of the GvL effect and there is the risk of re-transplanting residual LSCs.

1.6 Core binding factor leukaemias

Core binding factor leukaemia (CBFL) is characterised by the chromosomal rearrangements t(8;21)(q22;q22) or inv(16)(p13;q22)/t(16;16)(p13;q22) which generate the fusion proteins RUNX1-RUNX1T1 (AML1-ETO) and CBFβ-MYH11 respectively. These fusion proteins disrupt the normal function of core binding factor (CBF). The CBF factor is a heterodimeric transcription factor composed of a DNA-binding CBFα subunit (RUNX1, RUNX2 or RUNX3) and a non-DNA binding counterpart subunit CBFβ. RUNX1 (AML-1) binds to core enhancer sequences (TGT/cGGT) within promoters or enhancers of haematopoietic-specific lineage genes and recruits CBFβ, which strengthens the DNA binding affinity of RUNX1 (Reilly, 2005). Other lineage-specific transcription factors are then recruited to the RUNX1/CBFβ complex, which drives transcription of myeloid lineage genes such as myeloperoxidase (*MPO*), interleukin 3 (*IL3*), colony stimulating factor 1 receptor (*CSF1R*) and granulocyte-macrophage colony stimulating factor (*GM-CSF*).

In t(8;21) leukaemia, the RUNX1 protein becomes fused at the C-terminus to the co-repressor protein ETO, otherwise known as RUNX1T1. The RUNX1-RUNX1T1 fusion protein still retains its ability to bind to RUNX1 DNA targets and its binding partner CBFβ, however the ETO protein functionally dominates (Licht, 2001). The ETO protein recruits a repressor complex comprised of mSin3A, N-Cor and histone deacetylase (HDAC), which blocks transcription of key myeloid differentiation genes (Licht, 2001). Inv(16) generates a fusion protein between the major contractile protein smooth muscle myosin heavy chain 11 (MYH11) and CBFβ. The CBFβ-MYH11 fusion protein retains its ability to bind to RUNX1 and contains an additional CBFβ binding site that increases its binding affinity for RUNX1. The MYH11 component interacts with the repressor proteins mSin3A, N-Cor and HDAC, leading to transcriptional repression of RUNX1-transcribed genes. The CBFβ-MYH11 protein also actively retains RUNX1 either in the cytoplasm, in deposits on cytoskeletal filaments, or within the nucleus within rod-like complexes (Adya *et al.*, 1998;Reilly, 2005). This further limits the amount of RUNX1 available for transcription of myeloid genes. *In vitro* studies have shown both fusion proteins promote self-renewal while causing a block in myeloid differentiation (Kuo *et al.*, 2006;Elagib & Goldfarb, 2007). However, the fusion proteins alone are not capable of inducing AML in murine models and require additional co-

operating mutations in signalling genes such as *FLT3* or *c-KIT* to induce AML (Yuan *et al.*, 2001;Higuchi *et al.*, 2002;de Guzman *et al.*, 2002;Wang *et al.*, 2011;Zhao *et al.*, 2012).

1.7 c-KIT

1.7.1 c-KIT structure and function

The c-KIT proto-oncogene, also referred to as stem cell factor receptor (SCFR) or CD117, is a class III transmembrane receptor tyrosine kinase (RTK). The *c-KIT* gene is located on chromosome 4q11-q12 and is encoded by 21 exons. c-KIT is a 976 amino acid protein comprised of five immunoglobulin-like loops within the extracellular domain (ECD), a transmembrane domain (TMD), a juxtamembrane domain (JMD), two tyrosine kinase domains (TKD1 and TKD2) linked by a kinase insert domain (KID), and an activating loop domain (ALD) (Figure 1.2a). The first 3 immunoglobulin-like domains of the c-KIT receptor form a binding site for its ligand, stem cell factor (SCF) (Orfao *et al.*, 2007). Binding of SCF to c-KIT causes the receptor to dimerise. This is stabilised by the 4^{th} and 5^{th} loops of the ECD and results in autophosphorylation of specific tyrosine residues in the cytoplasmic domain of the receptor. Four such residues are Y547, Y553, Y568, and Y570, which are critical for maintaining the auto-inhibitory structure of the JMD. When the receptor dimerises, these residues become phosphorylated (DiNitto *et al.*, 2010). This causes a conformational change releasing the JMD from the kinase domain and switching of the ALD from a packed position to an extended form, allowing ATP and protein substrates into the catalytic site, as illustrated in Figure 1.2b. Phosphorylation of residue Y823 stabilises the ALD in the active conformation. Numerous docking proteins are capable of interacting with specific tyrosine phosphorylation sites within c-KIT, as shown in Table 1.6. c-KIT can therefore activate an array of signal transduction pathways including the Janus kinase/Signal Transducer and Activator of Transcription (JAK/STAT), Phosphatidylinositol 3-kinases/protein kinase B/mammalian target of rapamycin (PI3K/AKT/mTOR) and rat sarcoma/proto-oncogene c-RAF/extracellular signal-regulated kinases pathways (RAS/RAF/ERK). c-KIT mediates a number of functions including cell proliferation, differentiation, survival and migration (Malaise *et al.*, 2009). c-KIT is also involved in cellular processes including haematopoiesis, melanogenesis and gametogenesis.

Tyrosine residue	568	570	703	721	730	900	936
Docking protein	SFKs, APS, SHP2, Cbl, Lnk, SOCS6 CHK	SFKs, SHP1	Grb2	p85α	PLCy-2	P85α (Crk)	Grb2,APS Cbl, Grb7

Table 1.6 The docking sites in c-KIT that are phosphorylated upon receptor activation and the proteins that subsequently bind to specific residues. Adapted from Masson & Ronnstrand, (2009).

(a)

(b)

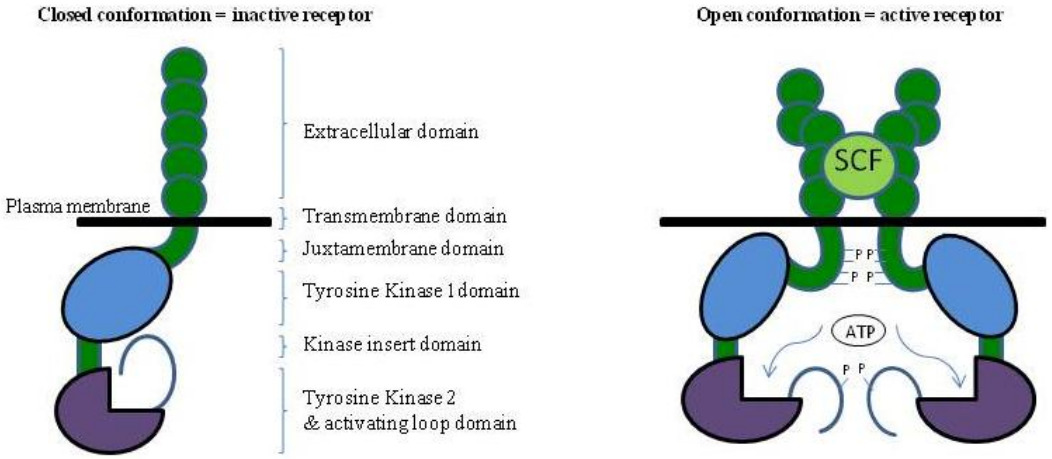

Figure 1.2 Schematic diagrams showing the functional domains of c-KIT in its inactive and active form. (a) c-KIT in its monomeric inactive form (b) c-KIT when the receptor dimerises in the presence of SCF causing structural reconfiguration leading to the activation of the receptor.

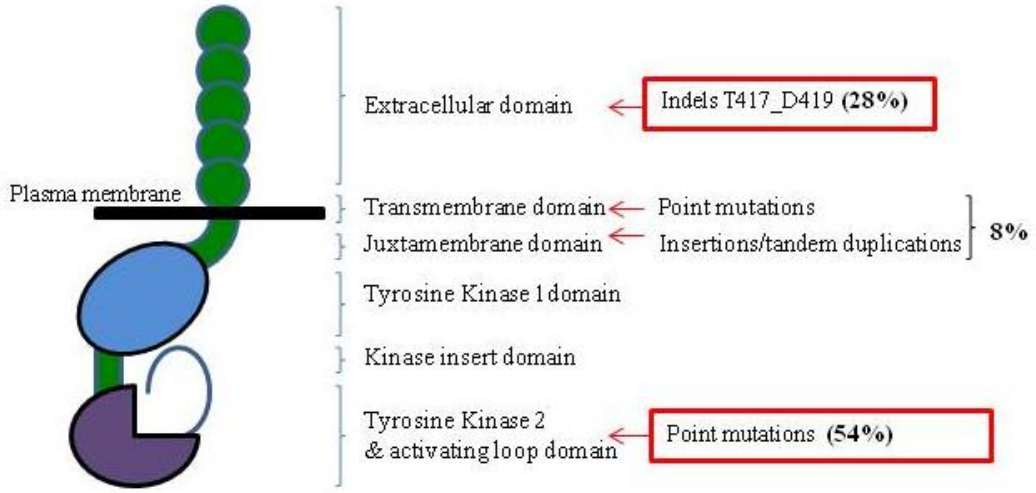

Figure 1.3 A diagram highlighting the domains in which *c-KIT* mutations commonly occur in CBFL. Two hot spots are highlighted in red, one in the ECD and one in the TKD2. Point mutations and insertions/tandem duplications have been found in the TMD and JMDs respectively, but at a lower frequency.

1.7.2 c-KIT isoforms

The mRNA of c-KIT can be alternatively spliced into two different isoforms. The two isoforms are characterised by the presence or absence of the Gly-Asn-Asn-Lys (GNNK) amino acid sequence found in the JMD. Both isoforms co-exist in different tissues such as the lung, BM, fetal liver, mast cells, brain, ovary and testis (Piao *et al.*, 1994). However, the GNNK- transcript has been identified as the predominant isoform. Different cell signalling capabilities have been associated with the different isoforms. Ba/F3 cells transduced with constructs expressing either c-KIT GNNK- or c-KIT GNNK+ showed that cells expressing the GNNK- isoform activated PI3K/AKT more strongly, resulting in increased cell survival/proliferation in comparison to cells expressing the GNNK+ isoform (Pedersen *et al.*, 2009). In AML, GNNK- is the main transcript expressed and one study suggested that patients with AML expressing just the GNNK- transcript had a better 3 year OS and progression free survival (PFS) in comparison to patients expressing the GNNK+ and the GNNK- transcripts (Guerrini *et al.*, 2007).

1.7.3 *c-KIT* mutations in AML

Somatic mutations in *c-KIT* have been identified in a host of diseases including gastrointestinal stromal tumours (GIST), melanoma, systemic mastocytosis, myeloproliferative diseases and leukaemias. In AML, c-KIT is highly expressed on 60-80% of myeloblasts and is mutated in approximately 5% of all AML (Beghini *et al.*, 2004). *c-KIT* mutations are, however, more commonly found in CBFL. The largest study to date of 199 adult patients with t(8;21) and 155 with inv(16) reported 28% of patients had a *c-KIT* mutation, with a greater frequency of mutations occurring in inv(16) in comparison to t(8;21) (35% versus 23%, p=0.02) (Allen *et al.*, 2013). In contrast, a study of 203 paediatric patients with CBFL reported a lower incidence of *c-KIT* mutations of 19% (Pollard *et al.*, 2010). Other studies have reported that the incidence of *c-KIT* mutations in CBFL can range from 13-46% (Care *et al.*, 2003;Beghini *et al.*, 2004). In CBFL, *c-KIT* mutations localise to mutational hotspots. Allen et al (2013) reported that 54% of *c-KIT* mutations occur in exon 17 (ALD) as point mutations, 28% occur within exon 8 (ECD) in the form of inframe indels and 8% occur either as point mutations in exon 10 (TMD) or insertions/tandem duplications in exon 11 (JMD) (Figure 1.3). Table 1.7 lists some of the *c-KIT* mutations identified in patients with AML and the domains they target. Of note, point mutations in exon 17 primarily reside at residues D816 and N822 and inframe indels occur between residues 417-419 (Care *et al.*, 2003;Goemans *et al.*, 2005;Wang, 2005;Paschka *et al.*, 2006;Shimada *et al.*, 2007).

The structural impact of *c-KIT* mutations depends on their location. Mutations in the JMD are proposed to disrupt the auto-inhibitory structure of c-KIT, leading the receptor to spontaneously dimerise in the absence of SCF (Kitamura & Hirotab, 2004). Mutations in the ALD most likely stabilise the ALD in the extended configuration, therefore shifting the conformation equilibrium to the active state (Vendome *et al.*, 2005;Gajiwala *et al.*, 2009). Bioinformatic analysis of c-KIT-D816V X-ray structures has suggested that mutations at this residue can remodel the JMD by favouring removal of the JMD from the TKD, further triggering transition from an inactive to an active state (Laine *et al.*, 2011). Based on this model the presence of mutations in the ALD may not require receptor dimerisation for activation.

1.7.4 Impact of *c-KIT* mutations in AML models

The role of numerous *c-KIT* mutations has been assessed *in vitro* in factor-dependent cell line models. Mutations in the ALD including N822K, D816V, D816F, D816H and D816Y lead to autophosphorylation of c-KIT, ligand-independent growth and activation of STAT5, STAT3, PI3K, AKT and ERK (Ning *et al.*, 2001;Growney *et al.*, 2005;Schittenhelm *et al.*, 2006;Wang *et al.*, 2011). The D816V mutation is the most common *c-KIT* mutation and has therefore been extensively studied. The IL3-dependent lymphoid Ba/F3 cell line transfected with a construct expressing *c-KIT*-D816V showed constitutive activation of downstream proteins including ERK, AKT Gab2, Shc, SHP-2 and Cbl, which was not observed with cells expressing the WT receptor (Pedersen *et al.*, 2009;Sun *et al.*, 2009). Comparative analysis of WT and D816V c-KIT signalling revealed that, unlike the WT receptor, the *c-KIT*-D816V mutation did not require the Src kinase to phosphorylate c-KIT (Sun *et al.*, 2009). The functional consequence of AML specific JMD mutations has not been investigated extensively. However, *c-KIT* mutations I571del14(ESVDPTQLPYDHKW) and L576P have been shown to constitutively activate c-KIT in murine IL3 dependent 32D and Ba/F3 cells respectively, with the former also showing ligand-independent growth (Antonescu *et al.*, 2007;Wang *et al.*, 2011). JMD mutations identified in GIST and mastocytosis patients have also been reported to be activating in *in vitro* cell line models (Growney *et al.*, 2005). Mutations in the ECD are particularly heterogeneous within AML (Table 1.7). Unlike the activating mutations in the ALD and JMD, the presence of an indel in exon 8 renders the receptor hypersensitive to SCF (Kohl *et al.*, 2005). Exon 8 mutations also cause the receptor to spontaneously dimerise, leading to the removal of factor dependency in cell lines such as Ba/F3 and FDC-P1 (Kohl *et al.*, 2005;Growney *et al.*, 2005;Nick *et al.*, 2011).

Exon	Mutation	Domain location	Mutation reported in t(8;21) or inv(16)
8	D419 deletion	ECD	t(8;21)
8	T417del and D419del	ECD	t(8;21)
8	ΔT417_D419 + insertion I	ECD	Both
8	ΔT417_D419 + insertion V	ECD	inv(16)
8	ΔT417_D419 + insertion W	ECD	inv(16)
8	ΔT417_D419 + insertion IP	ECD	t(8;21)
8	ΔT417_D419 + insertion NG	ECD	inv(16)
8	ΔT417_D419 + insertion RG	ECD	inv(16)
8	ΔD419_L421 + insertion VHV	ECD	inv(16)
8	ΔY418 + insertion GFF	ECD	inv(16)
9	502(AYFNF) repeat	ECD	t(8;21)
10	I538V	TMD	t(8;21)
10	V540L	TMD	t(8;21)
10	V530I	TMD	Inv(16)
11	L576P	JMD	t(8;21)
11	Q575ins17 (EFCELPYDHKWEFPRNR)	JMD	t(8;21)
11	I571del14(ESVDPTQLPYDHKW)	JMD	t(8;21)
16	I748T	KID	t(8;21)
17	D816Y	TKD-2	Both
17	D816V	TKD-2	Both
17	D816H	TKD-2	Both
17	D816I	TKD-2	inv(16)
17	A814S	TKD-2	t(8;21)
17	N822K	TKD-2	t(8;21)
17	N822T	TKD-2	t(8;21)
17	N822Y	TKD-2	t(8;21)
17	V825I	TKD-2	t(8;21)
17	V825A	TKD-2	t(8;21)
17	L773S	TKD-2	t(8;21)

Table 1.7 *c-KIT* mutations reported in CBFL and the domains they target.

A comparison of the leukaemogenic potential of ECD and ALD *c-KIT* mutations has been assessed *in vivo*. Haematopoietic stem/progenitor cells were retrovirally co-transduced with constructs expressing the murine *c-KIT*-D814V (homolog to D816V in humans) or *c-KIT*-T417IΔ418-419 in conjunction with RUNX1/RUNX1T1 and transplanted into mice. Mice co-expressing c-KIT-D814V and RUNX1/RUNX1T1 generated a transplantable aggressive AML phenotype in nine of twenty mice, a myeloproliferative phenotype in seven of twenty mice or a pre-B-cell leukaemia in four of twenty mice whereas, mice co-expressing c-KIT -417IΔ418-419 and RUNX1/RUNX1T1 exclusively generated an AML phenotype in nineteen of thirty-seven mice (Nick *et al.*, 2011). Of note, expression of just c-KIT-D814V or c-KIT-T417IΔ418-419 alone did not generate an AML phenotype but the mice did develop either a myeloproliferative disease (MPD), B-ALL or T-ALL. Mice receiving just RUNX1/RUNX1T1 rarely developed leukaemia. Other *c-KIT* mutations have also been examined *in vivo*, including the common ALD mutation N822K. A hybrid mouse/human c-KIT-N822K receptor was capable of rendering murine 32D cells factor-independent. Transplantation of murine BM cells transduced with the hybrid c-KIT-N822K receptor and RUNX1/RUNX1T1 generated an AML phenotype in BALB/c mice (Wang *et al.*, 2011). Expression of just the *c-KIT* N822K mutation generated an MPD phenotype, while no disease was observed in mice expressing just RUNX1/RUNX1T1.

This data therefore supports the two hit hypothesis of leukaemogenesis proposed by Kelly and Gilliland (2002). This model suggests the cooperation of two types of mutations, a type I and a type II. Type I mutations promote cell proliferation and are often an activated RTK e.g. c-KIT, whereas type II mutations cause a block in myeloid differentiation and promote self-renewal, e.g. RUNX1/RUNX1T1. Although the mouse models previously discussed support this, they do have a considerable disease latency suggesting other factors contribute to the pathogenesis and progression of AML. Whole genome or exome sequencing of samples from 200 de novo AML has revealed that, on average, 13 genes are mutated per patient (Ley, 2013). Recurrent mutations are identified in *NPM1*, tumour-suppressor genes, DNA methylation-related genes, signalling genes, chromatin-modifying genes, myeloid transcription factor genes, cohesion complex genes and spliceosome-complex genes. The emerging interplay of mutations between these genes/subgroups illustrates that a ‘2-hit’ model of leukaemogenesis is an over-simplification in AML.

1.7.5 Prognostic impact of *c-KIT* mutations

The presence of t(8;21) or inv(16) is usually associated with a favourable outcome in AML (Table 1.4). However, the presence of a *c-KIT* mutation in either subgroup has been associated with a significant increase in RR (Paschka *et al.*, 2006;Cairoli *et al.*, 2006;Allen *et al.*, 2013).

t(8;21)

Several groups have reported that patients with AML co-expressing t(8;21) and a *c-KIT* mutation have a significantly poorer OS and relapse-free survival/event-free survival (RFS/EFS) when compared to patients with inv(16) and a *c-KIT* mutation (Boissel *et al.*, 2006;Cairoli *et al.*, 2006;Park *et al.*, 2011b;Allen *et al.*, 2013). In particular, the presence of a *c-KIT* mutation in exon 17 has been associated with a significant poorer OS and EFS in t(8;21) patients (Park *et al.*, 2011b). More recent data showed that t(8;21) patients with a mutant level >25% (KIT^{high}) versus those with c-KIT-WT at 10 years from entry had a significant increase in RR (41% vs 25% respectively, p=0.05), with no significant impact on OS (45% versus 59% respectively, p=0.2) (Allen *et al.*, 2013).

Inv(16)

c-KIT mutations in exon 8 have been shown to occur more frequently in patients with inv(16) in comparison to those with t(8;21) and have subsequently been associated with a higher RR (Care *et al.*, 2003). Mutations in exon 17 have not been associated with the same poor prognosis in patients with inv(16) (Park *et al.*, 2011b). Patients with a mutant level >25% (KIT^{high}) versus those WT for *c-KIT* have not been associated with a significant increase in RR or decrease in OS (Cumulative Incidence Relapse: 63% vs 51%, p=0.2, and OS 48% vs 59%, p=0.4, for c-KIT^{high} and c-KIT-WT respectively) (Allen *et al.*, 2013). The discrepancy between different reports may be due to the differences in treatment and the relatively small samples sizes being examined. However, as proposed by Allen *et al* (2013) differences observed may be due to heterogeneity in mutant level.

The treatment options for patients with CBFL and a *c-KIT* mutation is unclear. Some authors have suggested that there is insufficient data supporting the use of *c-KIT* mutational status as a method for directing therapy (Marcucci *et al.*, 2011a). Others have suggested that patients with inv(16) or t(8;21) and a *c-KIT* mutation should be classified as intermediate risk and considered for either a matched sibling donor allogeneic haematological stem cell

transplantation (HSCT) or put forward for clinical trials using small molecule inhibitors (Park *et al.*, 2011a;O'Donnell *et al.*, 2012). Although HSCT has not been shown to improve outcome in t(8;21) leukaemia it does provide the most anti-leukaemic effect in comparison to autologous HSCT or consolidation therapy and therefore should be considered (Schlenk *et al.*, 2008b).

1.7.6 c-KIT inhibitors

The use of c-KIT inhibitors to treat CBFL is in its infancy. A variety of selective and non-selective inhibitors have been designed and tested in AML cell lines and primary AML cells, such as SU5416, SU6668, sorafenib, sunitinib, EXEL-0862, imatinib, dasatinib and masitinib. However, direct translation into clinical studies has been limited.

SU5416 and SU6668

SU5416 and SU6668 are potent ATP competitive inhibitors of RTKs such as vascular endothelial growth factor receptor 1/2/3 (VEGFR-1/2/3), FLT3 and c-KIT. *In vitro* studies using SU5416 and SU6668 on a human myeloid cell line MO7E and primary AML cells showed that both compounds inhibited SCF-stimulated c-KIT-WT phosphorylation and were capable of inhibiting proliferation and inducing apoptosis (Smolich, 2001).

Sorafenib and Sunitinib

Sorafenib and Sunitinib are both ATP competitive drugs shown to inhibit a range of RTKs including c-KIT, FLT3, VEGFR and platelet-derived growth factor receptor (PDGFR), that are FDA-approved for the treatment of advanced renal cell carcinoma (RCC). The effect of both drugs has been examined on a panel of AML cell lines and showed that they both potently inhibit proliferation and induce apoptosis in a time-and-dose dependent manner (Hu *et al.*, 2008). Sorafenib has also been shown to inhibit proliferation by ≥50% in six of nine primary AML cells and has been tested clinically in a cohort of 38 patients with AML, showing a short-term CR in only one patient (Crump *et al.*, 2010). Sunitinib is currently used as a therapeutic agent to treat imatinib-resistant GIST. An analogue of Sunitinib called SU11657 has been assessed in paediatric primary AML cells which showed that samples with either a *FLT3* or a *c-KIT* mutation were significantly more sensitive to SU11657 compared to samples WT for both receptors (Goodman *et al.*, 2007;Goemans *et al.*, 2010).

EXEL-0862

EXEL-0862 is an inhibitor of VEGFR, fibroblast growth factor receptor (FGFR), PDGFR, FLT3 and c-KIT. The binding mechanism of EXEL-0862 is currently unknown. In the human mast cell leukaemia cell lines HMC1.1 and HMC1.2, which harbour V560G and V560G and D816V *c-KIT* mutations respectively, EXEL-0862 was capable of inhibiting c-KIT phosphorylation in a dose-dependent manner, reducing cellular proliferation and inducing apoptosis (Pan *et al.*, 2007). EXEL-0862 appeared to be more potent in the HMC1.2 cells, suggesting this compound could be more effective against malignancies that harbour a D816V activating mutation.

Imatinib

Imatinib, commercially known as Gleevec, is an ATP competitive inhibitor of BCR-ABL (fusion protein found in chronic myelogenous leukemia (CML)), PDGFR, and c-KIT. Imatinib is the first line treatment for CML. Imatinib binds to the inactive conformation of c-KIT, locking it in this configuration. *In vitro* studies revealed that imatinib can bind and inhibit proliferation of cells expressing *c-KIT* mutations in the ECD, JMD and certain ALD mutations, e.g. N822K (Growney *et al.*, 2005). However, mutations at residue D816 are resistant to imatinib (Growney *et al.*, 2005;Shah *et al.*, 2006). Studies examining the effects of imatinib on c-KIT in the Kasumi-1 cells, a human CBFL cell line expressing the *c-KIT* N822K mutation, and patient samples expressing the N822K mutation showed a decrease in c-KIT phosphorylation and induction of apoptosis in a time/dose-dependent manner (Wang, 2005;Wang *et al.*, 2011). Treatment of 18 patients with relapsed or refractory AML/MDS with a daily dose of 400mg of imatinib showed no partial or complete responses to imatinib (Cortes *et al.*, 2003). These patients did express c-KIT however they were not screened for *c-KIT* mutations. A phase II pilot study of 21 patients with refractory AML expressing c-KIT (c-KIT+) received 600mg/day of imatinib for 6 months showing a haematological response in 5 patients (Kindler, 2004). In support of this, a phase I study of 21 patients with relapsed c-KIT+ AML treated with cytarabine, daunorubicin and imatinib showed a partial or complete response in 57% of patients (Advani *et al.*, 2010). A phase II study of patients with relapsed/refractory c-KIT+ AML used standard induction therapy in conjunction with escalating doses of imatinib (200-400mg/day) and showed a CR in twenty of thirty-one patients. Although initial results were promising, patients relapsed within a median of 6.8 months. The current clinical trials with imatinib have not taken into consideration *c-KIT* mutational status, therefore the therapeutic benefit of imatinib for patients with *c-KIT* mutations versus those without remains to be determined.

Dasatinib

Dasatinib is an ATP-competitive BCR-ABL, SRC, c-KIT inhibitor. In a panel of cell lines with varying *c-KIT* mutations, dasatinib was capable of inhibiting c-KIT phosphorylation and decreasing cellular proliferation in cell lines with *c-KIT*-WT, ALD (including D816V) and JMD mutations (Schittenhelm *et al.*, 2006;Shah *et al.*, 2006;Guerrouahen *et al.*, 2010). In a long term culture system, dasatinib potently inhibited proliferation of LSCs from primary AML cells with a *c-KIT* or *BCR-ABL* mutation while having a limited impact on healthy CD34+ cells (Han *et al.*, 2010). A recent study combining dasatinib with daunorubicin or ara-C resulted in enhanced apoptosis and inhibition of proliferation compared to either drug alone in primary AML cells (Dos Santos *et al.*, 2013). *In vivo*, a combination of daunorubicin or ara-C and dasatinib reduced the ability of murine AML stem cells to regenerate leukaemia in secondary recipient mice (Dos Santos *et al.*, 2013). Dasatinib is beginning to be assessed within the clinic. A phase I dose escalation study in paediatric patients (1-21 years of age) with relapsed/refractory leukaemia has been completed and showed no clinical responses in any patients with AML (Zwaan *et al.*, 2013). Of note, none of the patients included in the study had a *c-KIT* mutation. Investigations are now ongoing assessing the role of dasatinib as a monotherapy and in conjunction with standard chemotherapy in patients with CBFL (clinical trials NCT00850382 and NCT01876953).

Masitinib

Masitinib is an ATP-competitive inhibitor against c-KIT and PDGFR α/β. Masitinib was capable of decreasing c-KIT phosphorylation and inhibiting cell growth in Ba/F3 cells expressing *c-KIT*-WT and *c-KIT*-JMD mutations but not those expressing *c-KIT*-D816V (Dubreuil *et al.*, 2009). A nude mouse model injected with Ba/F3 cells expressing the murine *c-KIT*-Δ27 mutation (deletion of codons 547-555) treated with masitinib demonstrated inhibition of tumour growth and an increase in the median survival time in comparison to mice without treatment (Dubreuil *et al.*, 2009). The impact of masitinib in AML has yet to be assessed.

1.8 FLT3

1.8.1 FLT3 structure and function

FLT3, also known as CD135 or FLK2 (fetal liver tyrosine kinase 2) is a membrane bound class III tyrosine kinase receptor. The *FLT3* gene is located on chromosome 13q12 and generates a 993 amino acid protein with a predicted molecular weight of 130-143kDa when unglycosylated. The structure of FLT3 is similar to other RTKs such as c-KIT and PDGFR. The receptor contains an ECD comprised of 5 immunoglobulin-like repeats, a TMD, a JMD, two tyrosine kinase domains (TKD1 and TKD2) linked by a kinase insert domain (KID) and an ALD (Figure 1.4a). Unstimulated FLT3-WT is unphosphorylated and in an inactive monomeric form. This is maintained by the JMD adopting a 'wedged shape' with the activating loop folded back between TKD1 and 2, blocking the ATP binding site and substrate loading (closed conformation) (Meshinchi & Appelbaum, 2009) (Figure 1.4a). Activation of the receptor is controlled by binding of the FLT3 ligand (FL) to the 3 distal immunoglobulin-like repeats. FL is a cytokine that functions to stimulate proliferation, survival and differentiation of haematopoietic progenitor cells (Wodnar-Filipowicz, 2003). Once FL is bound, the 2 immunoglobulin-like repeats closest to the receptor mediate dimerisation of two monomeric FLT3 units (Figure 1.4b). This leads to phosphorylation of Y589 and Y591 residues within the JMD, destabilising the autoinhibitory structure and releasing the ALD. The tyrosine residues within the activation loop are then available to be phosphorylated, freeing the ATP binding site and rendering the receptor active (open conformation) (Meshinchi & Appelbaum, 2009). ATP and other substrates can then bind to the receptor, resulting in phosphorylation and activation of downstream target proteins including PI3K, Ras GTPase, phospholipase C-γ, Shc, growth factor receptor-bound protein (Grb2) and Src family tyrosine kinases (Takahashi, 2011). These proteins can then subsequently activate AKT, mTOR, STAT5 and MAPK, which are implicated in a host of cellular processes including proliferation, apoptosis and the development of multipotent stem cells.

(a) (b)

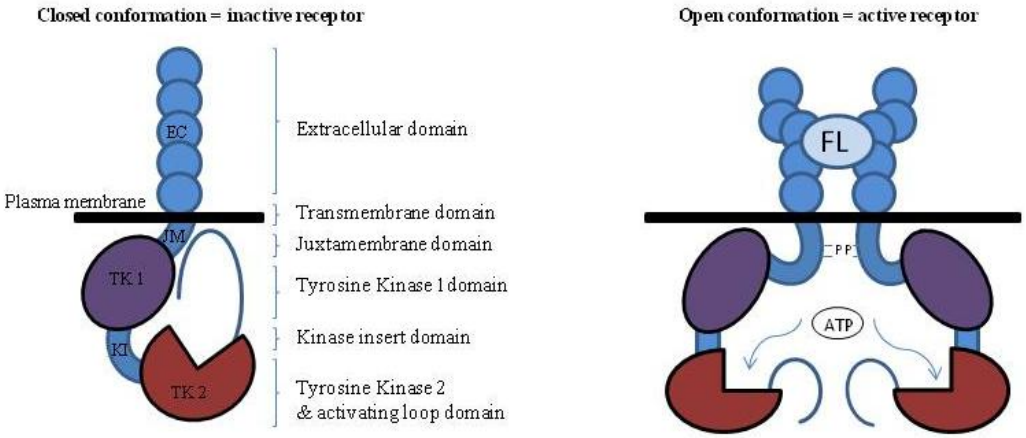

Figure 1.4 Schematic diagrams showing the functional domains of FLT3 in its active and inactive form. (a) FLT3 in its monomeric inactive form. (b) FLT3 when the receptor dimerises in the presence of FL causing structural reconfiguration leading to the activation of the receptor.

(a) (b)

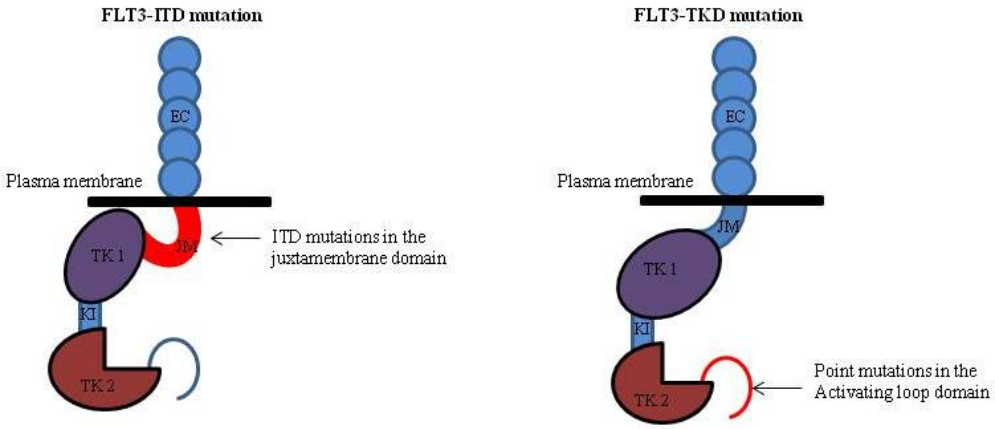

Figure 1.5 Diagrams of the two most frequent *FLT3* mutations in AML. (a) *FLT3*-ITDs in the JMD or (b) point mutations in the ALD (*FLT3*-TKD).

1.8.2 *FLT3* mutations in AML

FLT3 is highly expressed in 70-100% of AML cases and is frequently mutated in AML. *FLT3* is mutated in approximately 30% of AML by either internal tandem duplications (ITDs) within the JMD or point mutations in the second tyrosine kinase domain (TKD).

1.8.3 *FLT3*-ITD mutations

FLT3-ITD mutations occur within exons 14-15 in approximately 25% of adult AML cases and vary in size (3 to >400 base pairs) and location (Nakao *et al.*, 1996;Gilliland & Griffin, 2002). The incidence of *FLT3*-ITDs is age-dependent ranging from 12-15% in 0.2-19.8 year olds versus 54% for AML patients 35-54 years of age (Kottaridis *et al.*, 2001;Meshinchi *et al.*, 2001;Meshinchi *et al.*, 2006). Expression of *FLT3*-ITD mutations in murine 32D and Ba/F3 cells have demonstrated constitutive activation of FLT3 in the absence of ligand, constitutive activation of downstream target proteins (STAT5, AKT/PI3K and RAS/MAPK) and cytokine-independent growth (Mizuki *et al.*, 2000;Hayakawa *et al.*, 2000). Murine BM cells retrovirally transduced with *FLT3*-ITDs were capable of generating a MPD phenotype in a BM transplantation assay (Kelly *et al.*, 2002). However, the presence of a *FLT3*-ITD alone was not sufficient to induce AML. The exact mechanism of auto-dimerisation resulting from a *FLT3*-ITD is unknown. Crystal structural analysis of the receptor suggests that the presence of ITD mutations may disrupt the auto-inhibitory conformation controlled by residues Y589 and Y591, thereby generating a more relaxed structure which more readily allows auto-dimerisation (Meshinchi *et al.*, 2008).

The presence of *FLT3*-ITD mutations is also associated with an increased production of reactive oxygen species (ROS), both in AML cell lines and primary AML cells. Increased levels of ROS, as a result of *FLT3*-ITD mutations, has been shown to cause genomic instability mediated by an increase in double strand breaks resulting in erroneous DNA repair (Sallmyr *et al.*, 2008). These authors also showed that an increase in ROS levels by *FLT3*-ITD mutations appeared to be mediated by STAT5 signalling activating RAC1, a key GTPase protein required to activate NADPH oxidases.

1.8.4 Clinical impact of *FLT3*-ITDs

FLT3-ITDs are associated with a high white blood cell count, an elevated percentage of PB and BM blasts and a normal karyotype (Frohling *et al.*, 2002). The CR rate in patients positive for a *FLT3*-ITD (*FLT3*-ITD+ AML) is not significantly reduced, but there are increased RR, decreased disease free survival (DFS) rates and poor OS rates resulting in it being identified in many studies as a poor prognosis marker (Kottaridis *et al.*, 2001;Frohling

et al., 2002;Thiede *et al.*, 2002). The mutant level has been reported to vary from 1-96% in *FLT3*-ITD+ AML (Gale *et al.*, 2008). The allelic ratio of FLT3-WT to mutant receptor can impact on prognosis with a high ITD:WT allele ratio associated with a negative impact on RR and OS (Thiede *et al.*, 2002;Gale *et al.*, 2008). The variation in mutant level suggested that patients with a high mutant level (>50%) may have lost the WT allele, potentially by uniparental disomy (UPD), in a proportion of cells. An intermediate mutant level indicated a heterozygous mutation in the majority of cells or UPD of a mutant allele in up to 50% of the cells. A low mutant level (1-24%) implied that the acquisition of a *FLT3*-ITD mutation was a secondary event that occurred in a sub clone of cells. The impact of the size of the ITD on prognosis remains contradictory. Different groups have shown that both larger and shorter insertions can lead to an inferior prognosis, while others have reported no difference on outcome (Kusec *et al.*, 2006;Ponziani *et al.*, 2006;Meshinchi *et al.*, 2008;Gale *et al.*, 2008). More recently the actual site of the ITD has been examined. Kayser *et al* (2009) categorised ITDs into two classes, those occurring either within the JMD between amino acids 572 and 609 (69.5% of the *FLT3*-ITDs examined) or 3' of the JMD within the beta1-sheet of the TKD1 (30.5% of the *FLT3*-ITDs examined). Samples with insertion sites in the beta1-sheet TKD1 were associated with poorer a OS and an increased RR in comparison to patients with insertions sites outside of this region.

1.8.5 *FLT3*-TKD mutations

FLT3-TKD mutations occur in 5-10% of patients with AML (Frohling *et al.*, 2007;Mead *et al.*, 2007). Numerous *FLT3* point mutations have been described primarily occurring in the ALD in exon 20, called *FLT3*-TKD mutations (Table 1.8). The most frequent *FLT3*-TKD, accounting for 50% of *FLT3*-TKD mutations, is the substitution of aspartic acid 835 for a tyrosine residue (D835Y) (Mead *et al.*, 2007;Bacher *et al.*, 2008). Residue D835 can also be deleted or substituted for numerous amino acids, as listed in Table 1.8. Mutations in the ALD do not just reside at D835, other residues have also been found to be mutated including G831, R834, I836, D839, N841 and Y842 (Kindler *et al.*, 2005;Mead *et al.*, 2007;Frohling *et al.*, 2007;Smith *et al.*, 2013). Rare mutations (1% of adult patients with AML) have also been found within the ECD, JMD and KID (Table 1.8) (Reindl *et al.*, 2006;Frohling *et al.*, 2007;Smith *et al.*, 2012). The crystal structure of FLT3 suggests that residues D835 and Y842 are critical for stabilising the inactive conformation of the ALD (Smith *et al.*, 2012). Therefore, mutations at residues D835, Y842 or in close proximity to these residues are proposed to destabilise the inactive conformation, shifting the equilibrium to the active state and resulting in the ALD being maintained in the open (active) conformation.

In vitro studies assessing the functionality of *FLT3*-TKD mutations have demonstrated autophosphorylation of the receptor, activation of downstream signalling pathways (RAS/MAPK, STAT5 and PI3K/mTOR) and induction of ligand-independent growth in factor-dependent cell lines (Reindl *et al.*, 2006;Rocnik *et al.*, 2006;Frohling *et al.*, 2007;Smith *et al.*, 2012). Mice receiving primary BM cells retrovirally transduced with *FLT3*-TKD mutations generated a lymphoid-proliferative disease, whereas mice receiving BM cells transduced with *FLT3*-ITD mutations develop a MPD (Grundler *et al.*, 2005). This stark contrast in disease progression mediated by the two different mutations showed that different signalling pathways were involved. In support of this, *FLT3*-ITDs but not *FLT3*-TKD mutations have been shown to activate downstream STAT5 proteins (CIS and PIM-2), and microarray analysis of cells from patients with FLT3-ITD+ AML or FLT3-TKD+ AML showed differential gene expression profiles (Choudhary *et al.*, 2005;Neben *et al.*, 2005). *In vitro* studies have also shown that primary AML cells expressing *FLT3*-ITD mutations were significantly more sensitive to the FLT3 inhibitor lestaurtinib than cells expressing *FLT3*-TKD mutations (Mead *et al.*, 2008). The coincidence of a *FLT3*-ITD and a *FLT3*-TKD mutation occurs infrequently implying that in the absence of a selection pressure, such as the FLT3 inhibitor AC220, the presence of a double mutation may have no benefit. This suggests that *FLT3*-ITDs and TKDs have different mutational mechanisms.

Exon	Mutation	Domain
5	T167A	ECD
5	V194M	ECD
9	Y364H	ECD
11	S451F	ECD
14	Y572C	JMD
14	V579A	JMD
14	V592A	JMD
14	V592G	JMD
14	F594L	JMD
14	E608K	JMD
16	N676K	TKD1
17	F691L	TKD1
18	M737I	KID
20	G831E	ALD
20	R834Q	ALD
20	D835Y	ALD
20	D835E	ALD
20	D835H	ALD
20	D835N	ALD
20	D835A	ALD
20	D835S	ALD
20	D835N	ALD
20	D835V	ALD
20	D835F	ALD
20	Δ835	ALD
20	ΔD835delinsGPGP	ALD
20	ΔD835_I836delinsVIPT	ALD
20	Δ836	ALD
20	D839G	ALD
20	N841I	ALD
20	N841K	ALD
20	N841Y	ALD
20	Y842C	ALD

Table 1.8 *FLT3* mutations currently reported in AML.

1.8.6 Clinical impact of *FLT3*-TKD mutations

As observed with FLT3-ITD+ AML, the presence of a *FLT*3-TKD mutation is associated with elevated PB and BM blast counts and a normal karyotype (Frohling *et al.*, 2002;Bacher *et al.*, 2008). Several groups have reported that the presence of a *FLT3*-TKD mutation correlates with an inferior OS and DFS (Thiede *et al.*, 2002;Moreno *et al.*, 2003;Yanada *et al.*, 2005;Whitman *et al.*, 2008). In contrast, *FLT3*-TKD mutations with a high mutant level median >25% have been reported to confer a more favourable OS and CIR in comparison to *FLT3*-WT (Mead *et al.*, 2007). Bacher *et al* (2008) reported that *FLT3*-TKD mutations had no significant impact on EFS or OS. However, stratification of *FLT3*-TKD mutant positive patients based on *NPM1, CEBPA* and *MLL-PTD* mutation status revealed that a combination of a *FLT3*-TKD mutation with either an *NPM1* or a *CEBPA* mutation further improved OS and EFS in comparison to just *NPM1* and *CEBPA* mutated cases, while co expression of a *FLT3*-TKD mutation and *MLL-PTD* further reduced the poor prognosis already associated with *MLL-PTD* (Bacher *et al.*, 2008). The differential prognostic impact observed between these reports is likely to have arisen due to sampling variability, small patient cohorts and differences in treatment regimes. Therefore, the impact of *FLT3*-TKD mutations on prognosis remains unclear.

1.8.7 Clinical impact of FLT3-WT over expression

Of interest, FLT3 is phosphorylated in approximately 60% of patients with AML, even in the absence of an activating mutation (Zheng *et al.*, 2004). Other RTKs have been shown to dimerise in the absence of ligand-receptor interactions (Lemmon & Schlessinger, 2010). Therefore, as FLT3 is highly expressed in patients with AML, it has been suggested that this may contribute to spontaneous phosphorylation and activation of downstream signalling (Ozeki *et al.*, 2004). Alternatively, FLT3 has been shown to be phosphorylated, in both AML cell lines and primary AML cells, by autocrine secretion of FL (Zheng *et al.*, 2004). This suggests that although mutations often occur in *FLT3* in AML, the WT receptor can also be activated, and that inhibitors that target the mutant and WT receptor may provide some clinical benefit.

1.8.8 FLT3 inhibitors

Inhibitors of FLT3 have been developed and examined extensively in pre-clinical models, with some now being tested within clinical trials. Some of the FLT3 inhibitors currently being assessed in clinical trials are reviewed in Table 1.9.

Inhibitor	Trial	No. *FLT3* WT/TKD/ITD patients	Median Age of patients with AML	Disease status	Clinical benefit	CR	Reference
Tandutinib	Phase I	32/0/8	70.5 (22-90)	Rf + R + U	2/5 evaluable *FLT3*-ITD patients had a reduction in PB/BM blasts. No significant anti-leukaemic effect observed in *FLT3*-WT patients.	0	(DeAngelo *et al.*, 2006)
Tandutinib	Phase II	0/0/23	Not available	Rf + R	15 patients evaluable: 2 had stable disease ≥50 days and 6 had a reduction in PB and BM blasts (1-3 month duration)	0	(De Angelo *et al.*, 2004)
Sorafenib	Phase I	3/1/7 (1x TKD + ITD)	34 (21-59)	Rf + R	3/7 patients with *FLT3*-ITD achieved a CR compared to 1/3 for patients with *FLT3*-WT	40%	(Ravandi *et al.*, 2010)
Sorafenib	Phase II	36/2/13	53 (18-65)	Rf + R	38 patients achieved a CR: 12/13 with a *FLT3*-ITD, 2/2 with a *FLT3*-TKD and 24/36 with *FLT3*-WT. Probability of survival at 12 months was 74%. *FLT3*-ITD patients achieving CR had potent inhibition of *FLT3*-ITD	75%	(Ravandi *et al.*, 2010)
Sunitinib	Phase I	24/2/3	67 (19-82)	Rf + R	≥200mg of sunitinib inhibited FLT3 phosphorylation in 50% of patients expressing the WT receptor and 100% in patients with mutant FLT3	0	(O'Farrell *et al.*, 2003)
Sunitinib	Phase I	10/2/2	72 (54-80)	Rf + R + U	1 *FLT3*-TKD patient achieved a morphological remission, 1 *FLT3*-TKD and 2 *FLT3*-ITD patients achieved PRs. 2/7 patients without a *FLT3* mutation also achieved a PR. All responses were of short duration (4-16 weeks).	0	(Fiedler *et al.*, 2005)
Lestaurtinib	Phase I/II	0/1/16	61 (18-74)	Rf + R	5 patients displayed a significant reduction in PB/BM blast counts (>50%), with one patient sustaining a CR with a decrease in BM blasts to <5%. Clinical responses corresponded to sustained inhibition of p-FLT3 and toxicities were mild	6%	(Smith *et al.*, 2004;Levis *et al.*, 2006)
Lestaurtinib	Phase II	24/3/2	73 (67-82)	U	3/5 *FLT3* mutant patients achieved haematologic responses as demonstrated by a reduction in PB blasts. 5/22 patients with *FLT3*-WT also showed a decrease in BM blasts. The 8 patients with clinical responses corresponded to sustained inhibition of p-FLT3.	0	(Knapper *et al.*, 2006)

Rf = refractory AML, R= relapsed AML, U= unfit for standard chemotherapy, PR= partial remission, CRi=CR with incomplete haematologic recovery, CRc= CR+ CRp (CR with incomplete platelet recovery) + CRi.

Table 1.9 Clinical trials using FLT3 inhibitors in patients with AML.

Lestaurtinib	Phase II	Control arm: 0/8/97 (6x ITD + TKD) Lestaurtinib arm: 0/9/101 (2x ITD + TKD)	Control arm: 54 (21-79) Lestaurtinib arm:59 (20-81)	First relapse after first remission	There were no differences between patients treated with chemotherapy alone or in combination with lestaurtinib, either in OS or response rates. FLT3 blockade did correlate with those patients achieving CR	Control arm 21% Lestaurtinib arm 26% (P =0.35)	(Levis *et al.*, 2011;Levis *et al.*, 2012)
Midostaurin	Phase II	0/2/18	62 (29-78)	Rf + R	14 patients achieved a 50% reduction in PB counts while 6 patients saw a 50% reduced in BM blast count (2 to <5%)	0	(Stone *et al.*, 2005)
Midostaurin	Phase Ib	27/4/9	50 (18-60)	Rf + R	Midostaurin and standard induction chemotherapy showed that patients with mutant *FLT3* and *FLT3*-WT had equivalent 2 year OS rates of 62% and 59% respectively	74% *FLT3*-WT 92% *FLT3*-mutant	(Stone *et al.*, 2009)
Midostaurin	Phase IIb	60/9/26	≥18	Rf + R + U	Only one patient (1%) experienced a PR	0	(Fischer *et al.*, 2010)
Ponatinib	Phase I	0/0/7	49 (30-72)	Rf + R	2/7 patients with a *FLT3*-ITD achieved a CRi	0	(Smith *et al.*, 2013)
KW-2449	Phase I	32/0/5	Not available	Rf + R	5 patients with a *FLT3*-ITD did have a >50% reduction in PB blasts.	0	(Pratz *et al.*, 2009)
AC220	Phase I	47/0/18	60 (23-86)	Rf + R + U	9 *FLT3*-ITD patients responded (1 CR, 3CRi and 2 PR). 9 *FLT3*-WT patients responded (1 CRi, 2 CRp, 6 PR).The median duration of response was 14 weeks (4-64+)	12%	(Cortes *et al.*, 2009)
AC220	Phase II	38/-/99 (TKD status not given)	ITD+50 (19-77) ITD-55 (30-73)	Rf + R	34% of *FLT3*-ITD- patients achieved a CRc with a median duration of 5 weeks. 44% of *FLT3*-ITD+ patients showed a CRc with a median duration of 11.3 weeks.	3% *FLT3*-WT 4% *FLT3*-ITD+	(Levis *et al.*, 2012)
AC220	Phase II	41/-/92 (TKD status not given)	ITD- 69 (60-78) ITD+ 70 (54-85)	Rf + R	44% of *FLT3*-ITD- patients achieved CRc with a median duration of 22.1 weeks. 39% of *FLT3*-ITD+ patients showed a CRc with a median duration of 12.7 weeks.	2% *FLT3*-ITD- 0 *FLT3*-ITD+	(Cortes *et al.*, 2012)

Table 1.9 (continued)

The efficacy of FLT3 inhibitors in patients with AML has been disappointing (Table 1.9). This could be due to the kinetics of the individual compounds, such as the potency of the inhibitors to bind and maintain inhibition of FLT3, the biological half-life of the compounds and the dosing frequency. The disease features of AML may also impact on the response to FLT3 inhibitors, such as the allelic burden, the type and the site of mutation. There is some evidence to suggest that FLT3 may not be the driver mutation in all patients with AML. For example, relapse samples can lose their *FLT3* mutation (Kottaridis *et al.*, 2002). This suggests the *FLT3* mutation may occur in a sub-clone population of cells. In contrast there is emerging evidence that *FLT3*-ITD mutations can be the driving genetic lesion (Ding *et al.*, 2012). Patients with FLT3-ITD+ AML treated with AC220 have been shown to acquire secondary mutations within the TKD that confer resistance to AC220 (Smith *et al.*, 2013). Secondary mutations have primarily been detected in the activation loop at residue D835 (D835Y/V/F) and the 'gate keeper' residue F691 (F691L). The 'gate keeper' residue is defined as a large hydrophobic residue found in the ATP binding cleft of protein kinases. *In vitro* investigation of these secondary mutations has demonstrated cross resistance to sorafenib. This highlights that in these patients the leukaemic cells are dependent on FLT3 signalling, and therefore targeting the receptor is a valid therapeutic target.

1.9 AML and PI3K/ AKT, mTOR and MEK signalling

The PI3K/AKT, mTOR and MEK signalling pathway are involved in a host of key regulatory roles including cell cycle progression, differentiation, survival and apoptosis. PI3K, AKT, mTOR and MEK have all been shown to be constitutively active in primary AML cells (Grandage *et al.*, 2005). The function of these proteins in normal haematopoiesis is discussed below in conjunction with the proposed mechanism of dysregulation in AML, including current methods for inhibiting these activated pathways.

1.9.1 PI3K /AKT

PI3K exists in three classes, I-III, each with its own substrate specificity. The class IA PI3K is activated downstream of growth factors and is composed of a catalytic subunit of either p110α, p110β or p110δ in conjunction with one of the regulatory subunits p50, p55 or p85 (Park *et al.*, 2010). The *PIK3CA* gene, which encodes the p110α subunit, is frequently mutated in a range of cancers including breast, liver, gastric, brain and colon cancers (Karakas *et al.*, 2006). Class I PI3Ks function by phosphorylating phosphatidylinositol bisphosphate (PIP2), which produces phosphatidylinositol trisphosphate (PIP3) (Figure 1.6). PIP3 recruits AKT and phosphoinositide-dependent protein kinase-1 and 2 (PDK1/PDK2) to the plasma membrane. AKT is phosphorylated by PDK1 within the ALD at residue T308, while PDK2 (otherwise known as mTORC2) phosphorylates residue S473 at the C-terminus; both are required to fully activate AKT (Park *et al.*, 2010). AKT regulates a host of proteins such as Bcl-2-associated death promoter (BAD), IκB kinase α/β (IKKα/β), E3 ubiquitin-protein ligase (MDM2), forkhead family of transcription factors (FOXO), cyclin D, mTORC1, endothelial nitric oxide (eNOS), Apoptosis signal-regulating kinase 1 (ASK1) and the cell cycle regulators p21/p27. PI3K activation is negatively regulated by phosphatases and a key protein is Phosphatase and tensin homolog (PTEN), which dephosphorylates PIP3 to PIP2 and antagonises the PI3K/AKT/mTOR pathway (Figure 1.6) (Martelli *et al.*, 2010).

1.9.2 mTOR

Mammalian target of Rapamycin (mTOR) is a member of the PI3K-related kinases. It occurs in two distinct complexes, mTOR Complex 1 (mTORC1) and mTOR Complex 2 (mTORC2). mTORC1 is comprised of mTOR, DEP domain-containing mTOR-interacting protein (DEPTOR), regulatory-associated protein of mTOR (RAPTOR), PRAS40 and the mTOR subunit LST8 (Zoncu *et al.*, 2011). This complex, as illustrated in Figure 1.6, is regulated by upstream proteins including AKT, the tumour suppressor tuberous sclerosis proteins 1 and 2 (TSC1/TSC2), and the GTP-binding protein RHEB complex. AKT functions by

phosphorylating TSC2, which disrupts the binding of RHEB to the TSC1/TSC2 complex (Long *et al.*, 2005). RHEB-GTP is then free to directly activate the mTORC1 complex. Once activated the mTORC1 complex functions to activate p70 S6K kinase and eukaryotic initiation factor 4E binding protein 1 (4E-BP1). Activation of p70 S6K leads to phosphorylation of 40S ribosomal protein S6, which drives translation of specific mRNAs (Martelli *et al.*, 2009). Phosphorylation of 4E-BP1 by mTORC1 causes it to dissociate from the eukaryotic initiation factor 4E (elF4E), allowing it to recruit eIF4G and form part of the translation initiation complex (Martelli *et al.*, 2009). The mTORC1 complex is essential for controlling biosynthesis of cell cycle progression proteins (cyclin D1, c-Myc, CDK2 and p27) and cell survival proteins (Mcl-1 and Bcl-x).

The mTORC2 complex is comprised of mTOR, DEPTOR, rapamycin-insensitive companion of mTOR (RICTOR), LST8, mammalian stress-activated protein kinase-interaction protein 1 (mSIN1), and protein observed with Rictor-1 (PROTOR). The mTORC2 complex phosphorylates AKT at residue S473, and activates the kinases glucocorticoid regulated kinase (SGK) and protein kinase C (PKC) (Figure 1.6). The full mechanism of mTORC2 activation is still unclear, however the mTORC2 complex does regulate cell survival, cytoskeleton organisation and cell cycle progression.

1.9.3 MEK

The mitogen-activated protein kinase (MAPK) signal cascade is pivotal for cell proliferation, differentiation and survival. The MAPK family are serine/threonine kinases that fall into 3 broad groups: extracellular signal-regulated kinases (ERKs), c-Jun NH2–terminal Kinases (JNK), and p38 members. ERKs are activated by the presence of growth factors/cytokines, while the JNK and p38 members are stimulated in response to radiation, oxidative stress, DNA damage and cytokines (Molina & Adjei, 2006). The MAPK pathway becomes activated when a RTK becomes stimulated. Two extensively characterised RTKs that activate MAPK are the epidermal growth factor receptor (EGFR) and the platelet-derived growth factor receptor (PDGFR). When ligand binds to EGFR, it activates the kinase domain allowing tyrosine autophosphorylation. This allows adaptor proteins such as growth factor receptor-bound protein 2 (Grb2) to bind to the receptor and recruit factors including guanine nucleotide exchange factors (GEFs) that mediate exchange of GDP for GTP, such as Son of sevenless (SOS), cell division cycle 25 phosphatase (CDC25) and Shc (Schlessinger, 2000). The GEFs, once at the plasma membrane, activate RAS by exchanging GDP for GTP. RAS-GTP then stimulates its effector molecule the serine/threonine kinase RAF which in turn phosphorylates MAPK (MEK) and activates ERK1/2 (p42/p44) (Figure 1.6) (Molina &

Adjei, 2006). ERK1/2 regulates the transcription of cell cycle progression proteins including Myc, Fos and ELK1.

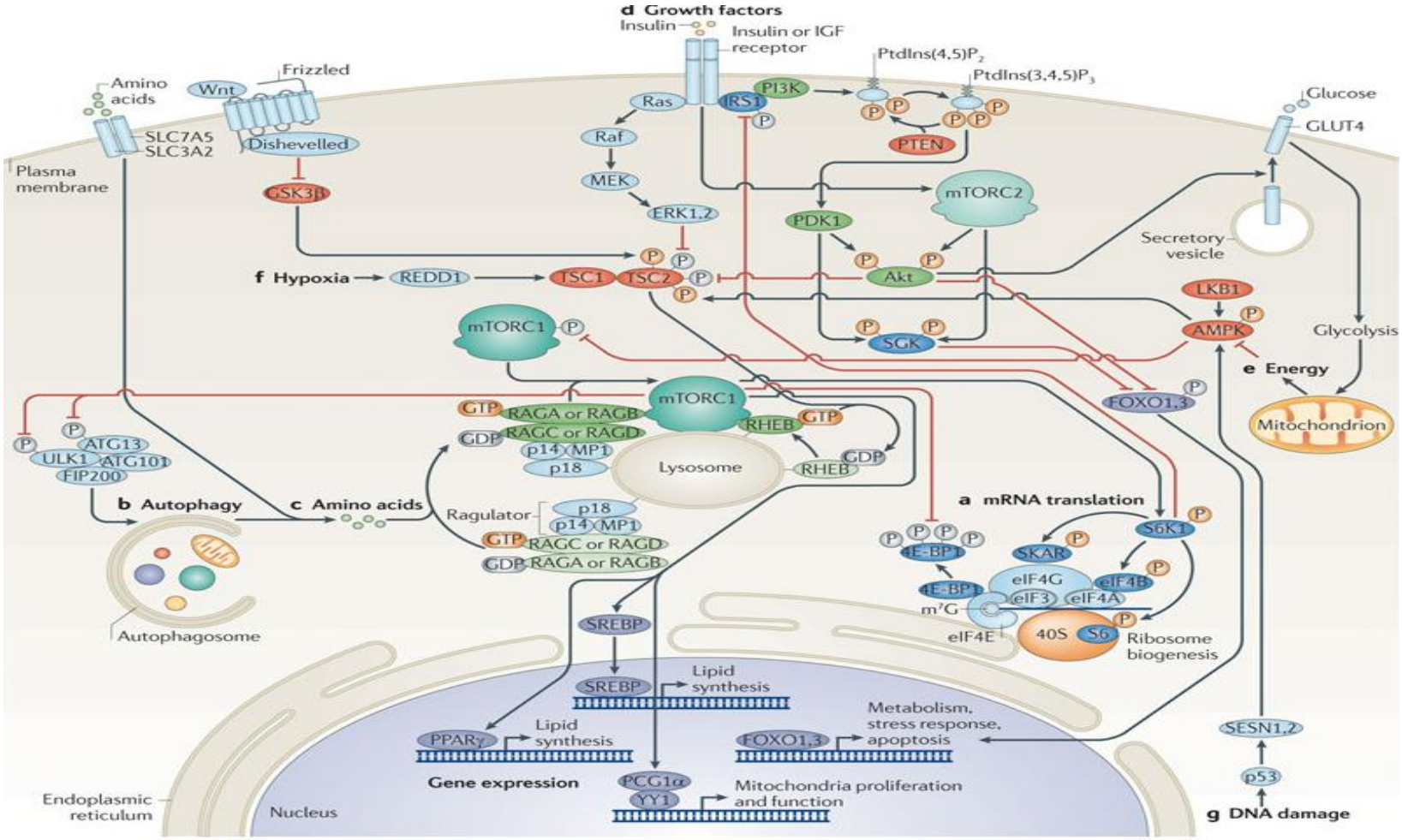

Figure 1.6 The protein signalling networks of PI3K/AKT, mTOR and MEK and their respective downstream targets. Taken from Zoncu *et al* (2011). Permission to reproduce this has been granted by Dr. Roberto Zoncu.

1.9.4 PI3K/AKT/ mTOR and MEK activation in AML

Constitutive activation of the PI3K/AKT, mTOR and MEK signalling pathways has been reported to be present in 50-80%, >90% and 75-80% of AML blast cells respectively (Xu *et al.*, 2003;Grandage *et al.*, 2005;Brandts *et al.*, 2005;Ricciardi *et al.*, 2005). Constitutive PI3K activation is associated with AKT phosphorylation at residues T308 and S473 and a significant increase in proliferation of primary leukaemic cells (Kubota *et al.*, 2004). The presence of phosphorylated AKT has been identified as a poor prognostic marker in AML, corresponding to a shorter DFS and OS (Min *et al.*, 2003;Kornblau *et al.*, 2006). The PI3K/AKT pathway can control expression of the multidrug resistance protein 1 (MRP1), which can exclude chemotherapeutic agents from leukaemic cells (Tazzari *et al.*, 2007). Therefore, constitutive PI3K/AKT activity is proposed to drive expression of MRP1 leading to chemoresistance. This could explain the poor prognosis of patients with AML associated with activated PI3K/AKT. However, Tamburini *et al* (2007) found that patients with activated PI3K/AKT had a more favourable outcome, with a lower RR and better OS. A more favourable outcome may be the result of constitutive PI3K activity driving the leukaemic cells into S phase of the cell cycle, making them more sensitive to DNA damaging chemotherapeutics. The discrepancies between these studies could arise from different culture conditions used to maintain primary AML cells, which could affect the level of PI3K/AKT activation. The prognostic implication of PI3K/AKT activation in AML remains unclear. The impact of mTOR dysregulation on prognosis in AML has not currently been assessed, however the presence of p-ERK has been associated with an independent poor prognosis (Kornblau *et al.*, 2006).

1.9.5 Mechanisms for PI3K/AKT/mTOR and MEK activation in AML

The precise mechanisms of constitutive PI3K/AKT/mTOR and MEK activation in AML are unclear, but mutations in RTKs such as c-KIT and FLT3 or in K/N-RAS have all been shown to activate proteins within the PI3K/AKT/mTOR and MEK networks (Birkenkamp *et al.*, 2004;Pedersen *et al.*, 2009;Sun *et al.*, 2009;Muranyi *et al.*, 2009;Chen *et al.*, 2010). Although RTK mutations can activate the PI3K/AKT/mTOR and MAPK signalling pathways, there is not always an association between a RTK mutation and constitutive PI3K/AKT/mTOR and MEK activation when examining primary AML cells *in vitro* (Iida et al., 1999, Martelli et al 2009). Other mechanisms of PI3K activation include over-expression of the PI3Kδ/β subunits, signalling through the insulin-like growth factor receptor (IGF-1R), autocrine/paracrine secretion of VEGF, interactions between β1 integrins (expressed on blast cells) and fibronectin (expressed on BM stromal cells) leading to up-regulation of integrin-linked kinase 1 (ILK1), and high very late antigen (VLA)-4 expression (Sujobert *et al.*,

2005;Billottet *et al.*, 2006;Martelli *et al.*, 2010). No activating mutations have been identified in the PI3K p110α or δ subunits or in the AKT1 (PH domain) in AML. *PTEN*, the negative regulator of PI3K, which is commonly deleted and mutated in acute lymphoblastic leukaemia (ALL), is infrequently deleted/mutated in AML (Liu *et al.*, 2000).

The activation of mTORC1 in AML blasts has been shown to be independent of PI3K/AKT and can be constitutively activated through the Src kinase Lyn, non-receptor kinase SYK and the ERK/MAPK pathway (Park *et al.*, 2010;Carnevale *et al.*, 2013). ERK activation can be mediated by genetic mutations of K/N-RAS, other cytoplasmic kinases or inhibition of specific phosphatases (Platanias, 2003). However, the presence of N-RAS mutations does not always correspond to ERK/MAPK activation in primary AML cells (Iida *et al.*, 1999). In AML there are currently no known mutations in *MAPK* genes or *mTOR*, and neither chromosomal location is currently associated with recurrent genomic gains or losses. Therefore, numerous factors appear to contribute to the activation of the PI3K/AKT/mTOR and MEK pathways. This suggests that several intrinsic and extrinsic pathways may contribute to the activation of these target proteins or there may be other mutated or dysregulated G-proteins/signalling molecules in AML that are currently unknown.

1.9.6 The use of PI3K/mTOR/AKT and MEK inhibitors in AML

As PI3K/mTOR/AKT and MEK activation is found in a high proportion of patients with AML, numerous inhibitors have been developed to target these pathways listed in Table 1.10.

PI3K Inhibitors

The first characterised PI3K inhibitors were Wortmannin and LY294002, which are cell-permeable and have a low molecular weight. Wortmannin is a potent irreversible inhibitor of class I, II and III PI3Ks (IC50=~5nM), binding to the p110 catalytic subunit (Vanhaesebroeck *et al.*, 2001). LY294002 is a synthetic flavonoid-based compound that competitively binds to the ATP binding site of the PI3K p110 catalytic subunit. LY294002 inhibits class I, II and III PI3Ks at an IC50 of ~1-20μM (Martelli *et al.*, 2009). Although Wortmannin and LY294002 have been used in *in vitro* models of AML, their clinical use has been limited due to high toxicities and poor stability in aqueous solutions.

One derivative of Wortmannin is pegylated-17-hydroxywortmannin (PWT-458). PWT-458 has improved drug stability and water solubility and has demonstrated anti-tumour activity in xenograft models of glioma, renal cell carcinoma and non-small cell lung cancer in nude

mice (Yu *et al.*, 2005). Other PI3K inhibitors have been examined in solid tumours, including an analog of Wortmannin, PX-866, which inhibits PI3Kα, γ, and δ (IC50 = 5.5, 9.0, and 2.7 nM, respectively), and inhibited tumour growth in xenograft tumour models (Garcia-Echeverria, 2009). An optimised water-soluble pan-PI3K/mTOR LY294002 derivative, SF1126, demonstrated inhibition of all PI3K classes (IC50= 0.5–5.7μM) and has been examined in a phase I clinical trial in solid tumours (trial NCT00907205l) (Martelli *et al.*, 2009). However these inhibitors have not currently been evaluated in AML.

IC87114, a selective inhibitor of the PI3K p110δ isoform, led to a reduction in proliferation, down-regulation of p-AKT/p-FOXO3a and synergistic cell killing of primary AML cells when combined with etoposide (Billottet *et al.*, 2006). A dose escalation phase I clinical trial of IC87114 (CAL-101) in relapsed and refractory haematological malignancies including AML has been completed, but the results are yet to be published (trial NCT00710528). Recently, more potent PI3K inhibitors have been developed including ZSTK-474 and BEZ-235. ZSTK-474 has shown potent inhibition of all class I isoforms of PI3K (~5-50nM) (Kong & Yamori, 2007). *In vitro* testing showed a reduction in proliferation in ALL cell lines and it is currently entering a phase I clinical trial in advanced solid malignancies to evaluate its safety profile (Levy *et al.*, 2009). Although PI3K inhibitors can effectively decrease proliferation in *in vitro* AML models, they have not demonstrated effective cell killing.

AKT inhibitors

Several different AKT inhibitors have been designed and examined in AML. Perifosine, an orally available alkyl-phospholipid inhibitor, functions by preventing AKT localisation to the plasma membrane. Perifosine inhibits phosphorylation of AKT and ERK and induces apoptosis in primary AML cells and AML cell lines (Papa *et al.*, 2008). CD34+ AML cells with constitutive AKT activity (AKT+) treated with perifosine reduced the clonogenicity of the cells while having a minimal impact on normal CD34+ cells. Perifosine has entered a phase I clinical trial in combination with UCN-01 (a PDK1 inhibitor) (trial NCT00301938) and a phase II trial in refractory and relapsed leukaemia (trial NCT00391560). The results of these trials have yet to be released. Triciribine, a synthetic reversible tricyclic nucleoside AKT1/2/3 inhibitor, is also being used in a phase I trial in adult patients with advanced haematological malignancies (trial NCT00642031).

Akti-1/2, a reversible AKT1/AKT2 isoform-specific allosteric inhibitor, has been shown to reduce proliferation, decrease clonogenicity and induced apoptosis in primary AML cells

with high risk cytogenetics (Gallay *et al.*, 2009). The limitation of this inhibitor is that the isoform(s) expressed in AML blasts is unknown. AZD5363, a orally available ATP competitive inhibitor of AKT1/2/3, has demonstrated potent anti-proliferative (<3μM) effects in several haematological cell lines (Davies *et al.*, 2012). AZD5363 is currently entering a phase I clinical trial in advanced solid tumours (trial NCT01226316).

mTOR inhibitors

The mTOR pathway is activated in almost all AML cells and has become an attractive pathway to target with inhibitory molecules. Rapamycin and its derivates, including temsirolimus, everolimus and deforolimus, also referred to as rapalogs, do not bind directly to mTORC1 but bind to the immunophilin FK506 binding protein 12 (FKBP12). The rapamycin/FKBP12 complex can then bind to mTORC1 and inhibit downstream targets. Treatment of primary AML cells with rapamycin has demonstrated a potent reduction in mTOR target proteins, i.e. p-4EB-P1 and p-p70 S6K but only slightly decreased cell survival (Xu *et al.*, 2003). In AML cell lines rapamycin has been shown to block transition from G_0-G_1 of the cell cycle and impair the clonogenicity of primary AML cells while normal CD34+ HSCs were unaffected (Recher *et al.*, 2005). Rapamycin has also been used in a preclinical study as a single agent, which showed a partial response in four of nine patients with refractory or relapsed AML (trial NCT00780104) (Recher *et al.*, 2005). Everolimus has also been assessed in a phase I clinical trial in relapsed or refractory haematological diseases, including AML, and showed no-dose limiting toxicities, however there was no complete/partial responses in patients with AML (trial NCT00544999) (Yee *et al.*, 2006). Other approaches have combined rapamycin with other cytotoxic agents. A combination of rapamycin and etoposide has demonstrated an enhanced cytotoxicity in primary AML cells and reduced the potential of these cells to engraft in NOD/SCID mice, suggesting specific killing of the LSC compartment (Recher *et al.*, 2005). Various phase II clinical trials are currently ongoing combining rapamycin, everolimus or temsirolimus with different chemotherapeutic drugs such as cytarabine and daunorubicin (Table 1.10). In addition, the multi-drug target kinase inhibitors PKC412 and nilotinib are currently being assessed in conjunction with everolimus (trials NCT00819546 and NCT00762632).

The modest efficacy of rapamycins in the clinic may be due to insufficient blockade of mTORC2. As a consequence, this has led to the development of second-generation ATP competitive inhibitors targeting mTORC1 and mTORC2. Targeting both mTORC1 and mTORC2 is proposed to reduce the positive feedback mechanism, described below, on PI3K/AKT and ERK/MAPK. Ku-0063794 and WYE-354 are two novel ATP competitive

inhibitors which target mTORC1 and mTORC2 directly. Ku-0063794 has demonstrated potent inhibition of mTORC1 and mTORC2 *in vitro* and *in vivo*, showing more efficient inhibition of p-4E-BP1 than rapalogs (Garcia-Echeverria, 2009). WYE-354 has shown potent down-regulation of mTORC1 substrates p-4E-BP1 and p-S6K (T389) and the mTORC2 substrate p-AKT S473 in different cancer cell lines (Yu *et al.*, 2009). WYE-354 also been shown to inhibit p-AKT S473 in nude mice bearing PC3MM2 tumours (prostate tumours). The use of WYE-354 has not yet been assessed in AML models. Current data suggests that second-generation inhibitors may have more clinical efficacy as they appear to more potently block protein translation and mTORC2 substrates in comparison to rapamycin and its rapalogs.

1.9.7 Dual PI3K/mTOR inhibition

The poor response to PI3K or mTOR inhibitors alone may be the result of complex compensatory feedback mechanisms. In AML cell lines everolimus can promote PI3K/AKT activation which up-regulates an autocrine IGF-1/IGF1-R activating loop (Tamburini *et al.*, 2008). One group has reported that inhibition of mTORC1 can lead to activation of ERK/MAPK signalling (Carracedo *et al.*, 2008). mTORC1 can also be activated independently of PI3K. This therefore provides a rationale for blocking both PI3K/AKT and mTOR simultaneously to circumvent some of these compensatory feedback mechanisms. In support of this, combined inhibition of PI3K and mTOR with IC87114 and everolimus respectively has shown an additive reduction in proliferation in AML cells (Tamburini *et al.*, 2008). As a result, dual PI3K/mTOR inhibitors have been developed. PI-103, a PI3K/mTOR inhibitor, has demonstrated pro-apoptotic effects in primary AML cells, including those cells in the LSC compartment ($CD34^{+}$, $CD38^{low/neg}$,$CD123^{+}$) (Park *et al.*, 2008). Unfortunately, PI-103 has not entered clinical trials due to its rapid metabolism *in vivo*. Novartis have subsequently developed an ATP competitive PI3K/mTOR inhibitor BEZ-235, which has shown inhibition of mTORC1, mTORC2 and PI3K in AML cell lines and primary AML cells (Chapuis *et al.*, 2010). BEZ-235 can induce a significant level of apoptosis in primary AML progenitors while showing a minimal effect on normal CD34+ haematopoietic progenitors (Chapuis *et al.*, 2010). The striking level of cell killing seen with BEZ-235 is thought to be attributable to potent inhibition of p-4E-BP1 resulting in a block in protein translation in conjunction with PI3K blockade. BEZ-235 has already been used in a dose escalation clinical trial in solid tumours (trial NCT00620594) and is currently being used in a phase I dose finding study in patients with relapsed or refractory AML (trial NCT01756118).

1.9.8 MEK inhibitors

A number of different inhibitory molecules have been used to target the RAF/MEK/ERK pathway including U0126, PD184352 (both non competitive ATP inhibitors of MEK1/2) and PD98059 (a non-ATP competitive inhibitor of MEK1). All of these inhibitors have demonstrated potent inhibition of proliferation and varying degrees of apoptosis in AML cell lines and primary AML cells (Kerr *et al.*, 2003;Lunghi *et al.*, 2003;Milella *et al.*, 2007;Zhang *et al.*, 2008). U0126 and PD98059 have not entered clinical trials due to poor pharmacokinetics and solubility. A phase II clinical trial of PD184352, otherwise known as CI-1040, in advanced non-small-cell lung, breast, colon and pancreatic tumours has been completed but showed no complete or partial responses (trial NCT00034827) (Rinehart *et al.*, 2004).

Subsequently, second-generation MEK inhibitors are now being developed. AZD6244, an allosteric MEK1/2 inhibitor, has displayed cytostatic effects in AML cell lines but failed to induce apoptosis (Zhang *et al.*, 2010). However, blocking MEK and MDM2 with AZD6244 and Nutlin3a respectively could induce significant cell killing in AML cell lines (Zhang *et al.*, 2010). AZD6244 is currently in several clinical trials for solid tumours. PD-0325901 is a non-ATP competitive MEK1/2 inhibitor which is more potent than its derivative PD184352. PD-0325901 has shown potent inhibition of cell growth in AML cell lines and primary AML cells (Ricciardi *et al.*, 2012). Combined PD0325901 and temsirolimus treatment resulted in synergistic growth inhibition in OCI-AML3 and MOLM-13 AML cell lines (Ricciardi *et al.*, 2012). PD0325901 has entered phase I and II clinical trials in solid tumours, however patients suffered more severe side effects than with PD184352 and as a result its use has been discontinued (trials NCT00174369, NCT00147550). The use of MEK inhibitors as single agents in AML models has been disappointing. This suggests that MEK blockade is not sufficient alone to eradicate leukaemic cells.

Inhibitor name	Target	Method of binding	Clinical status
Akti-1/2	AKT1/AKT2 isoforms	Allosteric	Preclinical
AZD5363	AKT1/2/3	ATP competitive	NCT01226316
AZD6244	MEK1/2	Allosteric	Numerous clinical trials
BEZ-235	Pan class I P13K and mTOR	ATP competitive	NCT00620594, NCT01756118
Everolimus	Immunophilin, FK506 binding protein 12	Allosteric	NCT00544999, NCT00544999, NCT00636922, NCT00819546, NCT00762632
IC87114	PI3K P110 δ subunit	ATP competitive	NCT00710528
Ku-0063794	mTORC1 and mTORC2	ATP competitive	Preclinical
LY294002	PI3K p110 catalytic subunit	ATP competitive	Preclinical
PD-0325901	MEK1/2	Non-ATP competitive	NCT00174369, NCT00147550
PD184352	MEK1/2	Non-ATP competitive	NCT00034827
PD98059	MEK1 inhibitor	Non-ATP competitive	Preclinical
Perifosine	PH domain of AKT	Non-ATP competitive	NCT00301938, NCT00391560
PI-103	Class I PI3K and mTOR	ATP competitive	Preclinical
PWT-458	PI3K p110 catalytic subunit	Not available	Preclinical
PX866	PI3Kα, γ, and δ	Irreversible	Preclinical
Rapamycin	Immunophilin, FK506 binding protein 12	Allosteric	NCT00780104, NCT00634244
SF1126	Pan PI3K/mTOR	Not available	NCT009072051
Sorafenib	RAF/ VEGFR1/2 /PDGFR and c-KIT kinases	ATP competitive and Non-ATP competitive	Numerous clinical trials
Temsirolimus	Immunophilin, FK506 binding protein 12	Allosteric	NCT00084916
Triciribine	AKT1/2/3	Non-ATP/substrate competitive	NCT00642031
U0126	MEK1/2	Non-ATP competitive	Preclinical
Wortmannin	PI3K p110 catalytic subunit	Irreversible	Preclinical
WYE-354	mTORC1 and mTORC2	ATP competitive	Preclinical
ZSTK-474	Pan-class I PI3K inhibitor	ATP competitive	NCT01280487

Table 1.10 PI3K, AKT, mTOR, PI3K+mTOR and MEK inhibitors currently available illustrating their targets, the mechanisms of binding to their targets and current clinical status of each inhibitor.

1.9.9 Novel therapeutic approaches

Overall there is an urgent requirement for new therapeutic options for treating non-APL AML. The use of small molecule inhibitors may be one such approach. A variety of small molecule inhibitors have been designed targeting an array of dysregulated proteins and signalling pathways, as discussed previously. However the majority, with the exception of AC220, have had disappointing clinical responses as single agents. This suggests that targeting just one genetic lesion or dysregulated signalling pathway is not enough to effectively eradicate leukemic blast cells in AML.

1.10 Aims

The following research aimed to:

- Investigate which c-KIT isoforms, GNNK- or GNNK+ is most common in a cohort of unselected patient samples with AML.
- Evaluate the impact of AML specific *c-KIT* mutations on receptor activation and downstream signalling in cells that express endogenous *c-KIT* mutations and a human cell line engineered to express *c-KIT* mutations in different domains.
- Examine the response of cells that express endogenous *c-KIT* mutations, a human cell line engineered to express AML specific *c-KIT* mutations and primary AML samples with *c-KIT* mutations to small molecule inhibitors of c-KIT, PI3K/AKT and mTOR.
- Investigate the functionality of a novel AML specific *FLT3* mutation identified during this project.

2. Materials and methods

All reagents used, unless otherwise specified, are from VWR International Ltd, Lutterworth, UK. Some specific methods are given in the relevant result chapters.

2.1 Cell culture

2.1.1 Cell lines

Cell line	Origin	Suspension/ Adherent	Growth factor dependent/independent
293T	Embryonal kidney cell line	Adherent	Independent
32Dcl3	Mouse Bone Marrow	Suspension	Dependent (IL3 - final concentration 2ng/mL)
HMC1.2	Human Mast Cell leukaemia	Suspension	Independent
Kasumi-1	Human acute myeloid leukaemia (AML FAB M2) t(8;21)	Suspension	Independent
ME-1	Human acute myeloid leukaemia (AML FAB Me40) inv(16)	Suspension	Independent
MOLM-13	Human acute myeloid leukaemia (AML FAB M5a)	Suspension	Independent
MV4-11	Human acute monocytic leukaemia (AML FAB M5)	Suspension	Independent
PL-21	Human acute promyelocytic leukaemia (AML FAB M3)	Suspension	Independent
SKNO.1	Human acute myeloid leukaemia (AML FAB M2) t(8;21)	Suspension	Dependent (GM-CSF - final concentration 10ng/mL)
UT-7	Human acute myeloid leukaemia (AML M7)	Suspension	Dependent (GM-CSF - final concentration 5 ng/mL)

2.1.2 Cell culture reagents

- 0.25% Trypsin-EDTA (PAA Laboratories Ltd, Somerset, UK)
- CASY Ton (Diagnostics Corporation, Indianapolis)
- Dimethyl sulfoxide (DMSO) (Sigma Aldrich, Poole, UK)
- Dulbecco's modified Eagle medium (DMEM) (PAA Laboratories Ltd, Somerset, UK)
- Dulbecco's Phosphate Buffered Solution (PBS) without calcium/magnesium (PAA Laboratories Ltd, Somerset, UK)
- Ficoll-Paque™ gradient (Amersham Biosciences, Bucks, UK)
- Foetal calf serum (FCS) heat-inactivated (PAA Laboratories, Pasching, Austria and BioSera, Boussens, France)
- Penicillin/streptomycin 100X (PAA Laboratories Ltd, Somerset, UK)
- Retronectin (TAKARA BIO INC, Saint-Germain-en-Laye, France)
- RPMI Medium 1640 with L- glutamine (PAA Laboratories Ltd, Somerset, UK)
- StemSpan™ H3000 (STEMCELL Technologies SARL, Grenoble, France)
- XtremeGene9 DNA transfection reagent (Roche Diagnostics Limited, West Sussex, UK)

2.1.3 Cell culture plastics

- 24 well non-treated tissue culture plates (BD biosciences, Oxford)
- 6, 12, 24, 48 and 96 well tissue culture plates (PAA Laboratories Ltd, Somerset, UK)
- $25cm^2$, $75cm^2$ and $175cm^2$ tissue culture flasks (Thermo Scientific, UK)

2.1.4 Small molecule inhibitors

Inhibitor	Targets	Source	Location
ZSTK-474	PI3K	Selleck	Newmarket, Suffolk
WYE-354	mTOR	Axon MedChem	Groningen, The Netherlands
BEZ-235	PI3K + mTOR	Axon MedChem	Groningen, The Netherlands
PD184352	MEK	Merck	Hertfordshire, UK
AZD5363	AKT	Astra Zeneca	Cheshire, UK
Dasatinib	BCR-ABL + c-KIT	Source BioScience LifeSciences	Nottingham Business Park, Nottingham
Imatinib	BCR-ABL + c-KIT	Axon MedChem	Groningen, The Netherlands
AC220	FLT3	Axon MedChem	Groningen, The Netherlands
Ponatinib	Abl,PDGFRα,VEGFR2,FGFR1 Src and FLT3	Selleck	Newmarket, Suffolk
Masitinib	PDGFRα/β and c-KIT	Selleck	Newmarket, Suffolk

2.1.5 Recombinant Growth Factors

- Murine IL3 (PeproTech, London, UK)
- Human GM-CSF (PeproTech, London, UK)
- Human SCF (PeproTech, London, UK)
- Human FLT3 (PeproTech, London, UK)
- Human TPO (PeproTech, London, UK)
- Human IL3 (PeproTech, London, UK)

2.1.6 Thawing of cells and cryo-preservation

Primary AML cells and cell lines were quickly thawed in a water bath at 37°C and decanted into a 50mL universal. Pre-warmed RPMI containing 10% FCS and 1% penicillin and streptomycin (R1) or RPMI containing 20% FCS and 1% penicillin and streptomycin (R2) was added to cell lines and primary AML cells respectively in a dropwise fashion every 2-3

seconds up to 10mLs with gentle shaking. A further 10mLs of R1/R2 was then added to the cells and they were centrifuged at 450g for 5 minutes. Cell lines were re-suspended in R1 or R2 at a seeding density of $1x10^6$ cells/mL and incubated at 37°C in a humidified atmosphere containing 5% CO_2. Primary AML cells were re-suspended at $2\text{-}5x10^5$ cells/mL in StemSpan medium (R3) containing 20ng/mL of human SCF, FLT3, TPO and IL3, in a relevant sized flask and incubated overnight at 37°C in a hypoxic atmosphere containing 5% CO_2 and 5% O_2. After 24 hours, viable primary AML cells were isolated by density centrifugation, as described in section 2.1.8 and re-suspended in R3 without growth factors. For cryo-preservation, cell lines were frozen down at a cell density recommended by Deutsche SammLung von Mikroorganismen und Zellkulturen GmbH (DSMZ), approximately $5x10^6$cells/mL, using a freezing mix of 70% RPMI, 20% FCS and 10% DMSO and stored in liquid nitrogen.

2.1.7 Cell counting and cell viability using the Casy Counter system

The Casy Counter system is an electric field multi-channel cell counting system that utilises the resistance measurement principle and pulse area analysis to determine cell number and cell viability. The Casy®Ton solution is a buffer specially designed for cell counting and aspiration through a pore of specific geometry at a constant flow rate. When measured, the cells displace a given volume of buffer which is equivalent to the volume of the cells. Cell viability is assessed on the integrity of the plasma membrane, as living cells have an intact cell membrane whereas dead or dying cells have ruptured or porous cell membranes. When cells with an intact cell membrane are exposed to a low voltage they can be described as electric insulators, whereas cells that are dead (ruptured or porous) allow the voltage to pass through the cells and are recorded by the size of their nucleus, therefore this allows live and dying cells to be distinguished based on size. Measurements are carried out by diluting the cell suspension 1:200 in Casy®Ton solution and analysing the diluted suspension on the Casy Counter. The results provide a diameter-linear size distribution, which indicates the volume, viability and concentration of the sample tested.

2.1.8 Ficoll centrifugation

A volume of 10mL Ficoll-Paque™ was layered underneath 5mL of R1/R2 in a 50mL falcon. Cells were washed with R1 and centrifuged at 450g for 5 minutes then re-suspended to approximately $1\text{-}5x10^6$cells/mL, layered on top of the R1/R2 layer and centrifuged at 352g for 25 minutes. Cells within the interface between the Ficoll-Paque™ and RPMI were aspirated, washed with 20mL of R1 and re-suspended to the desired concentration in either in R1/R2 or R3.

2.2 Retroviral production

2.2.1 Reagents for retroviral production

- **X-tremeGENE 9 DNA Transfection Reagent** (Roche Diagnostics Limited, West Sussex, UK)

2.2.2 Transfection of 293T cells

A total of $4.5x10^6$ 293T cells were seeded on to a $10cm^2$ tissue culture dish in 10mL DMEM containing 10% FCS and 1% penicillin and streptomycin (R4). After 24 hours, the 293T cells were checked to see that they were approximately 50-60% confluent prior to transfection. For each plate, 36µL of X-tremeGENE 9 DNA Transfection Reagent (3µL/µg DNA to be transfected) was diluted in 1.2mL of serum-free RPMI and incubated at room temperature for 5 minutes. A total of 12µg of plasmid DNA was transfected per plate, (4.6785µg of the gag/pol expressing plasmid (PeqPam), 3.125µg of the envelop plasmid (RD114 or Ecotropic) and 4.6785µg of the respective Moloney murine leukaemia virus based (SFG) plasmids (kindly provided by Martin Pule)) and incubated at room temperature for 5 minutes. The DNA mix was then added, to the X-tremeGENE 9:RPMI mix and incubated at room temperature for 30 minutes. DNA:X-tremeGENE 9 mix was added dropwise to each respective plate and placed into the incubator. Viral supernatant was harvested after 48 hours and stored at 4°C. Fresh R4 (10mLs) was then added to each plate. After a further 24 hours the viral supernatant was harvested again and pooled with the 48 hour supernatant. The viral supernatants were then aliquoted into cryotubes and either snap frozen in a dry ice ethanol bath and stored at-80°C or stored directly at -80°C.

2.3 Immunoblotting

2.3.1 Reagents for immunoblotting

- Bovine Serum Albumin (BSA) fraction V (Sigma Aldrich, Poole, UK)
- Complete, Mini Protease Inhibitor Cocktail Tablets (Roche Diagnostics Limited, West Sussex, UK)
- DC™ protein assay (BIO- RAD Laboratories Ltd, Richmond, CA)
- Enhance chemiluminescence kit (ECL Prime) (GE Amersham Life Sciences, Bucks, UK)
- Full range Amersham Rainbow Marker (GE Healthcare Life Sciences, Bucks, UK)
- Hybond-C-Extra nitrocellulose membrane (Amersham Life Sciences, Bucks, UK)
- Hyperfilm™ high performance autoradiography film (GE Amersham Life Sciences, Bucks, UK)
- Methanol (VWR International Ltd, Lutterworth, UK)
- Non-fat dried milk (MARVEL)
- NuPAGE® 4-12% Bis-Tris Gel 1.0 mm, 10/12/15 wells (Life Technologies Limited, Paisley, Scotland)
- NuPAGE® Antioxidant (Life Technologies Limited, Paisley, Scotland)
- NuPAGE® LDS Sample Buffer (4X) (Life Technologies Limited, Paisley, Scotland)
- NuPAGE® Novex 7% Tris-Acetate Gel 1.0 mm, 12 Well (Life Technologies Limited, Paisley, Scotland)
- NuPAGE® Sample Reducing Agent (10X) (Life Technologies Limited, Paisley, Scotland)
- PhosSTOP phosphatase Inhibitor Cocktail Tablets (Roche Diagnostics Limited, West Sussex, UK)
- Pierce ECL Western Blotting Substrate (Thermo Scientific, UK)
- Protein G-Sepharose 4 Fast Flow (Sigma-Aldrich Company Ltd, Dorset, UK)
- Tween-20 (Sigma Aldrich, Poole, UK)

2.3.2 Antibodies

- Anti-phosphotyrosine 4G10 (Millipore, Temecula)
- Bcl-2 (BD transduction, Oxford, UK)
- Bcl-x (BD transduction, Oxford, UK)
- BIM (Cell Signalling Technology, Hitchin, UK)
- Flt-3/ Flk-2 (C20) (Santa Cruz biotechnology, Middlesex, UK)
- GAPDH (Cell Signalling Technology, Hitchin, UK)
- Mcl-1 (Santa Cruz biotechnology, Middlesex, UK)
- Mouse IgG, HRP-linked (Cell Signalling Technology, Hitchin, UK)
- Pan c-Kit (D13A2) XP (Cell Signalling Technology, Hitchin, UK)
- PARP (Cell Signalling Technology, Hitchin, UK)
- Phycoerythrin (PE) Mouse Anti-Human CD117 (BD Pharmingen™)
- Phycoerythrin (PE) Mouse Anti-Human CD135 (BD Pharmingen™)
- Phospho 4E-BP1 (Thr37/46) (Cell Signalling Technology, Hitchin, UK)
- Phospho STAT5 (Tyr694) (Cell Signalling Technology, Hitchin, UK)
- Phospho-AKT (Ser 473) (Cell Signalling Technology, Hitchin, UK)
- Phospho-c-KIT (Tyr719) (Cell Signalling Technology, Hitchin, UK)
- Phospho-FLT3 (Tyr589/591) (Cell Signalling Technology, Hitchin, UK)
- Phospho-MAPK p42/44 (Thr 202/Tyr204) (Cell Signalling Technology, Hitchin, UK)
- Phospho-S6 Ribosomal Protein (Ser235/236) (Cell Signalling Technology, Hitchin, UK)
- P-p70-S6K (Thr389) (Cell Signalling Technology, Hitchin, UK)
- Pro-caspase 3 (Cell Signalling Technology, Hitchin, UK)
- Pro-caspase 9 (Cell Signalling Technology, Hitchin, UK)
- Rabbit IgG, HRP-linked (Cell Signalling Technology, Hitchin, UK)

Buffers:

Lysis buffers:

Protein lysis buffer (50mML HEPES pH 7.5, 100mM NaCl, 1% Triton X-100, 1mM EDTA, 1mM EGTA, 20mM NaF, 1mM Na orthovanadate, 1mM Pefabloc, 10µg/mL each of aprotinin, pepstatin, and leupeptin).

RIPA lysis buffer, 10X (0.5M Tris-HCl, pH 7.4, 1.5M NaCl, 2.5% deoxycholic acid, 10% NP-40, 10mM EDTA) diluted to 1X using Double Distilled Water (DDW) with 1 Complete Mini Protease Inhibitor Cocktail Tablet and 1 PhosSTOP Phosphatase Inhibitor Cocktail Tablet for each 10mLs.

Running buffer: NuPAGE® MOPS SDS Running Buffer (20X) (Life Technologies Limited, Paisley, Scotland) diluted to 1X using DDW.

Transfer Buffer: 10X stock (4.8mM Tris, 39mM Glycine, 0.038% SDS made to pH 9.1) diluted to 1X in 20% methanol.

Tris Buffered Saline (TBS): 10X solution 0.5M TRIS, 3.76M NaCl diluted in 1.25L of DDW, made to pH7.5

TBS-Tween-20 (TBST) Wash Buffer: 1L 10X TBS, 100mL 10% Tween-20 in PBS, made up to 10L with DDW.

2.3.3 DC™ protein assay

Working reagent A' was prepared by adding 20µL of reagent S to each mL of reagent A needed. For each run a BSA standard curve of 10mg/mL, 7.5mg/mL, 5mg/mL, 2.5mg/mL, 1mg/mL and 0.5mg/mL was used. For each standard or sample 5µL was pipetted into a 96 well microtiter plate, 25µL of reagent A' was added to each well then 200µL of reagent B. The protein lysate/reagent mix was incubated at room temperature for 15 minutes and the absorbance read at 750nm on the Varioskan® Flash microplate reader (Thermo Scientific). A standard curve was generated using the absorbance values from the known concentrations of BSA solution. Protein concentrations of the samples analysed were then determined using the equation of the straight line.

2.3.4 Western blotting

Cells (5-10x10^6) were harvested, washed with ice cold PBS and lysed in 50µL of protein lysis buffer or 1X RIPA lysis buffer supplemented with PhosSTOP phosphatases and Complete Mini Protease Inhibitor Cocktail Tablets (Modified RIPA) for 30 minutes on ice. Lysates were then centrifuged at 20,000g at 4°C for 10 minutes. The protein concentration in the supernatant was calculated using the DC™ protein assay (section 2.3.3). NuPAGE® LDS Sample Buffer (4X) was prepared with a final concentration of 10% NuPAGE® Sample Reducing Agent. Based on the protein concentration 25-80µg of protein lysate was standardised in 16µL lysis buffer. To each sample 4µL of the prepared NuPAGE sample buffer was added and boiled for 10 minutes. The NuPAGE gels were prepared prior to use by removing the combs and protective strips and placed into the Invitrogen Novex Mini cell Electrophoresis apparatus. The gels were then immersed in 1X MOPS buffer, and 500µL of anti-oxidant was added to the central chamber. The protein was then loaded onto the gels, with 5-10 µL of the Full Range Amersham Rainbow Marker and run at 150V until sufficient protein size separation was achieved (judged by Rainbow Marker migration). The gels were removed and soaked in transfer buffer and transferred to a nitrocellulose membrane using the Trans-Blot® SD Semi-Dry Transfer Cell (Bio-Rad) at 25V for 30mins.

Membranes were blocked in TBST with 4% MARVEL (MARVEL-TBST) or TBST with 5% BSA (BSA-TBST) for 1 hour at room temperature. Membranes were then washed 3 times in TBST. All membranes were incubated overnight at 4°C with primary antibody at dilutions specified by the manufacturer in BSA-TBST. The following day the primary antibody was removed and the membranes were washed 3 times for 5 minutes each in TBST. The relevant species-specific secondary antibody (conjugated to horseradish peroxidase) was diluted 1:15,000 in 3% MARVEL-TBST and incubated for 1 hour. Membranes were then washed 3 times in TBST for 5 minutes and proteins were detected using chemiluminescence with ECL prime or Pierce ECL Western Blotting Substrate according to the manufacturer's instructions. The membranes were then exposed to Hyperfilm for ranging times, dependent on the band intensity. The film was then developed in an automated film developer (Konica Minolta SRX-101A).

2.4 Flow cytometry

2.4.1 Reagents for flow cytometry

- Annexin buffer (150mM NaCl, 10mM HEPES pH7.4 and 10mM $CaCl_2$)
- Annexin V-Fluorescein isothiocyanate (FITC) conjugate (Roche Diagnostics, Mannheim, Germany)
- Flow-Check Fluorospheres (Beckman Coulter UK Ltd)
- Normocin^{TM} (50mg/mL) (InvivoGen, San Diego, USA)
- PBS with 0.5% BSA (0.5% BSA/PBS)
- Propidium iodide solution (PI) (diluted in filtered PBS at 2.5mg/mL) (Sigma Aldrich, UK)

2.4.2 Annexin V / PI staining

A total of 200µLs of cell suspension was added to 100µL of the following master mix: 20µL Flow-Check Fluorospheres, 100µL Annexin Buffer, 2.5µL PI solution and 0.25µL Annexin V-FITC conjugate and incubated for 15 minutes at room temperature. Samples were analysed on either the CyAn^{TM} ADP Analyzer (Beckman Coulter) or the BD FACSVerse^{TM} (BD Biosciences) flow cytometer machines. To analyse cells bivariant dot plots of log side scatter (SS) versus linear forward scatter (FS) were generated. Beads were identified by their unique forward scatter and side scatter properties and an electronic gate applied to them. Two thousand bead events were assayed in each case. An electronic gate was applied to the cell populations and data from this gate was plotted on a second bivariant dot plot of PI versus Annexin V. Quadrants were applied identifying cells which were PI/Annexin V double negative (live cells), PI negative/Annexin V positive (early apoptotic cells) and PI/Annexin double positive (late apoptotic/dead cells).

2.4.3 Flow cytometry examining BFP expression

All constructs used expressed the enhanced Blue Fluorescent Protein (eBFP) as a marker and was used to determine the percentage of cells that had been transfected. Cells were re-suspended to $1x10^6$/500µL in 0.5% BSA/PBS and analysed on the flow cytometer by gating the live cell population, based on their SS and FS. Data from this gate was then plotted on a second bivariant dot plot of BFP versus SS. The native cell line was used as a negative control to set the level of BFP expression to approximately 1%, hence anything above this threshold was considered positive.

2.4.4 Staining of cells with PE-conjugated antibodies

Cells were re-suspended to $1x10^6$/100µL in 0.5% BSA/PBS. Following the manufacturers' guidelines, the relevant amount of PE-conjugated antibody was added. The cell suspension was incubated for 1 hour on ice, then 400µL of 0.5% BSA/PBS was added. The live cell population was gated based on the cells SS and FS and from this gate the data was plotted onto a second bivariant dot plot of BFP versus PE. The appropriate native cell line was used as a negative control to set the level of BFP/PE expression to approximately 1%, and anything above this 1% threshold was considered positive.

2.4.5 Cell sorting

Cells were re-suspended to 1-$10x10^6$/mL in R1 or R2 containing 100µg/mL of Normocin™ and placed into sterile 5mL polystyrene round-bottom tubes and kept on ice. Cells were sorted based on BFP expression using a MoFlo™ XDP machine (Beckman Coulter UK Ltd). Following sorting cells were washed in 1mL of PBS and re-suspended in 300 - 1000µL of R1 or R2 containing 100µg/mL of Normocin™ and incubated at 37°C in a humidified atmosphere containing 5% CO_2.

2.5 Molecular Biology

2.5.1 Molecular biology reagents

- Agar (Sigma-Aldrich Company Ltd, Dorset, UK)
- Agarose (Bioline, London, UK)
- Ampicillin (Invitrogen, Paisley, UK)
- Bioline buffer and magnesium chloride (Bioline, London, UK)
- BIOTAQ™ DNA polymerase (Bioline, London, UK)
- CEQ™ DNA Size Standard Kit – 400/600 (Beckman Coulter UK Ltd, Buckinghamshire, UK)
- CEQ™ Separation Buffer (Beckman Coulter UK Ltd, Buckinghamshire, UK)
- Chloroform (VWR International Ltd, Lutterworth, UK)
- dNTPs (Bioline, London, UK)
- Ethanol 100% (VWR International Ltd, Lutterworth, UK)
- Ethidium Bromide (1mg/ml) (Invitrogen, Paisley, UK)
- Human c-KIT cDNA clone SC120061 (OriGene Technologies, Inc. Rockville, USA)
- Hyperladder I and IV (Bioline, London, UK)
- LB tablets (Sigma-Aldrich Company Ltd, Dorset, UK)

- One Shot® Stbl3™ Chemically Competent E. Coli (Life Technologies Limited, Paisley, Scotland)
- Optimase buffer and magnesium sulphate (Transgenomic Ltd, Glasgow, UK)
- Optimase™ DNA polymerase (Transgenomic Ltd, Glasgow, UK)
- PeqGOLD MicroSpin Cycle-Pure Kit (Peqlab, Sarisbury Green)
- Phusion® High-Fidelity DNA Polymerase (New England BioLabs, Hitchin, Hertfordshire)
- Plasmid DNA purification NucleoBond® Xtra Midi Kit (MACHEREY-NAGEL Düren, Germany)
- Primers (Integrated DNA Technologies, Belgium)
- QIAGEN plasmid mini kit (Crawley, West Sussex, UK)
- QIAGEN QIAquick gel extraction kit (Crawley, West Sussex, UK)
- QIAGEN QIAquick PCR purification KIT (Crawley, West Sussex, UK)
- QIAGEN RNeasy Mini Kit (Crawley, West Sussex, UK)
- Quick Blunting™ Kit (New England BioLabs, Hitchin, Hertfordshire
- Restriction enzymes and the corresponding buffers (New England BioLabs, Hitchin, Hertfordshire)
- Sample loading solution (SLS) (Beckman Coulter UK Ltd, Buckinghamshire,UK)
- Sterile molecular water (Sigma Aldrich Company Ltd, Dorset, UK)
- Super Optimal Broth (S.O.C) (Invitrogen Life Technologies, Paisley, UK)
- SuperScript® III First-Strand Synthesis System for RT-PCR (Invitrogen Life Technologies, Paisley, UK)
- T4 DNA ligase (New England BioLabs, Hitchin, Hertfordshire)

Buffers

1x Tris/Borate/EDTA (TBE) solution: 89mM Tris base, 90mM boric acid and 2mM EDTA in 1L of ddH_2O

5x Loading buffer: 30% glycerol and 0.025% bromophenol blue in 1x TBE

Dodecyltrimethylammonium bromide (DTAB) solution: 260mM DTAB, 1.5M NaCl, 100mM Trizma and 50mM EDTA made up to 1L DDW.

2.5.2 DNA extraction

Cells were pelleted and suspended in PBS (100µL per 1 x 10^6). To this, twice the volume of DTAB solution was added, mixed and incubated for 5 minutes at 68°C. Samples were stored at -20°C until required. Samples were thawed at 37°C and an equal volume of chloroform added, mixed thoroughly by inversion. Samples were centrifuged at 2465g for 15 minutes at room temperature. The upper aqueous layer containing the DNA was removed and to this an equal volume of 100% ethanol was added. This was mixed gently to precipitate out the DNA then centrifuged for 5 minutes at 2465g. The supernatant was removed and the pellet was transferred to a 1.5mL eppendorf. The pellet was washed in 70% ethanol and centrifuged at 20,000g for 5 minutes. The ethanol was removed and the pellet was allowed to air dry. The pellet was then re-suspended in sterile water (100µL for 10-15 x10^6 cells lysed) and stored at 4°C.

2.5.3 RNA extraction

RNA was isolated from 1x10^6 cells following the RNeasy Mini Kit (QIAGEN) manufacturer's instructions.

2.5.4 Generation of cDNA

cDNA was made according to the SuperScript® III First-Strand Synthesis System (Invitrogen Life Technologies) for RT-PCR manufacturer's protocol.

2.5.5 Polymerase Chain Reaction (PCR)

PCR was used to amplify regions of interest in genomic DNA or cDNA, with repeated thermal cycling consisting of denaturation followed by annealing of specific forward and reverse primers complementary to the target sequence followed by an extension step of DNA polymerisation. BIOTAQ™, Optimase™ or Phusion® DNA polymerases were used according to the manufacturer's instructions. Master mixes were made for each PCR reaction prior to the addition of the DNA template to ensure reproducibility. A negative control of double-distilled water (DDW), in place of the DNA template, was also included within each PCR reaction to ensure there was no contaminating DNA template within the master mix. Denaturation was carried out at 95°C for 30 seconds. The primer annealing temperature was calculated based on the composition of the primers and was incubated for 30 seconds. The extension temperature was 72°C and the time of the extension step was calculated based on the number of base pairs in the PCR product. The general rule for calculating the extension time was 1 minute per kilobase of DNA. These steps were repeated and modified according

to the individual requirement of each PCR and will be specified in more detail within the relevant chapters. The final step was an extension step for 5-15 minutes at 72°C to ensure complete amplification of each DNA amplicon. The standard reaction mix for a 20µL PCR using BIOTAQ™ DNA polymerase contained 0.5U of BIOTAQ™ DNA polymerase, 1X NH_4 reaction buffer, 1mM $MgCl_2$, 200µM dNTP mix, 0.5µM of forward/reverse primers. The standard reaction mix for a 20µL PCR using Optimase™ DNA polymerase contained 0.5U of Optimase™ DNA polymerase, 1X Optimase buffer, 200µM dNTP mix, 0.5µM of forward/reverse primers. PCR reactions using BIOTAQ™ or Optimase™ DNA polymerase were cycled 35 times as described above.

The standard reaction mix for a 20µL PCR reaction using Phusion® DNA polymerase contained 0.2U of Phusion® DNA polymerase, 1X Phusion HF buffer, 200µM dNTPs, 0.5µM of forward/reverse primers. The cycling conditions were an initial 2 minute denaturation step at 98°C, followed by 35 cycles of denaturation at 98°C for 42 seconds, annealing of primers for 42 seconds and extension at 72°C for the relevant amount of time followed by a final extension step between 5-15 minutes. All PCR reactions used 10-100ng of DNA template.

2.5.6 Principle of overlapping extension PCR

Overlapping extension PCR can be used to replace, delete or insert nucleotides into a desired fragment of DNA. This PCR based technique requires the design of primers containing the altered sequence to both the sense and antisense strands of DNA template sequence. The length of the horizontal segment of the primers is determined by the number of nucleotides required to reach the desired melting temperature. The primers were extended at the 3 prime ends to contain sufficient DNA sequence of the opposite fragment so that the melting temperature of the overlapping sequence is as required. An example is illustrated in Figure 2.1. An initial PCR was required to amplify fragment (x) using primer pair (1) and (3) and fragment (y) with primer pair (2) and (4). A master mix of: 1x HiFid buffer, 200µM dNTPs, 1 unit Phusion® DNA polymerase, 1µM or forward (1,2) and reverse primer (3,4) 30ng template DNA made up to 50µL with water and cycled according to the conditions described in section 2.5.5. PCR products were visualised on a 1% agarose gel and gel extracted and purified with a QIAGEN QIAquick gel extraction kit. A second PCR was then used to anneal PCR product (x) and PCR product (y) together and amplify across the whole of fragment (xy). Annealing of the PCR products was mediated by the overhangs incorporated into the primers (2) and (3). A master mix of: 1x HiFid buffer, 200µM dNTPs, 1 unit Phusion® DNA polymerase, 1µM of forward (1) and reverse primer (4) and 40-120ng of

each cleaned PCR product (x) and (y) made up to 175µL with water and divided between 3 PCR tubes. The cycling conditions were the same as previously described (section 2.5.5). From the second PCR reaction 12µL was ran on a 1% agarose gel to confirm that fragment (x) and (y) had annealed and amplified. The remaining PCR product was then cleaned up using a QIAGEN QIAquick PCR purification kit and used for downstream cloning.

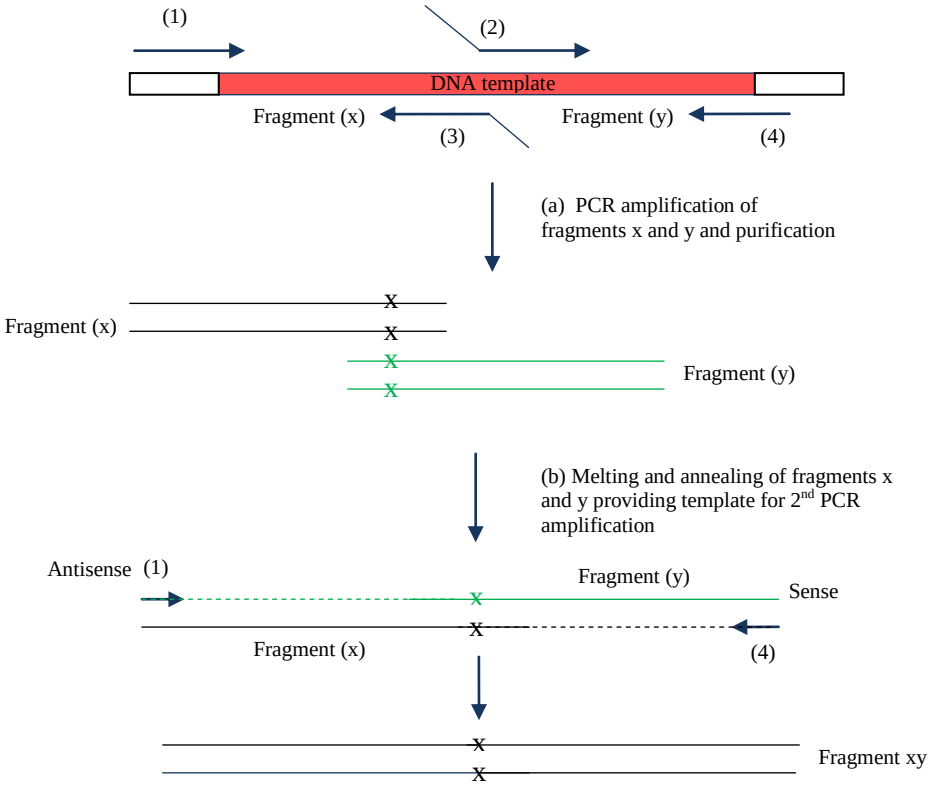

Figure 2.1 A schematic illustrating the principle of overlapping extension PCR.

2.5.7 Fragment size separation using the Capillary Electrophoretic Genetic Analysis System (CEQ)™ 8000

Size differences within PCR products were quantified using PCR incorporating a fluorescently labelled reverse primer. Approximately 50ng of DNA was amplified using the BIOTAQ™ DNA polymerase PCR conditions as described in section 2.5.5 but using 0.25µM of forward/reverse primers and 25-28 PCR cycles. CEQ™ DNA Size Standard Kit 400 or 600 (3.5µL) was added to 1mL of SLS. Each PCR product (2µL) was added to 38µL of SLS + CEQ™ DNA Size Standard mix. The PCR product/SLS mix was then loaded onto the sample plate and one drop of mineral oil was layered on top of each well. Separation buffer was also loaded on to the separation buffer plate. The samples were analysed by fragment separation on a CEQ 8000 Genetic Analysis System (Beckman Coulter). Following size separation of the PCR products, the area under each peak was determined by the instruments software algorithm. The relative proportion of each peak was determined by calculating the area under each peak as a percentage of the total alleles.

2.5.8 Agarose gel electrophoresis

PCR products or digested DNA products were visualised on 1-2% agarose gels. To make the gels, the required amount of agarose was added to 1X TBE. This was microwaved to dissolve the agarose. When cooled, ethidium bromide was added to the gel (final concentration 0.1µg/mL). This was then poured into a mould and allowed to set for 30 minutes. To run samples, the gels were submerged in 1X TBE containing 0.1µg/mL ethidium bromide. The desired amount of PCR product or digested DNA was added to the relevant amount of loading dye and loaded into a well within the gel. With each gel 4µL or either Hyperladder I or IV was also loaded to confirm the size of the DNA products. Samples were electrophoresed at 75mA for 30-45 minutes. DNA products were visualised under a UV transilluminator and a polaroid image was taken.

2.5.9 Agar plates and LB broth

LB broth was made with 25 LB tablets in 1L of DDW and autoclaved. Agar plates were made with 8 LB tablets and 7.5g of Agarose, made up to 500mL with DDW and autoclaved. When both the LB broth and Agar were cool to touch, ampicillin was added to a final concentration of 100µg/mL. Agar plates were poured in the presence of a bunsen burner and allowed to set before storing at 4°C.

2.5.10 Restriction enzyme digests

Amplified DNA or plasmid constructs were digested overnight using restriction enzymes, according to the manufacturer's instructions.

2.5.11 Sequencing

PCR products for sequencing were generated following the BIOTAQ^{TM} PCR conditions (section 2.5.5). PCR products were cleaned up using the PeqGOLD MicroSpin Cycle-Pure Kit and diluted to a concentration of 1ng/µL per 100bp. For plasmid constructs, 100ng/µL samples were prepared. Samples were sent for sequencing by the Scientific Support Services (SSS) at UCL cancer institute.

2.5.12 Cloning

PCR products were generated from template DNA using the high-fidelity proof-reading Phusion® DNA polymerase and were visualised on a 1% agarose gel and purified using a QIAGEN QIAquick gel extraction kit. Extracted PCR products and the retroviral plasmid vector (SFG) were digested with restriction enzymes and purified using a QIAGEN QIAquick PCR purification kit. Ligation reactions were carried out using either T4 DNA Ligase or Quick T4 DNA Ligase. For the T4 DNA Ligase reaction 3µL of digested PCR product (10-30ng/µL) was ligated to 1µL of digested vector (50-100ng/µL) using 1X T4 DNA Ligase Buffer and 400 NEB units of T4 DNA Ligase and incubated at 16°C overnight. Ligation reactions using the Quick T4 DNA Ligase were carried out with the same ratio of digested insert:vector but using 1X Quick Ligation Buffer, 2000 units of Quick T4 DNA Ligase in a total volume of 20µL, incubated at 25°C for 5 minutes and stored at 16°C. The ligated vector (1µL) was transformed into One Shot® Stbl3™ Chemically Competent E. Coli by heat shock at 42°C for 45 seconds and incubated on ice for 2 minutes. To the cells 250µl of SOC medium was added per vial and the cells were incubated in a shaking incubator to recover for 1 hour at 37°C. The transformed E. Coli cells were diluted 1:4 in S.O.C medium, with 100µL plated onto pre-warmed agar plates containing 100µg/mL of ampicillin. Plates were incubated overnight at 37°C. Uptake of vector provided ampicillin resistance allowing for bacterial colonies to form. Several colonies from each plate were selected and expanded in 4mL LB containing 100µg/mL Ampicillin (starter culture) at 37°C in a shaking incubator. DNA was extracted from 3mL of the expanded colonies using a QIAGEN plasmid mini kit as described by the manufacturer's instructions. Following isolation of the DNA from the individual clones, restriction enzyme digests were carried out to confirm the presence of the correct insert size and run on a 1% agarose gel. If the insert

was present at the correct size, then the remaining 1mL of starter culture was added in to 250mL LB with 100µg/mL ampicillin and incubated overnight at 37°C in a shaking incubator. DNA was isolated from the bulked up cultures using a Plasmid DNA purification NucleoBond® Xtra Midi Kit following the manufacturer's instructions. To confirm that the insert was still present at the expected size in the midi prep, a restriction enzyme digest was carried out and the products were run on a 1% agarose gel. If the insert corresponded to the expected size, then the insert was sequenced in its entirety.

3. Chapter 3: Functional consequence of *c-KIT* mutations in the UT-7 AML cell line

3.1 Introduction

CBFL is defined by the presence of t(8;21)(q22;q22) or inv(16)(p13;q22) which generate the fusion proteins RUNX1-RUNX1T1 and CBFβ-MYH11 respectively. Both t(8;21) and inv(16) are associated with a favourable clinical outcome, however, 40-50% of patients with these translocations eventually relapse (Grimwade *et al.*, 2010). c-KIT is expressed on 60-80% of myeloblast cells and is mutated in 28% of CBFL (Beghini *et al.*, 2004;Allen *et al.*, 2013). In CBFL, *c-KIT* mutations are found as indels in exon 8 (extracellular domain - ECD), point mutations in exon 10 (transmembrane domain - TMD), insertions/tandem duplications in exon 11 (juxtamembrane domain - JMD) or point mutations in exon 17 (activating loop domain - ALD). The presence of *c-KIT* mutations is associated with an increased RR in CBFL (Paschka *et al.*, 2006;Cairoli *et al.*, 2006;Allen *et al.*, 2013). As a result, c-KIT has become an attractive therapeutic target for this subset of patients. Dasatinib, an inhibitor of wild-type and mutant *c-KIT* isoforms has been shown to inhibit c-KIT phosphorylation and induce apoptosis in human AML cells harbouring *c-KIT*-WT, *c-KIT*-V560G or *c-KIT*-D816V and in murine Ba/F3 cells expressing *c-KIT*-D816V, *c-KIT*-D816F or *c-KIT*-D816Y (Schittenhelm *et al.*, 2006;Guerrouahen *et al.*, 2010). Most studies have focused on evaluating the response of cells expressing *c-KIT* mutations in individual domains i.e. ALD to small molecule inhibitors. Therefore, there has been no direct comparison evaluating the response of a human AML cell line expressing *c-KIT* mutations occurring in different domains to c-KIT inhibitors.

This chapter aimed to evaluate whether there are differences in proliferation and cell signalling between the *c-KIT* Δ417-419>Y, L576P, D816V and N822K mutations in the factor-dependent UT-7 megakaryoblastic leukaemia cell line. UT-7 cells expressing c-KIT-Δ417-419>Y, c-KIT-L576P, c-KIT-D816V and c-KIT N822K and were treated with c-KIT inhibitors to investigate if the mutation location impacted on the response to inhibitory molecules.

3.2 Methods

3.2.1 Cell lines

UT-7, a human GM-CSF dependent megakaryocytic AML cell line, was cultured in R2 media supplemented with 5ng/mL GM-CSF. 293T cells were cultured in R4. All cell lines were incubated in 5% CO_2 at 37°C.

3.2.2 Screening of pCMV6-XL5-c-KIT (NM_000222 OriGene)

The pCMV6-XL-c-KIT construct, containing the *c-KIT* cDNA sequence, was purchased from OriGene. The entire coding sequence of *c-KIT* was sequenced directly from the plasmid using the primers listed in Table 3.1.

Exon	Primer	Sequence
5	c-KIT 5D	5'-TGGCATAACACATGAACACTCCAG-3'
7	c-KIT-7U	5'-CATTCCTAGTGTCCAATTCTGA-3'
9	c-KIT 9D	5'-GCCCAGATGAGTTTAGTGTCTGC-3'
19	c-KIT 19D	5'-CTTAGAATCGACCGGCATTCCAG-3'
17	c-KIT 17/F3	5'-GCCAGAAATATCCTCCTTACTCATG-3'

D= Exonic reverse primer, U = Exonic forward primer and R=Reverse primer

Table 3.1 Primers used to sequence the coding region of *c-KIT* from the pCMV6-XL5-c-KIT plasmid construct.

3.2.3 Quantification of the *c-KIT* GNNK+ isoform transcript in samples from AML patients

cDNA was available from the tissue bank held in the department from the MRC AML-15 trial. 70 unselected patients were screened for the presence of the *c-KIT* GNNK+ isoform transcript. PCR products were generated using the forward primer c-KIT 8F and a fluorescently labelled reverse primer, c-KIT 10R*, as listed in Table 3.2, at an annealing temperature of 63°C. DNA was amplified with the BIOTAQ^{TM} DNA polymerase following the manufacturer's instructions, as described in chapter 2 section 2.5.5. cDNA was amplified for 28 cycles producing a 258bp product for the c-KIT GNNK- transcript and a 270bp product for the GNNK+ transcript. The relative level of c-KIT GNNK +/- isoform transcripts was assessed by fragment separation using the CEQ 8000 Genetic Analysis System (Beckman Coulter) as described in chapter 2 section 2.5.7. The level of the two isoforms was determined by calculating the area under each peak as a percentage of the total alleles.

3.2.4 Screening of samples from AML patients for the presence of *c-KIT* CAG repeat

cDNA was amplified using c-KIT 3F and c-KIT 5R, as listed in Table 3.2, at an annealing temperature of 64°C using the BIOTAQ^{TM} DNA polymerase as described in chapter 2 section 2.5.5. cDNA was amplified for 35 cycles producing a 341bp product which was sequenced using c-KIT 3F.

Exon	Primer	Sequence	Annealing temperature (^{o}C)
3	c-KIT 3F	5'-CCATCGGCTCTGTCTGCATTG-3'	64
5	c-KIT 5R	5'-TGGCATAACACATGAACACTCCAG-3'	
8	c-KIT 8F	5'-GATTGGTATTTTTGTCCAGGAACTG-3'	63
10	c-KIT 10R*	5'-ACCAATCAGCAAAGGAGTGAACAG-3'	

F=Forward primer, R=Reverse primer and *= fluorescently labelled primer.

Table 3.2 PCR primers used to identify the presence or absence of the GNNK isoform and the additional CAG repeat.

3.2.5 Preparation of *c-KIT*-WT construct lacking the GNNK+ insert and CAG repeat

In order to remove the GNNK+ insert and the CAG repeat from the *c-KIT*-WT sequence overlapping extension PCR was used, illustrated in Figure 3.1. The pCMV6-XL5-c-KIT construct served as a DNA template and *c-KIT* was amplified using Phusion® DNA polymerase as described in chapter 2 sections 2.5.5 and 2.5.6. Three initial PCR reactions were carried out using the following primer pairs MP11224:F-fuse:.SalI.kozak and MP11225-R (794bp product), MP11226-F and MP11227-R (811bp product) and MP11228-F and MP11229-R-fuse:.MluI (1421 bp product) as listed in Table 3.3. Fragment 1 (794bp) contained 5' overhangs for the SFG vector and removed the CAG repeat, fragment 2 (811bp) removed the CAG repeat and the GNNK+ insert with sufficient overhangs for both fragments 1 and 3 and fragment 3 (1421bp) removed the GNNK+ insert and contained 3' overhangs for the SFG vector. PCR products were visualised on a 1% agarose gel to check they were the expected size, and purified using a QIAquick PCR purification kit. Fragments 1, 2 and 3 were annealed and amplified across using primers MP11224:F-fuse:.Sal.kozak and MP11229 R-fuse:.MluI producing a 2973bp PCR product (Figure 3.1).

3.2.6 Cloning of corrected *c-KIT*-WT into SFG-xm.eGFP.I2.eBFP2 vector

The SFG-xm.eGFP.I2.eBFP2 retroviral plasmid sequentially expresses eGFP, an internal ribosome entry site (IRES) and eBFP (8404bp), and was a kind gift from Martin Pule (haematology department, UCL). This cassette is flanked by two long tandem repeats (LTRs). The SFG vector has a SalI restriction site at the 5' end of the GFP sequence and a MluI site at the 3'end of the IRES sequence as illustrated in Figure 3.2. The PCR primers used to clone *c-KIT* from the pCMV6-XL5-c-KIT plasmid were designed with SalI and MluI restriction sites at the 5' and 3' of *c-KIT* respectively allowing it to be cloned directly into the SFG-xm.eGFP.I2.eBFP2 vector. This allowed direct replacement of GFP for c-KIT which produced SFG-xm.c-KIT.eBFP (subsequently referred to as SFG-c-KIT) constructs that use BFP as a selectable marker. A total of 0.5µg of corrected *c-KIT*-WT PCR product (2961bp) lacking the GNNK insert and CAG repeat and 1µg of SFG-xm.eGFP.I2.eBFP2 were each digested using MluI and SalI in a 100µL reaction at 37°C for 4 hours according to the manufacturer's instructions. Digested vector products were visualised on a 1% agarose gel and the desired band (7684bp) was cut out and purified using a QIAquick Gel Extraction Kit (QIAGEN). The digested *c-KIT*-WT PCR product was cleaned up using a QIAGEN PCR purification kit. The digested SFG-xm.eBFP2 vector and *c-KIT*-WT PCR product were ligated together as described in chapter 2 section 2.5.12 to create SFG-c-KIT-WT (Figure 3.2). Mini preps and midi preps of bacterial cultures were screened for *c-KIT* using a MluI and SalI digest. If *c-KIT* was present two bands were observed when run on a 1% agarose

gel, one at 7684bp corresponding to the vector backbone and a fragment at 2961bp corresponding to *c-KIT*. The coding region of *c-KIT* was sequenced using the primers listed in Table 3.1 to confirm that the GGTAACAACAAA insert and CAG repeat had been removed.

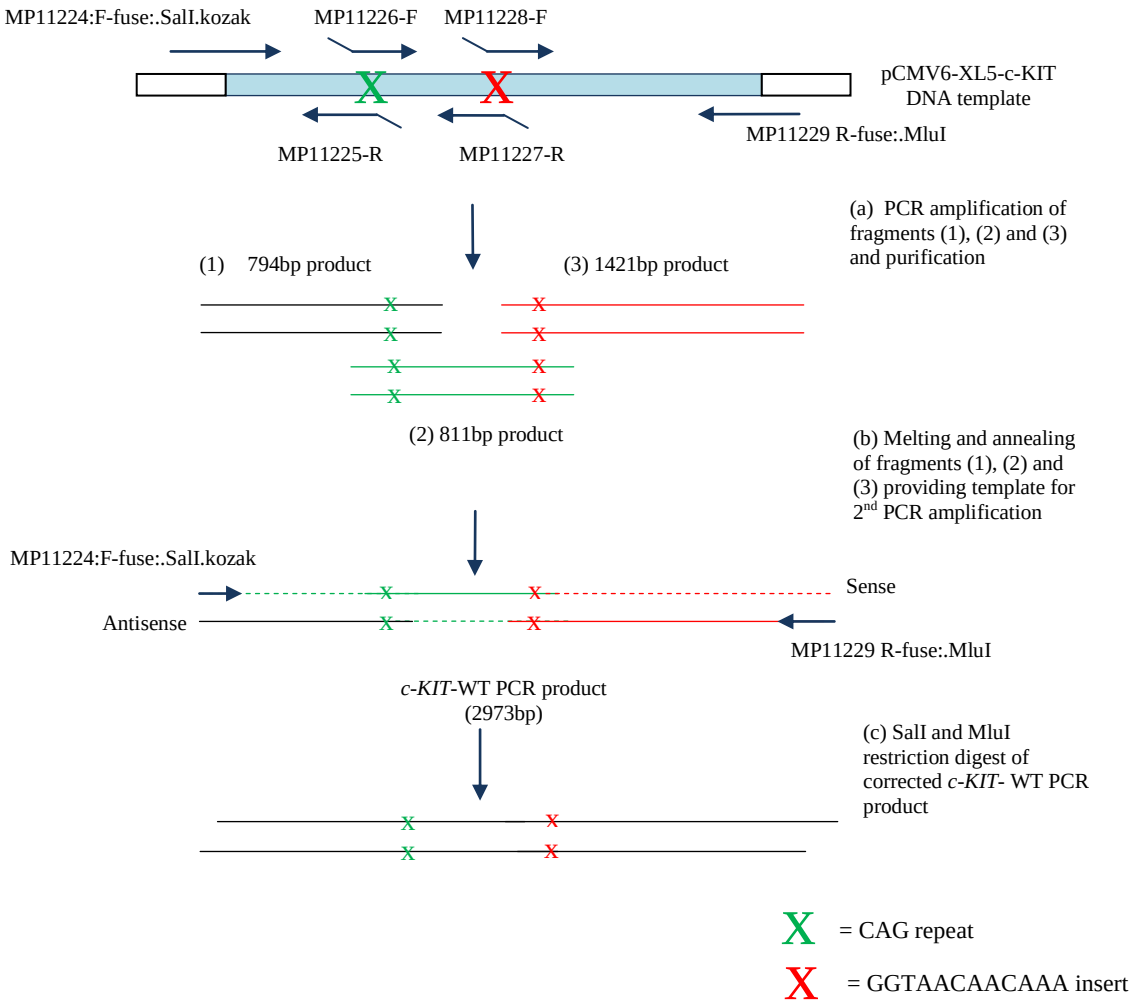

Figure 3.1 Amplification of *c-KIT* removing the GGTAACAACAAA insert and CAG repeat. *c-KIT* was amplified from the pCMV6-XL5-c-KIT construct with three PCR reactions using primer pairs MP11224:F-fuse:.SalI.kozak and MP11225-R, MP11226-F and MP11227-R and MP11228-F and MP11229-R-fuse.MluI. Fragments (1), (2) and (3) were gel extracted, annealed and amplified across using primers MP11224:F-fuse:.SalI.kozak and MP11229-R-fuse.MluI. The *c-KIT*-WT PCR product and SFGs.xm.eGFP.I2.eBFP vector were digested with SalI and MluI.

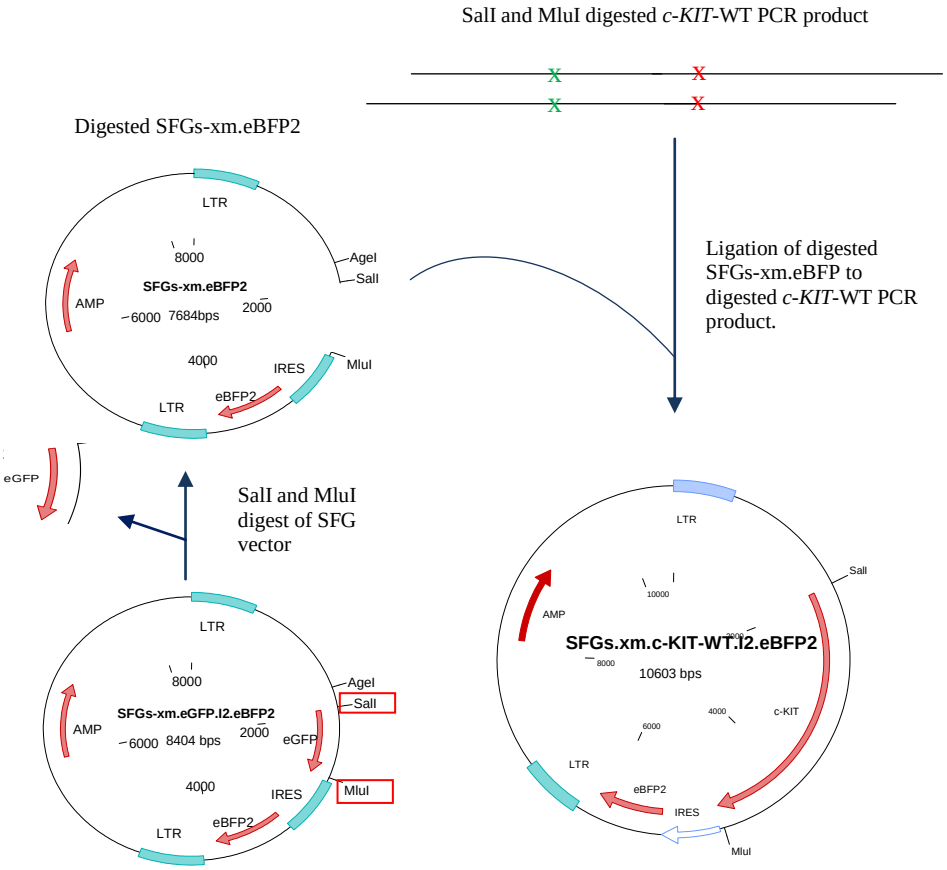

Figure 3.2 Schematic of the cloning strategy used to introduce *c-KIT*-WT into the SFG vector. SFG-xm.eGFP.I2.eBFP and *c-KIT*-WT PCR product were digested with MluI and SalI. The SFGs-xm.eBFP fragment was ligated to the digested *c-KIT*-WT PCR product to generate the SFG-c-KIT-WT construct.

Exon	Primer	Sequence	Annealing temperature (°C)
1	MP11224:F-fuse:.SalI.kozak	5'-CGATCGCGGACGGTCGACGCCACCATGAGAG GCGCTCGCGGCGCCT-3'	65
4-5	MP11225-R	5'-TCCTGTAGTTTAGTCTGACTGTTTTCTCTTTTC CACGTTGAGTAC-3'	
4-5	MP11226-F	5'-GTGGAAAAGAGAAAACAGTCAGACTAAACTA CAGGAGAAATATAATAGCTGGCATC-3'	65
9-10	MP11227-R	5'-TGTGGGGATGGATTTGCTCTTTAAATGCAAAG TTAAAATAGGCAGAAGTCTTG-3'	
9-10	MP11228-F	5'-TTGCATTTAAAGAGCAAATCCATCCCCACACC CTGTTC-3'	65
21	MP11229 R-fuse:.MluI	5'-CACCTTACGCTGACGCGTTCAGACATCGTCGT GCACAAGCAG-3'	

Green = SalI restriction site, Blue = kozak sequence, underlined = MluI restriction site

Table 3.3 *c-KIT* primers used to remove the GGTAACAACAAA insert and CAG repeat.

3.2.7 Generation of *c-KIT* mutant constructs

The *c-KIT* mutations Δ417-419>Y, L576P, D816V, and N822K were introduced with mismatch primers using splicing by overlap extension PCR as described in chapter 2 section 2.5.6. *c-KIT* was amplified from the SFG-c-KIT-WT construct using Phusion® DNA polymerase as described in chapter 2 sections 2.5.5 and 2.5.6. For each mutant two PCR amplicons were prepared using primers given in Table 3.4. One amplicon used the MP11224:F fuse:.SalI.kozak primer (1) and the mutant-specific reverse primer (3); the other amplicon used the mutant-specific forward primer (2) and MP11229 R-fuse:.MluI reverse primer (4) (Figure 3.3). The PCR products were visualised on a 1% agarose gel, cut out and extracted using the QIAquick Gel Extraction Kit. The two PCR products for each of the desired *c-KIT* mutations were annealed together and amplified across using primers MP11224:F fuse:.SalI.kozak (1) and MP11229 R-fuse:.MluI (4) (Figure 3.3). PCR products were run on a 1% agarose gel, gel extracted and digested with MluI and SalI in a 100µL reaction at 37°C for 4 hours according to the manufacturer's instructions. Each of the respective *c-KIT* mutant PCR products were then ligated together with digested SFG.xm-eBFP vector and cloned as described in chapter 2 section 2.5.12. MluI and SalI digests were used to screen mini preps and midi preps from bacterial cultures for the presence of *c-KIT* as

previously described. For each mutant construct, the entire coding sequence of *c-KIT* was sequenced using the primers listed in Table 3.1.

Exon	Primer	Sequence
1	MP11224:F-fuse:.SalI.kozak	5'-CGATCGCGGACGGTCGACGCCACCATGAGAGGCGCTCGCGGCGCCT-3'
17	c-KIT D816V-F	5'-GTCTAGCCAGAGTCATCAAGAATGA-3'
17	c-KIT D816V-R	5'-TCATTCTTGATGACTCTGGCTAGAC-3'
17	c-KIT N822K-F	5'-CATCAAGAATGATTCTAAGTATGTGGT-3'
17	c-KIT N822K-R	5'-ACCACATACTTAGAATCATTCTTGATG-3'
11	c-KIT L576P-F	5'-ACCCAACACAACCTCCTTATGATC-3'
11	c-KIT L576P-R	5'-GATCATAAGGAGGTTGTGTTGGGT-3'
8	Δ417-419+>Y-F	5'-ACCAGAAATCCTGTACAGGCTCGTGAATGGCAT-3'
8	Δ417-419+>Y-R	5'-ATTCACGAGCCTGTACAGGATTTCTGGTTTTGTATTCACA-3'
21	MP11229 R-fuse:.MluI	5'-CACCTTACGCTGACGCGTTCAGACATCGTCGTGCACAAGCAG-3'

Green = SalI restriction site, Blue = kozak sequence, underlined = MluI restriction site, Red = mutated codons.

Table 3.4 *c-KIT* primers used to introduce the Δ417-419>Y, L576P, D816V and N822K mutations.

3.2.8 Generation of SFG-EMPTY vector

In order to generate an SFG-EMPTY vector control the ends of the MluI and SalI digested SFG-xm.eBFP2 vector were blunted using the Quick Blunting™ KIT according to the manufacturer's guidelines, and the vector was then re-ligated using T4 DNA ligase as described in chapter 2 section 2.5.12. The ligated SFG-EMPTY vector was cloned as described in chapter 2 section 2.5.12.

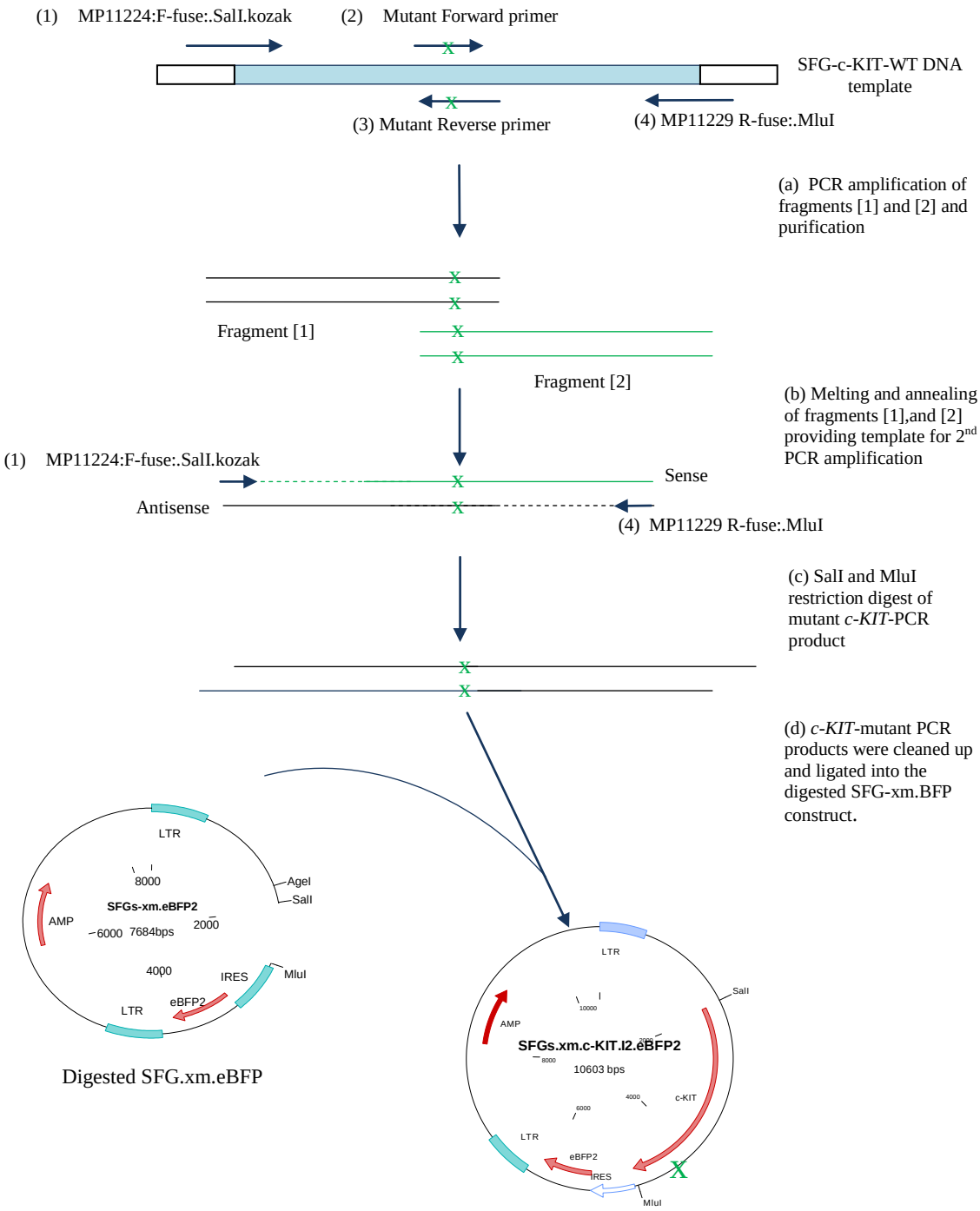

Figure 3.3 Schematic of the cloning strategy used to introduce *c-KIT* mutations into the SFG vector. *c-KIT* mutations were introduced by amplifying from the SFG-c-KIT-WT construct using mismatched primers. Two initial PCR reactions were carried out using MP11224:F-fuse:.SalI.kozak (1) and c-KIT mutant reverse primer (3) and c-KIT mutant forward (2) and MP11229-R-fuse.MluI (4). Products were gel extracted, annealed and amplified across using primers MP11224:F-fuse:.SalI.kozak (1) and MP11229-R-fuse.MluI (4). The amplified *c-KIT*-mutant PCR products were digested with SalI and MluI and ligated into the SFG-xm.BFP construct. The green crosses represent *c-KIT* mutations.

3.2.9 Retroviral production

Retroviral supernatant for each of the *c-KIT* constructs was made as described in chapter 2 section 2.2.2 using the RD114 envelope. Viral supernatants were directly stored at -80°C.

3.2.10 Transduction of UT-7 cells with SFG-c-KIT constructs

Non tissue culture treated 24 well plates were coated with 1µg/cm^2 of RetroNectin® per well overnight at 4°C. Retroviral supernatants were thawed on ice and 250µL was used to coat each RetroNectin® coated well for 30 minutes at room temperature. The viral supernatant was then removed from each well and discarded. UT-7 cells were re-suspended at 6x10^5 cells/mL in R2 with 5ng/mL GM-CSF and 500µL plated onto the RetroNectin® bound virus. The remaining viral supernatant (1.75mL) was gently overlaid on top of the UT-7 cells. The plate was centrifuged for 10 minutes at 1000g and incubated at 37°C in 5% CO_2 for 24 hours. The cells were then centrifuged, and re-suspended in fresh R2 with 5ng/mL GM-CSF and incubated at 37°C in a humidified atmosphere containing 5% CO_2. After 48 hours, cells were examined for BFP positivity by flow cytometry (see chapter 2 section 2.4.3) and then subsequently sorted based on BFP expression (see chapter 2 section 2.4.5).

3.2.11 Examination of CD117 expression

A total of 1x10^6 transduced and sorted cells were re-suspended in PBS/0.5% BSA and incubated with anti-CD117 PE conjugated antibody as described in chapter 2 section 2.4.4 and analysed on the flow cytometer.

3.2.12 Proliferation assay

UT-7 cells were washed 3 times in PBS, re-suspended at 5x10^{4}cells/mL in R2 and 100µL plated, in triplicate, into a 96 well plate in the presence or absence of 5ng/mL GM-CSF, with or without increasing concentrations of human SCF (5-50ng/mL). Cell proliferation was assessed every 24 hours using alamarBlue® following the manufacturer's guidelines. Measurements were corrected for background using absorbance values from wells containing media only.

3.2.13 Cytotoxicity assay

UT-7 cells at 5x10^{5}cells/mL were treated with increasing concentrations of dasatinib (0.1nM-1µM) or masitinib (0.1nM-10µM) for 72 hours in the presence of 100ng/mL SCF. Annexin V/PI staining was assessed as described in chapter 2 section 2.4.2. The live cell

fraction (Annexin and PI negative) and the absolute number of live cells were quantified by flow cytometry, and results expressed as a percentage of the control cells.

3.2.14 Data analysis

To examine if drug interactions were antagonistic, additive or synergistic at cell killing, the data was analysed using CalcuSyn software. This uses the Chou-Talalay method, which is based on the median-effect equation (Chou & Talalay, 1983;Chou & Talalay, 1984). The CI definitions are as follows: >1.1 antagonistic, 0.9-1.1 additive and <0.9 synergistic.

3.3 Results

3.3.1 Sequencing of the pCMV6-XL5-c-KIT (OriGene) construct

Sequencing of the OriGene pCMV6-XL5-c-KIT construct revealed that the *c-KIT* cDNA sequence contained a GGTAACAACAAA insert at the end of exon 9 which would result in expression of the c-KIT GNNK+ isoform (Figure 3.4a). The GGTAACAACAAA insert is not novel and has previously been reported as an alternative splice variant (Crosier *et al.*, 1993). The plasmid construct also had an additional CAG repeat at the end of exon 4 which would result in an additional glutamine (Q) that OriGene reported to be a naturally occurring polymorphism (SC120061) (Figure 3.4b). An unselected cohort of samples from AML patients were therefore assessed for the presence of these transcripts to identify which isoforms were predominant.

Expected WT: TTTAAA- - - - - - - - - - - - - - - GAGCAA

Construct : TTTAAAGGTAACAACAAAGAGCAA

Expected WT: TTTAGT- - - CTGACTGTT

Construct : TTTAGTCTGCTGACTGTT

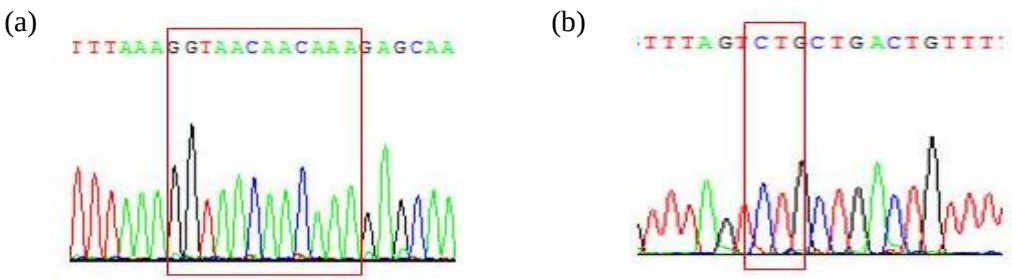

Figure 3.4 Sequencing chromatograms of *c-KIT* from the pCMV6-XL5-c-KIT construct showing the presence of the GNNK insert and CAG repeat. (a) Boxed sequence shows the presence of the GGTAACAACAAA repeat at the end of exon 9 sequenced in the forward direction. (b) Boxed sequence shows the presence of a CAG repeat at the end of exon 4, sequenced in the reverse direction.

3.3.2 Detection of *c-KIT* GNNK +/- isoforms in samples from patients with AML

The incidence of *c-KIT* GNNK+/- isoforms and their relative levels were quantified using cDNA from 70 samples with AML using PCR amplification with a fluorescently labelled primer and subsequent fragment size separation on the CEQ 8000 Genetic Analysis System. A sample with AML which expressed both the GNNK+ and GNNK- isoforms was identified and included in each fragment analysis run as a positive control to establish the variability within a single sample between repeats. The median GNNK- expression for the positive control was 96% (range 95-98%) and the median GNNK+ isoform expression was 4%

(range 2-5%). Two peaks at 258 and 270bp were identified for 44 (63%) of the samples corresponding to expression of both the *c-KIT* GNNK- and GNNK+ transcripts respectively (Figure 3.5a). In 26 samples (37%) only a single peak was detected at 258bp indicative of expression of only the GNNK- isoform (Figure 3.5b). In the 44 cases where the GNNK+ isoform was detected the median GNNK+ isoform expression was 5.5% ranging from 1-13% and the median GNNK- isoform expression was 94.5% ranging from 87-99%. The GNNK- isoform was identified as the predominant transcript within this AML cohort and therefore all constructs used in further experiments were GNNK-.

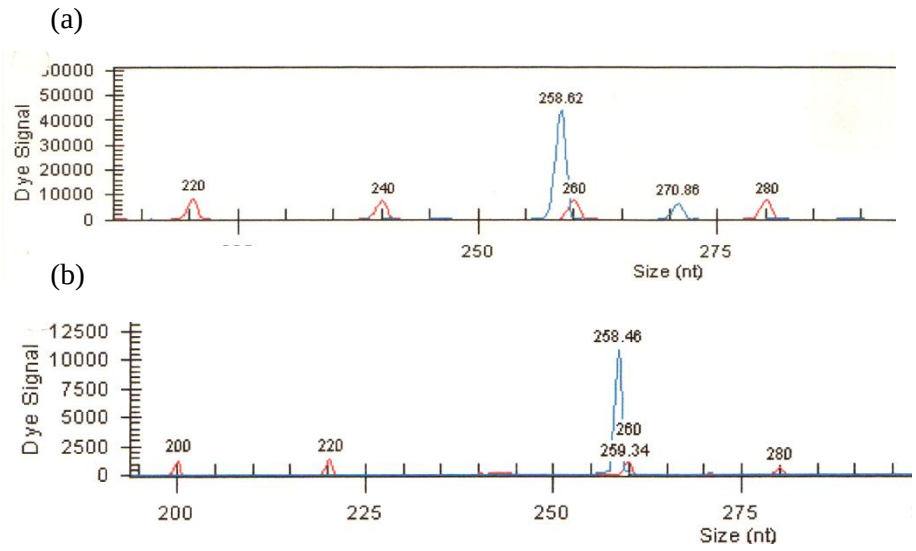

Figure 3.5 Chromatograms showing size separation of the GNNK- and GNNK+ isoforms. (a) A sample with AML in which two peaks at 258bp and 270bp were detected corresponding to expression of both the GNNK- and GNNK+ isoforms respectively. (b) A sample with AML in which only a single peak at 258bp was detected indicative of only the GNNK- transcript being expressed.

3.3.3 Sequencing of samples with AML for the additional CAG (Q) repeat

In order to determine the level of the CAG repeat isoform, exon 4 of *c-KIT* was sequenced from four samples with AML. A representative example is shown in Figure 3.6 indicating that the additional CAG isoform is a low level transcript. Therefore all constructs used in further experiments did not contain the additional CAG repeat.

Expected WT sequence : GAAAAGAGAAAACAGTCAG - - - ACTAAACTACAGGAGAAAT

Additional CAG repeat isoform : GAAAAGAGAAAACAGT CAGCAGACTAAACTACAGGAGAAAT

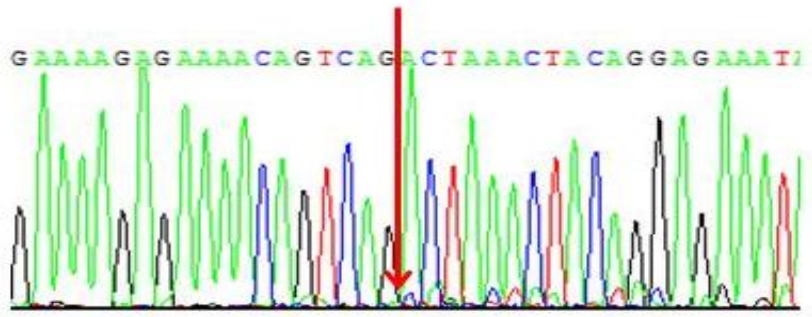

Figure 3.6 Sequencing chromatogram illustrating the additional CAG repeat isoform in a sample with AML. The red arrow indicates the presence of a low level transcript with the additional CAG repeat.

3.3.4 Transduction of UT-7 cells with SFG-c-KIT and SFG-EMPTY constructs

To investigate the impact of different *c-KIT* mutations on cell signalling, cell growth and response to small molecule inhibitors, UT-7 cells were transduced with constructs expressing SFG-c-KIT-WT, SFG-EMPTY, c-KIT-Δ417-419>Y, SFG-c-KIT-L576P, SFG-c-KIT-D816V and SFG-c-KIT-N822K. These mutations were selected as they are representative examples that occur across *c-KIT* in AML. UT-7 cells were selected as they are a factor dependent AML cell line and had no detectable mutations in exons 8, 10+11 and 17 of *c-KIT* and no mutations in exons 14-15 (*FLT3*-ITD) or exon 20 (*FLT3*-TKD) of *FLT3* (data not shown). UT-7 cells were successfully transduced with the various SFG-c-KIT and SFG-EMPTY constructs with transduction efficiencies ranging from 27-95% as assessed by BFP expression using flow cytometry. Cells were subsequently sorted based on BFP on the assumption that BFP expression is equivalent to c-KIT expression. Following cell sorting, BFP and CD117 (c-KIT) expression were simultaneously examined in each transduced cell line. As expected UT-7 native cells were negative for BFP (Figure 3.7a). UT-7 cells transduced with constructs expressing c-KIT-WT, SFG-EMPTY, c-KIT-Δ417-419>Y, SFG-c-KIT-L576P, SFG-c-KIT-D816V and SFG-c-KIT-N822K were all ≥ 97% BFP positive (Figure 3.7a). The UT-7 c-KIT-D816V cells were 97% BFP positive, however they were dimmer in comparison to the other generated cell lines. UT-7 native cells expressed very low levels of CD117 (5%) which was equivalent to UT-7 SFG-EMPTY cells (Figure 3.7b). UT-7 cells expressing c-KIT-WT were the only cells to have approximately equivalent BFP and CD117 expression (median MFI: 3.3 and 3.7 respectively) (Figure 3.7 a,b). In contrast CD117 expression was considerably lower in UT-7 cells expressing c-KIT Δ417-419>Y, c-KIT-L576P, c-KIT-D816V and c-KIT-N822K (median MFI: 1.0, 0.4, 0.5 and 0.7

respectively) (Figure 3.7b). Lower CD117 staining in the *c-KIT* mutant-expressing cells could be due to a lower expression of the 145kDa fully glycosylated mature membrane-bound c-KIT. Mutations in the ALD (D816V) and in the JMD have been reported to be retained in the endoplasmic reticulum and Golgi apparatus, reducing the amount of mature c-KIT receptor reaching the cell surface (Xiang *et al.*, 2007;Tabone-Eglinger *et al.*, 2008). This may explain why UT-7 cells transduced with c-KIT-L576P or c-KIT-D816V had particularly low surface CD117 expression (median MFI: 0.4 and 0.5 respectively) (Figure 3.7b). Western blotting confirmed that all UT-7 cells transduced with constructs expressing c-KIT-WT or mutant c-KIT over-expressed c-KIT in comparison to the UT-7 native or SFG-EMPTY transduced cells (Figure 3.8). UT-7 c-KIT-D816V cells had lower levels of c-KIT expression in comparison to the other c-KIT expressing cells, which is consistent with being dimmer for BFP. UT-7 cells expressing mutant c-KIT did not show a predominance of the 125kDa unglycosylated isoform of c-KIT.

(a) (b)

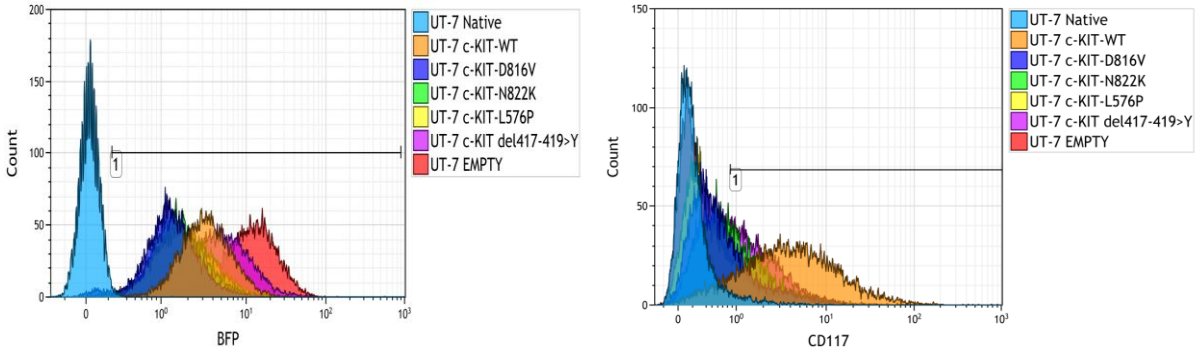

Ref. colour	Cell line	BFP (%[1])	BFP Median (MFI[2])	CD117 (%[1])	CD117 Median (MFI[2])
	UT-7 Native	1.1	0.0	5.1	0.2
	UT-7 c-KIT-WT	100.0	3.3	88.5	3.7
	UT-7 c-KIT-D816V	97.0	1.3	30.5	0.5
	UT-7 c-KIT-N822K	99.0	1.5	42.8	0.7
	UT-7 c-KIT-L576P	99.0	1.7	20.6	0.4
	UT-7 c-KIT-Δ417-419>Y	99.0	4.5	56.1	1
	UT-7 SFG-EMPTY	100.0	11.1	5.0	0.2

Figure 3.7 Examination of (a) BFP and (b) CD117 expression within UT-7 transduced cells. [1]refers to the gated area, [2] refers to the entire cell population.

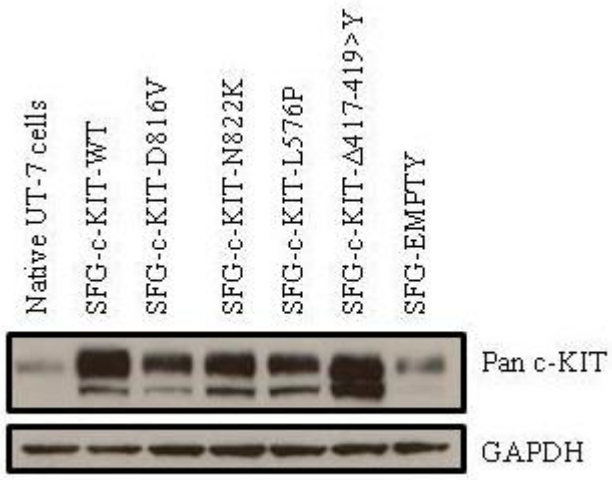

Figure 3.8 Western blotting of transduced UT-7 cells examining total c-KIT expression. GAPDH was used as a loading control.

3.3.5 Impact of *c-KIT* mutations on proliferation

The impact on proliferation of c-KIT-Δ417-419>Y, c-KIT-L576P, c-KIT-D816V and c-KIT-N822K mutants was assessed in transduced UT-7 cells compared with cells expressing c-KIT-WT or SFG-EMPTY (Figure 3.9 a-f). There were equivalent proliferation rates in all cells in the presence of 5ng/mL of GM-CSF and this was not increased by the addition of 5ng/mL or 50ng/mL SCF. UT-7 SFG-EMPTY cells did not proliferate in the absence of GM-CSF and subsequently died after 4-5 days. A low level of SCF (5ng/mL) did not increase proliferation whereas 50ng/mL SCF was sufficient to maintain a low level of proliferation (Figure 3.9a). UT-7 c-KIT-WT cells died in the absence of GM-CSF by day 4-5 and 5ng/mL SCF did not stimulate proliferation. In contrast, 50ng/mL promoted cell proliferation which was comparable to the levels observed in the presence of GM-CSF (Figure 3.9b). c-KIT-Δ417-419>Y expressing cells showed factor-independent growth, which was not significantly increased in the presence of SCF (Figure 3.9c). UT-7 c-KIT-D816V did not die in the absence of GM-CSF but maintained a low level of proliferation which was equivalent in the presence of only 5ng/mL of SCF (Figure 3.9d). Of note, UT-7 c-KIT-WT and c-KIT-D816V cells washed in PBS and starved of GM-CSF for four weeks showed that UT-7 c-KIT-D816V cells could proliferate in the absence of cytokines whereas c-KIT-WT cells died after one week (data not shown). This suggests that c-KIT-D816V can confer factor-independent growth and that 5 days was insufficient time to observe this. Addition of 50ng/mL SCF did increase proliferation rates of c-KIT-D816V expressing cells to an equivalent level to that observed in the presence of GM-CSF. For c-KIT-L576P and c-KIT-N822K expressing cells 5ng/ml SCF was not sufficient to promote proliferation (Figure 3.9 e,f). The presence of 50ng/mL SCF did stimulate cell proliferation in both cell lines, however this did not reach the levels observed in the presence of GM-CSF, and was only slightly greater than the level of proliferation seen treatment in the UT-7 SFG-EMPTY cells treated with 50ng/mL SCF. Overall, c-KIT-Δ417-419>Y and c-KIT-D816V were the only mutants capable of conferring ligand-independent growth.

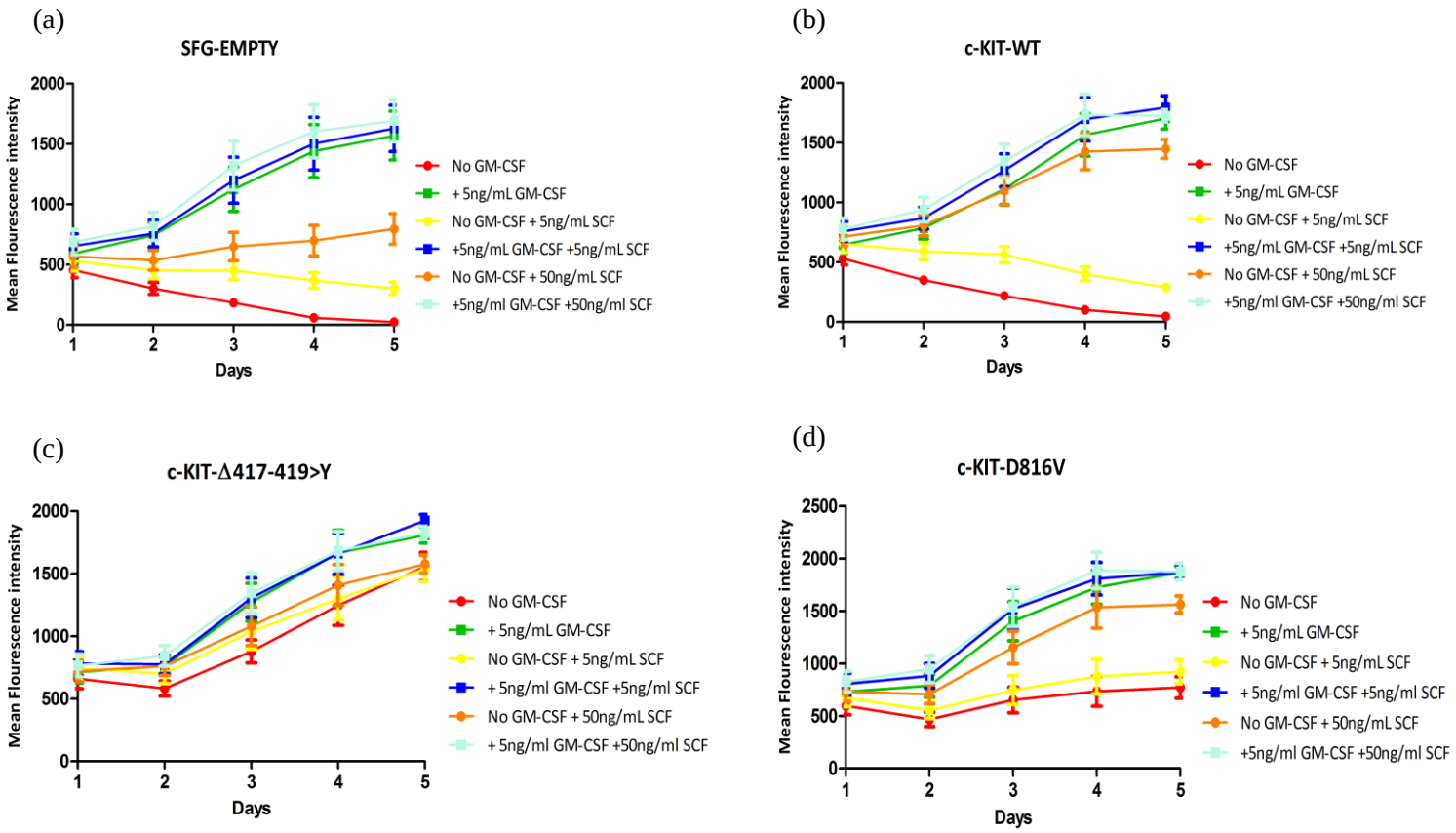
(a)
SFG-EMPTY
Mean Flourescence intensity
2000
1500
1000
500
0
1
2
3
4
5
Days
No GM-CSF
+ 5ng/mL GM-CSF
No GM-CSF + 5ng/mL SCF
+5ng/mL GM-CSF +5ng/mL SCF
No GM-CSF + 50ng/mL SCF
+5ng/ml GM-CSF +50ng/ml SCF
(b)
c-KIT-WT
Mean Flourescence intensity
2000
1500
1000
500
0
1
2
3
4
5
Days
No GM-CSF
+ 5ng/mL GM-CSF
No GM-CSF + 5ng/mL SCF
+5ng/mL GM-CSF +5ng/mL SCF
No GM-CSF + 50ng/mL SCF
+5ng/ml GM-CSF +50ng/ml SCF
(c)
c-KIT-Δ417-419>Y
Mean Flourescence intensity
2000
1500
1000
500
0
1
2
3
4
5
Days
No GM-CSF
+ 5ng/mL GM-CSF
No GM-CSF + 5ng/mL SCF
+ 5ng/ml GM-CSF +5ng/ml SCF
No GM-CSF + 50ng/mL SCF
+ 5ng/ml GM-CSF +50ng/ml SCF
(d)
c-KIT-D816V
Mean Flourescence intensity
2500
2000
1500
1000
500
0
1
2
3
4
5
Days
No GM-CSF
+ 5ng/mL GM-CSF
No GM-CSF + 5ng/mL SCF
+ 5ng/ml GM-CSF +5ng/ml SCF
No GM-CSF + 50ng/mL SCF
+5ng/ml GM-CSF +50ng/ml SCF

(e)

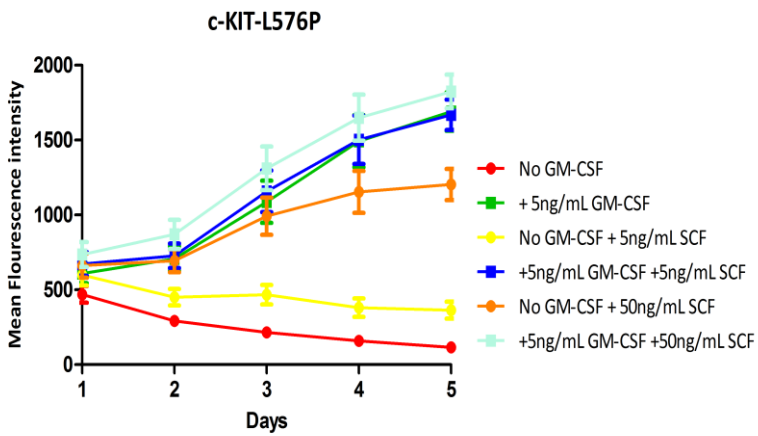

(f)

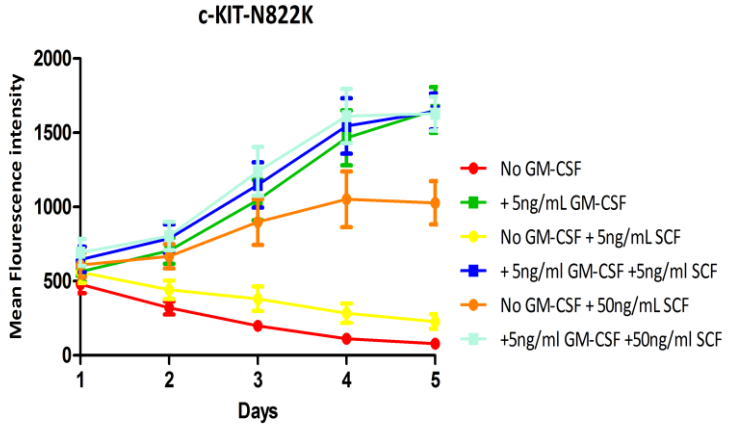

Figure 3.9 The impact of c-KIT-WT, SFG-EMPTY, c-KIT-Δ417-419>Y, c-KIT-D816V, c-KIT-L576P and c-KIT-N822K on proliferation in UT-7 cells. Each cell line were incubated with ± GM-CSF (5ng/mL) in the presence of increasing concentrations of SCF and treated with alamarBlue®. Data shown is the mean ± SEM of three individual experiments.

3.3.6 Impact of *c-KIT* mutations on downstream signalling

To assess differences in c-KIT activation and downstream signalling each cell line was washed with PBS and cultured for eight hours in the presence or absence of 50ng/mL SCF (Figure 3.10). UT-7 native and SFG-EMPTY cells showed no activation of c-KIT or downstream targets in the absence of SCF but stimulation with SCF caused low level phosphorylation of STAT5, MAPK and S6 and up regulation of PIM-1. In the absence of SCF, c-KIT-WT expressing cells showed no activation of c-KIT or downstream targets, but stimulation with SCF caused phosphorylation of c-KIT and activation of STAT5, AKT, MAPK and S6, and up regulation of PIM-1. As the WT receptor is over-expressed in these cells the activation of downstream target proteins was greater than observed in UT-7 native or UT-7 SFG-EMPTY cells.

In the absence of any growth factor, UT-7 c-KIT-Δ417-419>Y showed strong autophosphorylation of c-KIT which corresponded to constitutive activation of downstream target proteins (STAT5, MAPK, PIM-1 and S6) as indicated by the levels of p-STAT5, p-MAPK and p-S6. Of interest, AKT was not activated in these cells and MAPK, although constitutively active was only expressed at a low level. The addition of SCF did not further activate downstream signalling in these cells. In the absence of SCF UT-7 c-KIT-D816V cells showed autophosphorylation of c-KIT however this was weaker than UT-7 c-KIT-Δ417-419>Y cells. Autophosphorylation of c-KIT constitutively activated STAT5, PIM-1 and S6, with a very low level activation of MAPK. Stimulation of c-KIT-D816V expressing cells with SCF further increased activation of these downstream proteins and in addition stimulated low level phosphorylation of AKT. In contrast c-KIT-L576P or c-KIT-N822K expressing cells did not show constitutive c-KIT autophosphorylation nor activation of the majority of downstream target proteins. However, stimulation with SCF did cause phosphorylation of c-KIT, STAT5, AKT, MAPK and S6 and up regulation of PIM-1. There was no difference in activation in downstream signalling in the presence of SCF between UT-7 c-KIT-WT or c-KIT-c-KIT-L576P cells. However, c-KIT-N822K expressing cells did more strongly activate AKT and up regulate PIM-1 in the presence of SCF compared to c-KIT-WT expressing cells. Of note, there was residual S6 phosphorylation in the absence of SCF in these mutant c-KIT transduced cells but not in c-KIT-WT expressing cells suggesting that there may be low level constitutive activation of c-KIT.

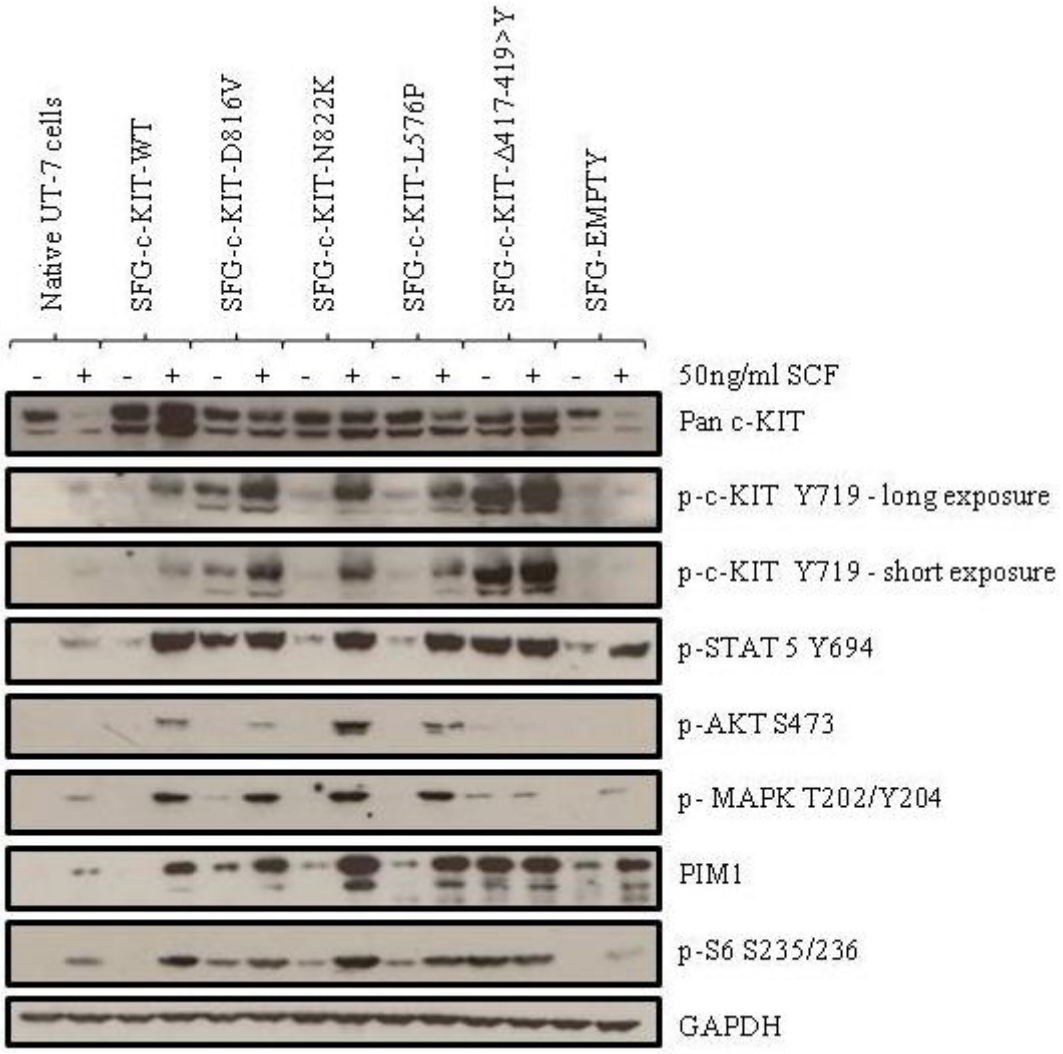

Figure 3.10 UT-7 cells transduced with c-KIT-WT and mutant constructs treated with or without 50ng/mL SCF for 8 hours. Cell lysates were analysed by western blotting using the indicated antibodies. GAPDH was used as a loading control.

3.3.7 Effect of dasatinib treatment on UT-7 cells expressing c-KIT

UT-7 cells transduced with SFG-EMPTY or c-KIT constructs were treated with dasatinib, a known c-KIT and SRC kinase inhibitor, for 72 hours in the presence of 100ng/mL SCF, to evaluate if the different c-KIT mutants had different responses to the inhibitor. UT-7 c-KIT-WT, SFG-EMPTY and c-KIT-L576P expressing cells treated with dasatinib showed no difference in growth inhibition (IC50s 19nM ± 5.8, 15.7nM ± 7.3, 23.1nM ± 3.9 c-KIT-WT, SFG-EMPTY and c-KIT-L576P respectively; WT vs EMPTY P = 0.73, unpaired t-test ; WT vs L576P P = 0.58, unpaired t-test) or cell killing (IC50s 29.4nM ± 5.3, 20.6nM ± 6.2, 29nM ± 2.3 c-KIT-WT, c-KIT-L576P and SFG-EMPTY respectively; WT vs

EMPTY $P = 0.32$, unpaired t-test ; WT vs L576P $P = 0.94$, unpaired t-test) (Figure 3.11 a,b) reflected in Table 3.5. UT-7 c-KIT-Δ417-419>Y cells treated with dasatinib showed no difference in growth inhibition in comparison to UT-7 c-KIT-WT expressing cells (IC50 27.4nM ± 5.4, c-KIT-Δ417-419>Y; WT vs Δ417-419>Y $P = 0.58$, unpaired t-test) however there was a suggestion that these cells were more resistant to cell killing (IC50 53.8nM ± 11.3, c-KIT-Δ417-419>Y; WT vs Δ417-419>Y $P = 0.1$, unpaired t-test). UT-7 c-KIT-D816V cells were significantly more resistant to dasatinib-mediated growth inhibition (IC50 181.2nM ± 39.8, c-KIT-D816V; WT vs D816V $P = 0.007$, unpaired t-test) and cell killing (IC50 316nM ± 50.6, c-KIT-D816V; WT vs D816V $P = 0.001$, unpaired t-test) in comparison to c-KIT-WT expressing cells. UT-7 c-KIT-N822K cells were also more resistant to dasatinib-mediated growth inhibition (IC50 41.4nM ± 3.3, c-KIT-N822K; WT vs N822K $P = 0.02$, unpaired t-test) and cell killing (IC50 77.3nM ± 13.5, c-KIT-N822K; WT vs N822K $P = 0.02$, unpaired t-test) in comparison to UT-7 c-KIT-WT cells.

To demonstrate that the differences in growth inhibition and cell killing were mediated by reduced activation of c-KIT and its downstream target proteins, cell signalling was examined. c-KIT-transduced and SFG-EMPTY cells were washed with PBS and exposed to 0.1, 1, 10, 100, 1000nM dasatinib in the presence of 50ng/mL SCF for 24 hours. In UT-7 c-KIT-WT, SFG-EMPTY, c-KIT-Δ417-419>Y and c-KIT-L576P cells, a concentration of 100nM dasatinib was sufficient to completely inhibit phosphorylation of c-KIT and activation of downstream target proteins (Figure 3.12). A concentration of 100nM dasatinib was also capable of decreasing the pro-survival protein Mcl-1 in these transduced cells. In UT-7 c-KIT-D816V cells 100nM dasatinib did not completely decrease the phosphorylation of c-KIT or activation of downstream target proteins whereas a concentration of 1000nM dasatinib was sufficient to potently decrease phosphorylation of c-KIT, AKT, MAPK and S6. Mcl-1 was only decreased at 1000nM dasatinib in UT-7 c-KIT D816V cells. c-KIT-N822K expressing cells were slightly more resistant to dasatinib at a concentration of 100nM in comparison to c-KIT-WT expressing cells as indicated by residual c-KIT, AKT and S6 phosphorylation. c-KIT-N822K expressing cells were more sensitive to dasatinib in comparison to UT-7 c-KIT-D816V cells.

(a) (b)

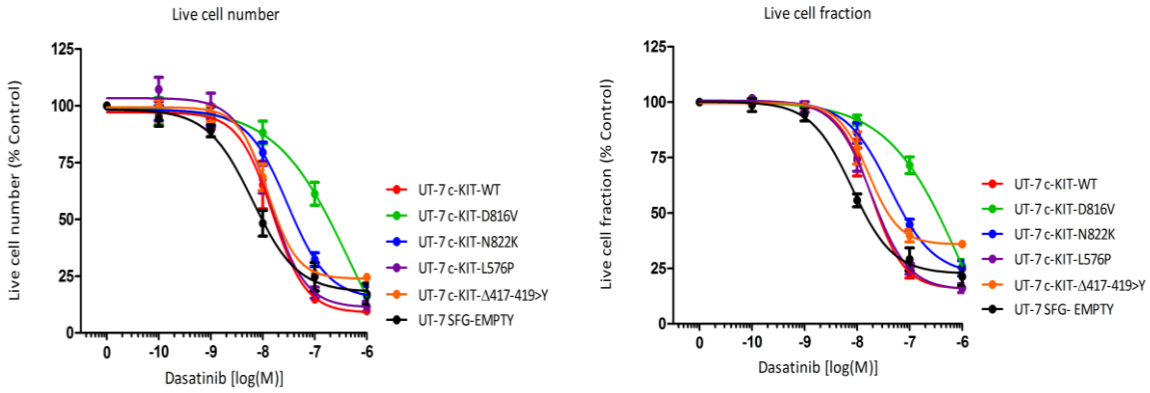

Figure 3.11 Response of transduced UT-7 cells to dasatinib in the presence of 100ng/mL SCF after 72 hours. (a) Total number of live cells. (b) Percentage of cells in the live cell fraction. Data shown is the mean ± SEM of four independent repeats.

Cell line	**Live cell number IC50 (nM)**	**Live cell fraction IC50 (nM)**
UT-7 c-KIT-WT	19 ± 5.8	29.4 ± 5.3
UT-7 c-KIT-D816V	181.2 ± 39.8	316 ± 50.6
UT-7 c-KIT-N822K	41.4 ± 3.3	77.3 ± 13.5
UT-7 c-KIT-L576P	23.1 ± 3.9	29 ± 2.3
UT-7 c-KIT-Δ417-419>Y	27.4 ± 5.4	53.8 ± 11.3
UT-7 SFG-EMPTY	15.7 ± 7.3	20.6 ± 6.2

Table 3.5 Live cell number and live cell fraction IC50 values from UT-7 transduced cells treated with dasatinib.

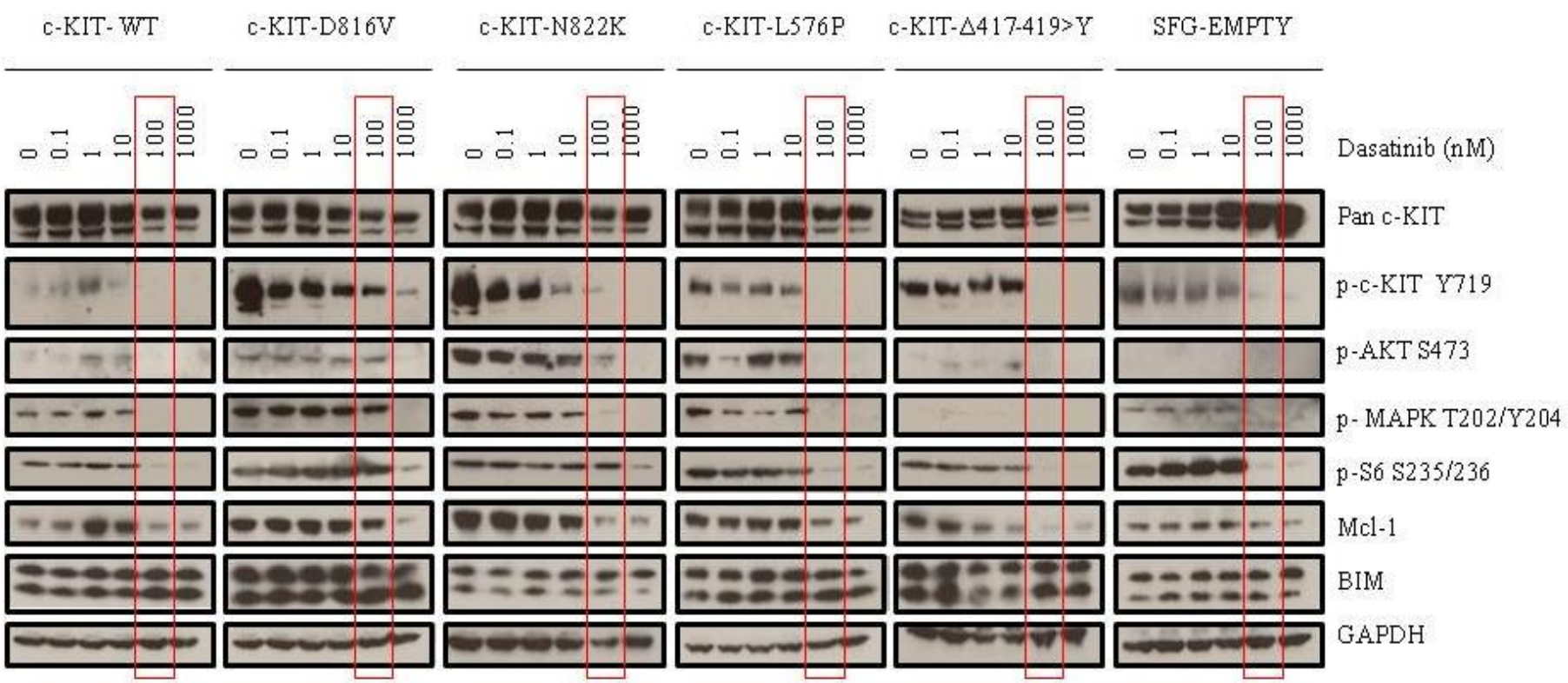

Figure 3.12 Western blots of UT-7 transduced cells treated with 0.1-1000nM of dasatinib, in the presence of 50ng/mL SCF for 24 hours. The boxed areas highlight differential responses to dasatinib between the respective cell lines. GAPDH was used as a loading control.

3.3.8 Response of UT-7 cells expressing c-KIT to dasatinib and BEZ-235

c-KIT-D816V and *c-KIT*-N822K mutations have previously been reported to activate PI3K/AKT and mTOR (Ning *et al.*, 2001;Growney *et al.*, 2005;Schittenhelm *et al.*, 2006;Wang *et al.*, 2011). In Figure 3.10 UT-7 cells expressing mutant c-KIT showed constitutive activation of mTOR, as indicated by phosphorylation of S6, but there was no detectable phosphorylation of AKT. It was therefore hypothesised that a combination of dasatinib and BEZ-235, the dual PI3K/mTOR inhibitor, may overcome the resistance to dasatinib observed and sensitise the cells to a greater level of cell killing. Each cell line was washed with PBS and treated with 12.5, 25, 50 and 100nM dasatinib in combination with 0.125, 0.25 and 0.5μM BEZ-235 in the presence of 100ng/mL SCF for 72 hours. c-KIT-WT, c-KIT-Δ417-419>Y and c-KIT-L576P expressing cells treated with dasatinib showed equivalent growth inhibition and cell killing (Figure 3.13 a,b,g,h,i,j). c-KIT D816V and c-KIT-N822K expressing cells were more resistant to dasatinib-mediated growth inhibition and cell killing in comparison to UT-7 c-KIT-WT cells, the former being most resistant (Figure 3.13 c,d,e,f) All of the transduced UT-7 cells treated with BEZ-235 showed an equivalent dose dependent decrease in cell proliferation and cell killing. A combination of dasatinib and BEZ-235 only slightly increased growth inhibition and cell killing, compared to dasatinib alone in c-KIT-WT, c-KIT-Δ417-419>Y and c-KIT-L576P expressing cells. A combination of dasatinib and BEZ-235 was capable of overcoming some of the resistance observed with dasatinib alone in UT-7 c-KIT-D816V and c-KIT-N822K cells, by sensitizing the cells to a greater level of growth inhibition and cell killing in comparison to either drug alone (Figure 3.13 c-f).

CalcuSyn was used to assess if the interactions between dasatinib and BEZ-235 was synergistic in each UT-7 c-KIT transduced cell line at inducing cell killing. Dasatinib and BEZ-235 showed a weak additive or slight synergistic effect in UT-7 cells harbouring c-KIT-WT and c-KIT-L576P at an ED50, ED75 or ED90 (Table 3.6). UT-7 cells expressing c-KIT-Δ417-419>Y and N822K were more sensitive to this drug combination as indicated by CI values at an ED90 of 0.61 and 0.59 respectively. Dasatinib and BEZ-235 showed the strongest synergistic effect in UT-7 c-KIT-D816V cells as indicated by CI values at an ED50, ED75 and ED90 of 0.54, 0.406 and 0.31 respectively. This data suggests that targeted blockade of c-KIT and PI3K/mTOR could specifically enhance cell killing in cells harbouring *c-KIT*-Δ417-419>Y, *c-KIT*-D816V or *c-KIT*-N822K mutations.

3.3.9 Impact of dasatinib and BEZ-235 on c-KIT and downstream signalling in c-KIT transduced UT-7 cells

Western blotting was used to examine the impact of dasatinib and BEZ-235 on downstream signalling in UT-7 transduced cells. Each cell line was washed with PBS and incubated with no inhibitor, 100nM dasatinib, 0.5μM BEZ-235 or a combination of both inhibitors for 24 hours in the presence of 50ng/mL SCF. Dasatinib alone reduced phosphorylation of c-KIT, STAT5 and MAPK in all UT-7 transduced cells however there was residual mTOR signalling, as indicated by p-4E-BP1, in all cell lines and p-S6 in UT-7 c-KIT-D816V and c-KIT-N822K cells (Figure 3.14). UT-7 c-KIT-D816V cells also had residual AKT signalling, as indicated by p-AKT. BEZ-235 alone reduced phosphorylation of PI3K/mTOR targets, as indicated by p-AKT and p-4E-BP1, in all cell lines but had little or no impact on p-c-KIT, p-STAT5, p-MAPK or p-S6. In the presence of dasatinib and BEZ-235 residual mTOR signalling was eliminated as demonstrated by a reduction in p-4E-BP1 in all transduced cells and a potent decrease in p-S6 in UT-7 c-KIT-D816V and c-KIT-N822K cells. Dasatinib and BEZ-235 also reduced residual AKT signalling in c-KIT-D816V expressing cells. Inhibition of residual mTOR and AKT signalling may have contributed to the decrease in cell proliferation and increase in apoptosis observed in Figure 3.13. In general the pro-survival protein Mcl-1 decreased in the presence of both dasatinib and BEZ-235 which corresponded with an increase in the pro-apoptotic protein BIM in all UT-7 transduced cells. The effect of dasatinib and BEZ-235, compared to either drug alone, was most prominent in c-KIT-D816V expressing cells which may explain why this drug combination showed the strongest synergistic effect on cell killing.

(a)

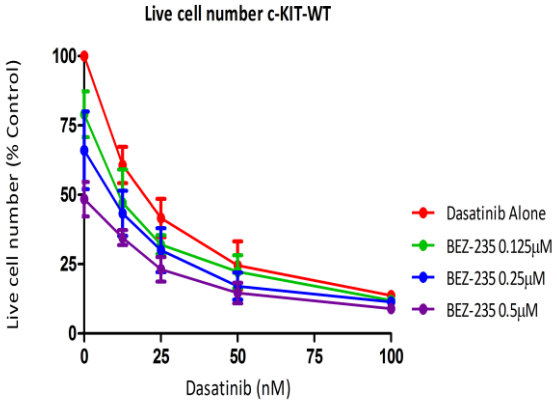
Live cell number c-KIT-WT
Live cell number (% Control)
100
75
50
25
0
0
25
50
75
100
Dasatinib (nM)
Dasatinib Alone
BEZ-235 0.125μM
BEZ-235 0.25μM
BEZ-235 0.5μM

(b)

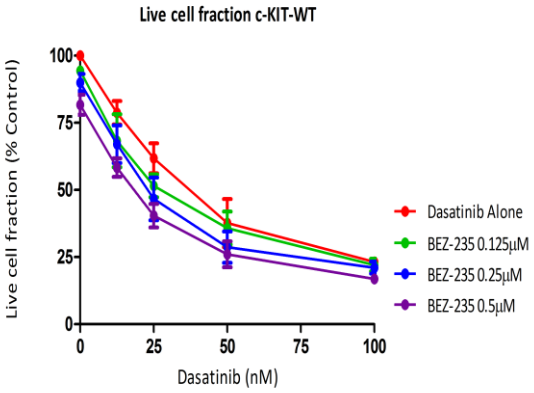
Live cell fraction c-KIT-WT
Live cell fraction (% Control)
100
75
50
25
0
0
25
50
75
100
Dasatinib (nM)
Dasatinib Alone
BEZ-235 0.125μM
BEZ-235 0.25μM
BEZ-235 0.5μM

(c)

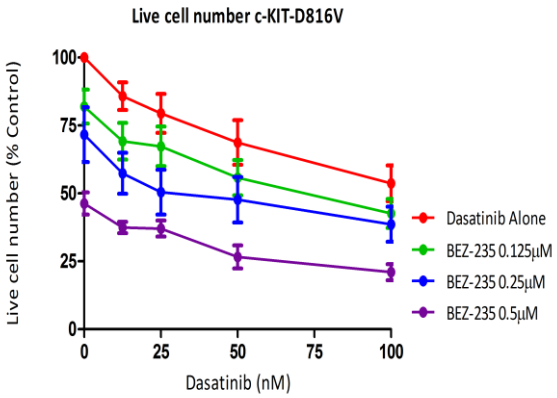
Live cell number c-KIT-D816V
Live cell number (% Control)
100
75
50
25
0
0
25
50
75
100
Dasatinib (nM)
Dasatinib Alone
BEZ-235 0.125μM
BEZ-235 0.25μM
BEZ-235 0.5μM

(d)

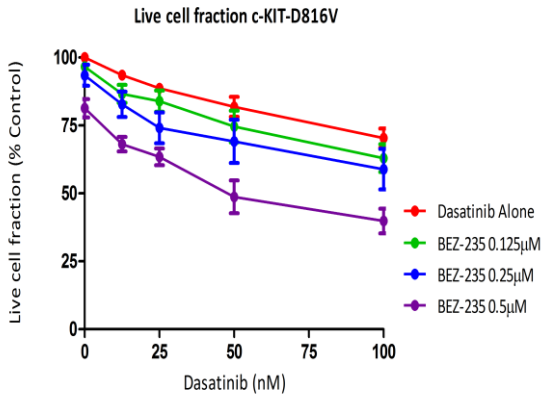
Live cell fraction c-KIT-D816V
Live cell fraction (% Control)
100
75
50
25
0
0
25
50
75
100
Dasatinib (nM)
Dasatinib Alone
BEZ-235 0.125μM
BEZ-235 0.25μM
BEZ-235 0.5μM

(e)

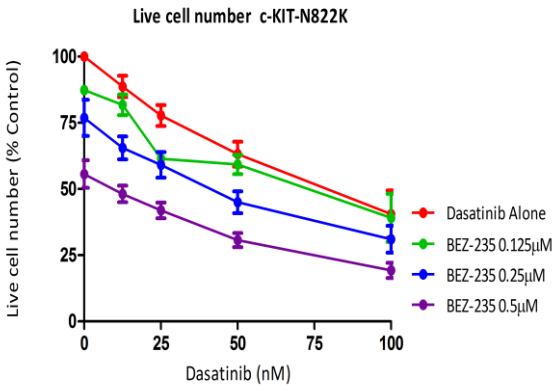
Live cell number c-KIT-N822K
Live cell number (% Control)
100
75
50
25
0
0
25
50
75
100
Dasatinib (nM)
Dasatinib Alone
BEZ-235 0.125μM
BEZ-235 0.25μM
BEZ-235 0.5μM

(f)

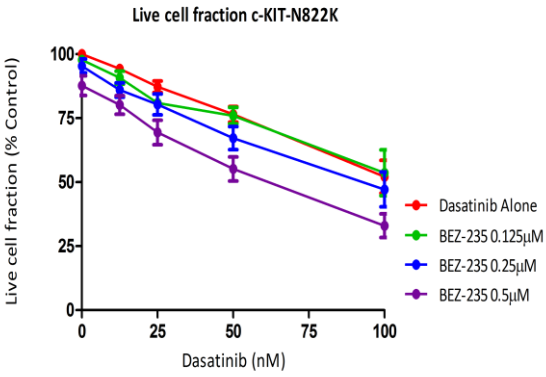
Live cell fraction c-KIT-N822K
Live cell fraction (% Control)
100
75
50
25
0
0
25
50
75
100
Dasatinib (nM)
Dasatinib Alone
BEZ-235 0.125μM
BEZ-235 0.25μM
BEZ-235 0.5μM

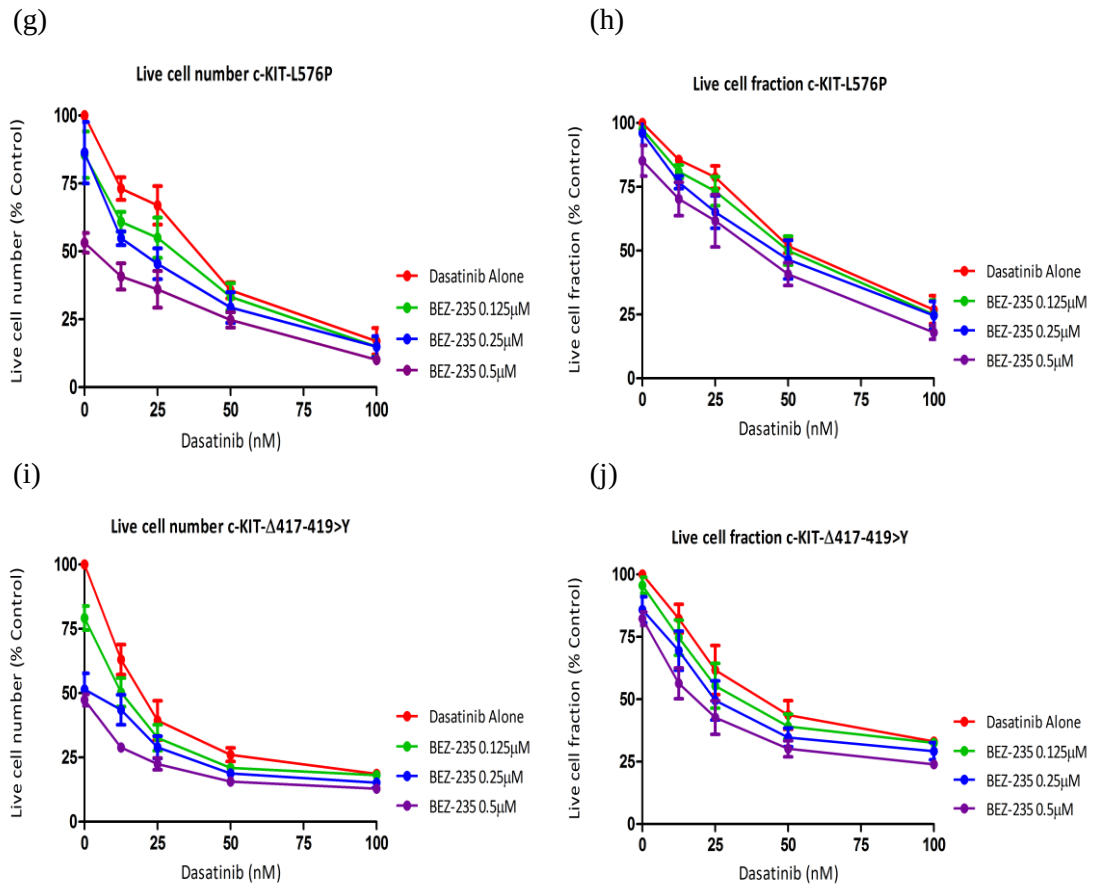

Figure 3.13 Response of transduced UT-7 cells to combinations of dasatinib and BEZ-235 in the presence of 100ng/mL SCF after 72 hours. (a,c,e,g,i) Total number of live cells. (b,d,f,h,j) Percentage of cells in the live cell fraction. Data shown is the mean ± SEM of three or four individual experiments.

		CI Values at:		
Drug Combination	**Cell line**	ED50	ED75	ED90
Dasatinib + BEZ-235 (1:5)	c-KIT-WT	0.76	0.76	0.76
Dasatinib + BEZ-235 (1:5)	c-KIT-D816V	0.54	0.406	0.31
Dasatinib + BEZ-235 (1:5)	c-KIT-N822K	0.76	0.676	0.59
Dasatinib + BEZ-235 (1:5)	c-KIT-L576P	0.94	0.876	0.81
Dasatinib + BEZ-235 (1:5)	c-KIT-Δ417-419>Y	0.78	0.69	0.61

CI = Combination Index value, ED = Effective dose

Table 3.6 CI values for the cell killing data of transduced UT-7 cells treated with dasatinib and BEZ-235.

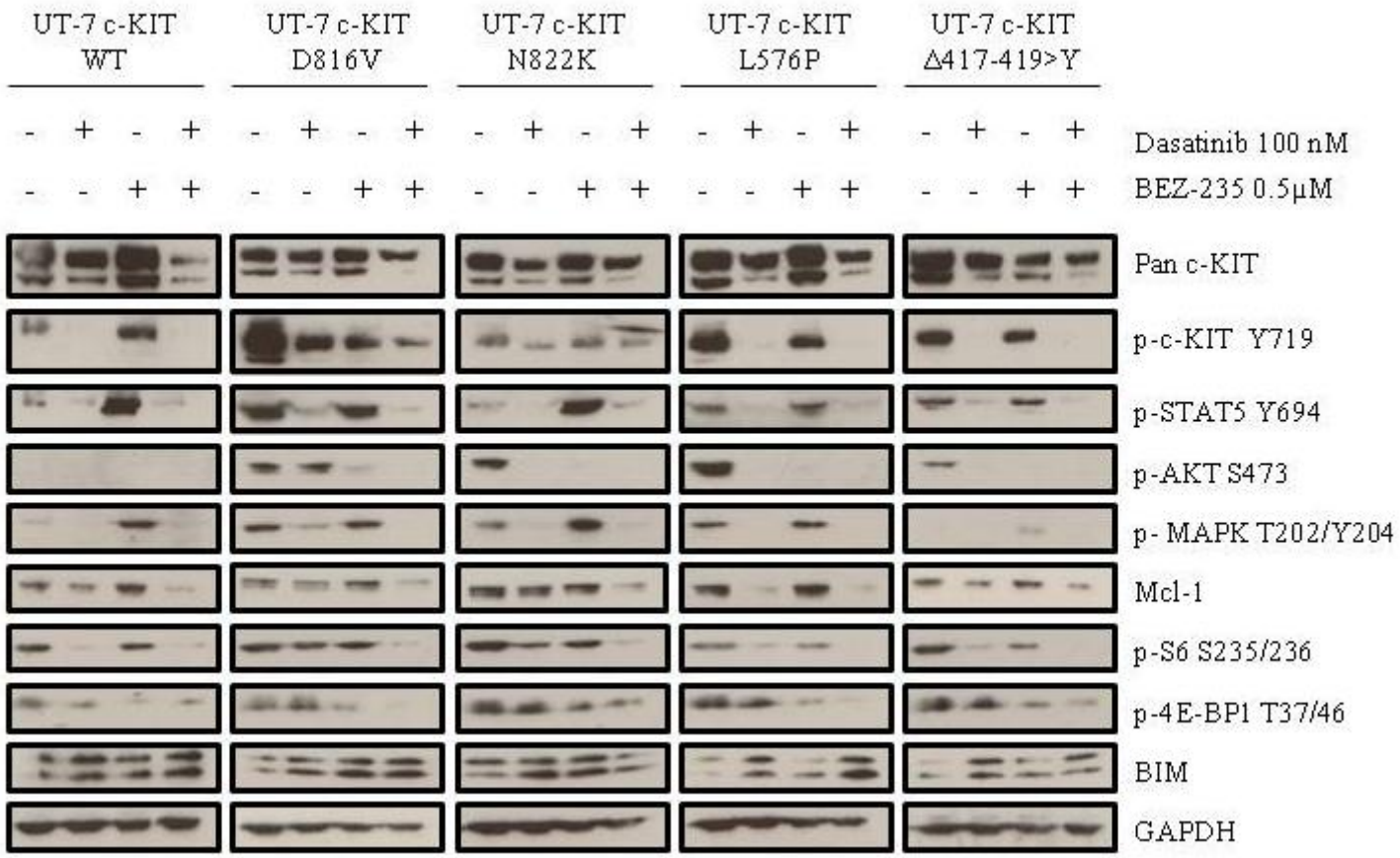

Figure 3.14 Effect of dasatinib and BEZ-235 on c-KIT and downstream signalling in UT-7 transduced cells. Cells were treated with each inhibitor for 24 hours in the presence of 50ng/mL SCF. Cell lysates were analysed by western blotting using the indicated antibodies. GAPDH was used as a loading control.

3.3.10 Effect of masitinib treatment on UT-7 cells expressing c-KIT

To examine if the differential response to dasatinib observed in the UT-7 c-KIT-expressing cells is limited to this inhibitor, the various cell lines were treated with another ATP competitive inhibitor, masitinib. Each cell line was washed with PBS and treated with 0.1, 1, 10, 100, 1000, 10,000nM masitinib, in the presence of 100ng/mL SCF for 72 hours. Treatment of UT-7 c-KIT-WT, SFG-EMPTY, c-KIT-Δ417-419>Y and c-KIT-L576P expressing cells with masitinib showed no significant difference in growth inhibition (IC50s 443nM ± 80, 258nM ± 27, 181nM ± 62, 236nM ± 27 c-KIT-WT, SFG-EMPTY, c-KIT-Δ417-419>Y and c-KIT-L576P respectively; WT vs SFG-EMPTY $P = 0.09$, unpaired t-test ; WT vs c-KIT-Δ417-419>Y $P = 0.06$, unpaired t-test ; WT vs c-KIT-L576P $P = 0.07$, unpaired t-test) or cell killing (IC50s 689nM ± 165, 358nM ± 11, 351nM ± 66, 236nM ± 17 c-KIT-WT, SFG-EMPTY, c-KIT-Δ417-419>Y and c-KIT-L576P respectively; WT vs SFG-EMPTY $P = 0.12$, unpaired t-test ; WT vs c-KIT-Δ417-419>Y $P = 0.13$, unpaired t-test ; WT vs c-KIT-L576P $P = 0.12$, unpaired t-test) (Figure 3.15 a,b), IC50s listed in Table 3.7. Of note, UT-7 c-KIT-WT expressing cells were less responsive to masitinib in comparison to SFG-EMPTY, c-KIT-Δ417-419>Y and c-KIT-L576P expressing cells. UT-7 c-KIT-D816V cells were significantly more resistant to dasatinib-mediated growth inhibition (IC50 5307nM ± 2378, c-KIT-D816V; WT vs D816V $P = 0.02$, unpaired t-test) and cell killing (IC50 12388nM ± 3005, c-KIT-D816V; WT vs D816V $P = 0.02$, unpaired t-test) in comparison to UT-7 c-KIT-WT expressing cells. c-KIT-N822K expressing cells were also significantly more resistant than UT-7 c-KIT-WT cells to masitinib-mediated growth inhibition (IC50 2104nM ± 295, c-KIT-N822K; WT vs N822K $P = 0.01$, unpaired t-test) and cell killing (IC50 3084nM ± 227, c-KIT-N822K; WT vs N822K $P = 0.001$, unpaired t-test). This suggests that mutations in the ALD may prevent masitinib from binding effectively to c-KIT. Comparing the IC50s listed in Table 3.5 and Table 3.7 for each UT-7 transduced cell line treated with either dasatinib or masitinib shows that dasatinib was more potent at inhibiting cell growth and cell killing.

(a) (b)

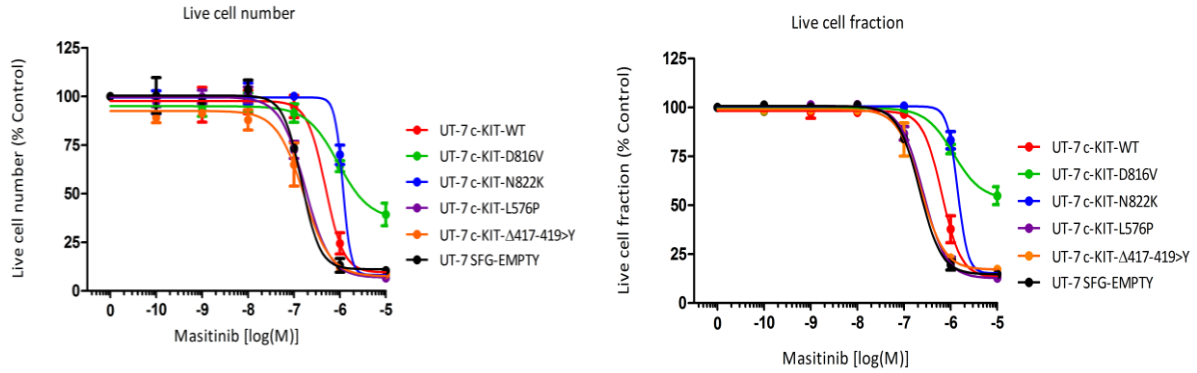

Figure 3.15 Response of transduced UT-7 cells to masitinib in the presence of 100ng/mL SCF after 72 hours. (a) Total number of live cells. (b) Percentage of cells in the live cell fraction. Data shown is the mean ± SEM three independent repeats.

Cell line	Live cell number IC50 (nM)	Live cell fraction IC50 (nM)
UT-7 c-KIT-WT	443 ± 80	689 ± 165
UT-7 c-KIT-D816V	5307 ± 2378	>10,000
UT-7 c-KIT-N822K	2104 ± 295	3084 ± 227
UT-7 c-KIT-L576P	236 ± 27	364 ± 17
UT-7 c-KIT-Δ417-419>Y	181 ± 62	351 ± 66
UT-7 SFG-EMPTY	258 ± 27	358 ± 11

Table 3.7 Live cell number and live cell fraction IC50 values from UT-7 transduced cells treated with masitinib.

3.4 Discussion

In order to investigate the functional consequence of *c-KIT* mutants, a construct containing the *c-KIT* coding sequence was purchased from OriGene. Sequencing of this construct revealed the presence of the GGTAACAACAAA (GNNK+) insert and CAG (Q) repeat. The GNNK+ isoform has previously been described as an alternative splice variant (Crosier *et al.*, 1993) while the additional CAG repeat at the end of exon 4 is reported by OriGene to be a naturally occurring polymorphism (SC120061). It was important to establish which of these *c-KIT* isoforms was the primary transcript as the c-KIT GNNK- protein has been shown to have stronger activation of PI3K/AKT than the c-KIT GNNK+ isoform, resulting in increased cell survival/proliferation in comparison to cells expressing the c-KIT GNNK+ protein (Pedersen *et al.*, 2009). Samples with AML were therefore evaluated for the presence or absence of the GNNK transcript. Expression of both the *c-KIT* GNNK- and GNNK+ isoforms were detected in 63% of the samples with a median GNNK+ isoform expression in of 5.5% (range 1-13%). This showed that the GNNK- isoform was the primary transcript in the samples with AML examined, consistent with a previous report (Guerrini *et al.*, 2007). As the GNNK+ isoform was identified as a low level transcript four samples with AML were sequenced directly to examine the level of the additional CAG (Q) repeat isoform. The additional CAG repeat was a minor transcript in all four samples. The functional consequence of this additional CAG repeat is currently unknown. As a result *c-KIT* was cloned by overlapping extension PCR from the pCMV6-XL-c-KIT construct removing the GNNK+ insert and the CAG repeat at the end of exon 4.

Plasmid constructs were generated expressing c-KIT-WT, SFG-EMPTY, c-KIT-Δ417-419>Y, c-KIT-L576P, c-KIT-D816V and c-KIT-N822K and transduced into UT-7 cells to investigate the functional consequence of different *c-KIT* mutations. These mutations were selected as they are representative examples of mutations that occur across the receptor in AML. The *c-KIT*-Δ417-419>Y mutation is representative of an ECD mutation as residues 417-419 are most commonly deleted in CBFL, the *c-KIT*-L576P mutation is an example of a JMD mutation that is also frequently found in melanoma and the *c-KIT*-D816V and *c-KIT* N822K mutations are the most common point mutations in the ALD (Care *et al.*, 2003;Goemans *et al.*, 2005;Wang, 2005;Paschka *et al.*, 2006;Shimada *et al.*, 2007). Mutations in the ECD have been shown to render c-KIT hyper-sensitive to SCF, stimulate autophosphorylation of the receptor and induce factor independent growth in murine Ba/F3 and FDC-P1 cell lines (Kohl *et al.*, 2005;Growney *et al.*, 2005;Nick *et al.*, 2011). The *c-KIT*-Δ417-419>Y mutation has not been assessed in an *in vitro* system. The *c-KIT*-L576P mutation has been stably expressed in Ba/F3 cells which showed autophosphorylation of c-

KIT however the impact on growth has not been examined (Antonescu *et al.*, 2007;Wang *et al.*, 2011). Mutations in the ALD including *c-KIT*-D816V and N822K have also been shown to cause autophosphorylation of c-KIT, ligand-independent growth and activation of STAT5, STAT3, PI3K, AKT and ERK in murine and human factor dependent cell line models (Ning *et al.*, 2001;Growney *et al.*, 2005;Schittenhelm *et al.*, 2006;Wang *et al.*, 2011).

UT-7 c-KIT-Δ417-419>Y, c-KIT-L576P, c-KIT-D816V and c-KIT-N822K cells expressed 4, 9, 7 and 5 times respectively lower cell surface c-KIT in comparison to c-KIT-WT expressing cells. Total c-KIT protein level was assessed by western blotting which showed equivalent expression between c-KIT-WT, c-KIT-L576P and c-KIT-N822K expressing cells. In contrast UT-7 c-KIT-D816V cells had slightly lower total c-KIT levels in comparison to c-KIT-WT cells whereas c-KIT-Δ417-419>Y expressing cells had twice as much total c-KIT protein. This suggests that the mutant receptors may be retained in the endoplasmic reticulum and/or Golgi apparatus in the transduced cells, which has been reported in other studies using c-KIT transduced cell line models (Xiang *et al.*, 2007;Tabone-Eglinger *et al.*, 2008). Alternatively, it has been shown that c-KIT-D816V can constitutively phosphorylate Cbl leading to ubiquitin degradation of the receptor (Sun *et al.*, 2009). This may have contributed to a lower expression of c-KIT in the mutant c-KIT expressing cells; in particular it may explain why surface expression and total c-KIT was lower in c-KIT-D816V expressing cells.

Initial experiments investigated the impact of the different *c-KIT* mutations on proliferation. Expression of c-KIT-L576P or c-KIT-N822K did not confer factor independent growth, and there was low/no detectable autophosphorylation of c-KIT and activation of downstream proteins. Previous reports have shown that expression of c-KIT-L576P or c-KIT-N822K in Ba/F3 cells led to constitutive activation of c-KIT and factor independent growth (Growney *et al.*, 2005;Antonescu *et al.*, 2007). Discrepancies may relate to other studies selecting their transduced cells for antibiotic resistance prior to use whereas this study sorted transduced cells based on BFP expression. Alternatively it could be due to the different properties of the cell line models used. Only UT-7 cells expressing c-KIT-Δ417-419>Y and c-KIT-D816V exhibited factor independent growth; greater in UT-7 c-KIT-Δ417-419>Y cells than UT-7 c-KIT-D816V cells. UT-7 c-KIT Δ417-419>Y cells showed a higher level of c-KIT autophosphorylation and activation of STAT5, S6 and up regulation of PIM-1 in comparison to UT-7 c-KIT-D816V expressing cells which may explain why UT-7 c-KIT Δ417-419>Y cells had a greater growth advantage. Similar mutations in the ECD and the D816V mutation have previously been reported to constitutively active c-KIT and confer factor independent

growth in cell line models (Kohl *et al.*, 2005;Growney *et al.*, 2005;Pedersen *et al.*, 2009;Sun *et al.*, 2009;Nick *et al.*, 2011).

Investigation of cell signalling in UT-7 cells expressing mutant c-KIT revealed that c-KIT-Δ417-419>Y only weakly activated p-MAPK and p-AKT, even in the presence of SCF, whereas c-KIT-WT, c-KIT-L576P, c-KIT-D816V and c-KIT-N822K expressing cells treated with SCF increased phosphorylation of both these proteins. This suggests that mutations in the ECD may activate different cell signalling molecules compared to mutations in the ALD or JMD. This is supported by mouse model data showing co-expression of c-KIT T417IΔ418-419 and RUNX1/RUNX1T1 exclusively generated an AML phenotype whereas mice co-expressing c-KIT-D814V and RUNX1/RUNX1T1 variably developed AML, a myeloproliferative disease or a pre-B-cell leukaemia (Nick *et al.*, 2011).

As the UT-7 transduced cells had various transforming capabilities it was of interest to assess the response of each cell line to dasatinib and masitinib, c-KIT inhibitors. In the data shown here, c-KIT-WT, c-KIT-Δ417-419>Y and c-KIT-L576P expressing cells were all approximately equivalent in their sensitivity to dasatinib-mediated growth inhibition, cell killing and reduction in phosphorylation of c-KIT. UT-7 c-KIT-D816V cells were more resistant to growth inhibition, cell killing and reducing phosphorylation of c-KIT and downstream target proteins. For example UT-7 c-KIT-D816V cells were ten times more resistant to dasatinib-mediated cell killing compared to UT-7 c-KIT-WT cells. The UT-7 c-KIT-N822K cells were more resistant to dasatinib than UT-7 c-KIT-WT cells, however this was less pronounced than UT-7 c-KIT-D816V cells. The reason for these differences may relate to conformational changes conferred by the different mutations. When c-KIT is in its inactive form it adopts an autoinhibited conformation whereby the ALD folds back into the ATP-binding cleft, blocking the loading of substrates (Mol *et al.*, 2004). In this conformation, the Asp810-Phe811-Gly812 (DFG) motif, found at the amino-terminal end of the ALD, is flipped away from the active site (DFG OUT). When SCF binds to c-KIT it causes the receptor to dimerise. This results in phosphorylation of key residues in the cytoplasmic domain (Y547, Y553, Y568, and Y570), causing a conformational change which releases the JMD from the kinase domain (DiNitto *et al.*, 2010). This releases the ALD from a 'packed' position to an 'extended' form whereby the DFG motif adopts an 'IN' position, allowing ATP and substrates to bind to the catalytic site. Modelling of the binding mechanism of dasatinib to c-KIT indicated that it is a type I inhibitor showing preferential binding to the catalytic site of the receptor in its active conformation (Shah *et al.*, 2006). Modelling of dasatinib binding to the c-KIT-D816V mutation suggested that mutations at this residue should not significantly alter binding to c-KIT (Shah *et al.*, 2006). Data presented here

demonstrates that mutations in the ALD may cause secondary changes in the ATP-binding cleft reducing the affinity of dasatinib for the mutant receptors.

To try and overcome some of the resistance to dasatinib observed in the c-KIT-D816V expressing cells, each cell line was treated with a combination of dasatinib and varying concentrations of BEZ-235, a dual PI3K/mTOR inhibitor. BEZ-235 was selected as c-KIT mutations are known to activate PI3K/AKT and mTOR (Ning *et al.*, 2001;Growney *et al.*, 2005;Schittenhelm *et al.*, 2006;Wang *et al.*, 2011). In UT-7 c-KIT-D816V expressing cells dasatinib did reduce phosphorylation of c-KIT in a dose dependent manner, however there was still strong activation of PI3K/AKT and mTOR targets including AKT and S6 (Figure 3.12). Therefore, it was proposed that targeted blockade of c-KIT and PI3K/mTOR may sensitise c-KIT-D816V expressing cells to a greater level of cell killing. UT-7 c-KIT-D816V expressing cells treated with dasatinib and BEZ-235 showed the strongest synergistic effect on cell killing which was most likely mediated by a reduction in residual AKT and mTOR signalling compared with either inhibitor alone. Dasatinib and BEZ-235 showed a moderate additive or synergistic effect on cell killing in UT-7 c-KIT-WT, c-KIT-Δ417-419>Y, c-KIT-L576P and c-KIT-N822K cells which may be due to an enhanced reduction in the pro-survival protein Mcl-1 and an increase in BIM, not observed with either drug alone. This indicated that a combination of dasatinib and BEZ-235 had beneficial effects in all of the c-KIT transduced cells.

Finally, each c-KIT transduced cell line was treated with masitinib to examine if the dose responses observed to dasatinib were restricted to this drug. Masitinib was selected as this is also a type I inhibitor that can target the WT receptor and certain *c-KIT* mutations. Masitinib was not as potent at inhibiting cell growth and inducing cell killing as dasatinib which is indicated when the IC50 values are compared for each cell line treated with each drug (Table 3.5 and Table 3.7). SFG-EMPTY, c-KIT-Δ417-419>Y and c-KIT-L576P expressing cells were most sensitive to masitinib. The c-KIT-Δ417-419>Y and c-KIT-L576P mutations may be more sensitive to masitinib because these mutations are thought to stabilise the ALD in a more active conformation, thereby increasing the binding affinity for masitinib. c-KIT-WT expressing cells were approximately 2 fold more resistant to growth inhibition and cell killing in comparison to SFG-EMPTY, c-KIT-Δ417-419>Y and c-KIT-L576P cells. The differences in response of c-KIT-WT and SFG-EMPTY expressing cells to masitinib may be due to differences in drug receptor occupancy. UT-7 c-KIT-WT cells express a higher level of c-KIT compared to SFG-EMPTY expressing cells which suggests a greater concentration of masitinib would be required to saturate the receptors and mediate a response. In contrast, UT-7 c-KIT-D816V and c-KIT-N822K cells were considerably more

resistant to masitinib-mediated growth inhibition and cell killing in comparison to c-KIT-WT, SFG-EMPTY, c-KIT-Δ417-419>Y and c-KIT-L576P cells. Recent bioinformatic analysis of c-KIT-D816V X-ray structures has suggested that mutations at this residue not only modify the ALD but can also remodel the JMD by favouring removal of the JMD from the TKD, and this is proposed to further activate the receptor (Laine *et al.*, 2011). This supports the notion that mutations in the ALD may cause secondary structural changes that could prevent effective binding of inhibitors such as dasatinib and masitinib to the active site of c-KIT. This may pose implications not only for the treatment of AML but also for other diseases including systemic mastocytosis (SM). The presence of the *c-KIT*-D816V mutation has been reported to occur in 93% of patients with SM and has become an attractive therapeutic target for this disease (Garcia-Montero, 2006). However, clinical trials using dasatinib to treat SM have yielded disappointing results (Purtill *et al.*, 2008;Verstovsek *et al.*, 2008). This could be due to dasatinib being less effective at inhibiting c-KIT in the presence of the D816V mutation.

In summary this chapter aimed to evaluate if all *c-KIT* mutations should be considered the same. To address this UT-7 cells were transduced with c-KIT-Δ417-419>Y, c-KIT-L576P, c-KIT-D816V and c-KIT-N822K as representative examples of mutations that occur in AML. This is the first direct comparison of *c-KIT* mutations occurring in different domains expressed in a human AML cell line. There were intrinsic differences in signal strengths between the mutants examined, only c-KIT-Δ417-419>Y and c-KIT-D816V expressing cells constitutively activated c-KIT in the absence of SCF and conferred ligand-independent growth. There were also differences in the level of factor independent growth and downstream signalling between these two mutants. Each *c-KIT* mutant expressing cell line was treated with RTK inhibitors including dasatinib and masitinib. UT-7 cells expressing *c-KIT* mutations in the ALD were more resistant to dasatinib or masitinib-mediated cell killing in comparison to cells expressing *c-KIT* mutations in the ECD and JMD. The resistance to dasatinib observed in UT-7 cells expressing c-KIT-D816V or c-KIT-N822K could be overcome by co-blockade of c-KIT and PI3K/mTOR. This data suggests that all c-KIT mutations cannot be considered the same and that screening for mutations in *c-KIT* may be imperative as the domain they occur in can affect the sensitivity to c-KIT inhibitors. The impact of c-KIT inhibitors in CBFL patients is currently ongoing in several clinical trials (trials NCT00850382 and NCT02013648).

4. Chapter 4: Identification and functional analysis of a novel *FLT3* activating mutation in CBFL

4.1 Introduction

FLT3-TKD mutations occur in 5-10% of patients with AML (Frohling *et al.*, 2007;Mead *et al.*, 2007). Mutations within the TKD constitutively activate FLT3, promoting ligand-independent growth and activation of downstream target proteins such as AKT and MAPK (Reindl *et al.*, 2006;Rocnik *et al.*, 2006;Frohling *et al.*, 2007). The clinical implications of *FLT3*-ITD mutations on prognosis in AML have been assessed in large patient cohorts showing an adverse impact on outcome, but the impact *FLT3*-TKD mutations have on outcome is unclear (Mead *et al.*, 2007;Whitman *et al.*, 2008). Although the prognostic significance of *FLT3*-TKD mutations is debatable, patients with *FLT3*-TKD mutations have shown clinical responses to FLT3 inhibitors (Fiedler *et al.*, 2005). Of note, patients without a *FLT3*-ITD or a TKD mutation have also shown clinical responses to FLT3 inhibitors, which may highlight the presence of unknown activating mutations outside of the currently screened domains. In accordance with this, point mutations, although rare (1% of adult patients with AML) have been found outside the TKD in regions including the ECD, JMD and KID and are listed in Table 1.8 (Reindl *et al.*, 2006;Frohling *et al.*, 2007;Smith *et al.*, 2012).

Frohling *et al* (2007) highlighted the importance of distinguishing which of these mutations are so-called 'driver' or 'passenger' mutations. 'Driver' mutations which constitutively activate FLT3 and confer a proliferative advantage are proposed to respond to targeted inhibition. Although 'passenger' mutations do not activate FLT3 or confer a proliferative advantage, they may have an alternative role. The identification of new 'driver' *FLT3* mutations is therefore important as they may be sensitive to RTK inhibitors. This suggests that as diagnostic screening improves, patients with AML and these less frequent FLT3 mutations could be eligible for clinical trials using FLT3 inhibitors. This chapter reports studies investigating a novel *FLT3* mutation T820N identified in the ME-1 cell line. The functional properties of FLT3-T820N were examined by expression in the factor-dependent 32D cell line.

4.2 Methods

4.2.1 Cell lines

MV4-11, MOLM-13, MV4-11, PL-21 and HMC1.2 AML cell lines were cultured in R1 or R2 media. 32D clone 3 (32Dcl3) IL3 dependent immature myeloid cell line was cultured in R1 plus 2ng/mL of murine IL3 (mIL3). 293T cells were cultured in R4. All cell lines were incubated in a humidified environment at 37°C in 5% CO_2.

4.2.2 Identification of *FLT3* T820N mutation

PCR was used to amplify exons 14-15 (328bp product) and 20 (278bp) of *FLT3* and exons 8 (206bp), 10-11 (454bp) and 17 (201bp) of *c-KIT* using 30ng of ME-1 gDNA. gDNA was amplified for 35 cycles with primers and the corresponding annealing temperatures listed in (Table 4.1). PCR products were obtained using the BIOTAQ™ DNA polymerase or Optimase™ following the manufacturer's instructions and visualised on a 2% agarose gel as described in chapter 2 section 2.5.5. PCR products were sequenced using the appropriate primers.

Exon/Domain	Primer	Sequence	Annealing temperature (°C)
KIT ex8	8F2	5'-TCCAGCACTCTGACATATGGCCAT-3'	62.0
	8R2	5'-TGCAGTCCTTCCCCTCTGCAT-3'	
KIT ex10+11	10+11F	5'-GACTGAGTGGCTGTGGTAGAG-3'	61.0
	10+11R	5'-TAAAGTCACTGTTATGTGTACCCA-3'	
KIT ex17	17/F3	5'-GCCAGAAATATCCTCCTTACTCATG-3'	62.0
	17/R3	5'-GACAGGATTTACATTATGAAAATCACAG-3'	
FLT3-ITD	14F	5'-GCAATTTAGGTATGAAACC-3'	60.0
	15R	5'-CTTTCAGGATTTTGACGGCA-3'	
FLT3-TKD	20/F2	5'-CATCACCGGTACCTCCTACTG-3'	63.0
	20/R3	5'-TAACGACACAACACAAAATAGC-3'	

F= forward primer and R= reverse primer

Table 4.1 PCR primers used to screen for common *FLT3* and *c-KIT* mutations.

4.2.3 RNA extraction and cDNA amplification from ME-1 cells

RNA was isolated from $1x10^6$ ME-1 cells were using the RNeasy mini Kit (QIAGEN) according to the manufacturer's instructions. cDNA was subsequently made following the SuperScript® III First-Strand Synthesis System (Invitrogen Life Technologies) manufacturer's protocol.

4.2.4 PCR of *FLT3* WT and T820N from ME-1 cDNA

Full length *FLT3* WT and T820N cDNA were amplified from the transcriptional start site to the stop codon using 30ng of cDNA from ME-1 cells illustrated in Figure 4.1. DNA was amplified with primer pair SFG-FLT3-For and FLT3-reverse (2982bp product) listed in Table 4.2 using Phusion® DNA polymerase (New England BioLabs) following the cycling conditions described in chapter 2 sections 2.5.5 and 2.5.6 (Figure 4.1a). *FLT3* could not be cloned into the SFG vector using the SalI restriction site as it is also found within the *FLT3* sequence. To circumvent this *FLT3* was cloned into the SFG vector using the restriction sites AgeI and MluI. A portion of the SFG vector containing the AgeI restriction site was amplified using primer pair MP1835 and SFG-FLT3-Inv/Rev (376bp) as this sequence is essential for transgene expression (Table 4.2 and Figure 4.1b). To anneal the SFG PCR product to the *FLT3* PCR product overlapping primer extension PCR was performed using MP1835 and FLT3-reverse primers (3367bp) (Table 4.2) as illustrated in Figure 4.1c. PCR products were visualised and purified as described in chapter 2 section 2.5.6 and 2.5.12. All primer combinations from Table 4.2 used an annealing temperature of 65°C.

Primer	Sequence
MP1835	5'-CCCTTGTAAACTTCCCTGACC-3'
SFG-FLT3-For	5'-ATCCTCTAGACTGTCGACGCCACCATGCCGGCGTTGGCGCGCGAC-3'
SFG-FLT3-Inv/Rev	5'-GTCGCGCGCCAACGCCGGCATGGTGGCGTCGACAGTCTAGAGGAT-3'
FLT3-reverse	5'-CACCTTACGCTGACGCGTCTACGAATCTTCGACCTGAGCCTG-3'
FLT3-D835Y-Forward	5'-GGTGAAGATATGTGACTTTGGATTGGCTCGATATATCATGAGTGA-3'
FLT3-D835Y-Reserve Inverse	5'-TGCCCCTGACAACATAGTTGGAATCACTCATGATATATCGAGCCA-3'

Blue = kozak sequence, under lined = MluI restriction site and red = mutated codon D835

Table 4.2 PCR primers used to clone *FLT3* and to introduce the *FLT3*-D835Y point mutation.

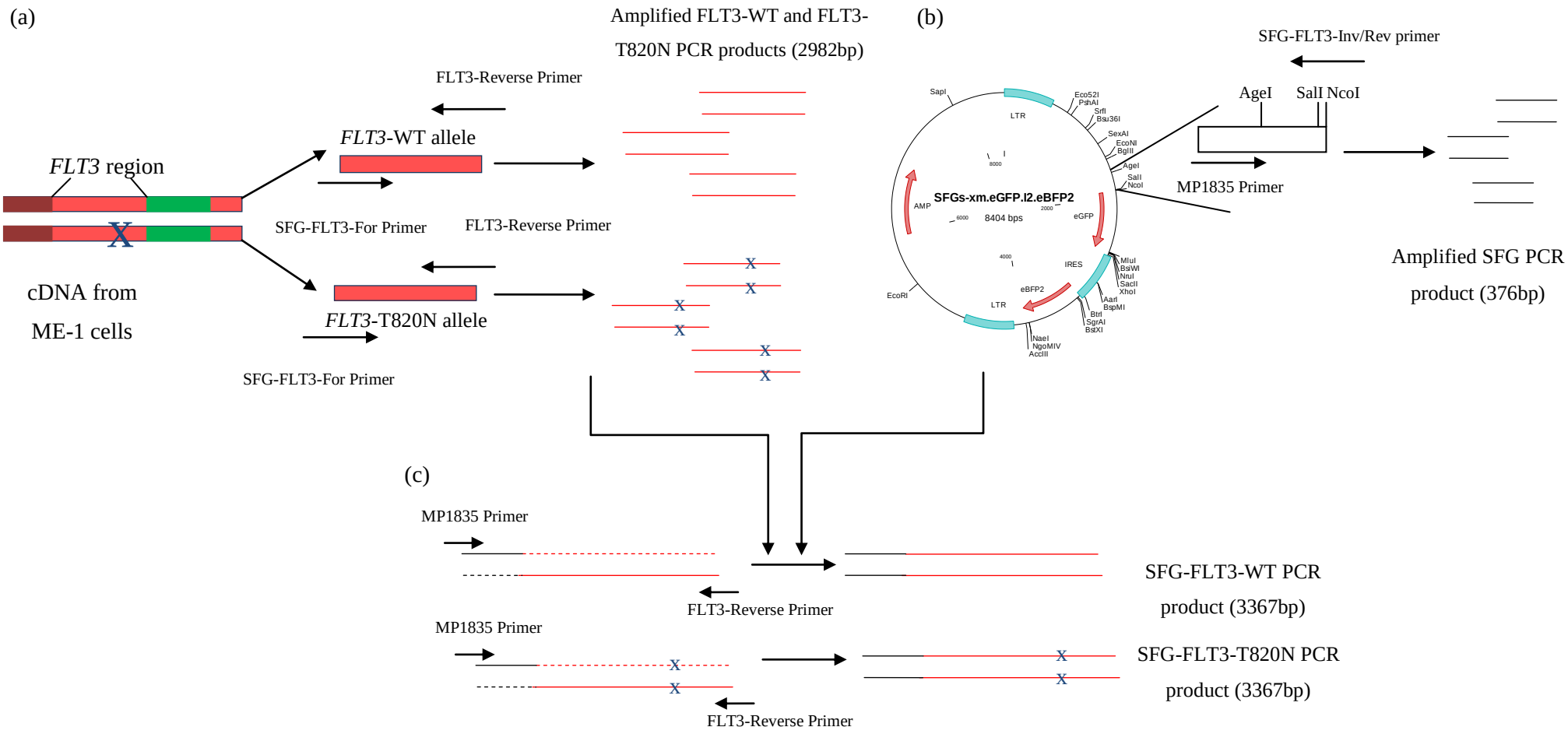

Figure 4.1. Amplification of FLT3 and subsequent cloning into the SFG vector backbone. (a) Amplification of FLT3-WT and FLT3-T820N from cDNA taken from the ME-1 cells. (b) Amplification of 376bp of the SFG vector containing the AgeI restriction site. (c) Overlapping by extension PCR of FLT3-WT and FLT3-T820N PCR products to the SFG PCR product. Blue cross denotes T820N mutation.

4.2.5 Cloning of FLT3 WT and T820N cDNA into the SFG-xm.eGFP.I2.eBFP2 retroviral vector

Approximately 0.5µg SFG-FLT3-WT and SFG-FLT3-T820N PCR products and 1µg of SFG-xm.eGFP.I2.eBFP2 vector were sequentially digested with MluI and AgeI in a 100µL reaction for 4 hours at 37°C following the manufacturer's guidelines illustrated in Figure 4.2 a,b. Digested plasmid vector was visualised on a 1% agarose gel and the desired band (7472bp) was cut out and purified as described in chapter 2 section 2.5.12. The digested SFG-xm.eBFP2 vector was ligated with the cut SFG-FLT3-WT or SFG-FLT3-T820N PCR products and cloned as described in chapter 2 section 2.5.12 (Figure 4.2c). Mini preps and midi preps were screened for the presence of *FLT3* using an EcoR1 digest. If FLT3 was present two fragments were visualised when run on a 1% agarose gel one at 7183bp and another at 3500bp. Clones with FLT3 were sequenced directly using primers listed in Table 4.3.

4.2.6 Removal of the D7G polymorphism in the SFG-FLT3-WT construct

After the SFG-FLT3-WT and SFG-FLT3-T820N constructs were sequenced a 20A>G nucleotide change, which would result in a D7G SNP, was identified in the SFG-FLT3-WT construct. To maintain the same background and examine the effect of just the T820N mutation, the D7G SNP was removed by correcting the SFG-FLT3-WT sequence with the SFG-FLT3-T820N sequence which did not have the SNP. The SFG-FLT3-WT and SFG-FLT3-T820N constructs were digested with AgeI-HF and MfeI for 3 hours at 37°C. Digested fragments were visualised on a 1% gel and the SFG-FLT3-WT backbone product (8805bp) and the SFG-FLT3-T820N 1861bp (with no D7G SNP) product were gel extracted, illustrated in Figure 4.3a. These two fragments were then ligated together, cloned into the SFG-xm.eBFP2 vector and sequenced as described in chapter 2 section 2.5.11 (Figure 4.3b).

Primer	Sequence
MP1835	5'-CCCTTGTAAACTTCCCTGACC-3'
FLT3/ex5U	5'-GTCTGCATATCTGAGAGCGTTC-3'
FLT3/ex5D	5'-GAACGCTCTCAGATATGCAGAC-3'
FLT3/ex9U	5'-CAGATGTACGTGGACCTTCTC-3'
FLT3/11F	5'-GCAATTTAGGTATGAAAGCC-3'
FLT3/17F	5'-CCGCCAGGAACGTGCTTG-3'
FLT3-Reverse	5-'CACCTTACGCTGACGCGTCTACGAATCTTCGACCTGAGCCTG-3'

U = exonic forward primer, D = exonic reverse primer, F = forward primer and underlined = MluI restriction site

Table 4.3 Primers used to sequence the entire *FLT3* gene within the plasmid constructs.

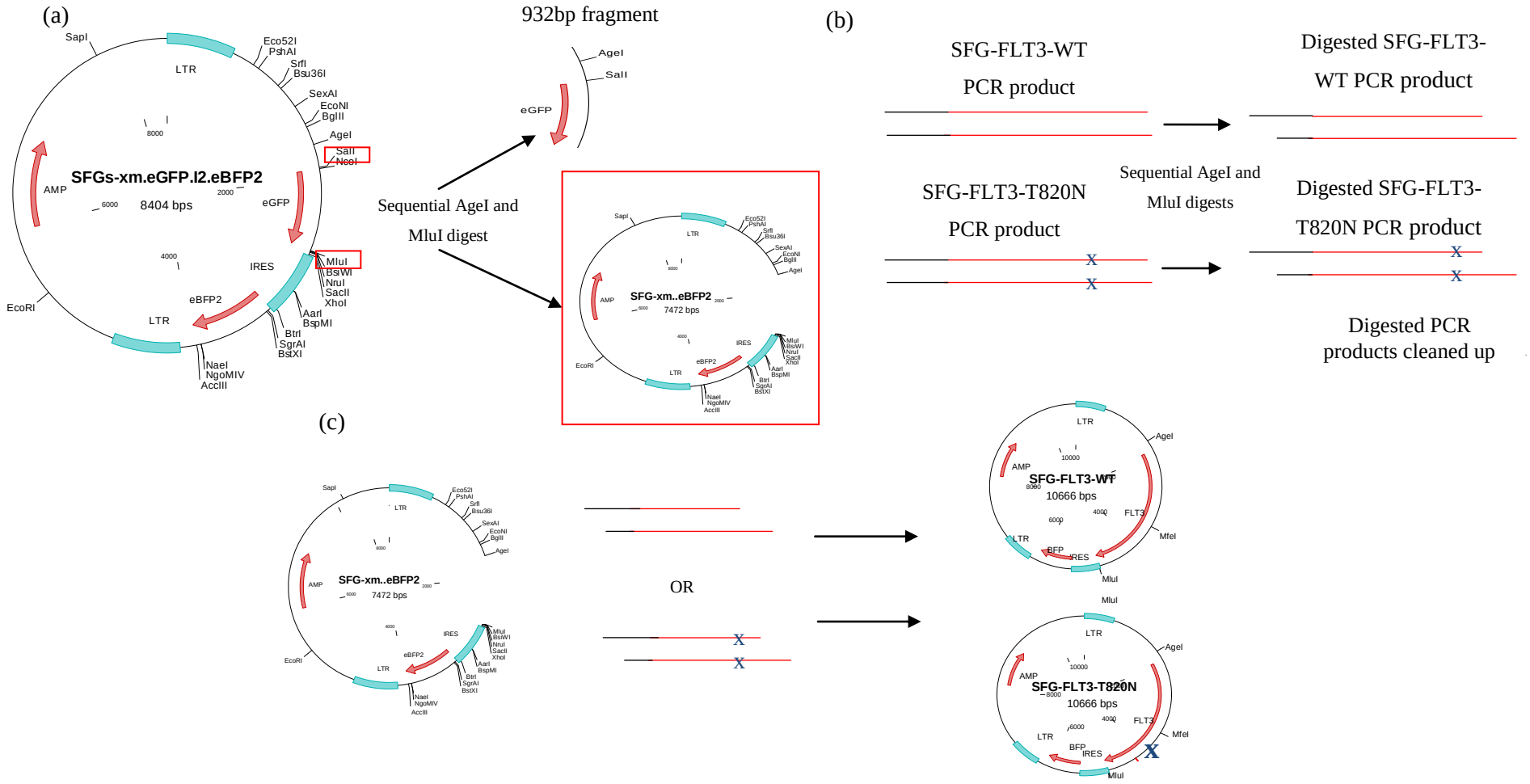

Figure 4.2 Cloning FLT3-WT and FLT3-T820N into the SFG vector. (a) Sequential digest of SFGs-xm.eGFP.I2.eBFP with AgeI and MluI restriction enzymes. (b) Sequential digest of SFG-FLT3-WT and SFG-FLT3-T820N PCR products with AgeI and MluI restriction enzymes. (c) Ligation and cloning of SFG-FLT3-WT and SFG-FLT3-T820N into the SFG-xm.eBFP2 vector. Blue cross denotes T820N mutation.

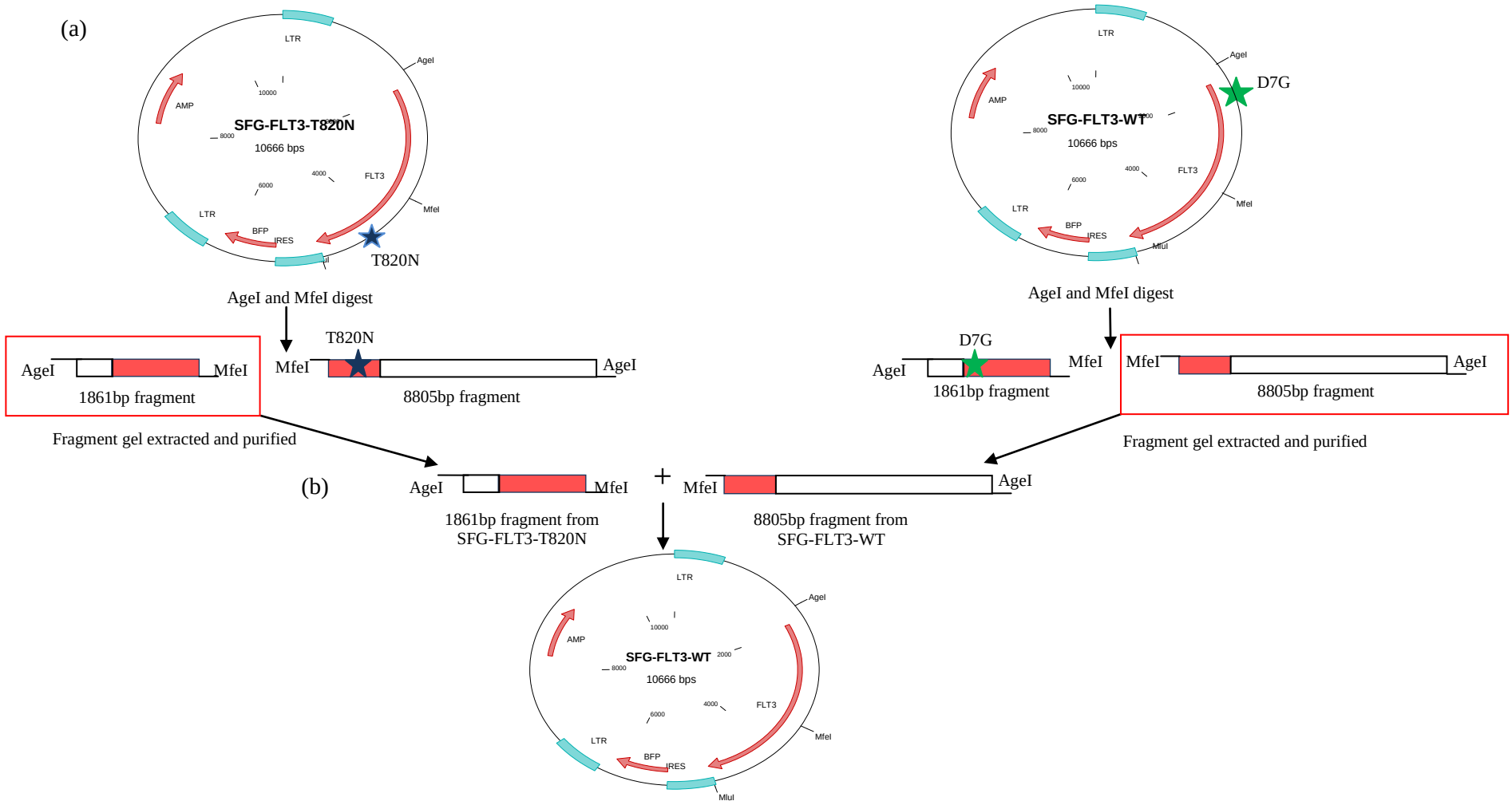

Figure 4.3 Removal of D7G SNP from the SFG-FLT3-WT construct. (a) SFG-FLT3-WT and SFG-FLT3-T820N plasmid constructs were both digested with AgeI and MfeI restriction enzymes. (b) Ligation of 1861bp fragment from the SFG-FLT3-T820N construct, without the D7G SNP, to the 8805bp fragment from the SFG-FLT3-WT, WT at residue T820. Blue star denotes T820N mutation and green star denotes D7G SNP.

4.2.7 Generation of SFG-FLT3-D835Y construct

FLT3 D835Y is the most common *FLT3*-TKD in AML and therefore was used as a positive control. The *FLT3*-D835Y mutation was introduced by amplifying *FLT3* from the SFG-FLT3-WT construct using splicing by overlap extension PCR as described in chapter 2 section 2.5.6. Two initial PCR reactions were carried out the first using primers MP1835 and FLT3-D835Y Reverse-Inverse (2894bp) and the second using FLT3-D835Y Forward and FLT3 Reverse (517bp) (Figure 4.4). A total of 30ng of the SFG-FLT3-WT construct was used as a DNA template and amplified for 35 cycles using the Phusion® DNA polymerase following the cycling conditions described in chapter 2 sections 2.5.5 and 2.5.6. Products of the correct size were gel extracted and purified. MP1835 and FLT3-Reverse primers were used to anneal and amplifying across the 2894bp and 517bp FLT3-D835Y PCR products (Figure 4.4). The PCR reaction used 105-280ng of each purified PCR product and was carried out as specified in chapter 2 section 2.5.6. The amplified SFG-FLT3-D835Y PCR product (3367bp) was sequentially digested with AgeI and MluI and gel extracted. The cut SFG-FLT3-D835Y PCR product was ligated into the SFG-xm.BFP construct and cloned as described in chapter 2 section 2.5.12. The entire coding sequence of FLT3 was sequenced.

4.2.8 Retroviral production.

Retroviral supernatant for each of the FLT3 constructs was made as described in chapter 2 section 2.2.2 using an Ecotropic envelope. Viral supernatant was snap frozen in an ethanol/dry ice bath and stored at -80°C.

4.2.9 Transduction of 32D cells

Non tissue culture treated 24 well plates were coated with 1µg/cm^2 of RetroNectin® per well overnight at 4°C. Retroviral supernatants were thawed on ice and 250µL was used to coat each RetroNectin® coated well for 30 minutes at room temperature. The viral supernatant was then removed from each well and discarded. 32D cells were re-suspended at 6x10^5 cells/mL in R1 with 2ng/mL mIL3 and 500µL plated onto the RetroNectin® bound virus. The remaining viral supernatant (1.75mL) was gently overlaid on top of the 32D cells. The plate was centrifuged for 10 minutes at 1000g and incubated at 37°C in 5% CO_2 for 24 hours. The cells were then harvested, re-suspended in fresh R1 with 2ng/mL mIL3 and incubated at 37°C in a humidified atmosphere containing 5% CO_2. After 48 hours, cells were examined for BFP positivity by flow cytometry (see chapter 2 section 2.4.3) and then subsequently sorted based on BFP expression (chapter 2 section 2.4.5).

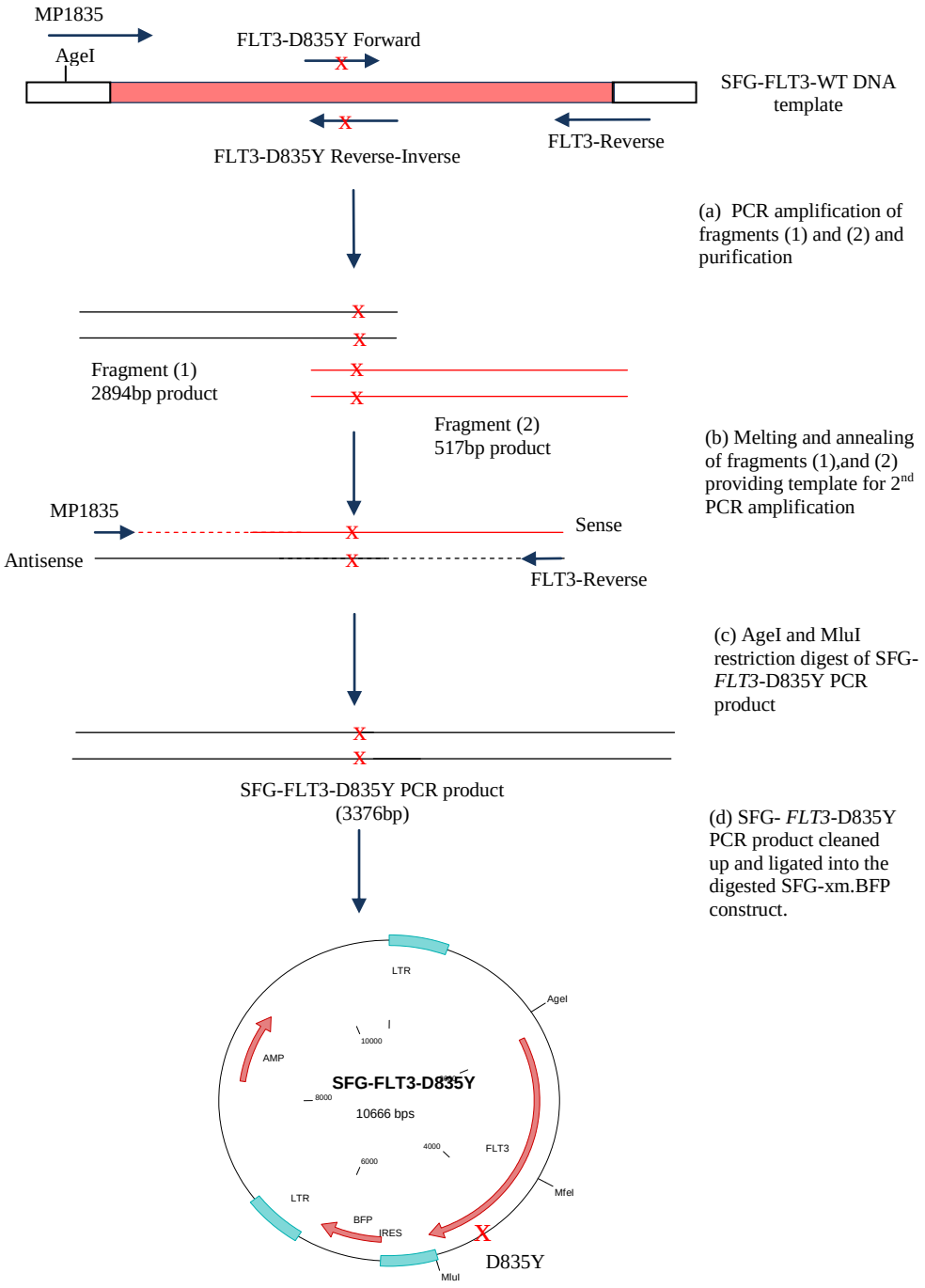

Figure 4.4 Cloning of FLT3-D835Y into the SFG vector. The FLT3-D835Y mutation was introduced by amplifying *FLT3* from the SFG-FLT3-WT construct using splicing by overlap extension PCR. Two initial PCR reactions were carried out using primers MP1835 and FLT3-D835Y Reverse-Inverse and FLT3-D835Y Forward and FLT3-Reverse. Fragments (1) and (2) were gel extracted, annealed and amplified across using primers MP1835 and FLT3-Reverse. The amplified SFG-FLT3-D835Y PCR product was sequentially digested with AgeI and MluI and ligated into the SFG-xm.BFP construct. Red crosses represent the *FLT3*-D835Y mutation.

4.2.10 Examination of CD135 expression

A total of $1x10^6$ transduced and sorted cells were re-suspended in PBS/0.5% BSA and incubated with anti-CD135 PE conjugated antibody as described in chapter 2 section 2.4.4 and analysed by flow cytometry.

4.2.11 Proliferation assay

32D cells were washed 3 times in PBS, re-suspended at $2.5x10^4$cells/mL in R1 and 100µL plated, in triplicate, into a 96 well plate in the presence or absence of mIL3 (2ng/mL), with or without increasing concentrations of human FL (1.56-6.25ng/mL). Cell proliferation was assessed every 24 hours using alamarBlue® following the manufacturer's guidelines. Measurements were corrected for background using absorbance values from wells containing media only.

4.2.12 Cytotoxicity assay

MV4-11, MOLM-13, MV4-11, PL-21 and HMC1.2 cells at $4x10^5$cells/mL were treated with the indicated amounts of AC220 for 72 hours (see Figures 4.6). 32D cells at $4x10^5$cells/mL were treated with increasing concentrations of AC220 (range 0.1-100nM) or Ponatinib (range 3.125-200nM) for 48 hours with various cytokine combinations. Annexin/PI staining was assessed as described in chapter 2 section 2.4.2. The live cell fraction (Annexin and PI negative) and the absolute number of live cells were quantified by flow cytometry, and results expressed as a percentage of the control cells.

4.2.13 Detection of Reactive Oxygen Species (ROS)

A total of $10x10^6$ cells from each transduced cell line were washed three times in 20mL of PBS. For each cell line $5x10^6$ cells/mL were re-suspended in 5mL of R1 either with or without FL (10ng/mL) and returned to the incubator for 8 hours. After 8 hours cells were centrifuged at 448g for 5 minutes and re-suspended in 0.5% BSA/PBS at $1x10^6$ cells/mL. A total of $1x10^6$ cells/mL was aliquoted into individual 5mL polystyrene round-bottom tubes and centrifuged. Cells were then pre-loaded with CM-H_2DCFDA by adding to each tube 500µL of a master mix containing 495µL of Hank's Balanced Salt solution (HBSS) and 5µL of CM-H_2DCFDA and incubated at 37°C for 30 minutes in the dark. To each tube 1mL of 0.5% BSA/PBS was added and centrifuged at 448g for 5 minutes. Working stocks of hydrogen peroxide (H_2O_2) 0.25mM, 0.5mM, 1mM and 5mM were made fresh for each biological repeat. Cells were re-suspended in 500µL of 0.25mM, 0.5mM, 1mM, 5mM of H_2O_2 or 500µL HBSS for untreated cells and incubated for 15 minutes at 37°C 5% CO_2 in

the dark. Cells were washed with 1mL of 0.5% BSA/PBS and centrifuged at 448g for 5 minutes. Cells were re-suspended in 500µL 0.5% BSA/PBS and kept on ice until analysed on the flow cytometer. Live cells were gated based on their forward and side scatter properties. Cells within this gate were plotted onto a separate histogram with log CM-H_2DCFDA on the X axis and counts on the Y axis. The mean fluorescence intensity (MFI) was recorded for each point.

4.3 Results

4.3.1 Screening of ME-1 cells for *c-KIT* and *FLT3* mutations

The ME-1 cell line is derived from a patient carrying inv(16) and therefore may be a useful model for studying signalling in CBFL. ME-1 cells were screened for mutations in known hotspots in *c-KIT* and *FLT3*. For each PCR reaction two controls were used - a negative control, the HL60 cell line, and a no DNA template control. There were no mutations in exons 8, 10+11 and 17 of *c-KIT* and they did not have a *FLT3*-ITD mutation (WT fragment size is 328bp) (Figure 4.5a). Sequencing of the *FLT3*-TKD region (278bp) revealed a heterozygous C>A DNA nucleotide substitution that would result in a missense Thr820Asn (T820N) amino acid change (Figure 4.5b). Of note this change fell outside of the TKD domain.

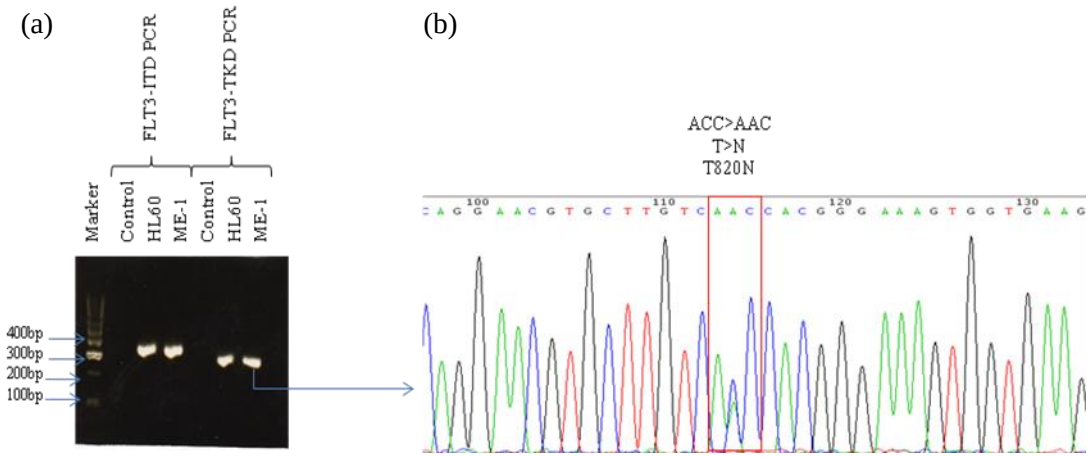

Figure 4.5 Analysis of *FLT3*-ITD and *FLT3*-TKD PCR products from HL60 and ME-1 cells highlighting the identification of the *FLT3* T820N mutation in ME-1 cells. (a) *FLT3*-ITD and *FLT3*-TKD PCR products amplified from HL60 and ME-1 cells and run on a agarose gel. (b) A sequence chromatogram from the ME-1 *FLT3*-TKD PCR product highlighting a C>A nucleotide change resulting in a T820N amino acid substitution.

4.3.2 Response of ME-1 cells to the FLT3 inhibitor AC220

ME-1 cells expressing *FLT3*-T820N, MV4-11, MOLM-13 and PL-21 cells, all carrying a *FLT3*-ITD, and *FLT3*-WT HMC1.2 cells were all treated with increasing concentrations of AC220 for 72 hours. MV4-11 and MOLM-13 cells were very sensitive to AC220 as demonstrated by potent growth inhibition (IC50s: 1.4 and 2.6nM respectively) and cell killing (IC50s: 4.5 and 8nM respectively) (Figures 4.6 a,b). PL-21 cells showed a clear decrease in the live cell number and the live cell fraction between 1.25µM and 10µM AC220 (Figures 4.6 c,d). In contrast, AC220 had minimal effect on growth inhibition or cell killing in ME-1 and HMC1.2 cells, up to 10µM concentration (Figures 4.6 c,d).

(a) (b)

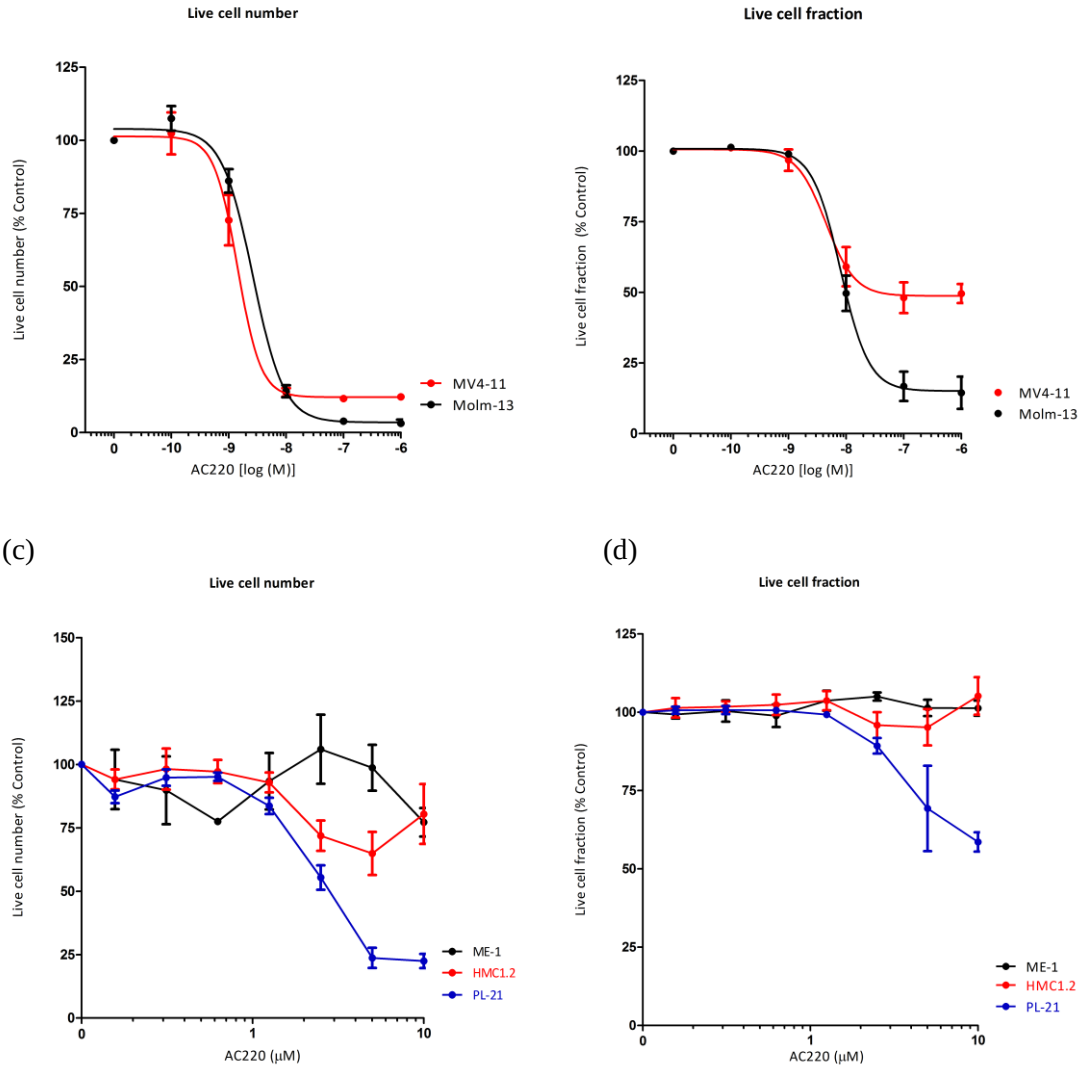

Figures 4.6 Growth inhibition and cell killing of MV4-11, MOLM-13, PL-21, HMC1.2 and ME-1 cells treated with AC220 for 72 hours. (a,c) Total number of live cells. (c,d) Percentage of cells in the live cell fraction. Data shown is the mean ± SEM of three individual experiments.

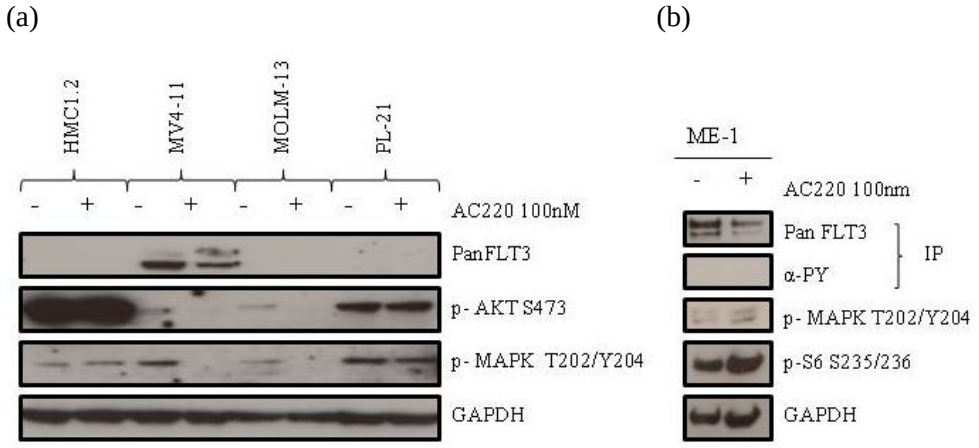

Figure 4.7 Effect of AC220 on signalling downstream of FLT3 in the HMC1.2, MV4-11, MOLM-13, PL-21 and ME-1 cells. (a) Western blotting of HMC1.2, MV4-11, MOLM-13 and PL-21 cells treated in the presence or absence of AC220 for 4 hours. (b) IP of FLT3 and western blotting from ME-1 cells treated in the presence or absence of AC220 for 4 hours. GAPDH was used as a loading control.

Western blotting was used to assess the effect of AC220 on signalling downstream of FLT3 in MV4-11, MOLM-13, PL-21, ME-1 and HMC1.2 cells. A concentration of 100nM of AC220 was used as this potently inhibited cell growth and induced cell killing in MV4-11 and MOLM-13 cells. AC220 did not reduce phosphorylation of AKT, MAPK or S6 in the ME-1, HMC1.2 or PL-21 cells (Figure 4.7 a,b). In contrast, although MV4-11 and MOLM-13 cells express low levels of phosphorylated AKT and MAPK there was a reduction in p-AKT and p-MAPK which is mediated by inhibition of FLT3 autophosphorylation (see chapter 5 section 5.3.12). Immunoprecipitation of FLT3 showed that ME-1 cells do not express active FLT3, as indicated by no detectable p-FLT3, which could explain the lack of response to AC220 (Figure 4.7b). This data suggests that *FLT3*-T820N is not constitutively active in ME-1 cells.

4.3.3 Transduction of 32D cells with SFG-FLT3 and SFG-EMPTY constructs

To investigate the function of the *FLT3*-T820N mutation further, 32D cells were transduced with SFG-FLT3-T820N and for comparison SFG-FLT3-WT, SFG-FLT3-D835Y and SFG-EMPTY constructs. 32D cells were successfully transduced with the various SFG-FLT3 and SFG-EMPTY constructs with transduction efficiencies ranging from 10-70% as assessed by BFP expression via flow cytometry. Cells were subsequently sorted based on BFP on the assumption that expression of BFP indicates expression of FLT3. Following sorting BFP and cell surface CD135 (FLT3) expression were simultaneously examined in each cell line. 32D

native cells were negative for BFP and CD135 expression whereas 32D cells transduced with FLT3-WT, FLT3-T820N, FLT3-D835Y and SFG-EMPTY vector were all 95-99% BFP positive (Figure 4.8a). Although 32D FLT3-D835Y cells were 95% BFP positive, they were dimmer in comparison to the other generated cell lines. For 32D cells expressing FLT3-WT or FLT3-T820N, the median MFI for BFP was 11.1 and 14.8 respectively which was roughly equivalent to the median MFI for CD135 11.5 and 13.1 respectively (Figure 4.8). In contrast CD135 expression was considerably lower in 32D FLT3-D835Y cells (median MFI: 0.8) (Figure 4.8 a,b). The lower CD135 staining within these cells may be due to a lower expression of the 160KDa fully glycosylated (membrane bound) FLT3 as a previous study has reported that FLT3-D835Y is retained within the endoplasmic reticulum, preventing it from reaching the cell surface (Choudhary *et al.*, 2005). Western blotting confirmed a predominance of the 130KDa unglycosylated isoform in 32D FLT3-D835Y cells (Figure 4.9). There was equivalent total FLT3 expression between 32D FLT3-WT and FLT3-T820N cells (Figure 4.9). Total FLT3 expression was considerably less in 32D FLT3-D835Y cells in comparison to FLT3-WT and FLT3-T820N expressing cells which is consistent with a dimmer BFP level.

4.3.4 Impact of FLT3-T820N on proliferation

The impact on proliferation of the FLT3-T820N mutation was examined in transduced 32D cells in comparison to 32D cells expressing FLT3-WT, FLT3-D835Y and SFG-EMPTY cells. 32D SFG-EMPTY cells did not proliferate in the absence of mIL3 and subsequently died after 3/4 days; they were unresponsive to FL (Figure 4.10a). FLT3-T820N expressing cells showed factor-independent growth which was significantly greater, from day 3 onwards, when compared to 32D SFG-EMPTY (P <0.001, Two-way analysis of variance (ANOVA) with Bonferroni's multiple comparisons post-test) and FLT3-WT expressing cells (P <0.01, Two-way ANOVA with Bonferroni's multiple comparisons post-test) (Figure 4.10b). 32D FLT3-D835Y cells also showed factor-independent growth but this was not increased further by the addition of FL (Figure 4.10c). The level of factor-independent growth was not statistically different on days 1-5 between cells expressing FLT3-D835Y and FLT3-T820N (P >0.05, Two-way ANOVA with Bonferroni's multiple comparisons post-test) however it was when comparing 32D FLT3-D835Y cells to SFG-EMPTY and FLT3-WT expressing cells from day 4 onwards (D835Y vs EMPTY P <0.0001; D835Y vs WT P <0.01, Two-way ANOVA with Bonferroni's multiple comparisons post-tests). In the absence of any growth factor, 32D FLT3-WT cells did not die but maintained a very low level of proliferation which was considerably lower than observed for 32D FLT3-T820N or FLT3-D835Y cells (Figure 4.10d). There was no statistical difference in proliferation rate between

FLT3-WT and SFG-EMPTY expressing cells in the absence of any growth factors between days 1-5 (P >0.05, Two-way ANOVA with Bonferroni's multiple comparisons post-test). The addition of FL did increase the proliferation rates, however they did not reach the levels achieved in cells expressing FLT3-T820N. Both the FLT3-D835Y and FLT3-T820N expressing cells showed ligand-independent growth which was greater than FLT3-WT expressing cells.

(a) (b)

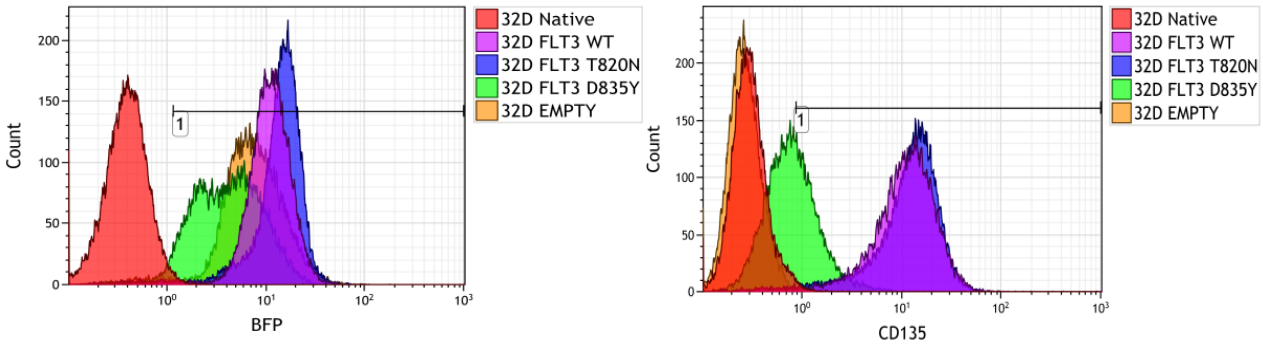

Ref. colour	Cell line	BFP (%[1])	BFP Median (MFI[2])	CD135 (%[1])	CD135 Median (MFI[2])
	32D Native	1.0	0.4	1.1	0.3
	32D FLT3-WT	98.7	11.1	98.5	11.5
	32D FLT3-T820N	97.8	14.8	98.1	13.1
	32D FLT3-D835Y	95.3	4.2	41.0	0.8
	32D EMPTY	97.0	7.4	0.2	0.3

Figure 4.8 Examination of (a) BFP and (b) CD135 expression within 32D transduced cells. [1]refers to the gated area, [2] refers to the entire cell population.

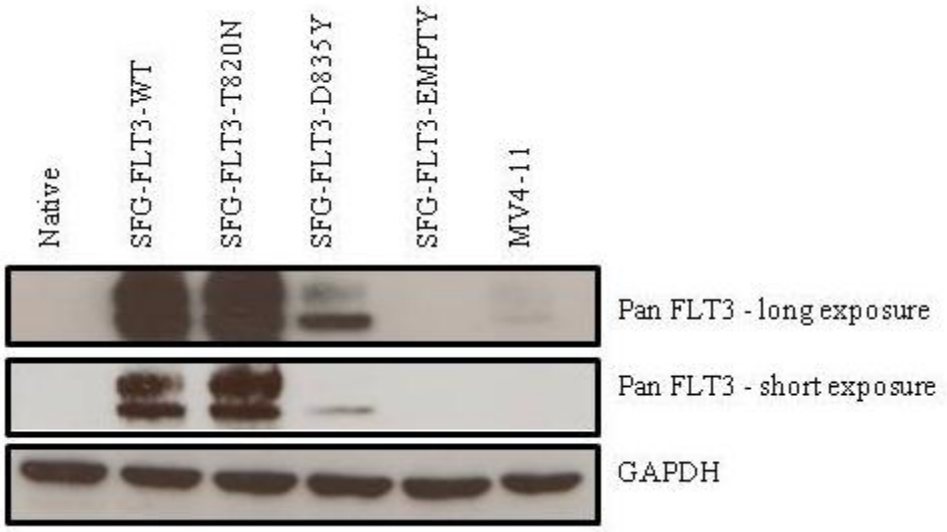

Figure 4.9 Western blotting of transduced 32D cells examining total FLT3 expression. GAPDH was used as a loading control.

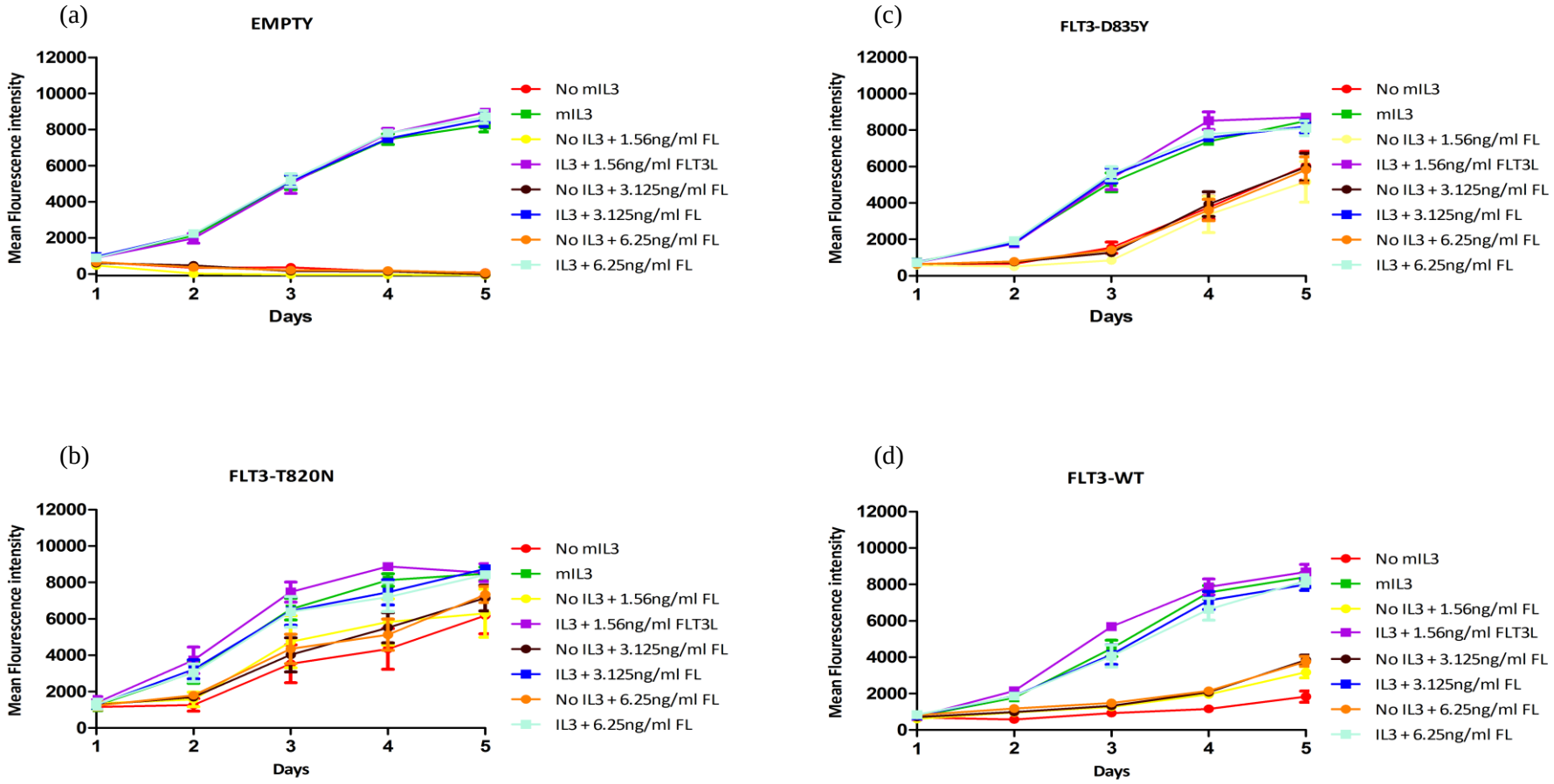

Figure 4.10 The impact of FLT3-T820N on proliferation in 32D cells in comparison to FLT3-WT, FLT3-D835Y and SFG-EMPTY expressing cells. Each cell line were incubated with ± IL3 (2ng/mL) in the presence of increasing concentrations of FL and treated with alamarBlue®. Data shown is the mean ± SEM of three individual experiments.

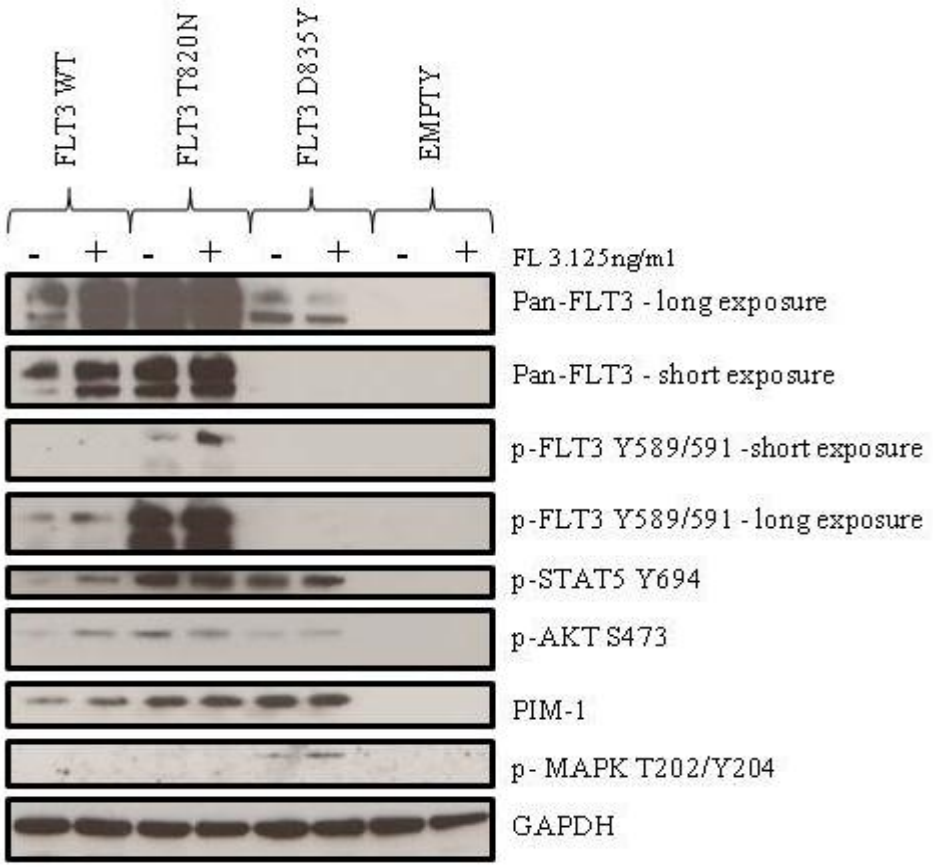

Figure 4.11 Examining FLT3 signalling in 32D FLT3-T820N, FLT3-WT, FLT3-D835Y and SFG-EMPTY cells ± 3.125ng/mL FL for 4 hours. GAPDH was used as a loading control

4.3.5 Impact of FLT3-T820N on downstream signalling

32D FLT3-T820N cells demonstrated factor-independent growth, therefore the FLT3-transduced and SFG-EMPTY cells were washed with PBS and cultured for four hours in the presence or absence of FL to evaluate differences in FLT3 downstream signalling. Autophosphorylation of FLT3 was used as a measure of FLT3 activity as indicated by phosphorylation of residues Tyr589/591. In the absence of any growth factor, 32D FLT3-T820N cells showed autophosphorylation of FLT3 and constitutive activation of downstream target proteins (STAT5, AKT and PIM-1) as indicated by p-STAT5 and p-AKT (Figure 4.11). Stimulation of 32D FLT3-T820N cells with FL further phosphorylated FLT3, however there was no corresponding up regulation of downstream target proteins. Although 32D FLT3-D835Y cells had no detectable p-FLT3, they did show constitutive activation of STAT5, AKT, PIM-1 and MAPK. The addition of FL did not further activate downstream signalling. In contrast, 32D FLT3-WT cells starved of FL showed low/absent constitutive activation of FLT3, STAT5, AKT and PIM-1 in comparison to FLT3-WT cells stimulated

with FL (Figure 4.11). Stimulation of 32D FLT3-WT cells with FL increased phosphorylation of FLT3 resulting in activation of downstream target proteins. This suggests that constitutive activation of FLT3, STAT5, AKT and PIM-1 may contribute to the factor-independent growth observed in 32D FLT3-T820N cells. Interestingly, 32D FLT3-WT cells had detectable p-FLT3 in the absence of FL. This suggests that the WT receptor can autophosphorylate, providing a rationale as to why FLT3-WT expressing cells did not die following continued growth factor starvation. 32D SFG-EMPTY cells treated with or without FL showed no detectable activation of FLT3, STAT5, AKT, PIM-1 or MAPK.

4.3.6 Effect of AC220 treatment on 32D FLT3-expressing cells

32D EMPTY, FLT3 WT, FLT3-T820N and FLT3-D835Y cells were treated with increasing concentrations of AC220 in the presence of mIL3 alone (2ng/mL), FL alone (10ng/mL) or in the presence of both cytokines for 48 hours examining growth inhibition and cell killing. In the absence of mIL3, 32D EMPTY cells died after 48 hours. In the presence of FL and mIL3 or mIL3 alone 32D EMPTY cells were relatively resistant to AC220-mediated growth inhibition and cell killing (≤100nM) (Figure 4.12 a,b). 32D SFG-EMPTY cells did respond to 1000nM of AC220 as indicated by growth inhibition and cell killing, however as these cells do not express FLT3 the effects observed were most likely off-target effects.

32D FLT3-T820N, FLT3-D835Y and FLT3-WT cells stimulated with FL and mIL3, mIL3 alone or FL alone and treated with AC220 had similar dose responses in terms of growth inhibition and cell killing (Figure 4.12 c-h). The presence of FL and mIL3 or mIL3 alone did protect 32D FLT3 expressing cells to a certain extent from AC220 mediated growth inhibition and cell killing, however they were considerably more sensitive to AC220 when compared to 32D SFG-EMPTY cells at concentrations ≥100nM of AC220.

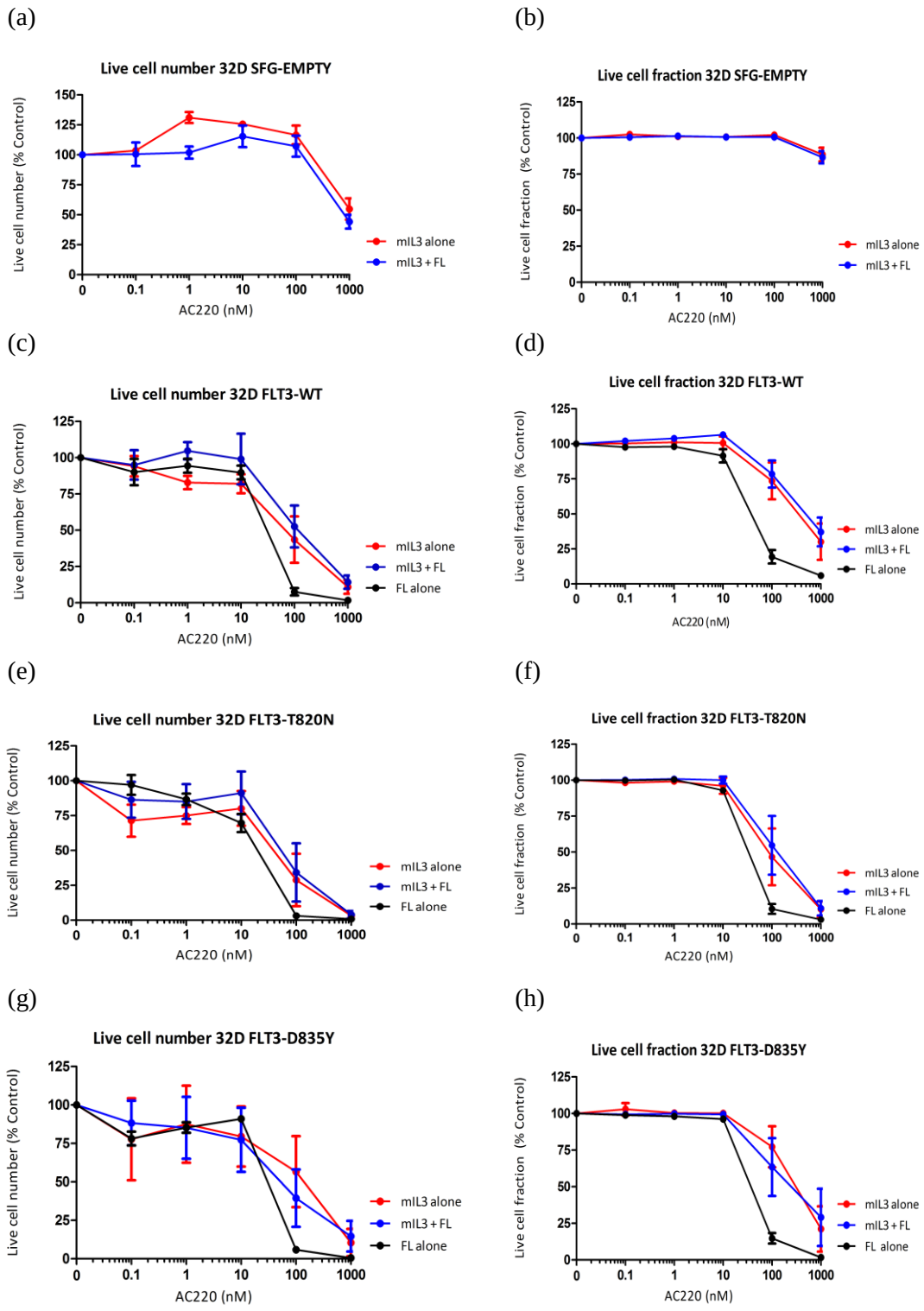

Figure 4.12 32D SFG-EMPTY, FLT3-WT, FLT3-T820N and FLT3-D835Y cells treated with AC220 in the presence or absence of 2ng/mL mIL3 with or without 10ng/mL FL for 48 hours. (a,c,e,g) Total number of live cells. (b,d,f,h) Percentage of cells in the live cell fraction. Data shown is the mean ± SEM of three individual experiments.

AC220 treatment in the presence of FL

Data in Figure 4.12 did not show any striking differences between the FLT3 transduced cells in response to AC220 therefore each cell line was treated with a narrower dose range of AC220, between 6.25nM and 100nM, in the presence of FL (Figure 4.13). 32D FLT3-T820N cells were significantly more sensitive to AC220-mediated growth inhibition (IC50 = 17.6nM ± 2.3) compared to 32D FLT3-D835Y cells (IC50 = 52.2nM ± 11.1, *P* = 0.01, unpaired t-test) but not compared to 32D FLT3-WT cells (IC50 = 24.5nM ± 4.7, *P* = 0.25, unpaired t-test). 32D FLT3-T820N cells were significantly more sensitive to AC220-mediated cell killing compared to both 32D FLT3-D835Y and FLT3-WT cells (IC50s 26 ± 2.5, 61.1nM ± 11.8, 39.9nM ± 4.6, FLT3-T820N, FLT3-D835Y and FLT3-WT respectively; T820N vs D835Y *P* = 0.008, unpaired t-test ; T820N vs WT *P* = 0.03, unpaired t-test). To demonstrate that the difference in growth inhibition and cell killing were mediated by differences in sensitivity to FLT3 blockade, the level of phosphorylation of FLT3 target proteins was assessed. FLT3-transduced cells were washed with PBS and exposed to 6.25, 12.5, 25, 50 and 100nM AC220 in the presence of 10ng/mL FL for 24 hours. In 32D FLT3-T820N cells, concentrations ≥25nM of AC220 potently reduced phosphorylation of FLT3, STAT5 and AKT whereas concentrations ≥50nM were required to completely block p-FLT3 and downstream signalling in 32D FLT3-WT cells (Figure 4.14). A concentration ≥50nM of AC220 reduced phosphorylation of AKT in FLT3-D835Y cells whereas 100nM of AC220 was required to slightly reduce phosphorylation of FLT3 and STAT5.

AC220 treatment in the absence of FL

Similar results were obtained in the absence of FL (Figure 4.15). 32D FLT3-T820N cells were significantly more sensitive to AC220 mediated growth inhibition (IC50 = 7.9nM ± 0.9) in comparison to 32D FLT3-D835Y cells (D835Y: IC50 = 38.7nM, *P* = 0.04 unpaired t-test) but not 32D FLT3-WT cells (WT: IC50 = 14.3nM ± 2.6, T820N vs WT *P* = 0.08, unpaired t-test). AC220 induced significantly more cell killing in 32D FLT3-T820N cells in comparison to 32D FLT3-D835Y cells (IC50 = 42.1nM ± 2.8, *P* = 0.0004, unpaired t-test) but not 32D FLT3-WT cells (IC50 = 20 ± 5.8, *P* = 0.18, unpaired t-test) (Figure 4.15). FLT3-transduced cells were washed with PBS and exposed to concentrations between 6.25 and 100nM AC220 in the absence of FL for 24 hours. In the absence of FL, a concentration ≥25nM AC220 most potently reduced p-FLT3, p-STAT5 and p-AKT in 32D FLT3-T820N cells, whereas both 32D FLT3-WT and FLT3-D835Y expressing cells were more resistant requiring 100nM of AC220 to reduce phosphorylation of FLT3 and downstream target proteins (Figure 4.16).

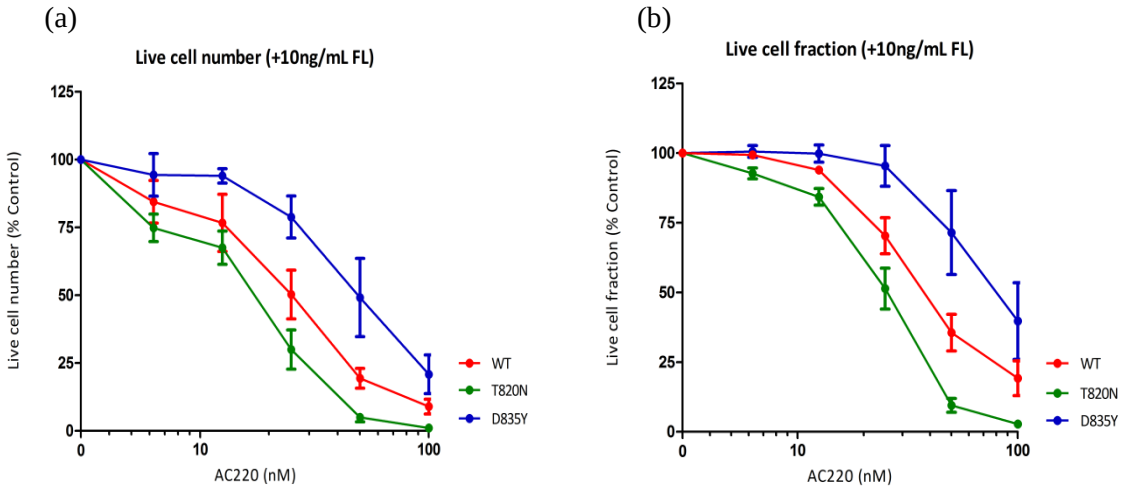

Figure 4.13 Response of 32D FLT3 WT, FLT3-T820N and FLT3-D835Y cells to a narrower dose range of AC220 in the presence of 10ng/mL FL after 48 hours. (a) Total number of live cells. (b) Percentage of cells in the live cell fraction. Data shown is the mean ± SEM of WT n=6, T820N n=5 & D853Y n=4 independent repeats.

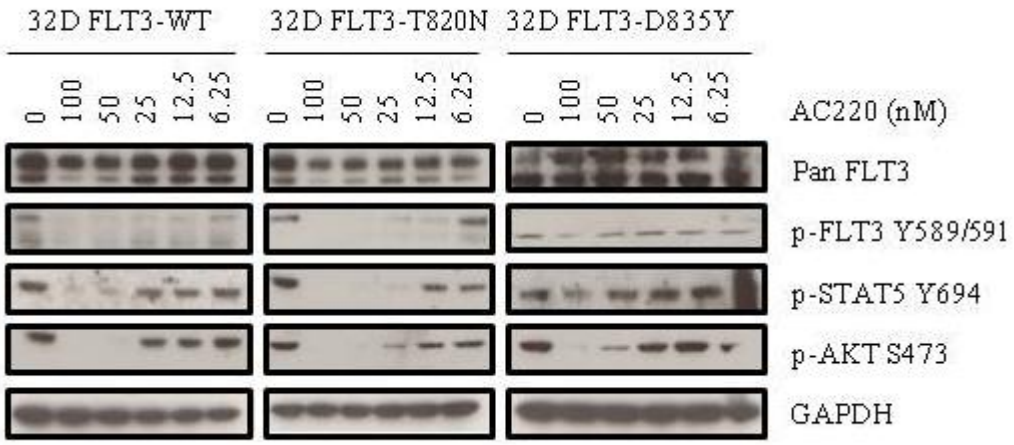

Figure 4.14 Western blots of 32D FLT3-WT, FLT3-T820N and FLT3-D835Y expressing cells treated with 6.25-100nM of AC220, in the presence of 10ng/mL FL for 24 hours. GAPDH was used as a loading control.

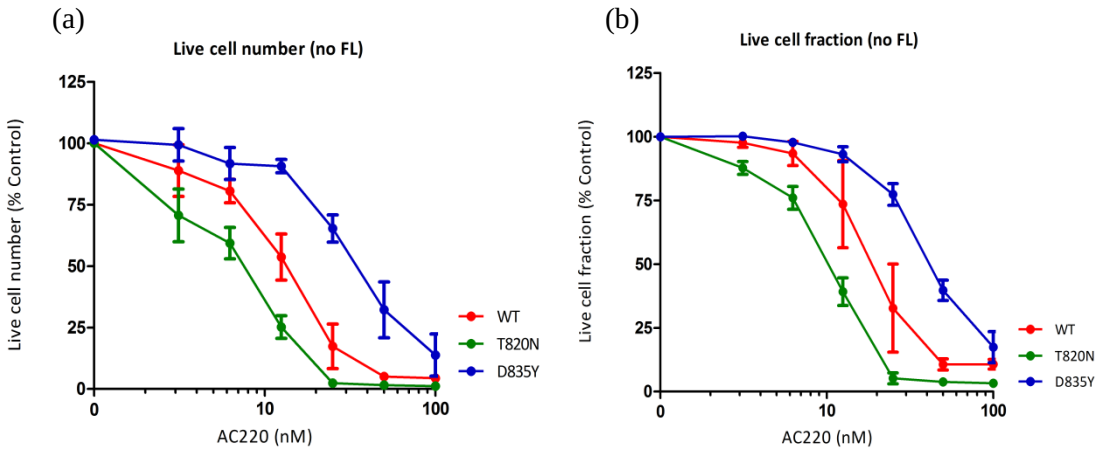

Figure 4.15 Response of 32D FLT3 WT, FLT3-T820N and FLT3-D835Y cells to a narrower dose range of AC220 in the absence of FL after 48 hours. (a) Total number of live cells. (b) Percentage of cells in the live cell fraction. Data shown is the mean ± SEM of three individual experiments.

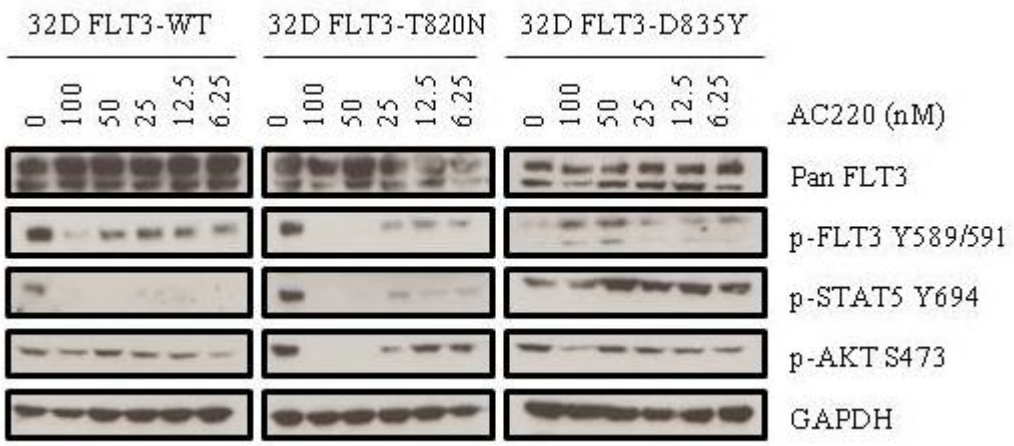

Figure 4.16 Western blots of 32D FLT3-WT, FLT3-T820N and FLT3-D835Y expressing cells treated with 6.25-100nM of AC220, in the absence of FL for 48 hours. GAPDH was used as a loading control.

4.3.7 Response of FLT3-expressing cells to ponatinib

To examine if the differential response to AC220 observed in 32D FLT3-expressing cells is limited to this inhibitor, the various cell lines were treated with another type II FLT3 inhibitor, ponatinib. Treatment of 32D EMPTY cells with increasing concentrations of ponatinib in the presence of mIL3 did not inhibit cell growth or induce cell killing (Figure 4.17 a,b). Ponatinib, in the presence of FL, inhibited cell growth at equivalent levels in 32D FLT3-T820N (IC50 = 20.6nM ± 2.3) and FLT3-WT cells (IC50 = 18.7nM ± 4, *P*=0.69, unpaired t-test) whereas FLT3-T820N cells were significantly more sensitive to growth inhibition than FLT3-D835Y cells (IC50 = 68.2nM ± 9, *P* = 0.002, unpaired t-test) (Figure 4.17a). There was no differential response to ponatinib-mediated cell killing between 32D FLT3-T820N (IC50 = 25.6nM ± 3) and FLT3-WT cells (IC50 = 26.6nM ± 2.8, *P* = 0.8, unpaired t-test) whereas FLT3-T820N cells were significantly more sensitive to cell killing when compared to 32D FLT3-D835Y (IC50 = 88nM ± 12.2, *P* = 0.002, unpaired t-test) (Figure 4.17b). In the absence of FL, there was no differential response to ponatinib-mediated growth inhibition between 32D FLT3-T820N (IC50 = 28.3nM ± 1) and FLT3-WT cells (IC50 = 38.4nM ± 8, *P*= 0.25, unpaired t-test) (Figure 4.17c). There was, however a trend for FLT3-T820N cells to be more sensitive to ponatinib-mediated cell killing than 32D FLT3-WT cells (T820N: IC50 = 28.3nM ± 1 and WT: IC50 = 63.8nM ± 9, *P* = 0.07, unpaired t-test) (Figure 4.17d). 32D FLT3-D835Y cells were more resistant to ponatinib when compared to 32D FLT3-T820N and FLT3-WT cells requiring concentrations ≥100nM to inhibit cell growth or induce cell killing (Figure 4.17c,d).

4.3.8 Level of Reactive Oxygen Species (ROS) in FLT3-expressing cells

The level of ROS was investigated in each cell line to ascertain whether this may contribute to the proliferative advantage observed in 32D FLT3-T820N cells. Each cell line was washed and treated with or without 10ng/mL FL for 8 hours. Each cell line was then incubated with the fluorescent probe CM-H2DCFDA and treated with H_2O_2 (Figure 4.18). Oxidation of CM-H2DCFDA produces a fluorescent adduct that becomes trapped within the cell, therefore providing a quantitative measure of ROS that can be assessed by flow cytometry. The basal level of ROS was not significantly different between the variant cells lines, whether in the presence or absence of FL (*P* >0.05, Two-way ANOVA with Bonferroni's multiple comparison post-test) (Figure 4.18). The level of ROS was also measured in the presence of increasing concentrations of H_2O_2, with or without FL, in each variant cell line. The level of ROS did not significantly alter between the variant cell lines at

any H_2O_2 concentration, whether in the presence or absence of FL (P >0.05, Two-way ANOVA with Bonferroni's multiple comparison post-test) (Figure 4.18).

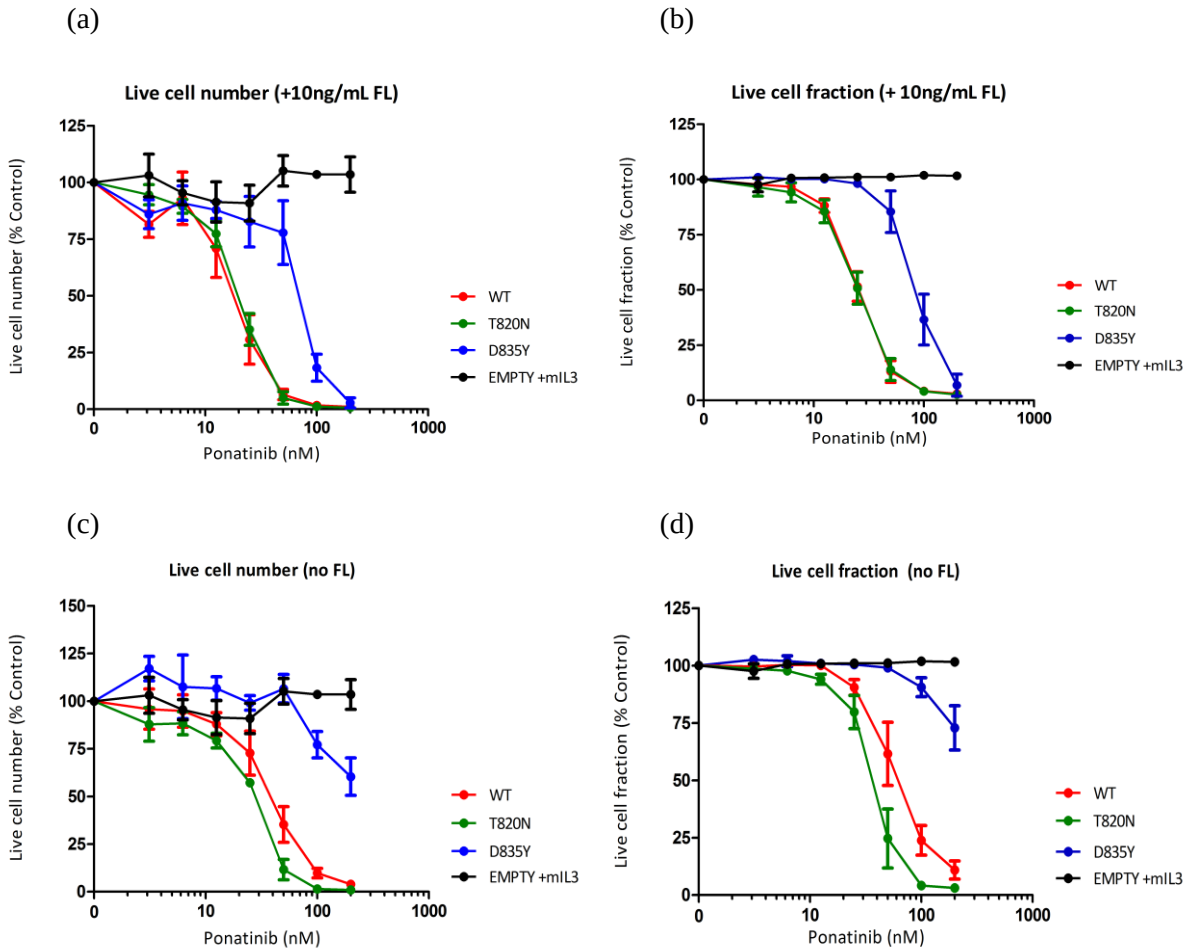

Figure 4.17 Response of 32D FLT3-WT, FLT3-T820N and FLT3-D835Y expressing cells to ponatinib in the presence or absence of 10ng/mL FL after 48 hours. 32D SFG-EMPTY cells were treated with ponatinib in the presence of 2ng/mL mIL3. Data shown is the mean of FLT3-WT, FLT3-T820N, FLT3-D835Y n=4 & SFG-EMPTY n=3 independent repeats ± SEM.

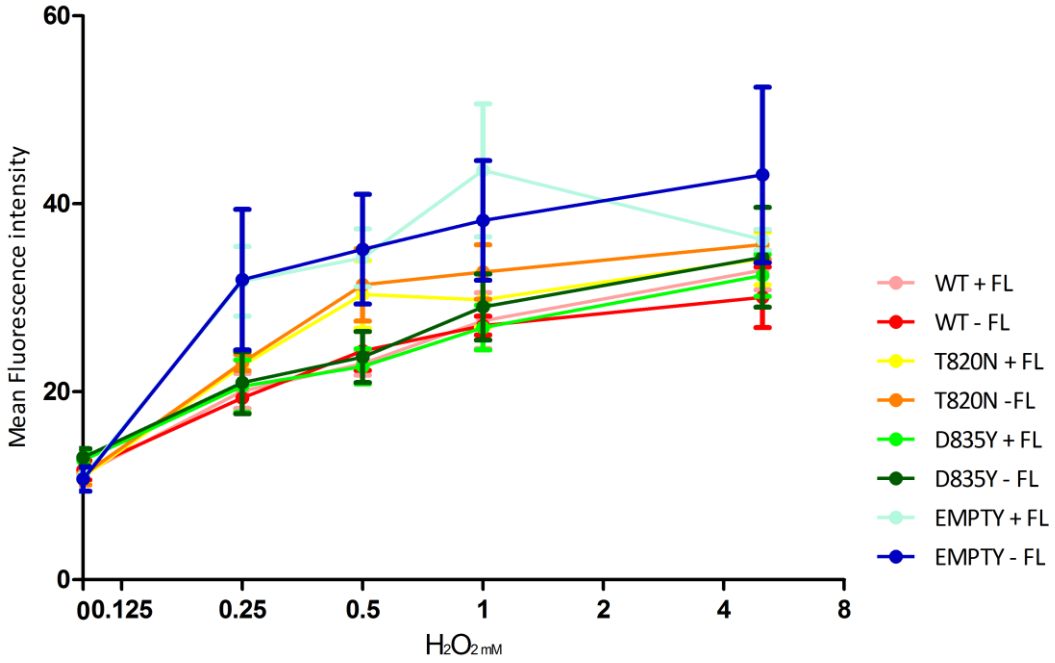

Figure 4.18 Examining the level of ROS in 32D FLT3-WT, FLT3-T820N, FLT3-D835Y and SFG-EMPTY cells pre-incubated with or without 10ng/mL FL for 8 hours and subsequently treated with H_2O_2. Data shown is the mean ± SEM of three individual experiments.

4.4 Discussion

Various different *FLT3* point mutations have been identified and the functional consequence of these mutations examined *in vitro*. This is the first report of the *FLT3*-T820N mutation being identified in the ME-1 cell line and the functional consequence investigated. In AML the majority of activating point mutations in *FLT3* occur in the ALD at residues D835 or N841. The *FLT3*-T820N mutation falls outside the ALD and lies just after the catalytic loop domain. This indicated that the *FLT3*-T820N mutation was not a 'classical' *FLT3* mutation and therefore warranted further investigation. Initially ME-1 cells were treated with AC220 to identify whether the mutation conferred resistance or increased sensitivity to growth inhibition or cell killing. These cells were completely resistant to AC220-mediated growth inhibition, cell killing or reducing phosphorylation of FLT3 target proteins. Immunoprecipitation of FLT3 from the ME-1 cell line revealed an absence of active FLT3. One explanation for this could be that the FLT3-T820N mutation has become redundant, suggesting that with multiple *in vitro* passages this mutation has been superseded by acquisition of a more potent driver mutation. Additional driver mutations were not indentified in mutational hotspots of *c-KIT* or *FLT3* as initially investigated (Figure 4.5). AC220 is a type II inhibitor that binds to the inactive conformation of FLT3. ME-1 cells do not have active FLT3 signalling hence AC220 treatment did not impact on downstream signalling, cell killing or inhibition of growth. The reason why FLT3 is not autophosphorylated in ME-1 cells is not clear. It could be that a phosphatase has been up regulated in these cells resulting in FLT3 being constantly dephosphorlyated. Further investigation would be required to address this. HMC1.2 cells did not express detectable FLT3, explaining why they did not respond to AC220. There was also no detectable FLT3 in PL-21 cells which suggested the growth inhibition and cell killing observed between 1.25μM-10μM AC220 was most likely the result of off-target effects. In contrast, MV4-11 and MOLM-13 cells were sensitive to AC220-mediated growth inhibition and cell killing, demonstrating that AC220 is a potent inhibitor of activating *FLT*3 mutations (addressed further in Chapter 5).

In order to investigate the functional consequence of the *FLT3*-T820N mutation 32D cells were transduced with constructs containing FLT3-WT, FLT3-T820N, FLT3-D835Y and SFG-EMPTY. Initial experiments examined the impact of the FLT3-T820N mutation on proliferation compared to cells expressing FLT3-WT, FLT3-D835Y and SFG-EMPTY. In the absence of mIL3, 32D EMPTY cells did not proliferate and died after 3/4 days (Figure 4.10). 32D FLT3-D835Y expressing cells conferred factor-independent growth, which is consistent with previous reports (Abu-Duhier *et al.*, 2001;Spiekermann *et al.*, 2003). 32D

FLT3-T820N expressing cells were capable of factor-independent growth which was equivalent to 32D FLT3-D835Y cells, suggesting that *FLT3*-T820N is a gain of function mutation. FLT3 was autophosphorylated by the T820N mutation in the absence of any growth factor, resulting in strong activation of STAT5, PIM-1 and AKT which corresponds with other known activating FLT3 mutations (Figure 4.10) (Reindl *et al.*, 2006;Rocnik *et al.*, 2006;Frohling *et al.*, 2007;Smith *et al.*, 2012). 32D FLT3-WT cells were capable of surviving without cytokines but only had a very low level of proliferation (Figure 4.10d). Reports have suggested that over-expression of the WT receptor may induce spontaneous phosphorylation of FLT3 and activate downstream signalling (Ozeki *et al.*, 2004). This is supported in Figure 4.11 which shows that 32D FLT3-WT expressing cells could autophosphorylate FLT3, although at low levels, when starved of FL which may explain why the 32D FLT3-WT cells did not die following cytokine removal.

As the FLT3-T820N mutation resulted in autophosphorylation of FLT3 conferring a proliferative advantage, it was of interest to examine the response of these cells to AC220. 32D SFG-EMPTY cells in the presence of mIL3 were resistant to AC220-mediated growth inhibition and cell killing at concentrations ≤100nM AC220. In contrast, mIL3 could not protect 32D FLT3-expressing cells from AC220-mediated growth inhibition or cell killing at 100nM concentration (Figure 4.12). As the FLT3-expressing cells did not die in the absence of mIL3 it suggests that these cells are less dependent on signalling via the IL3 receptor for cell survival, and that the IL3 receptor may be redundant and/or down-regulated in these cells. Another explanation could be that over-expression of FLT3 may swamp the endoplasmic reticulum machinery preventing as much IL3 receptor from being produced and expressed on the cell surface of these cells. Further experiments would be needed to explore this.

32D FLT3-T820N cells were more sensitive to AC220-mediated cell killing, inhibition of growth and reducing phosphorylation of FLT3 and other downstream target proteins in the presence or absence of FL when compared to 32D FLT3-WT or FLT3-D835Y cells. Although both FLT3-T820N and FLT3-D835Y mutations conferred a proliferative advantage to 32D cells, they resulted in very different responses to AC220. The crystal structure of FLT3 in the absence of FL suggests that the receptor adopts an inactive conformation whereby the activation loop folds back into the ATP-binding cleft, blocking the loading of substrates (Griffith *et al.*, 2004). In this conformation, the Asp829-Phe830-Gly831 (DFG) motif, which resides at the amino-terminal within the activating loop domain, is flipped away from the active site (DFG-OUT). To activate FLT3, the activating loop needs to be removed from the active site while the DFG motif needs to flip inward towards the

active site (DFG-IN). Modelling of AC220 binding to FLT3 suggests that it is a type II kinase inhibitor demonstrating preferential binding to the inactive receptor (DFG-OUT) (Wodicka *et al.*, 2010;Smith *et al.*, 2012). This suggests that AC220 would have a lower affinity for the active conformation (DFG-IN). Specific amino acid residues are thought to stabilise the inactive conformation of the ALD, including D835 and Y842, and it has been proposed that mutations at these residues destabilise the inactive conformation, shifting the equilibrium to the active state and therefore preventing effective AC220 binding (Smith *et al.*, 2012). This is consistent with the results presented here as 32D FLT3-D835Y cells were more resistant to AC220 in terms of inhibition of growth, cell killing and reducing phosphorylation of FLT3 in the presence or absence of FL in comparison to 32D FLT3-WT and FLT3-T820N cells. A similar response to AC220 has been observed in Ba/F3 cells expressing FLT3-D835Y which demonstrated that 100-1000nM AC200 was required to potently inhibit cell growth and reduce phosphorylation of FLT3 (Pauwels *et al.*, 2012).

Although the response of 32D FLT3-D835Y cells to AC220 is consistent with other published data, the response of 32D FLT3-T820N cells was more complex. The FLT3-T820N mutation constitutively activated FLT3 and was most sensitive to AC220 compared to cells expressing FLT3-D835Y and FLT3-WT. This suggests that AC220 may bind to alternative kinase conformations, other than the currently known inactive configuration, when the activation loop is phosphorylated (DFG-IN). In support of this, AC220 has demonstrated potent anti-tumour activity against *FLT3*-ITD mutations, both in AML cell lines, primary AML cells and in *in vivo* mouse models (Zarrinkar *et al.*, 2009;Pietschmann *et al.*, 2012). This reiterates that AC220 must be able to bind to alternative conformations when there is an activating *FLT3* mutation. Of note, all of the FLT3-expressing cell lines were more sensitive to AC220 in the absence of FL, supporting the notion that AC220 preferentially binds to the inactive conformation of FLT3. Currently the mechanism of how type II inhibitors such as AC220 bind to the activation loop region when phosphorylated is unknown (Liu & Gray, 2006).

To assess whether the response of the FLT3-expressing cells to AC220 was specific to this inhibitor, they were treated with another type II FLT3 inhibitor ponatinib. Ponatinib has demonstrated potent inhibition of FLT3 and cellular proliferation in *in vitro* and *in vivo* FLT3-ITD AML models (Gozgit *et al.*, 2011). 32D FLT3-T820N and FLT3-WT cells treated with ponatinib in the presence of FL showed no discernible differences between growth inhibition or cell killing, whereas in the absence of FL the FLT3-T820N expressing cells were more sensitive to ponatinib. 32D FLT3-D835Y cells were the most resistant to ponatinib-mediated inhibition of growth and cell killing compared to either 32D FLT3-WT

or FLT3-T820N cells. Current binding models suggest, that like AC220, ponatinib binds to the DFG-OUT, inactive FLT3 conformation (Smith *et al.*, 2013). The D835Y mutation is thought to destabilise this structure and therefore prevent ponatinib binding to FLT3, which explains the reduced toxicity observed when 32D FLT3-D835Y cells were treated with ponatinib. However, this cannot be the only mechanism of ponatinib binding to FLT3. FLT3-T820N cells were the most sensitive, in the absence of FL, to ponatinib. This suggests that the T820N mutation, although activating, generates a configuration that can more readily bind ponatinib. Of note, all of the FLT3-expressing cells were more resistant to ponatinib in the absence of FL, which is in stark contrast to what was observed under AC220 treatment. This suggests that in the absence of FL ponatinib cannot bind as readily to the FLT3 receptor, regardless of mutational status. Overall, AC220 was more potent at inhibiting the FLT3-T820N mutation in comparison to ponatinib.

FLT3-ITD mutations are reported to have increased endogenous levels of ROS, which has been associated with an increase in DNA damage and a decrease in end-joining fidelity (Sallmyr *et al.*, 2008). Currently, *FLT3*-TKD mutations have not been associated with elevated ROS levels. In contrast, the presence of a *FLT3*-ITD mutation can lead to STAT5 activation which can increase the level of ROS and contribute to driving cell proliferation (Sallmyr *et al.*, 2008). As the *FLT3*-T820N mutation falls outside the TKD, led to factor-independent growth and constitutively activated STAT5, it was hypothesised that ROS may be elevated in these cells. The basal level of ROS and response to H_2O_2 was assessed in each cell line. The basal level of endogenous ROS was equivalent across all the cell lines in the presence or absence of FL and there was no significant difference in response to H_2O_2 in the presence or absence of FL between the variant cell lines, suggesting that ROS do not play a significant role in cell growth in these cells.

In summary, the data in this chapter report the identification of a novel *FLT3*-T820N point mutation in the ME-1 cell line. FLT3-T820N expressed in 32D cells conferred ligand-independent growth and constitutively activated FLT3 in the absence of FL. 32D FLT3-T820N cells were more sensitive to AC220 in regards to cell killing, inhibition of growth, reducing phosphorylation of FLT3 and downstream target proteins in comparison to FLT3-WT and FLT3-D835Y expressing cells. The same mutation has been identified by the Wellcome Trust Sanger Institute in the acute erythremia KMOE-2 AML cell line. Although the same mutation has been identified in two AML cell lines, the current MRC screening strategy for identifying *FLT3*-TKD mutations would encompass the T820 residue and the mutation would be detected by dHPLC but no such mutation has been detected in over a 1000 patients screened (Rosemary Gale, personal communication). Therefore, as this

mutation has not been previously reported, it suggests that the T820N mutation is most likely a very rare mutation in AML.

5. Chapter 5: The impact of dasatinib and other small molecule inhibitors on AML cell lines and primary AML cells

5.1 Introduction

Activating mutations in *c-KIT* and *FLT3* occur in 28% of CBFL and 30% of AML respectively and have been discussed in detail in chapters 3 and 4 (Kottaridis *et al.*, 2001;Mead *et al.*, 2007;Allen *et al.*, 2013). Mutations in *c-KIT* or *FLT3* are associated with activation of key downstream signalling proteins including PI3K, AKT, mTOR and MEK. Activation of these signalling pathways is found in 50-90% of primary AML cells even in the absence of known RTK mutations, suggesting that these protein networks are intrinsic to the maintenance of AML cells (Xu *et al.*, 2003;Grandage *et al.*, 2005;Brandts *et al.*, 2005;Ricciardi *et al.*, 2005). Targeting individual cell signalling molecules with small molecule inhibitors has elicited disappointing results in early clinical trials in AML and other malignancies (Rinehart *et al.*, 2004;Yee *et al.*, 2006;Cortes *et al.*, 2012;Levis *et al.*, 2012;Zwaan *et al.*, 2013).

This chapter aimed to investigate the effect of combined RTK and AKT, mTOR, PI3K or PI3K + mTOR inhibition on cell growth, cell killing and signalling in AML cell lines and primary AML cells with and without activating RTK mutations.

5.2 Materials and methods

5.2.1 Cell lines

Kasumi-1, SKNO.1, MV4-11, MOLM-13 and PL-21 cells were all grown in R2 media whereas HMC1.2 cells were cultured in R1 media, as described in chapter 2 section 2.1.6. Primary AML cells were thawed and left overnight in R3 media containing 20ng/mL of human SCF, FLT3, TPO and IL3. After 24 hours viable primary AML cells were isolated by density centrifugation, re-suspended in fresh R3, treated with small molecule inhibitors and incubated in a hypoxic atmosphere containing 5% CO_2 and 5% O_2 as described in chapter 2 section 2.1.8.

5.2.2 Screening of AML cell lines and primary AML cells for *c-KIT* and *FLT3* mutations

PCR was used to amplify exons 14-15 and 20 of *FLT3* and exons 8, 10-11 and 17 of *c-KIT* using primers listed in Table 4.1 as described in chapter 2 section 4.2.2.

5.2.3 Annexin V/ PI assay

Performed as described in chapter 2 section 2.4.2.

5.2.4 Protein detection using western blotting

Performed as described in chapter 2 section 2.3.4.

5.2.5 Immunoprecipitation of FLT3 from MV4-11 and MOLM-13 cells

MV4-11 and MOLM-13 cells ($1x10^7$ cells/mL) were treated with AC220 for 4 hours. Cells were harvested and lysed in modified RIPA buffer (50mM TRIS HCL, 1% NP40, 0.25% sodium deoxycholate, 150mM NaCl, 1mM EGTA, 1mM PMSF, 1µg/mL leupeptin, 1µg/mL pepstatin A, 1mM NaF and 1mM Na_3VO_4). Harvested lysates were adjusted to contain equivalent amounts of protein using the DC™ assay as described in chapter 2 section 2.3.3. They were then pre-cleared with a 50% slurry containing an equal volume of Protein G-Sepharose 4 Fast Flow beads and RIPA lysis buffer for 1 hour at 4°C with end-over-end rotation. The beads were removed by centrifugation and the lysates were incubated with 2µg of FLT-3/Flk-2 antibody (C20) (Santa Cruz biotechnology) at 4°C over night with end-over-end rotation. They were then incubated again with a 50% slurry containing an equal volume of Protein G-Sepharose 4 Fast Flow beads and RIPA lysis buffer for 2-3 hours at 4°C with end-over-end rotation. Protein bound to the beads were then washed 3 times with ice cold

lysis buffer and re-suspended in 50µL of NuPAGE® LDS Sample Buffer containing 10% NuPAGE® sample reducing agent. The samples were boiled for 5 minutes and 10µL was loaded onto a NuPAGE® Novex 7% Tris-Acetate Gel 1.0 mm. Gels were electrophoresed and transferred as described in chapter 2 section 2.3.4.

5.2.6 Data analysis

To examine if drug interactions were antagonistic, additive or synergistic at cell killing, the data was analysed using CalcuSyn software. This uses the Chou-Talalay method, which is based on the median-effect equation (Chou & Talalay, 1983;Chou & Talalay, 1984). The CI definitions are as follows: >1.1 antagonistic, 0.9-1.1 additive and <0.9 synergistic.

5.3 Results

5.3.1 Confirmation of reported mutations in cell lines

gDNA from HMC1.2, SKNO.1, Kasumi-1, MV4-11, MOLM-13 and PL-21 cell lines was screened for mutations in *c-KIT* (exons 8, 10, 11 and 17) and *FLT3* (exons 14 and 15 [ITD] and 20 [TKD]) by sequencing and fragment size separation. The HMC1.2 cells had both a *c-KIT* V560G and D816V mutation (Figure 5.1). The Kasumi-1 and the SKNO.1 cells both had the *c-KIT* N822K mutation (Figure 5.1). The MV4-11, MOLM-13 and PL-21 cells were WT for *c-KIT*. Only MV4-11, MOLM-13 and PL-21 cells lines had a *FLT3*-ITD mutation, shown in Figure 5.2 and quantified in Figure 5.3. Quantification of the *FLT3*-ITDs revealed that the MV4-11 cells only expressed the mutant allele which suggests complete loss of the *FLT3*-WT allele. The mutant level in the MOLM-13 and PL-21 cells was not equivalent to every cell having a heterozygous mutation i.e. 50:50. The reason for this is unclear. In the MOLM-13 cells a higher mutant level could indicate a proportion of the cells have lost the WT allele, whereas a lower mutant level in the PL-21 cells might suggest loss of the mutant allele in a proportion of cells. The HL60 cell line was included as a control which only expressed the WT allele. None of the cell lines examined had a mutation in exon 20 of *FLT3*. The mutations identified in each cell line are consistent with previous reports (Furitsu *et al.*, 1993;Quentmeier *et al.*, 2003;Becker *et al.*, 2008).

5.3.2 Cytotoxic effects of dasatinib in Kasumi-1 and HMC1.2 cells

To examine the cytotoxic effect of targeting *c-KIT* mutations, the Kasumi-1 and HMC1.2 cells were treated with dasatinib. After 72 hours in the presence of dasatinib, Kasumi-1 cells showed a dose-dependent reduction in live cell number (IC50 = 9.2nM ± 0.57), and the percentage of live cells (IC50 = 21.4nM ± 2) (Figure 5.4 a,b). In contrast, HMC1.2 cells treated with dasatinib for 48 hours were more resistant to dasatinib-mediated growth inhibition (IC50 = 1.6 ± 0.2µM) and cell killing (IC50 = 3.1µM ± 0.6) (Figure 5.5 a,b).

Cell line	Gene	Exon	Sequencing chromatograph highlighting *c-KIT* mutations	Sequencing Direction
HMC1.2	*c-KIT*	10+11	GTT>GGT **V560G** 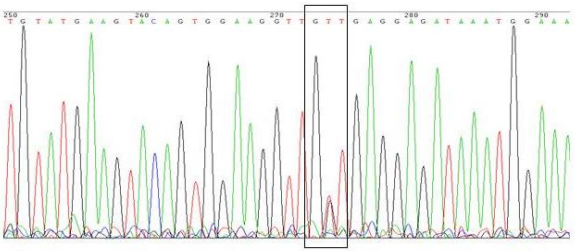	Forward
HMC1.2	*c-KIT*	17	GAC>GTC **D816V** 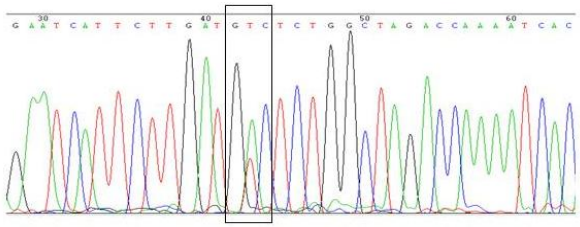	Reverse
SKNO.1	*c-KIT*	17	AAT>AAA **N822K** 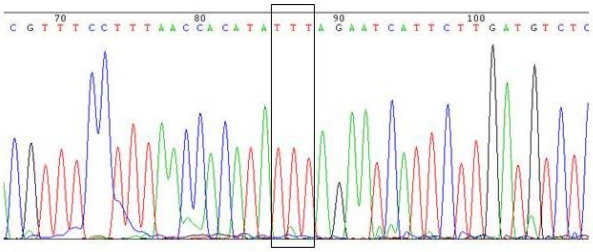	Reverse
Kasumi-1	*c-KIT*	17	AAT>AAA **N822K** 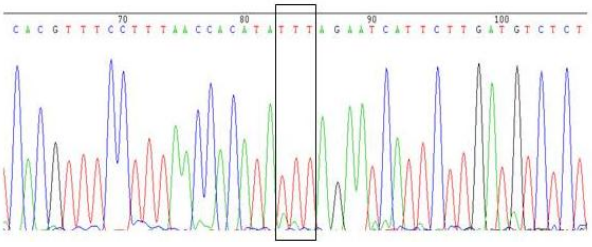	Reverse

Figure 5.1 Sequencing chromatograms showing the presence of *c-KIT* mutations in HMC1.2, SKNO.1 and Kasumi-1 cells.

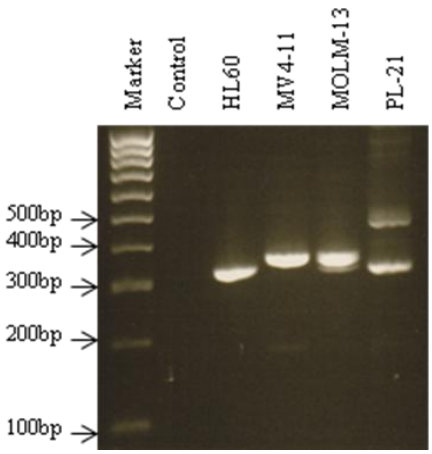

Figure 5.2 Identification of *FLT3*-ITD mutations in MV4-11, MOLM-13 and PL-21 cells. *FLT3*-ITD PCR products were amplified from HL60, MV4-11, MOLM-13 and PL-21 cells and run on a agarose gel. The HL60 cell line was used as a WT control (WT PCR fragment size 328bp).

Cell line	Gene	Exon	CEQ graphical data	WT:MUT allele	
				WT (%)	MUT (%)
HL60	*FLT3*	14-15	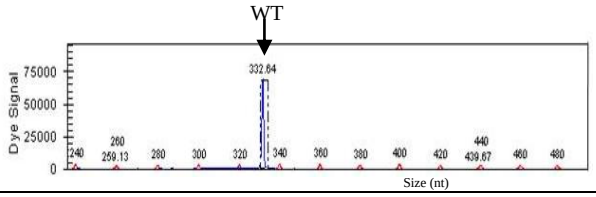	100	0
MV4-11	*FLT3*	14-15	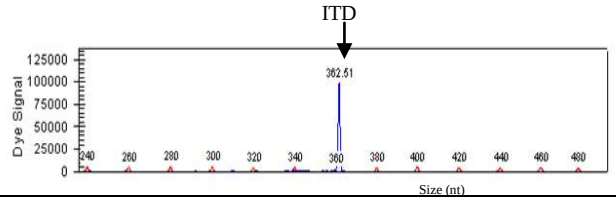	0	100
MOLM-13	*FLT3*	14-15	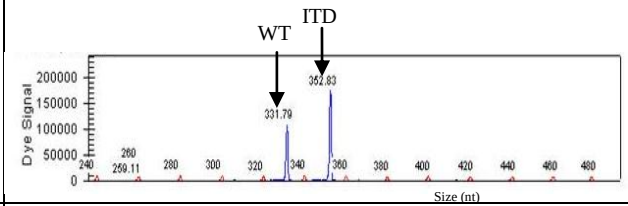	38	62
PL-21	*FLT3*	14-15	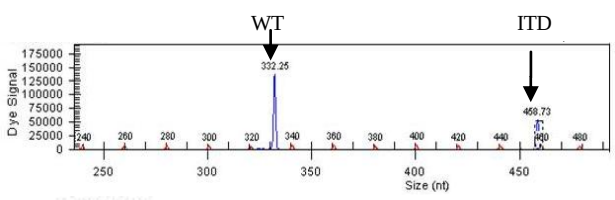	72	28

Figure 5.3 Fragment analysis of *FLT3*–ITD mutations in the MV4-11, MOLM-13 and PL-21 cells. The HL60 cell line was used as a WT control. WT = Wild-type, MUT = Mutant. Above is a representative example from three repeats.

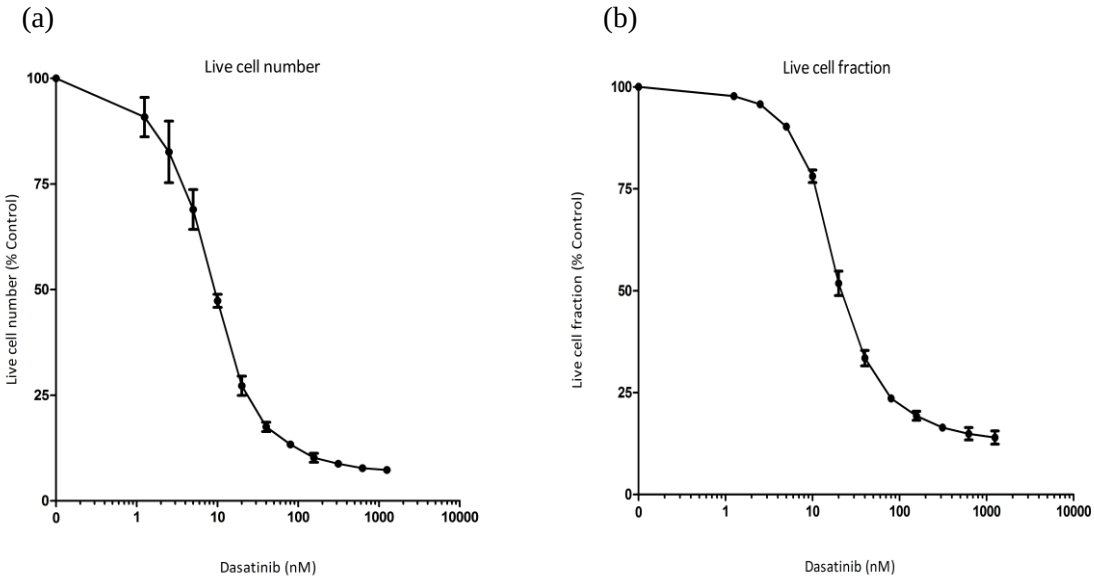

Figure 5.4 Response of Kasumi-1 cells to dasatinib after 72 hours (a) Total number of live cells. (b) Percentage of cells in the live cell fraction. Data shown is the mean ± SEM of three individual experiments.

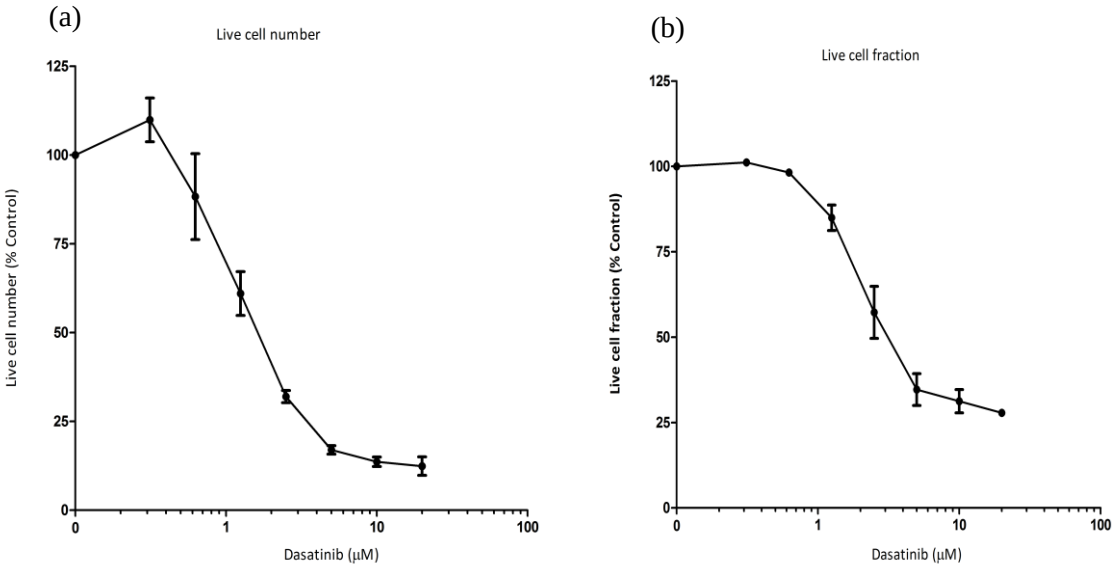

Figure 5.5 Response of HMC1.2 cells to dasatinib after 48 hours (a) Total number of live cells. (b) Percentage of cells in the live cell fraction. Data shown is the mean ± SEM of three individual experiments.

5.3.3 The effect of dasatinib on signalling in *c-KIT* mutant cell lines

As Kasumi-1 and HMC1.2 cells varied in their sensitivity to dasatinib-mediated growth inhibition and cell killing, the impact on targeting c-KIT and downstream signalling was assessed. Autophosphorylation of c-KIT was used as a measure of c-KIT activity as indicated by phosphorylation of residue Y719. Kasumi-1 cells treated with dasatinib for 4 hours caused a dose-dependent reduction in phosphorylation of c-KIT at residue Y719 between 20 and 80nM (Figure 5.6 a,b) There was also a corresponding reduction in phosphorylation of MAPK and S6 (Figure 5.6 a,b). The level of p-4E-BP1 was slightly reduced at dasatinib concentrations ≥ 40nM. In HMC1.2 cells, 0.3125-10μM dasatinib caused a dose-dependent reduction in phosphorylation of c-KIT corresponding with a reduction in phosphorylation of AKT, MAPK and S6 (Figure 5.7 a,b). Although c-KIT phosphorylation was potently reduced at concentrations between 0.3125μM and 1.25μM, the level of phosphorylation of AKT, MAPK and S6 remained disproportionately high. The level of p-4E-BP1 remained relatively unchanged following dasatinib treatment in the HMC.1.2 cells. A concentration of 2μM of imatinib did not reduce p-c-KIT levels in the HMC1.2 cell line.

The capability of dasatinib to reduce autophosphorylation of c-KIT in HMC1.2 cells was explored further by extending the dose response range. Figure 5.8 illustrates after 4 hours a concentration greater than 0.08μM of dasatinib reduced phosphorylation of c-KIT. This suggests that although c-KIT activity is potently reduced other signalling molecules may contribute to phosphorylation of AKT, MAPK and S6.

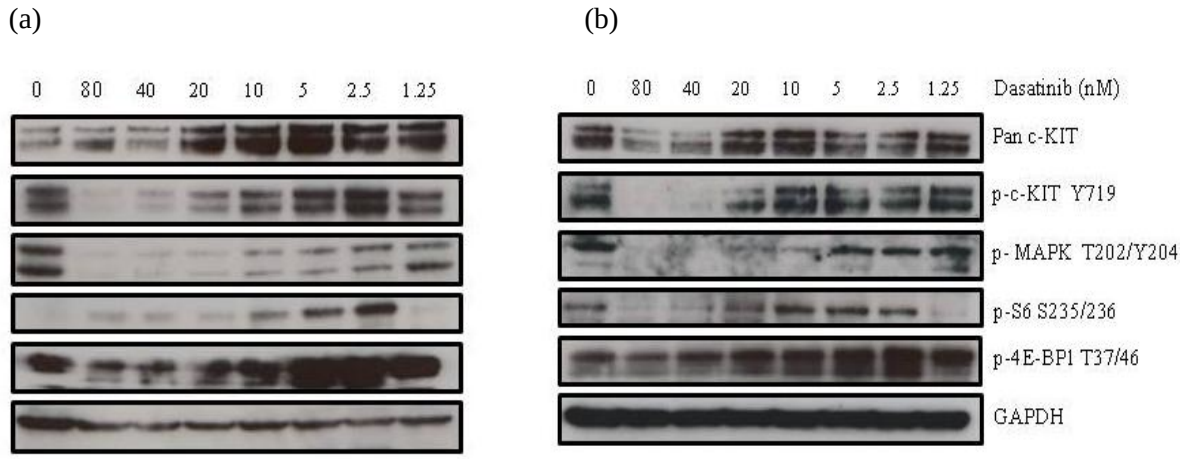

Figure 5.6 Effect of dasatinib on signalling downstream of c-KIT in Kasumi-1 cells after 4 hours. (a,b) Two independent repeats. GAPDH was used as a loading control.

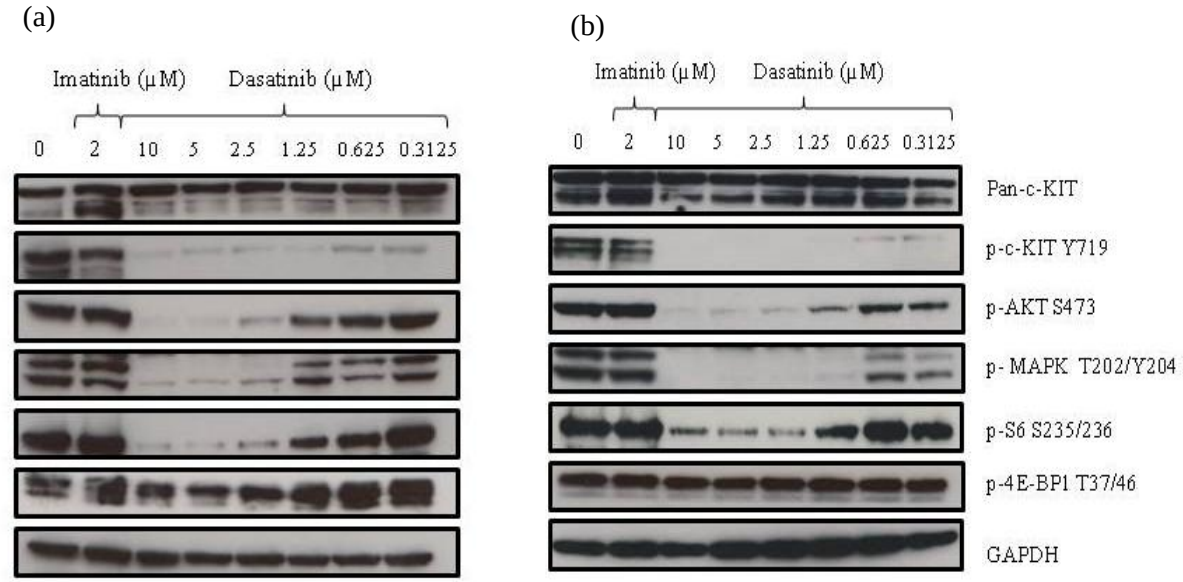

Figure 5.7 Effect of dasatinib on signalling downstream of c-KIT in HMC1.2 cells after 4 hours. (a,b) Two independent repeats. GAPDH was used as a loading control.

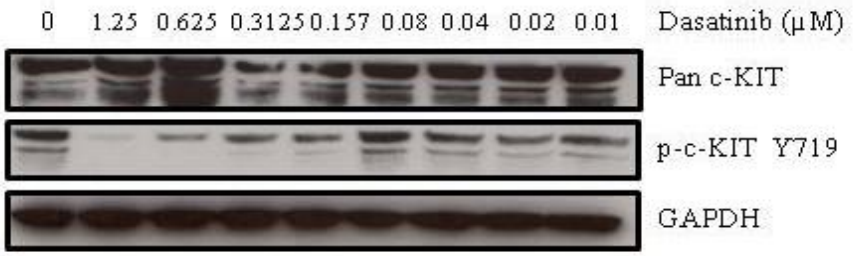

Figure 5.8 Effect of expanded dose range of dasatinib on c-KIT phosphorylation in HMC1.2 cells after 4hours. GAPDH was used as a loading control.

5.3.4 Cytotoxic effect of combining dasatinib with other small molecule inhibitors in Kasumi-1 and HMC1.2 cells

In Kasumi-1 cells, 40nM dasatinib completely blocked c-KIT phosphorylation and MEK but there was residual PI3K/mTOR signalling as indicated by the levels of p-4E-BP1 and p-S6 (Figure 5.6 a,b). In HMC1.2 cells, dasatinib reduced c-KIT autophosphorylation fully at 313nM, but there was also residual MEK, AKT, PI3K and mTOR signalling (Figure 5.7 a,b). Therefore, the effect of combining dasatinib with selective inhibitors of PI3K (ZSTK-474), mTOR (WYE-354), PI3K + mTOR (BEZ-235) and AKT (AZD5363) on cell survival and cell signalling was examined.

Kasumi-1 cells were treated with selected inhibitors for 48 hours. As shown previously, dasatinib as a single agent was capable of killing Kasumi-1 cells at 80nM. Kasumi-1 cells were sensitive to ZSTK-474, WYE-354, BEZ-235 or AZD5363 alone as indicated by potent growth inhibition and cell killing (Figure 5.9 a,b). Treatment of Kasumi-1 cells with a combination of dasatinib and ZSTK-474, WYE-354, BEZ-235 or AZD5363 showed an enhanced reduction in cell growth and cell killing, particularly combinations of dasatinib and ZSTK-474, WYE-354 or BEZ-235 (Figure 5.9 a,b). In contrast, HMC1.2 cells required a concentration >1.25μM dasatinib to induce substantial cell killing. HMC1.2 cells were relatively sensitive to growth inhibition and cell killing mediated by ZSTK-474, WYE-354, BEZ-235 or AZD5363 alone (Figure 5.10 a,b). As the HMC1.2 cells were more resistant to dasatinib a higher dose range of 0.3125, 0.625, 1.25 and 5μM was used in combination with ZSTK-474, WYE-354, BEZ-235 or AZD5363. These drug combinations showed an enhanced reduction in cell growth and cell killing, particularly combinations of dasatinib and ZSTK-474, WYE-354 or BEZ-235 (Figure 5.10 a,b). The effect of the drug combinations was less striking in Kasumi-1 cells which may be due to a greater level of cell killing observed with ZSTK-474, WYE-354, BEZ-235 or AZD5363 alone.

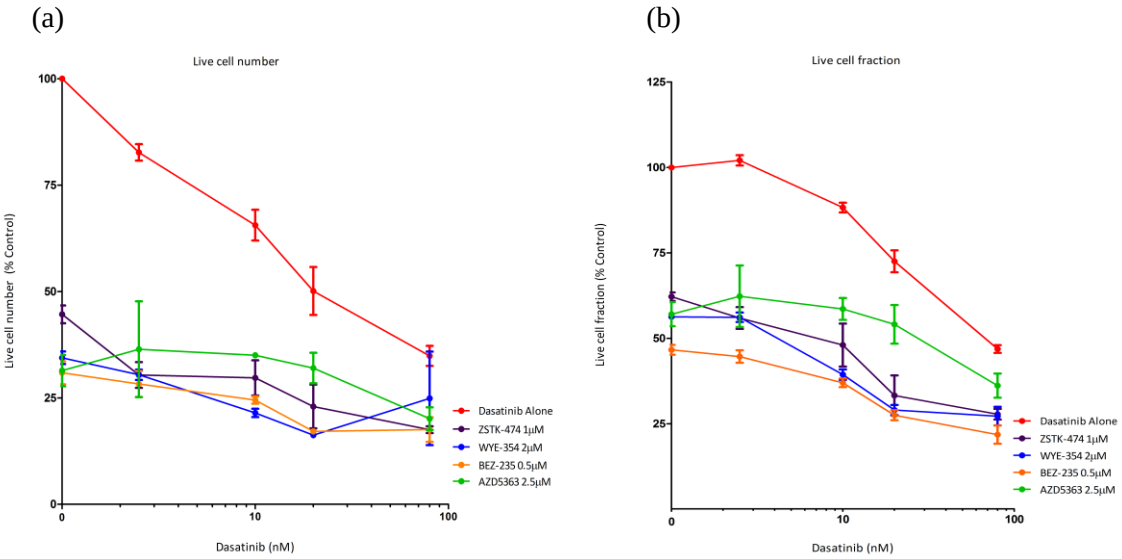

Figure 5.9 Response of Kasumi-1 cells to combinations of dasatinib and ZSTK-474, WYE-354, BEZ-235 or AZD5363 after 48 hours. (a) Total number of live cells. (b) Percentage of cells in the live cell fraction. Data shown is the mean ± SEM of three individual experiments

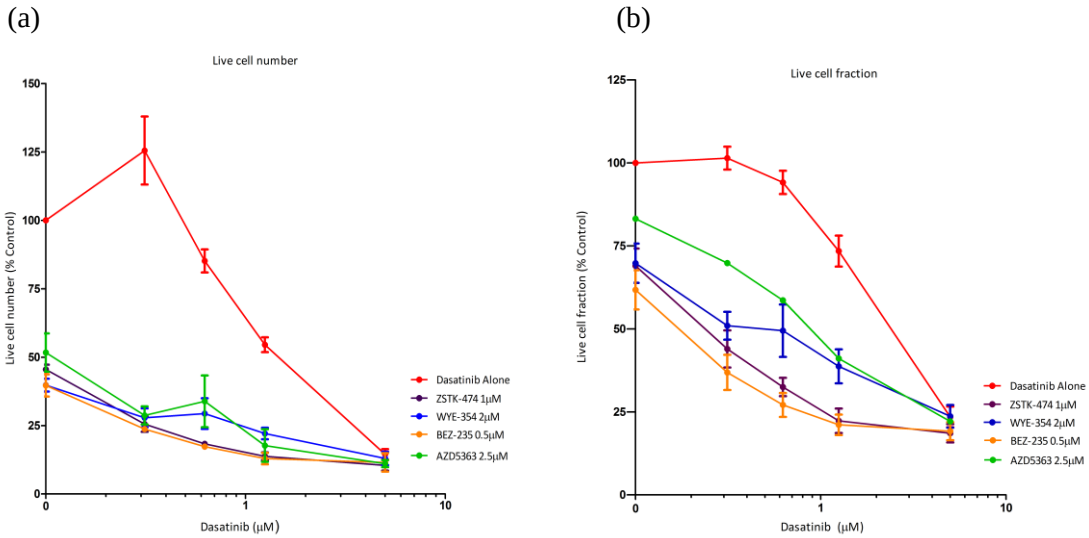

Figure 5.10 Response of HMC1.2 cells to combinations of dasatinib and ZSTK-474, WYE-354, BEZ-235 or AZD5363 after 48 hours. (a) Total number of live cells. (b) Percentage of cells in the live cell fraction. Data shown is the mean ± SEM of three individual experiments

5.3.5 Evaluation of synergy between dasatinib and PI3K/mTOR inhibitors

Kasumi-1 and HMC1.2 cells were treated with Dasatinib and PI3K/mTOR inhibitors to examine whether combinations of these drugs were additive or synergistic. Kasumi-1 cells were treated with a dose range of WYE-354, ZSTK-474 or BEZ-235 in combination with dasatinib for 72 hours. As shown in Figure 5.11 a-f BEZ-235 was the most potent PI3K/mTOR inhibitor at decreasing cell growth and inducing cell killing alone. Increasing concentrations of WYE-354, ZSTK-474 or BEZ-235 in combination with dasatinib, further inhibited cell growth and induced greater cell killing in comparison to either agent alone (Figure 5.11 a-f).

HMC1.2 cells were treated with a dose range of WYE-354, ZSTK-474 or BEZ-235 in combination with dasatinib for 48 hours. As shown in Figure 5.12 a-f BEZ-235 was the most potent PI3K/mTOR inhibitor at reducing cell growth, however the effect of the various PI3K/mTOR inhibitors on cell killing was comparable. A combination of dasatinib and WYE-354, ZSTK-474 or BEZ-235 enhanced growth inhibition and cell killing in comparison to either drug alone (Figure 5.12 a-f). In particular dasatinib and ZSTK-474 or BEZ-235 had the most potent effects. The effect of dasatinib and the PI3K/mTOR inhibitors was less pronounced in Kasumi-1 cells which is most likely the result of these cells being more sensitive to dasatinib in comparison to HMC1.2 cells (Figure 5.11 a-f and Figure 5.12 a-f).

CalcuSyn software was used to examine if the interactions between dasatinib and WYE-354, ZSTK-474 or BEZ-235 were synergistic at cell killing in each cell line (Table 5.1). In Kasumi-1 cells a combination of dasatinib and WYE-354, ZSTK-474 or BEZ-235 gave CI values at ED50 of <0.9, indicating that all drug combinations examined were synergistic (Table 5.1). In particular, dasatinib and the PI3K inhibitor ZSTK-474 showed the strongest synergy. In HMC1.2 cells, a combination of dasatinib plus WYE-354, ZSTK-474 or BEZ-235 also gave CI values at ED50 of <0.9, indicating that all drug combinations examined were synergistic (Table 5.1). Of note, as seen in Kasumi-1 cells, a combination of dasatinib and ZSTK-474 had the strongest synergistic interaction in HMC1.2 cells.

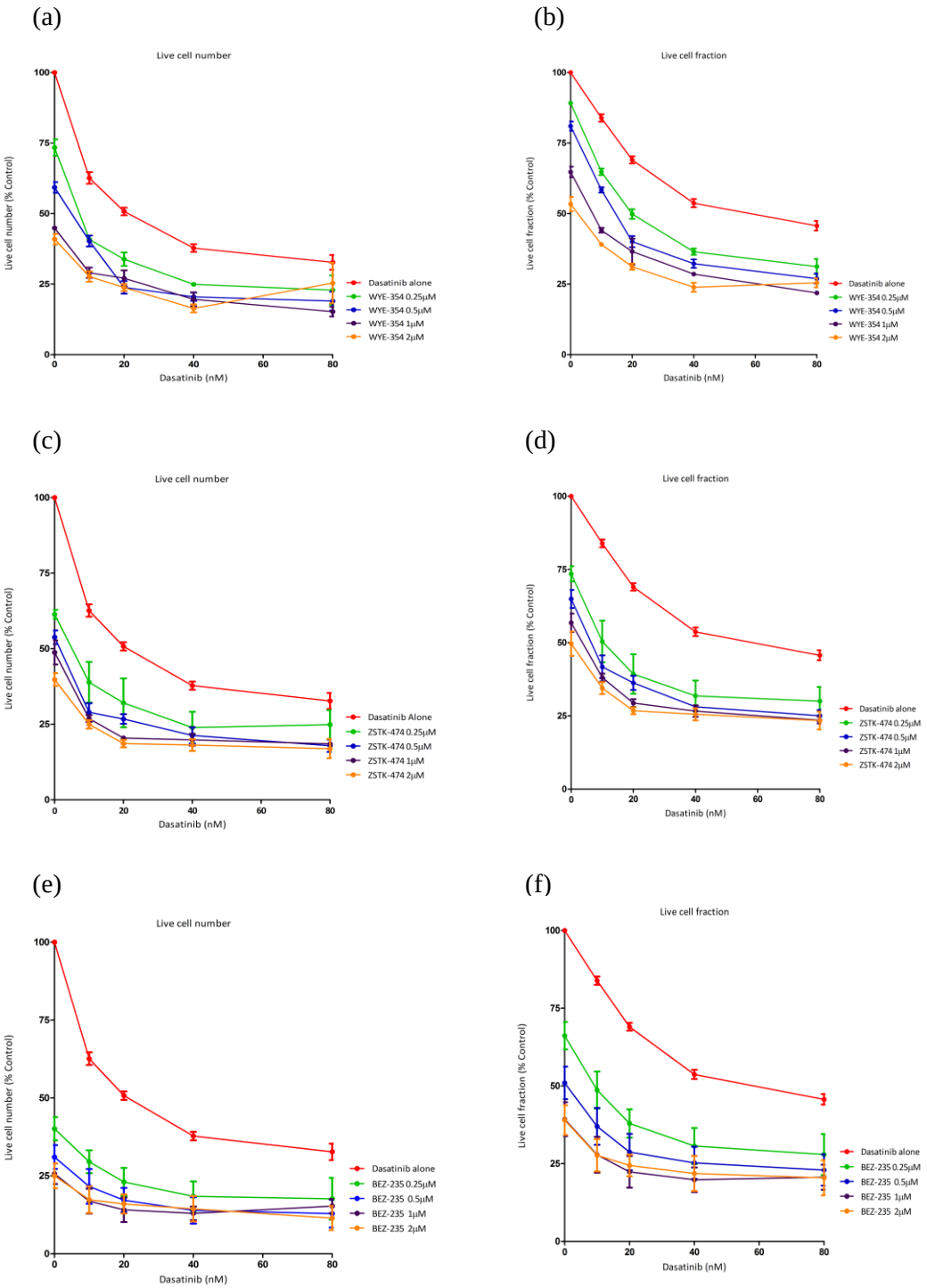

Figure 5.11 Response of Kasumi-1 cells to combinations of dasatinib and WYE-354, ZSTK-474 or BEZ-235 after 72 hours. (a,c,e) Total number of live cells. (b,d,f) Percentage of cells in the live cell fraction. Data shown is the mean ± SEM of three individual experiments

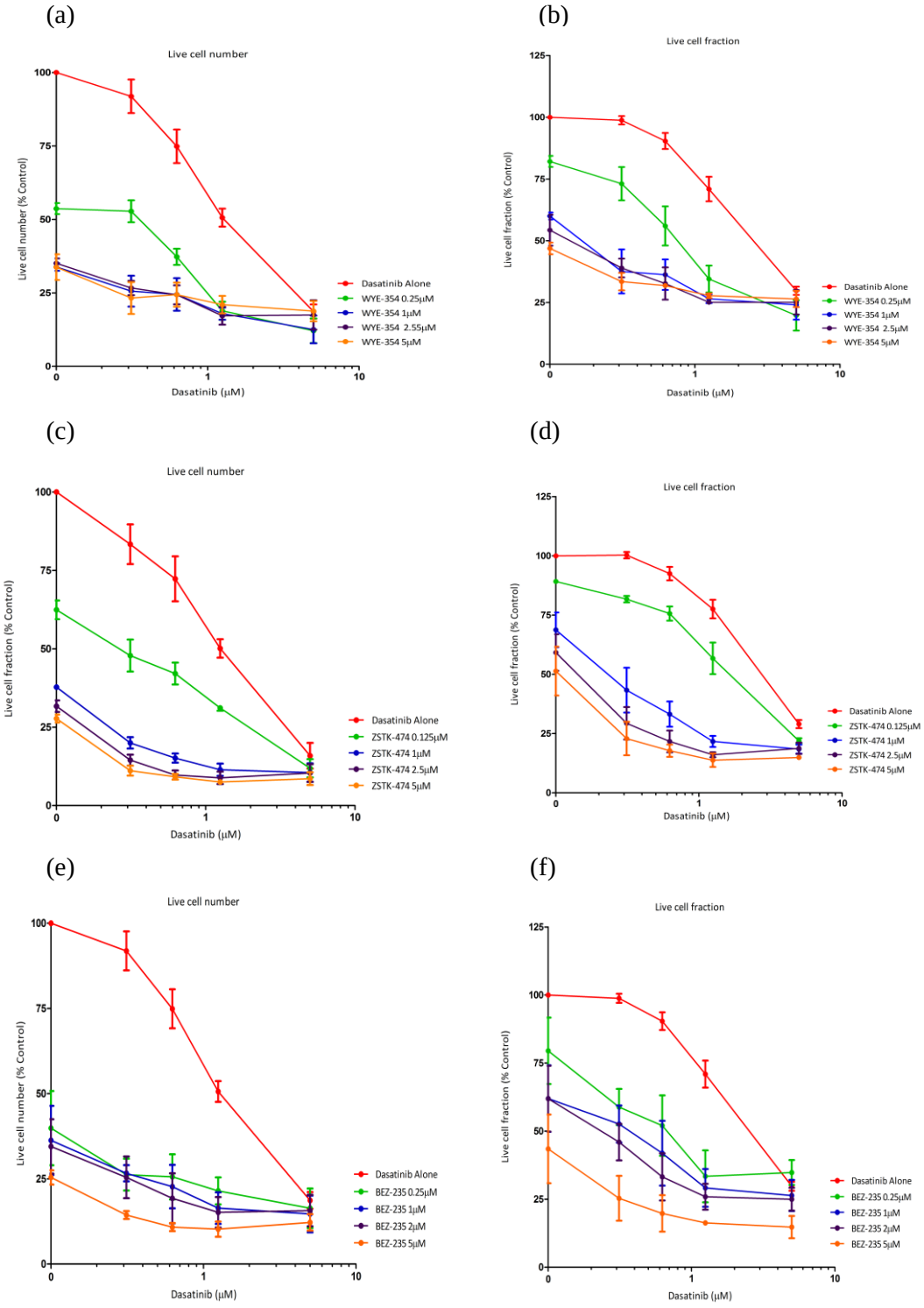

Figure 5.12 Response of HMC1.2 cells to combinations of dasatinib and WYE-354, ZSTK-474 or BEZ-235 after 48 hours. (a,c,e) Total number of live cells. (b,d,f) Percentage of cells in the live cell fraction. Data shown is the mean ± SEM of three individual experiments

.

		CI Values at:		
Drug Combination	**Cell line**	ED50	ED75	ED90
Dasatinib + WYE-354 (1:25)	Kasumi-1	0.479	0.567	0.678
Dasatinib + ZSTK-474 (1:25)	Kasumi-1	0.275	0.379	0.614
Dasatinib + BEZ-235 (1:25)	Kasumi-1	0.367	0.382	0.455
Dasatinib + WYE-354 (1:4)	HMC1.2	0.482	1.498	15.801
Dasatinib + ZSTK-474 (1:4)	HMC1.2	0.308	0.291	0.421
Dasatinib + BEZ-235 (1:4)	HMC1.2	0.562	0.432	0.533

CI = Combination Index value, ED = Effective dose

Table 5.1 CalcuSyn data providing the CI values at ED50, ED75 and ED90 from cell killing data of Kasumi-1 and HMC1.2 cells treated with dasatinib and WYE-354, ZSTK-474 or BEZ-235. Brackets indicate the respective ratio of each drug used.

5.3.6 Impact of combined inhibition of c-KIT and PI3K/mTOR on downstream signalling in Kasumi-1 and HMC1.2 cells

As combinations of dasatinib and WYE-354, ZSTK-474 or BEZ-235 showed synergistic cell killing (CI<0.9) in both Kasumi-1 and HMC1.2 cells, western blotting was used to examine the effect on downstream target proteins. Both cell lines were treated with inhibitory molecules for 4 hours. In Kasumi-1 cells, 40nM dasatinib potently reduced phosphorylation of c-KIT and MAPK. However, there was residual mTOR/PI3K signalling as indicated by levels of p-S6, p-p70-S6K and p-4E-BP1 (Figure 5.13a). WYE-354, ZSTK-474 or BEZ-235 alone potently inhibited PI3K/mTOR targets but p-c-KIT and p-MAPK remained at levels equivalent to the control. Combining dasatinib with WYE-354, ZSTK-474 or BEZ-235 markedly reduced residual PI3K and mTOR signalling compared with just dasatinib (Figure 5.13a). This pattern was most striking when Kasumi-1 cells were treated with dasatinib and BEZ-235, as there was no residual p-p70 S6K, p-S6 or p-4E-BP1 expression.

In HMC1.2 cells dasatinib alone potently reduced c-KIT autophosphorylation however there was residual MEK, AKT, PI3K and mTOR signalling at a concentration of 0.625μM (Figure 5.13b). Treatment of HMC1.2 cells with WYE-354, ZSTK-474 or BEZ-235 alone potently inhibited mTOR/PI3K signalling indicated by a marked decrease in phosphorylation of p70 S6K, AKT, S6 and 4E-BP1 (Figure 5.13b). Combinations of dasatinib and WYE-354, ZSTK-474 or BEZ-235 significantly reduced the levels of p-p70 S6K, p-MAPK, p-AKT, p-S6 and p-4E-BP1 compared to either drug alone. Of note, a combination of dasatinib and WYE-354 or BEZ-235 most potently decreased phosphorylation of downstream target proteins (Figure 5.13b).

(a)

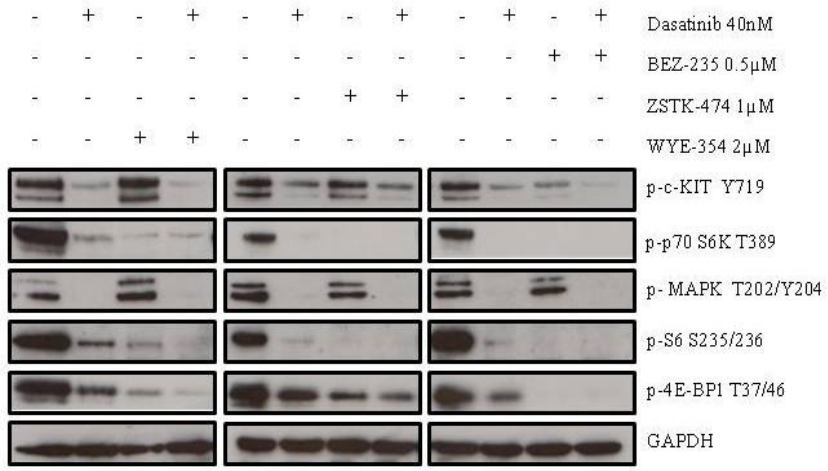

(b)

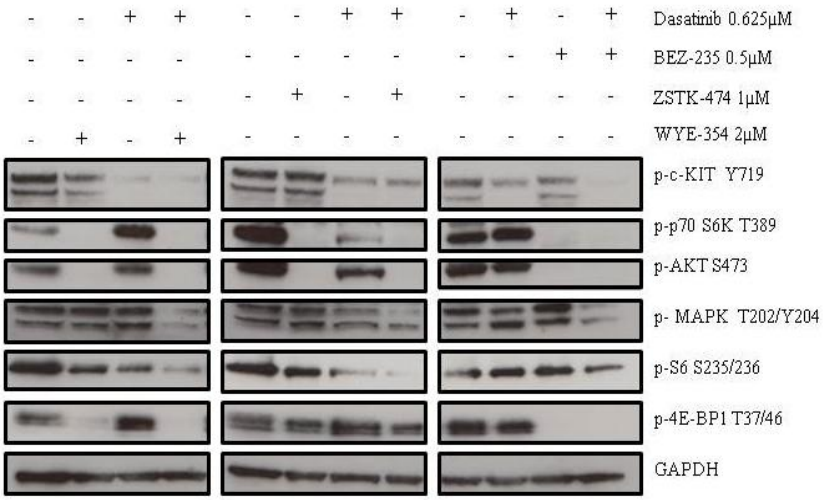

Figure 5.13 Effect of dasatinib and WYE-354, ZSTK-474 or BEZ-235 on c-KIT and downstream signalling in Kasumi-1 and HMC1.2 cells after 4 hours. Western blotting of Kasumi-1(a) and HMC1.2 cells (b) treated with dasatinib and WYE-354, ZSTK-474 or BEZ-235. GAPDH was used as a loading control.

5.3.7 A combination of dasatinib and inhibitors of PI3K/mTOR induces apoptosis

The mechanism of cell killing in Kasumi-1 and HMC1.2 cells was examined further by screening of pro-apoptotic and anti-apoptotic Bcl-2 family members at 4, 24 and 48 hours of treatment. Cells were treated with dasatinib and WYE-354, ZSTK-474 or BEZ-235 for 4 and 24 hours but showed little change in any apoptotic markers examined (data not shown). Therefore, cells were treated with inhibitor combinations for 48 hours. In Kasumi-1 cells treated with dasatinib alone there was no significant change in expression of the Bcl-2 family member proteins, pro-caspase 3 or PARP (Figure 5.14a). Treatment of Kasumi-1 cells with ZSTK-474 or BEZ-235 alone decreased expression of Mcl-1 corresponding with an increase in PARP cleavage but had a minimal effect on the other apoptotic proteins examined. WYE-354 alone did not decrease expression of Mcl-1 or Bcl-2 however there was an increase in PARP cleavage suggesting other Bcl-2 family proteins might be involved in driving apoptosis through this inhibitor. Combinations of dasatinib and WYE-354, ZSTK-474 or BEZ-235 led to a significant decrease in Mcl-1. Combining dasatinib and BEZ-235 also reduced expression of Bcl-2. Only a combination of dasatinib and BEZ-235 led to a decrease in pro-caspase 3 however all drug combinations induced PARP cleavage (Figure 5.14a). The level of BIM did not change under any of the drug combinations in Kasumi-1 cells.

HMC1.2 cells treated with dasatinib, WYE-354, ZSTK-474 or BEZ-235 alone did not significantly alter the expression of the Bcl-2 family member proteins examined and did not decrease expression of pro-caspases 3 or 9 (Figure 5.14b). Only a combination of dasatinib and ZSTK-474 or BEZ-235 significantly decreased both Mcl-1 and Bcl-x. These drug combinations also led to a decrease in pro-caspases 3 and 9 and an increase in PARP cleavage (Figure 5.14b). Dasatinib and WYE-354 did not decrease levels of Mcl-1 or Bcl-2 however there was an increase in PARP cleavage which suggests other proteins may be involved in driving cell killing through this drug combination. The effect of the drug combinations on BIM is inconclusive. Bcl-2 was not detected in HMC1.2 cells and Bcl-x and pro-caspase 9 were not detected in Kasumi-1 cells. Both Kasumi-1 and HMC1.2 cells were screened for changes in phosphorylation at residues S112 and S136 of the pro-apoptotic protein BAD however neither were detected in either cell line (data not shown). A combination of dasatinib and BEZ-235 had the most potent effects in both cell lines.

(a)

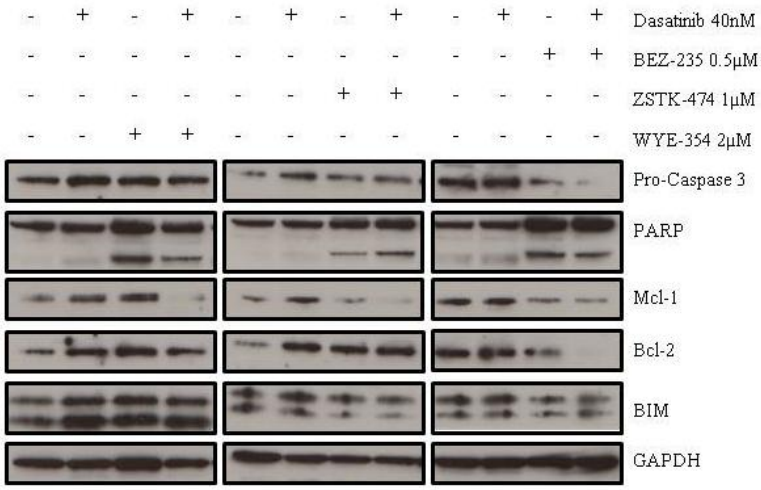

(b)

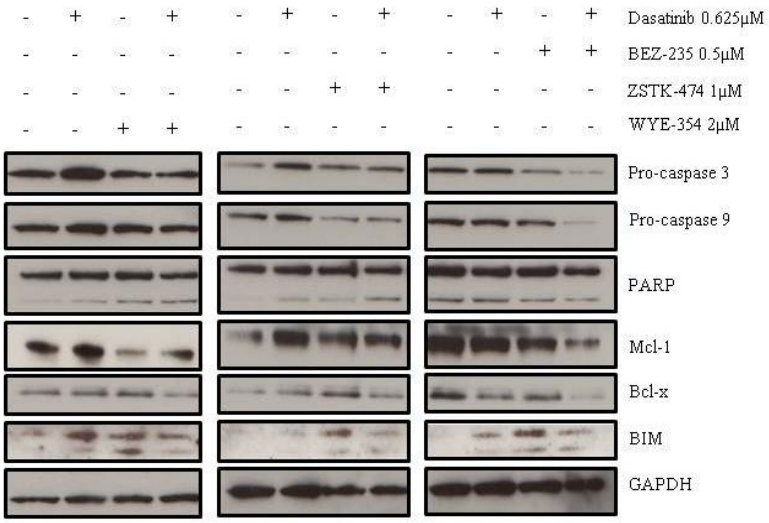

Figure 5.14 Effect of dasatinib and WYE-354, ZSTK-474 or BEZ-235 on apoptotic regulators in Kasumi-1 and HMC1.2 cells after 48 hours of treatment. Western blotting of Kasumi-1(a) and HMC1.2 cells (b) treated with dasatinib and WYE-354, ZSTK-474 or BEZ-235. GAPDH was used as a loading control.

5.3.8 Time course effect of dasatinib on c-KIT autophosphorylation in Kasumi-1 and HMC1.2 cells

Kasumi-1 and HMC1.2 cells were cultured with dasatinib for 4, 8, 24 and 48 hours to assess if dasatinib could reduce phosphorylation of c-KIT in a sustained of transient manner. Treatment of Kasumi-1 cells with 40nM dasatinib reduced the level of p-c-KIT at 4 and 8 hours which was completely decreased after 8 hours (Figure 5.15). The reduction in p-c-KIT corresponded with a complete decrease in phosphorylation of MAPK and S6. The level of p-4E-BP1 expression only appeared to decrease more substantially after 24 or 48 hours, in accordance with the cells beginning to die.

In HMC1.2 cells, 5μM dasatinib reduced c-KIT autophosphorylation at 4 and 8 hours of drug treatment and corresponded with a decrease in phosphorylation of AKT, MAPK and to a lesser extent S6. After 8 hours the level of c-KIT phosphorylation began to increase and by 48 hours there was detectable phosphorylation of AKT, MAPK and an increase in phosphorylation of S6. It is unclear why this occurs but it could be due dasatinib being more rapidly metabolised in these cells.

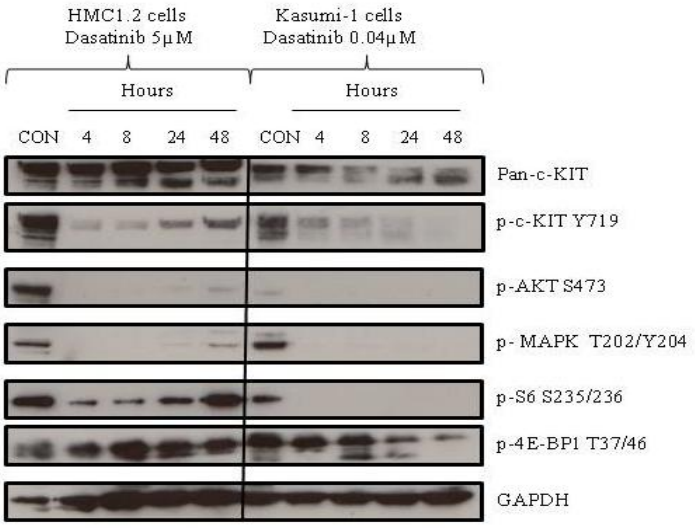

Figure 5.15 Time course effect of dasatinib on c-KIT autophosphorylation and downstream target proteins in Kasumi-1 and HMC1.2 cells. GAPDH was used as a loading control.

5.3.9 Cytotoxic effect of dasatinib in SKNO.1 cells

The SKNO.1 cell line expresses RUNX1/RUNX1T1 and bears a homozygous *c-KIT* N822K mutation. As SKNO.1 cells have similar genetic abnormalities to the Kasumi-1 cells it was of interest to assess the response of these cells to dasatinib. After 48 hours of treatment, dasatinib marginally decreased the number of live cells, in the presence or absence of GM-CSF (Figure 5.16 a,c). Conversely, dasatinib did not induce cell killing in the presence or absence of GM-CSF (Figure 5.16 b,d). SKNO.1 cells were subsequently treated with dasatinib in combination with ZSTK-474, WYE-354, BEZ-235 or AZD5363 for 72 hours in the absence of GM-CSF (Figure 5.17 a,b). None of the inhibitor combinations reduced the live cell number below 50% of the control (Figure 5.17a) or decreased the percentage of cells in the live fraction below 70% of the control (Figure 5.17b).

5.3.10 Effect of dasatinib on signalling in SKNO.1 cells

As SKNO.1 cells showed no cytotoxic effect following dasatinib treatment, western blotting was used to assess the impact of dasatinib on c-KIT and downstream target proteins. SKNO.1 cells did not express any detectable c-KIT phosphorylation at residue Y719 and only expressed the unglycosylated c-KIT isoform (120KDa), not the fully glycosylated c-KIT isoform (145KDa). Treatment of the SKNO.1 cells with 1.25μM or 5μM dasatinib did not show any reduction in phosphorylation of AKT (Figure 5.18). This suggests that in SKNO.1 cells, c-KIT is not the driver mutation and therefore the cells are not a good model to evaluate the therapeutic benefit of targeting c-KIT with small molecule inhibitors.

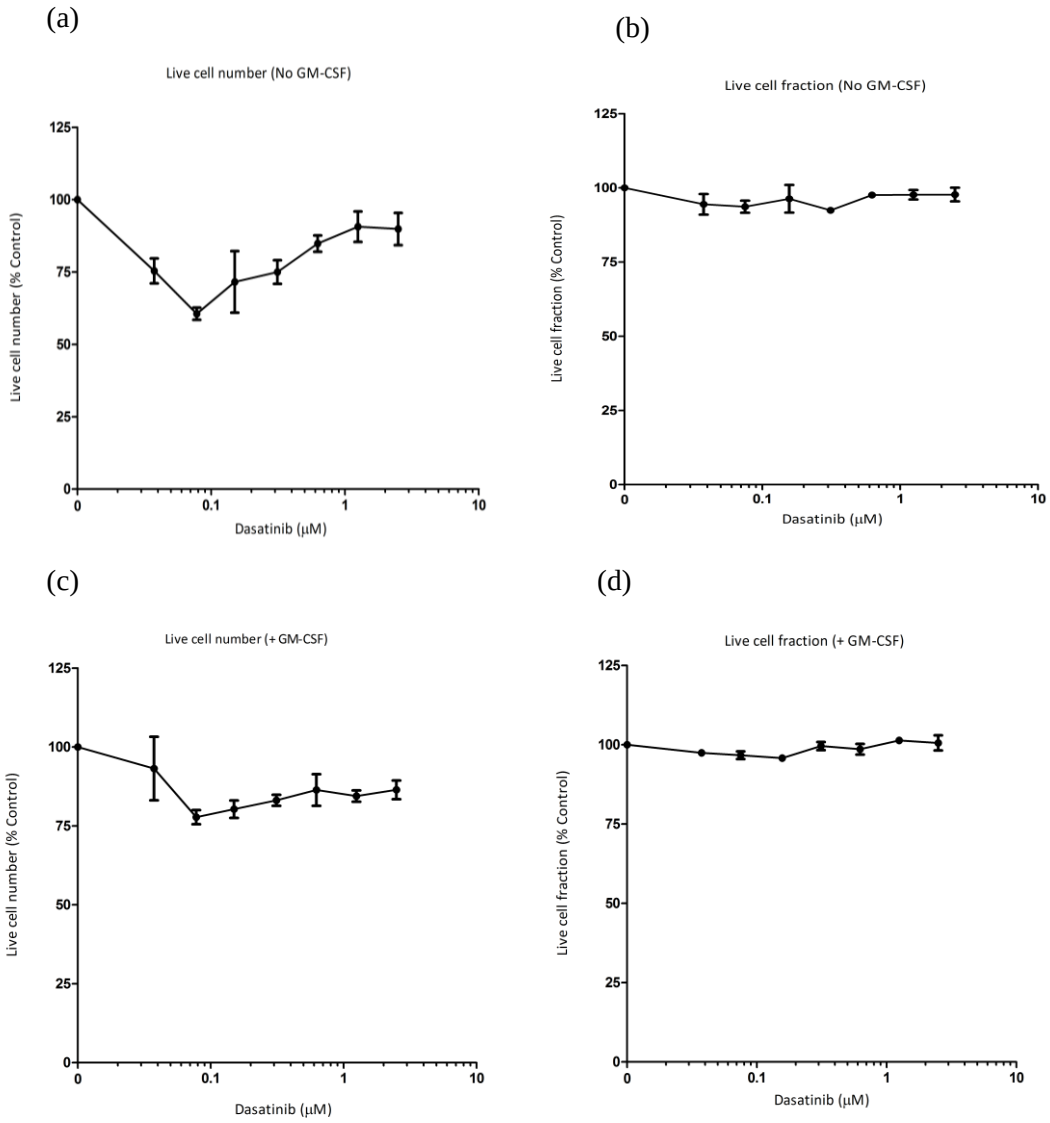

Figure 5.16 Response of SKNO.1 cells to dasatinib in the presence or absence of 10ng/mL GM-CSF for 48 hours. (a) Total number of live cells. (b) Percentage of cells in the live cell fraction. Data shown is the mean ± SEM of three individual experiments.

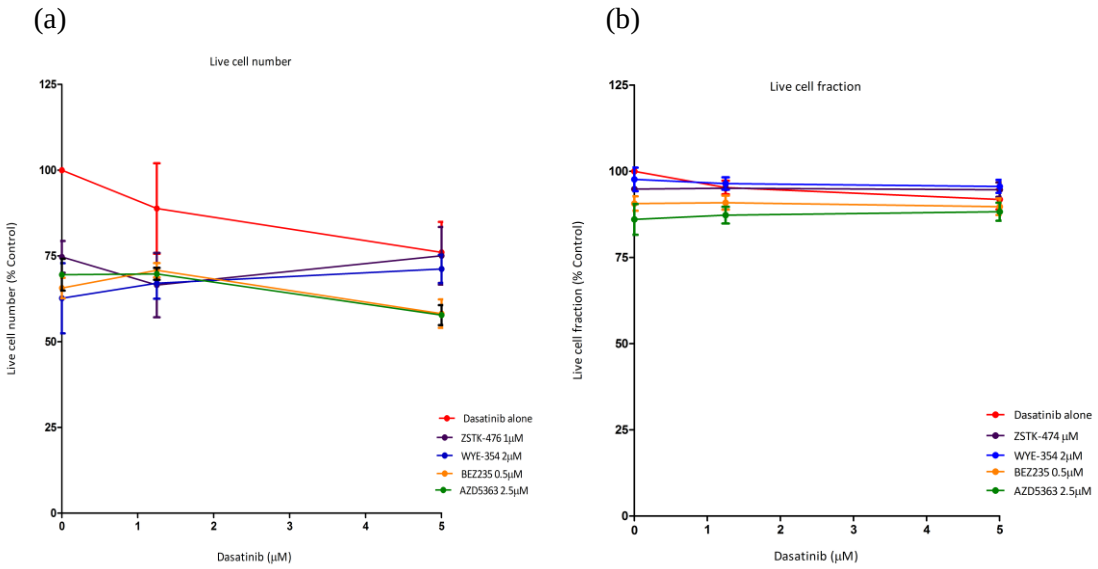

Figure 5.17 Response of SKNO.1 cells to combinations of dasatinib and ZSTK-474, WYE-354, BEZ-235 or AZD5363 in the absence of GM-CSF after 48 hours (a) Total number of live cells. (b) Percentage of cells in the live cell fraction. Data shown is the mean ± SEM of three individual experiments.

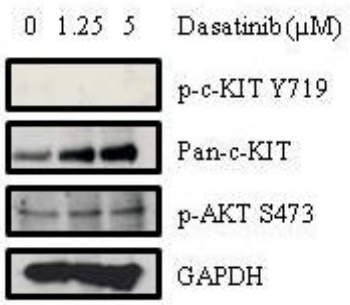

Figure 5.18 Effect of dasatinib on c-KIT and downstream signalling in SKNO.1 cells after 4 hours. GAPDH was used as a loading control.

5.3.11 Synergistic cell killing meditated by c-KIT and PI3K/mTOR blockade is limited to *c-KIT* mutant cells

Combined inhibition of c-KIT autophosphorylation and constitutively active PI3K/mTOR led to synergistic cell killing in Kasumi-1 and HMC1.2 cells. To demonstrate that the enhanced cell killing observed was specific to targeting mutant *c-KIT* and its downstream targets, three *c-KIT*-WT cell lines (PL-21, MV4-11 and MOLM-13) were treated with dasatinib in combination with BEZ-235. BEZ-235 was selected as it was the most potent of the inhibitors studied at decreasing phosphorylation of mTOR and P13K targets, and combinations of dasatinib and BEZ-235 showed the most striking impact on apoptotic regulators in Kasumi-1 and HMC1.2 cells. Dasatinib and BEZ-235 did not show synergistic cell killing in the PL-21, MV4-11 or MOLM-13 cells (Figure 5.19 a-f). However, MV4-11 and MOLM-13 cell lines were sensitive to BEZ-235 alone in regards to growth inhibition and cell killing (Figure 5.19 c-f). The effect of dasatinib and BEZ-235 on cell killing in PL-21, MV4-11 and MOLM-13 cells gave CI values at an ED50 of >1.1 indicating that drug interactions were antagonistic (Table 5.2).

		CI Values at:		
Drug Combination	**Cell line**	ED50	ED75	ED90
Dasatinib + BEZ-235 (2.5:1)	PL-21	1.268	1.224	1.186
Dasatinib + BEZ-235 (2.5:1)	MV4-11	1.137	1.588	2.220
Dasatinib + BEZ-235 (2.5:1)	MOLM-13	2.075	2.841	4.000

CI = Combination Index value, ED = Effective dose

Table 5.2 CalcuSyn data providing the CI values at ED50, ED75 and ED90 from cell killing data of PL-21, MV4-11 and MOLM-13 cells treated with dasatinib and BEZ-235.

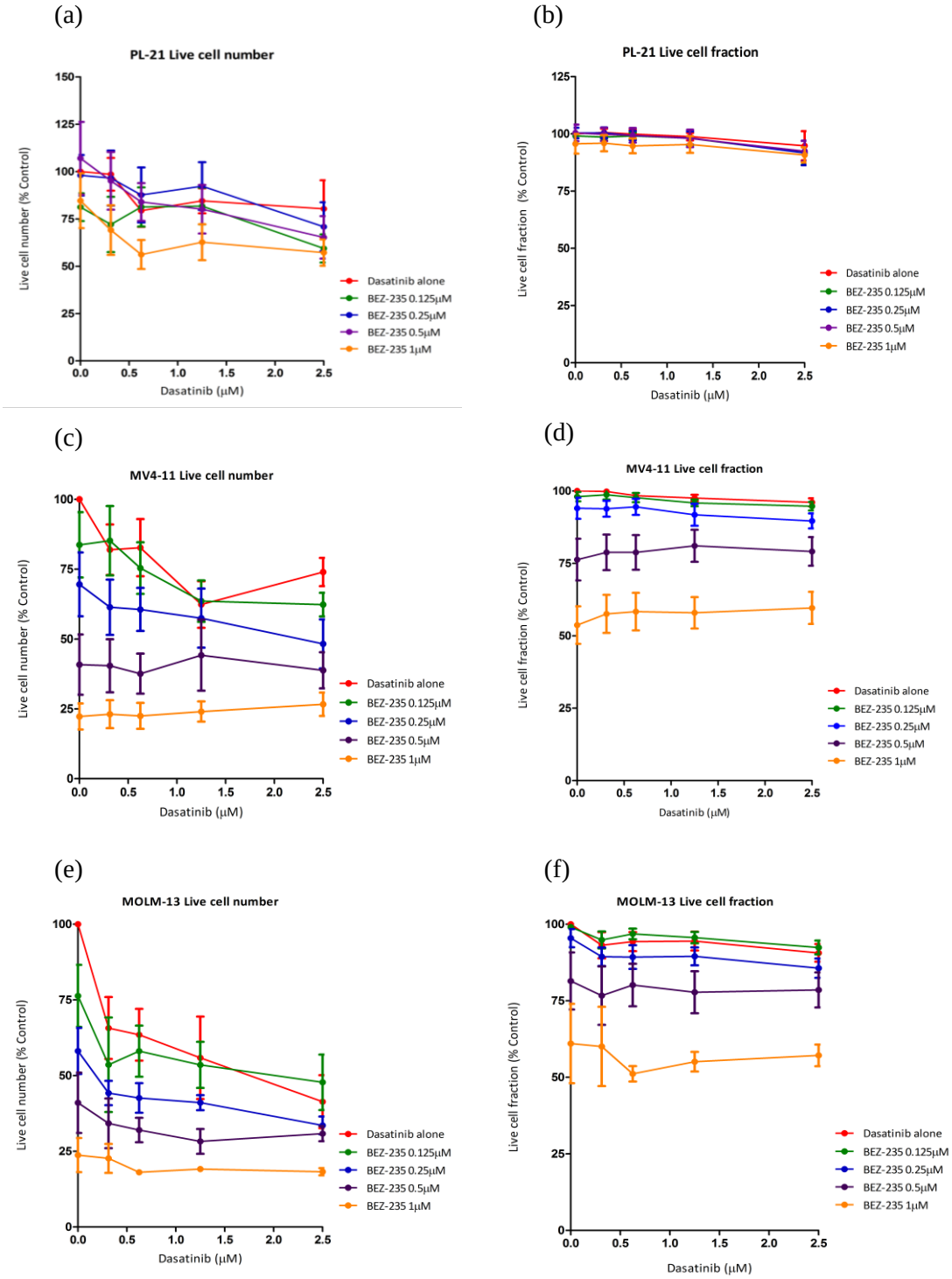

Figure 5.19 Response of PL-21, MV4-11 and MOLM-13 cells to combinations of dasatinib and BEZ-235 after 72 hours. (a,c,e) Total number of live cells. (b,d,f) Percentage of cells in the live cell fraction. Data shown is the mean ± SEM of three or four individual experiments.

5.3.12 MV4-11 and MOLM-13 cells treated with AC220

It was hypothesised that cell lines expressing *FLT3*-ITD mutations treated with AC220 and BEZ-235 may show a similar synergistic cell killing profile as observed when targeting c-KIT and PI3K/mTOR in *c-KIT* mutant cells. MV4-11 and MOLM-13 cells were treated with AC220 alone to ascertain a concentration range to use in combination with BEZ-235. MV4-11 and MOLM-13 cells treated with AC220 for 72 hours showed a dose dependent reduction in cell growth (IC50 1.4nM and 2.6nM respectively) and cell killing (IC50 4.5nM and 8nM respectively) (Figures 4.6 a,b). In accordance with this, 12.5-100nM AC220 potently reduced phosphorylation of FLT3, MAPK and S6 in MV4-11 cells (Figure 5.20a). The MOLM-13 cell line also showed a dose-dependent reduction in the level of p-FLT3 between 12.5 and 100nM AC220 (Figure 5.20b). The level of p-MAPK is very low in the MOLM-13 cells making any reduction in phosphorylation difficult to ascertain. The levels of p-4E-BP1 remained unchanged under AC220 treatment in both MV4-11 and MOLM-13 cells supporting the hypothesis that targeting PI3K and mTOR proteins in combination with AC220 may enhance cell killing.

(a) (b)

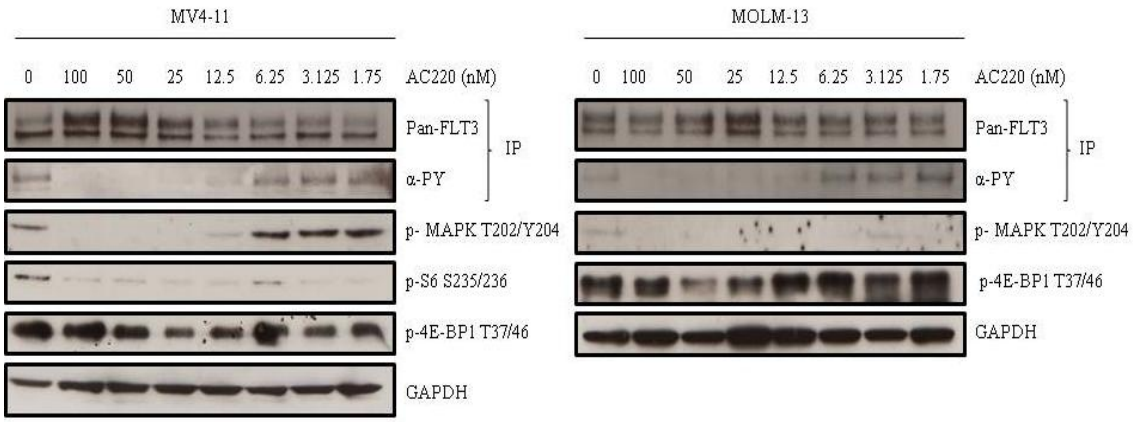

IP = Immunoprecipitation, α-PY = Anti-phosphotyrosine antibody

Figure 5.20 Effect of AC220 on phosphorylation of FLT3 and downstream target proteins in MV4-11 and MOLM-13 cells. IP of FLT3 and western blotting of (a) MV4-11 and (b) MOLM-13 cells treated with AC220 for 4 hours. GAPDH was used as a loading control.

5.3.13 Cytotoxic effect of combining AC220 and BEZ-235 in *FLT3*-ITD mutant cells

To examine the cytotoxic effects of targeting mutant FLT3 and constitutively active PI3K/mTOR, MV4-11, MOLM-13 and PL-21 cells were treated with AC220 and BEZ-235. As seen previously MV4-11 and MOLM-13 cells were sensitive to growth inhibition and cell killing mediated by AC220 or BEZ-235 alone (Figure 5.21 a-d). A combination of AC220 and BEZ-235 showed an increase in growth inhibition and cell killing compared to either drug alone (Figure 5.21 a-d). MOLM-13 cells were particularly sensitive to this drug combination (Figure 5.21 c-d). PL-21 cells were considerably more resistant to AC220 as demonstrated by only a small decrease in growth inhibition and very little cell killing (Figure 5.21 e,f). PL-21 cells were also relatively resistant to BEZ-235 requiring 1µM to significantly inhibit cell growth and induce some cell killing. A combination of AC220 and BEZ-235 only slightly enhanced growth inhibition and cell killing in comparison to either agent alone (Figure 5.21 e,f). The lack of response to AC220 in the PL-21 cells may be due to total FLT3 levels being undetectable (Figure 4.7).

A combination of AC220 and BEZ-235 were synergistic at cell killing in MV4-11 and MOLM-13 cells (CI values at ED50 of <0.9 for both cell lines) (Table 5.3). In contrast, AC220 and BEZ-235 were antagonistic in PL-21 cells CI value at ED50 of >1.1 (Table 5.3).

		CI Values at:		
Drug Combination	**Cell line**	ED50	ED75	ED90
AC220 + BEZ-235 (1:100)	MV4-11	0.888	0.771	0.678
AC220 + BEZ-235 (1:100)	MOLM-13	0.586	0.53041	0.484
AC220 + BEZ-235 (2.5:1)	PL-21	1.661	1.661	1.661

CI = Combination Index value, ED = Effective dose

Table 5.3 CalcuSyn data providing the CI values at ED50, ED75 and ED90 from cell killing data of MV4-11, MOLM-13 and PL-21 cells treated with AC220 and BEZ-235.

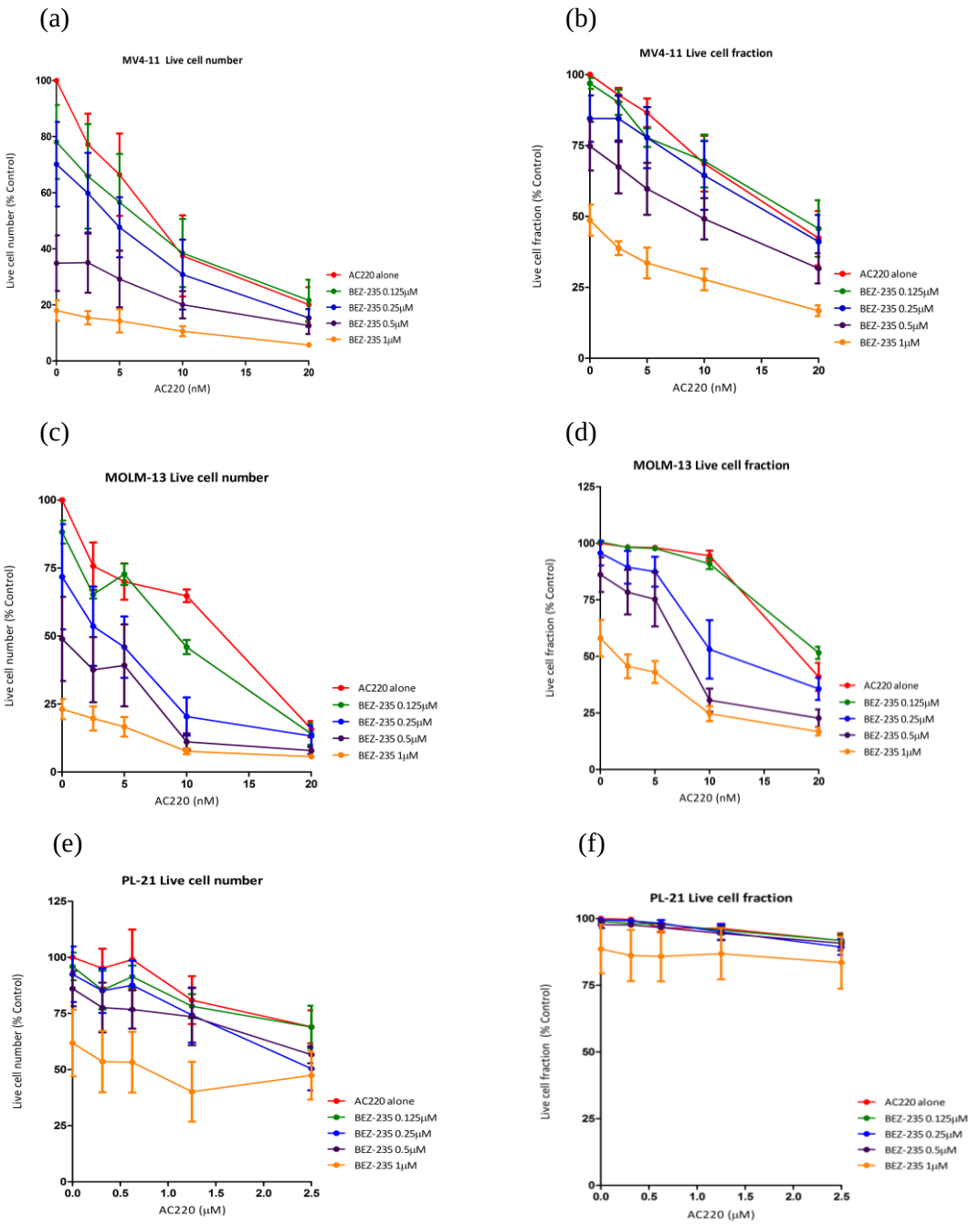

Figure 5.21 Response of MV4-11, MOLM-13 and PL-21 cells to combinations of AC220 and BEZ-235 after 72 hours. (a,c,e) Total number of live cells. (b,d,f) Percentage of cells in the live cell fraction. Data shown is the mean ± SEM of three or four individual experiments.

5.3.14 Impact of combined FLT3 and PI3K/mTOR blockade on cell signalling

As AC220 and BEZ-235 were synergistic at cell killing in MOLM-13 and MV4-11 cells, western blotting was used to investigate the impact on downstream signalling. In MV4-11 cells, AC220 (10nM) reduced phosphorylation of FLT3, MAPK and S6 whereas levels of p-4E-BP1 remained unchanged (Figure 5.22). A combination of AC220 and BEZ-235 inhibited FLT3 autophosphorylation and potently reduced phosphorylation of MAPK, S6 and 4E-BP1. In MOLM-13 cells, AC220 (10nM) reduced p-FLT3 (Figure 5.22). A combination of AC220 and BEZ-235 reduced phosphorylation of FLT3 and 4E-BP1.

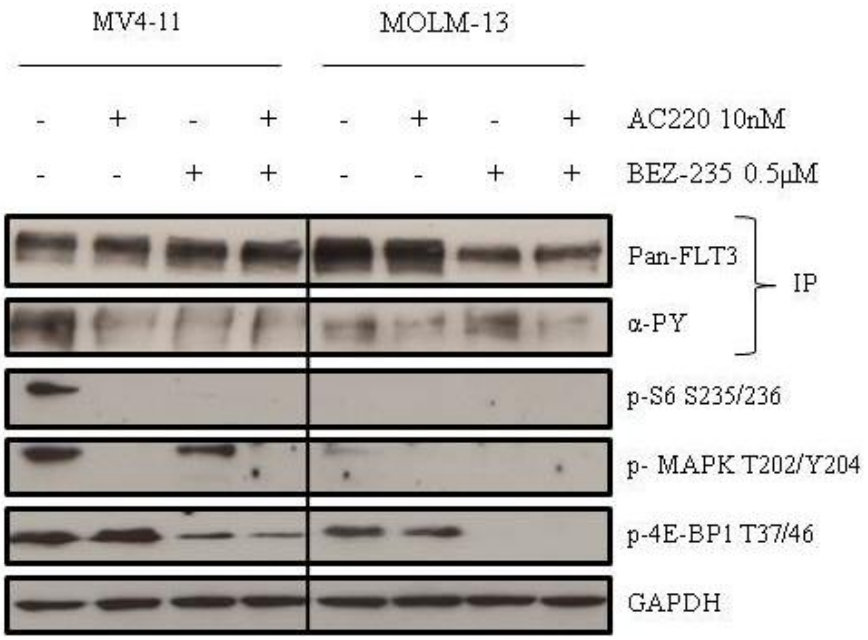

IP = Immunoprecipitation, α-PY = Anti-phosphotyrosine antibody

Figure 5.22 Effect of AC220 and BEZ-235 on phosphorylation of FLT3 and downstream target proteins in MV4-11 and MOLM-13 cells after 4 hours. GAPDH was used as a loading control.

5.3.15 Primary CBFL cells

To assess the impact of targeting c-KIT and PI3K/mTOR further CBFL primary cells were treated with dasatinib and BEZ-235. A total of 27 primary CBFL cells were thawed of which 20 had inv(16) and 7 had t(8;21). Following the overnight recovery step only 13 samples survived. Of the samples that did not recover 2 had the t(8;21) translocation and a *c-KIT* N822K mutation. Of the 13 samples that survived 11 had inv(16) and 2 had t(8:21). A total of 5 samples provided both cell killing and western blotting data, 4 samples only provided cell killing data due to insufficient cells for western blotting, 3 samples only had western blotting data due to cells not surviving long enough in liquid culture to assess the impact on cell killing and 1 sample did not provide any information. From the cells that thawed one was a relapse sample and only one sample had a *c-KIT* mutation. The reason for the poor number of *c-KIT* mutant samples is due to the variability in how CBFL cells thawed and the ability of the cells to survive long enough in liquid culture to access the impact of the drugs on growth inhibition and cell killing.

5.3.16 Impact of dasatinib and BEZ-235 on cell growth and cell survival in primary CBFL cells

As dasatinib and BEZ-235 resulted in synergistic cell killing, eliminated c-KIT auto-phosphorylation and markedly reduced residual MEK, AKT, PI3K and mTOR signalling in *c-KIT* mutant cell lines, it was hypothesised that a combination of dasatinib and BEZ-235 may enhance cell killing in primary CBFL cells, in particular those with a *c-KIT* mutation. A total of nine primary CBFL cells had a cell viability $\geq$ 45% at 48 hours following Annexin/PI staining, shown in Figure 5.23 a-r. The remaining four patients were <10% viable upon analysis at 48 hours and therefore excluded. All nine of the CBFL samples evaluable were *c-KIT*-WT. Dasatinib alone had a limited impact on inhibiting proliferation in the majority of samples however samples 1, 7, 8, 9 and 9 relapse did show a reduction in cell growth (Figure 5.23 a, g, i, k and m). In contrast, dasatinib alone did not induce a significant level of apoptosis in any of the samples examined (Figure 5.23 a-r). The response of the primary cells to BEZ-235 alone was varied. All samples except 10 or 11 demonstrated that BEZ-235 inhibited cell growth (Figure 5.23 a, c, e, g, i, k and m) with a modest effect on cell killing (Figure 5.23 b, d, f, h, j, l and n). A combination of dasatinib and BEZ-235 did not enhance inhibition of cell growth or cell killing in any of the CBFL samples examined.

(a) Live cell number

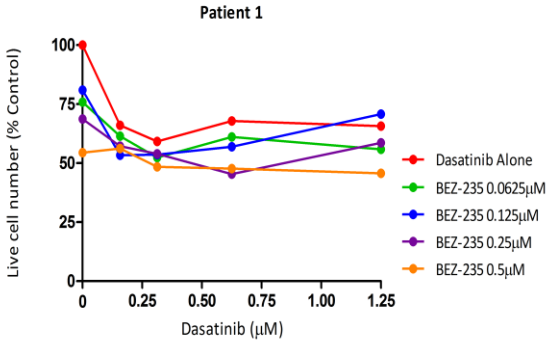

(b) Live cell fraction

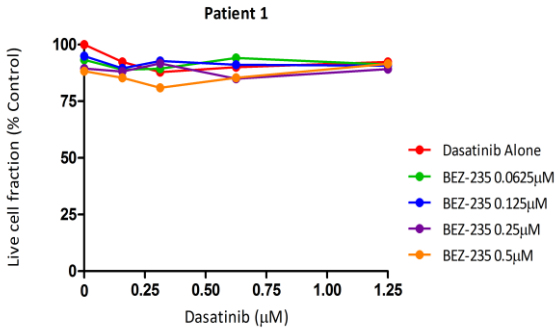

(c)

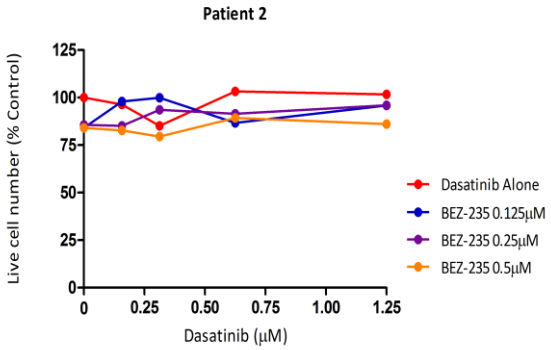

(d)

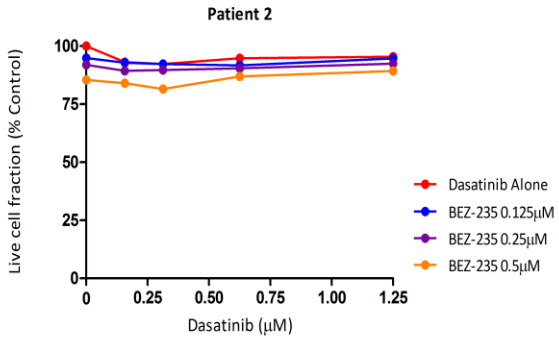

(e)

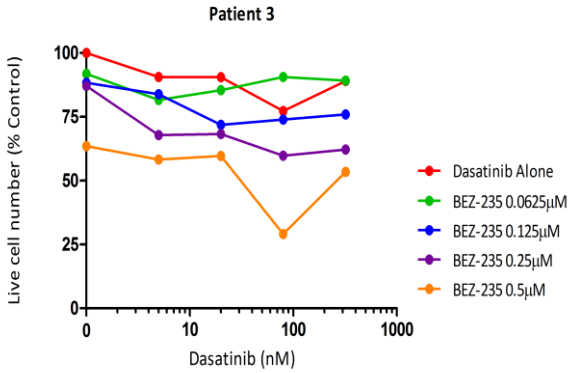

(f)

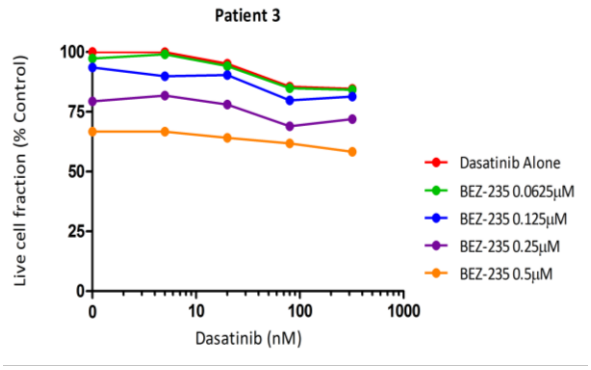

(g) Live cell number

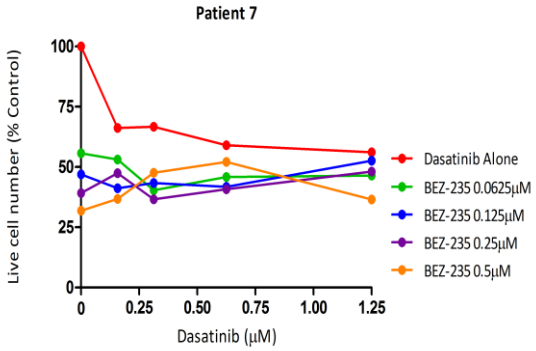

(h) Live cell fraction

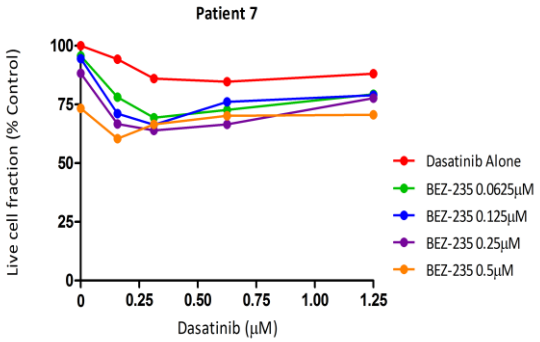

(i)

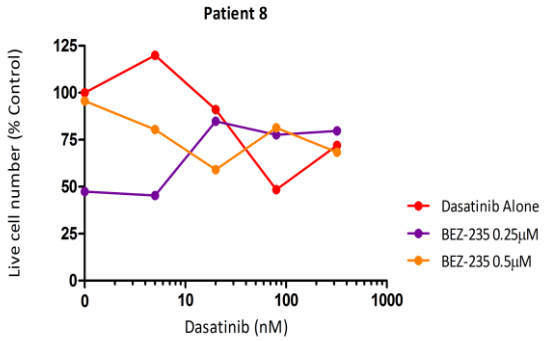

(j)

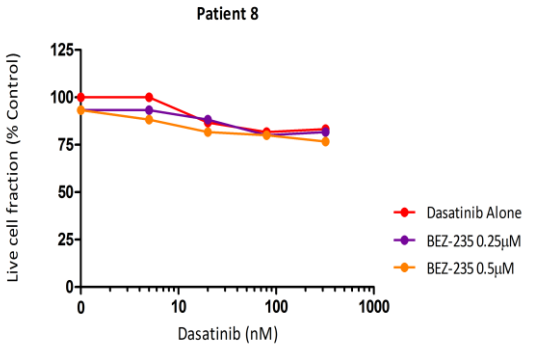

(k)

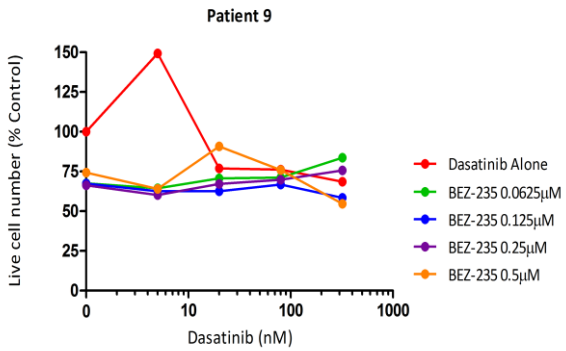

(l)

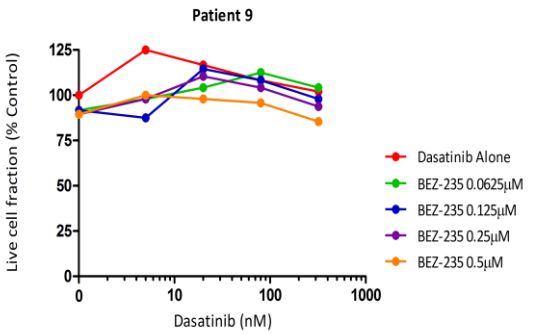

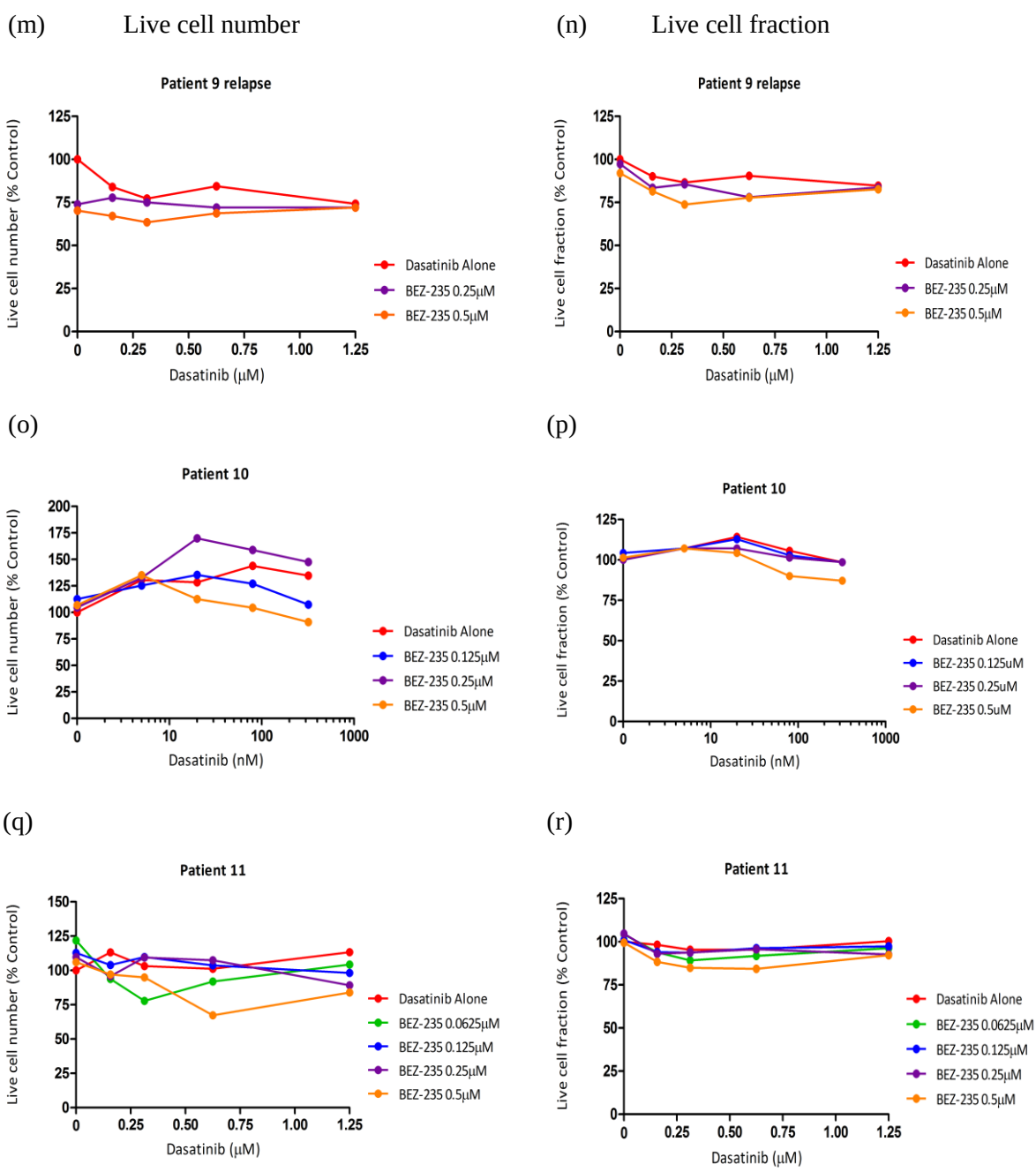

Figure 5.23 Response of primary CBFL samples to combinations of dasatinib and BEZ-235 after 48 hours. (a,c,e,g,i,k,m,o,q) Total number of live cells. (b,d,f,h,j,l,n,p,r) Percentage of cells in the live cell fraction.

5.3.17 The effect of dasatinib and BEZ-235 on downstream signalling in primary CBFL cells

Primary CBFL cells were cultured in the presence of dasatinib, BEZ-235, dasatinib and BEZ-235 or with no inhibitor for 4 hours. Total lysates were subsequently probed for phospho-specific antibodies against AKT, MAPK, 4E-BP1, S6 and p-70 S6K. Western blotting data was available for 8 patients, the other 4 samples did not have sufficient cell numbers for western blotting analysis. Seven patients had constitutive activation of MAPK, as indicated by p-MAPK, and all patients had constitutive activation of the mTOR pathway as shown by p-p70-S6K, p-S6 and p-4EB-P1 expression (Figure 5.24). Only 3 patients had constitutive activation of AKT. When the CBFL cells were cultured in the presence of dasatinib, there was a reduction in p-MAPK in 4 samples (patients 2, 4, 9, and 11) corresponding with a reduction in p-p-70-S6K and p-S6. BEZ-235 alone potently reduced phosphorylation of p-70 S6K, S6 and 4E-BP1 in 7 samples (patients 1, 2, 3, 4, 6, 11 and 12). A combination of dasatinib and BEZ-235 had a variable impact in the CBFL primary cells examined. Patients 2 and 11 showed a decrease in constitutive activation of p70 S6K, MAPK, S6, and 4E-BP1 in the presence of both dasatinib and BEZ-235 in comparison to either drug alone. In comparison, patients 1 and 4 showed an increase in p-S6 expression following dual inhibitor treatment. Patient 12 was the only sample with a *c-KIT* mutation, D816V. Dasatinib did not inhibit phosphorylation of AKT or PI3K/mTOR target proteins in this sample. In contrast patient 12 did show potent inhibition of p-p70 S6K, p-S6 and p-4E-BP1 when treated with BEZ-235 alone or dasatinib and BEZ-235. There were insufficient cells for patient 3 to examine the impact of dasatinib and BEZ-235.

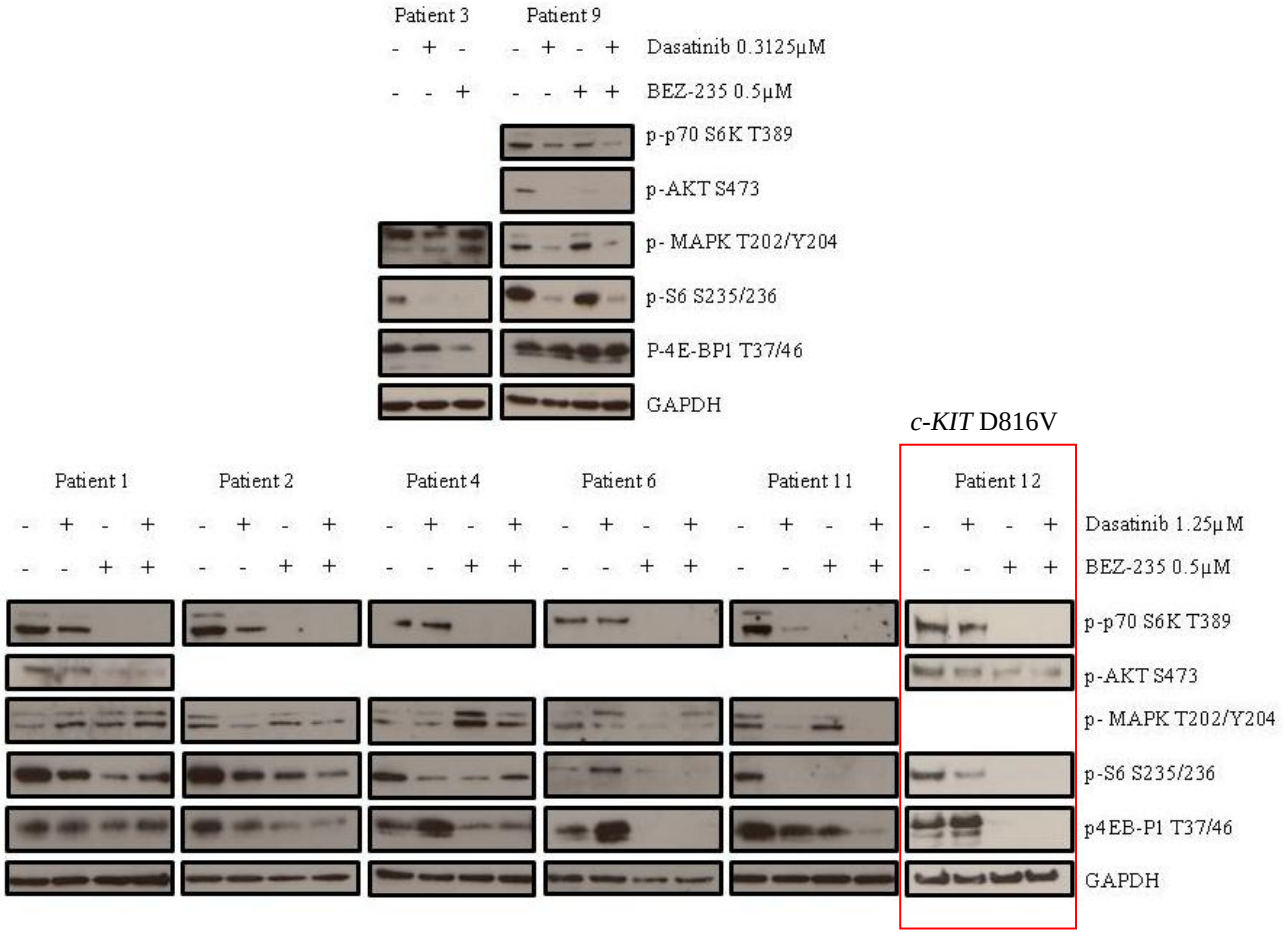

Figure 5.24 Impact of dasatinib and BEZ-235 on cell signalling in primary CBFL samples after 4 hours. Top panel treated with a lower dasatinib concentration in comparison to the bottom panel**.** Blank spaces indicate that the protein was not detected. GAPDH was used as a loading control.

5.4 Discussion

The use of small molecule inhibitors against mutated RTKs or activated signalling molecules has elicited a limited clinical response in AML (Rinehart *et al.*, 2004;Yee *et al.*, 2006;Cortes *et al.*, 2012;Levis *et al.*, 2012;Zwaan *et al.*, 2013). Therefore this chapter aimed to evaluate the response of AML cell lines and primary CBFL cells to inhibitors targeting either c-KIT or FLT3 in combination with inhibitors of downstream signalling molecules.

AML cell lines were first screened for mutations in *c-KIT* and *FLT3* and confirmed the presence of *c-KIT* N822K in Kasumi-1 and SKNO.1 cells, *c-KIT* V560G and D816V in HMC1.2 cells and the presence of *FLT3*-ITD mutations in MV4-11, MOLM-13 and PL-21 cells. The mutations identified in each cell line were consistent with previous reports (Furitsu *et al.*, 1993;Quentmeier *et al.*, 2003;Becker *et al.*, 2008). Quantification of the *FLT3*-ITD mutations in the MOLM-13 and PL-21 cells indicated there was not a heterozygous mutation in every cell. The higher *FLT3*-ITD level in the MOLM-13 cells could indicate a proportion of the cells are homozygous for the *FLT3*-ITD mutation. Cells with a homozygous mutation may have a greater proliferative advantage compared to those cells with a heterozygous mutation and might have begun to out compete those with the heterozygous mutation. In contrast a proportion of the PL-21 cells appear to have lost the *FLT3*-ITD. This may be due to the *FLT3*-ITD becoming redundant in these cells as data presented in chapter 4 showed there was no detectable FLT3 or any response to AC220. To investigate this further each cell line could be single cell sorted, expanded and the mutant level of each clone analysed. This would identify if some of the MOLM-13 cells have a homozygous *FLT3*-ITD or if a proportion of the PL-21 cells have lost the *FLT3*-ITD mutation.

Initial experiments showed that dasatinib was capable of potently inhibiting c-KIT phosphorylation in Kasumi-1(40nM) and HMC1.2 (157nM) cells, which corresponded to potent cell killing in the Kasumi-1 cells (IC50 21.4nM ± 2) whereas the HMC1.2 cells were more resistant to cell killing (IC50 3.1µM ±0.6). This is consistent with previous reports (Schittenhelm *et al.*, 2006;Mpakou *et al.*, 2013). HMC1.2 cells were more resistant to dasatinib-mediated inhibition of c-KIT phosphorylation which could be due to the presence of both the V560G and D816V mutations. Alternatively this may just be due to the presence of the *c-KIT* D816V mutation. Data presented in chapter 3 showed that UT-7 cells

expressing c-KIT-D816V were the most resistant to dasatinib-mediated inhibition of c-KIT phosphorylation in comparison to the other mutant expressing cells, including UT-7 c-KIT-N822K cells. HMC1.2 cells may be more resistant to dasatinib-mediated cell killing due to a high expression of p-AKT, p-S6 and p-MAPK even when c-KIT activity is eliminated (Figure 5.7). Activation of these proteins is associated with promoting cell survival and proliferation; therefore residual activation might be sufficient to keep the cells alive. Stimulation of AKT, S6 and MAPK, in the absence of c-KIT activity, also suggests other signalling molecules may activate these proteins. Of note the dose response observed between 1.25μM-10μM dasatinib in regards to the decrease in phosphorylation of AKT, MAPK and S6 is most likely mediated by off target effects.

HMC1.2 cells were also treated with imatinib however there was no decrease in c-KIT autophosphorylation or phosphorylation of downstream target proteins. Previous reports have shown that imatinib can inhibit c-KIT autophosphorylation in cells harbouring the *c-KIT* V560G mutation but not cells with the *c-KIT* D816V mutation (Frost *et al.*, 2002;Shah *et al.*, 2006). The *c-KIT* D816V mutation might therefore dominate over the V560G mutation in the HMC1.2 cells which might explain why there was no decrease in c-KIT activity or downstream target proteins.

SKNO.1 cells also express the *c-KIT* N822K mutation, however in this study there was no detectable phosphorylation of c-KIT. This may explain why dasatinib did not induce significant levels of apoptosis alone or in combination with other small molecule inhibitors in these cells. Dasatinib did inhibit cell growth in the absence of GM-CSF at concentrations <0.3125μM however this was not observed at higher concentrations. This is supported by a report that showed dasatinib significantly inhibited proliferation of SKNO.1 cells at 10nM concentration (Han *et al.*, 2010). The response observed might be mediated by dasatinib targeting Src tyrosine-protein kinase proteins which is only effective at nanomolar concentrations or it could be due to off target effects. As c-KIT did not appear to be the driver mutation in SKNO.1 cells, it was not considered a good model for assessing the effects of dasatinib against mutant *c-KIT* and these cells were not further investigated.

In both Kasumi-1 and HMC1.2 cells, combinations of dasatinib and inhibitors of PI3K, mTOR or PI3K and mTOR led to synergistic cell killing corresponding to a marked

reduction in residual constitutive activation of MEK, AKT, PI3K and mTOR target proteins. This indicates that both c-KIT and PI3K/mTOR signalling is essential for the survival of these cells. The most potent effects were observed with combinations of dasatinib and BEZ-235. There are several possible reasons why this drug combination was the most effective. Firstly, BEZ-235 simultaneously targets mTOR and P13K whereas the other inhibitors examined only target mTOR or PI3K. This is advantageous as previous reports have shown that mTORC1 can be activated independently of PI3K, and inhibition of mTOR can lead to complex compensatory feedback loops activating AKT and P13K (Tamburini *et al.*, 2008). Secondly, BEZ-235 was most potent at inhibiting phosphorylation of PI3K/mTOR target proteins in both cell lines compared to the other inhibitors examined. Thirdly, BEZ-235 alone decreased autophosphorylation of c-KIT in Kasumi-1 cells and dasatinib and BEZ-235 most strongly inhibited c-KIT activity in HMC1.2 cells (Figure 5.13). This could indicate a downstream feedback mechanism, mediated by BEZ-235 that could lead to an enhanced reduction in c-KIT activity. Finally, dasatinib and BEZ-235 was the only drug combination to significantly reduce expression of anti-apoptotic Bcl-2 family member proteins and decrease levels of caspase proteins in both cell lines.

Subsequently, the same approach was adapted to targeting mutant FLT3 and PI3K/mTOR in PL-21, MV4-11 and MOLM-13 cells. Treatment of MV4-11 and MOLM-13 cells with AC220 inhibited autophosphorylation of FLT3 at 12.5nM, which corresponded with potent cell killing, IC50 4.5nM and 8nM respectively, and is consistent with other reports (Zarrinkar *et al.*, 2009;Gunawardane *et al.*, 2013). AC220 and BEZ-235 did not enhance inhibition of cell growth or induce cell killing in PL-21 cells. As previously discussed in chapter 4, the poor response to AC220 is most likely due to an absence of FLT3 expression in PL-21 cells. In contrast, AC220 and BEZ-235 induced synergistic cell killing and reduced residual mTOR signalling in MV4-11 and MOLM-13 cells. In support of this, recently published data has shown that simultaneous blockade of FLT3 and PI3K with small molecule inhibitors in *FLT3*-ITD AML cell lines enhanced apoptosis in comparison to the individual agents in hypoxic and normoxic conditions (Jin *et al.*, 2013). In accordance with this finding, another study demonstrated that inhibition of FLT3 and AKT in *FLT3*-mutant cell lines and primary AML cells could synergistically inhibit cell growth in the presence or absence of stroma (Weisberg *et al.*, 2013). It would be of interest to examine the response of primary *FLT3* mutant AML cells to AC220 and BEZ-235 to determine whether this drug

combination might have a therapeutic benefit. AC220 has already been used in several clinical trials and has shown particular promise in patients with *FLT3* mutations whereas BEZ-235 is just beginning to enter phase I clinical trials in acute leukaemias (Cortes *et al.*, 2012;Levis *et al.*, 2012) (trial NCT01756118).

As a result of the promising data obtained from targeting c-KIT and mTOR/PI3K in *c-KIT* mutant cell lines, a cohort of primary CBFL cells were treated with dasatinib and BEZ-235. Of the CBFL samples examined all but one were wild-type for *c-KIT*. The reason for the low number of *c-KIT* mutant samples investigated was due to the variability in how individual patient samples thawed and the ability to maintain the AML samples long enough in culture to assess the impact of the drugs. The effects of dasatinib and BEZ-235 in primary *c-KIT* mutant CBFL cells therefore could not be assessed fully. However, as dasatinib can inhibit the kinase activity of the WT receptor at nanomolar concentrations and c-KIT is highly expressed on 60-80% of myeloblasts (Beghini *et al.*, 2004;Schittenhelm *et al.*, 2006), it did provide an opportunity to assess the impact of targeting the WT receptor in conjunction with PI3K and mTOR. Dasatinib alone inhibited cell growth in 5 samples but did not induce significant cell killing in any samples. BEZ-235 alone inhibited cell growth in 7 samples as well as having a modest impact on cell killing. None of the primary CBFL cells treated with dasatinib and BEZ-235 showed synergistic or additive effects on inhibiting cell growth or inducing cell killing. This indicates that dasatinib and BEZ-235 may not be an effective therapeutic approach for killing CBFL cells with WT *c-KIT*. These observations support the effects seen in *c-KIT*-WT cell lines treated with dasatinib and BEZ-235 (Figure 5.19). Of note, patient samples 2 and 11 showed dasatinib and BEZ-235 could reduce p-MAPK, p-S6 and p-4E-BP1 further than either drug alone but did not result in cell killing. This suggests that other signalling pathways may contribute to the survival of the leukaemic cells. A phase I dose escalation study in paediatric patients aged 1-21 with relapsed or refractory AML and *c-KIT*-WT showed no clinical responses to dasatinib. This may indicate that dasatinib alone has a limited impact in *c-KIT*-WT expressing patients. The data presented in this chapter provides evidence that combining dasatinib and BEZ-235 in *c-KIT*-WT AML cell lines or primary CBFL cells does not increase the sensitivity of these cells to growth inhibition or cell killing.

In summary, a combination of dasatinib and ZSTK-474, WYE-354 or BEZ-235 were synergistic in *c-KIT* mutant cell lines at cell killing, with similar results observed with AC220 and BEZ-235 in *FLT3*-ITD AML cell lines. The response of primary CBFL cells to dasatinib and BEZ-235 was limited to those with *c-KIT*-WT due to low numbers of samples having a *c-KIT* mutation. Primary CBFL cells with *c-KIT*-WT showed a limited response to dasatinib, BEZ-235 or a combination of dasatinib and BEZ-235. Further work is required to investigate the therapeutic potential of dasatinib and BEZ-235 in *c-KIT* mutant primary CBFL cells in conjunction with assessing the effect of AC220 and BEZ-235 in primary samples with AML and *FLT3* mutations.

6. **Conclusions and future directions**

Although there have been improvements in therapeutics and supportive care, the majority of patients with AML eventually succumb to the disease. This has led to the development of new therapeutic options for AML. One such approach is the use of small molecule inhibitors against frequently mutated RTKs or dysregulated signalling pathways. In AML RTKs such as *c-KIT* and *FLT3* are frequently mutated and key signalling pathways including PI3K/AKT, mTOR and MEK are constitutively activated in a large proportion of patients (Gilliland & Griffin, 2002;Grandage *et al.*, 2005;Frohling *et al.*, 2007;Allen *et al.*, 2013). Numerous reports have tried to exploit this by using small molecule inhibitors to target individual signalling proteins but clinical responses have primarily been cytostatic and not cytotoxic (Rinehart *et al.*, 2004;Yee *et al.*, 2006;Cortes *et al.*, 2012;Levis *et al.*, 2012;Zwaan *et al.*, 2013). The data in this thesis aimed to evaluate if all *c-KIT* mutations should be considered equivalent and to evaluate the efficacy of small molecule inhibitors against RTK mutations and activated downstream signalling molecules.

Clinical data has shown that patients with CBFL and a *c-KIT* mutation have an increased RR (Paschka *et al.*, 2006;Cairoli *et al.*, 2006;Allen *et al.*, 2013). Several studies have shown that *c-KIT* mutations, occurring across the receptor, can lead to constitutive activation of *c-KIT* and confer factor independent growth in cell line models (Ning *et al.*, 2001;Growney *et al.*, 2005;Schittenhelm *et al.*, 2006;Wang *et al.*, 2011). Data in chapter 3 showed that expression of *c-KIT*-Δ417-419>Y and *c-KIT*-D816V in UT-7 cells led to autophosphorylation of c-KIT and ligand independent growth. This suggested that c-KIT could be an attractive therapeutic target for patients with a *c-KIT* mutation. UT-7 cells engineered to express *c-KIT* mutations in different domains and cell lines with endogenous *c-KIT* mutations showed differential sensitivities to dasatinib-mediated growth inhibition, cell killing and inhibition of c-KIT phosphorylation (chapter 3 and 5). The *c-KIT*-D816V mutation was identified as being more resistant to dasatinib-mediated inhibition of c-KIT phosphorylation in engineered UT-7 c-KIT D816V cells and in the HMC1.2 AML cell line that has a naturally occurring D816V mutation. Although dasatinib was potent at inhibiting c-KIT phosphorylation there was residual mTOR and/or PI3K/AKT signalling in both UT-7 transduced cells and *c-KIT* mutant cell lines. A combination of c-KIT and PI3K/mTOR blockade reduced residual mTOR and/or PI3K/AKT signalling and enhanced cell killing in UT-7 transduced cells and cell lines

with endogenous *c-KIT* mutations. This drug combination was particularly potent against cells expressing *c-KIT*-D816V. In the primary CBFL samples examined all but one were wild-type for *c-KIT*. In these samples c-KIT and PI3K/mTOR blockade did not significantly inhibit cell growth or induce cell killing. This suggests the therapeutic efficacy of targeting c-KIT and PI3K/mTOR may be limited to patients with a *c-KIT* mutation.

Examining the effects of dasatinib and BEZ-235 in primary CBFL cells with *c-KIT* mutations was affected by difficulties in thawing and maintaining primary AML cells in culture. Further work would require investigating a greater number of samples with *c-KIT* mutations to evaluate if dasatinib and BEZ-235 is effective at inducing cell killing. The culture conditions used to maintain primary AML cells would need to be improved and one possible method would be to culture cells on murine MS-5 stroma. This method has previously been shown to decrease apoptosis (Konopleva *et al.*, 2002). To further investigate the effects of *c-KIT* mutations on AML progression a mouse model could be generated by transducing murine BM cells with constructs expressing *c-KIT*-WT, *c-KIT*-Δ417-419>Y, *c-KIT*-L576P, *c-KIT*-D816V or *c-KIT*-N822K in conjunction with constructs expressing either RUNX1-RUNX1T1 or CBFβ-MYH11. This would allow a direct comparison between mice expressing the same *c-KIT* mutation in the presence of t(8;21) or inv(16). This may show differences in disease biology and disease progression as certain mutations such as those in the ECD are more frequently found in patients with inv(16) (Care *et al.*, 2003) whereas ALD mutations are more frequently found in patients with t(8;21) (Park *et al.*, 2011b). It would also provide a model system to examine the efficacy of dasatinib and BEZ-235 *in vivo*. The effects of dasatinib, BEZ-235 or dasatinib and BEZ-235 would also need to be assessed in normal CD34 progenitor cells using long term colony formation assays, by the impact on engraftment in NOD/SCID mice and by characterising the effects on normal murine BM cells in the *in vivo* model of inhibitor treatment.

Identifying the domain in which *c-KIT* mutations occur will be important clinically, as different mutants have varying responses to c-KIT inhibitors. For example the *c-KIT*-D816V mutation has been reported to be resistant to imatinib (Growney *et al.*, 2005) and data in chapter 3 showed that UT-7 cells expressing *c-KIT*-D816V and *c-KIT*-N822K were relatively resistant to dasatinib and masitinib. This indicates that the region in which the *c-KIT* mutation occurs may govern which c-KIT inhibitors should be used. A recent study

examining *c-KIT* mutational status in paired presentation and relapse CBFL patients showed that 6 of 13 patients with a *c-KIT* mutation lost or changed their *c-KIT* mutation at relapse (Allen *et al.*, 2013). This shows that in some patients the acquisition of a *c-KIT* mutation is likely to be a secondary event and has implications for the use of c-KIT inhibitors.

FLT3-mutant AML cell lines treated with the FLT3 TK inhibitor AC220 and the PI3K/mTOR inhibitor BEZ-235 also showed a similar synergistic cell killing profile as *c-KIT* mutant cells treated with dasatinib and BEZ-235 (chapter 5). To explore this drug combination further primary AML cells both with and without *FLT3* activating mutations would need to be treated with AC220 and BEZ-235 to examine if this drug combination could enhance cell killing in samples with a *FLT3* mutation.

Chapter 4 reported the identification and functional consequence of the *FLT3*-T820N mutation in ME-1, a patient derived, AML cell line. Although the *FLT3*-T820N mutation autophosphorylated FLT3 and resulted in ligand-independent growth, the mutation has not been detected in approximately 1000 primary AML samples (Rosemary Gale, personal communication). This indicates this mutation occurs infrequently in AML. However, 32D FLT3-T820N cells were more sensitive to AC220-mediated inhibition of FLT3 phosphorylation and induction of cell killing in comparison to 32D cells expressing FLT3-WT and FLT3-D835Y. This reiterates that mutations outside the classical mutational hotspots can respond to FLT3 inhibitors. Therefore, as screening strategies improve, patients with AML and infrequent *FLT3* mutations could be eligible for clinical trials using FLT3 inhibitors.

In summary, this thesis examined the impact of AML specific *c-KIT* mutations, occurring across the receptor, showing that each mutation varied in its ability to activate c-KIT and its downstream targets. Dasatinib had variable effects on cells harbouring distinct *c-KIT* mutations and simultaneous blockade of mutated RTKs and PI3K/mTOR enhanced cell killing in AML cell lines. These observations may provide the basis for novel therapeutic approaches for patients with AML with specific RTK mutations.

References

Abu-Duhier, F. M., Goodeve, A. C., Wilson, G. A., Care, R. S., Peake, I. R. & Reilly, J. T. (2001) Identification of novel FLT-3 Asp835 mutations in adult acute myeloid leukaemia. *Br J Haematol,* **113,** 983-8.

Advani, A. S., Tiu, R., Saunthararajah, Y., Maciejewski, J., Copelan, E. A., Sobecks, R., Sekeres, M. A., Bates, J., Rush, M. L., Tripp, B., Salvado, A., Noon, E., Howard, M., Jin, T., Hsi, E., Egorin, M. J., Lim, K., Cotta, C. V., Price, C. & Kalaycio, M. (2010) A Phase 1 study of imatinib mesylate in combination with cytarabine and daunorubicin for c-kit positive relapsed acute myeloid leukemia. *Leukemia Research,* **34,** 1622-1626.

Adya, N., Stacy, T., Speck, N. A. & Liu, P. P. (1998) The leukemic protein core binding factor beta (CBF beta)-smooth-muscle myosin heavy chain sequesters CBF alpha 2 into cytoskeletal filaments and aggregates. *Molecular and Cellular Biology,* **18,** 7432-7443.

Allen, C., Hills, R. K., Lamb, K., Evans, C., Tinsley, S., Sellar, R., O'brien, M., Yin, J. L., Burnett, A. K., Linch, D. C. & Gale, R. E. (2013) The importance of relative mutant level for evaluating impact on outcome of KIT, FLT3 and CBL mutations in core-binding factor acute myeloid leukemia. *Leukemia,* **27,** 1891-1901.

Antonescu, C. R., Busam, K. J., Francone, T. D., Wong, G. C., Guo, T., Agaram, N. P., Besmer, P., Jungbluth, A., Gimbel, M., Chen, C. T., Veach, D., Clarkson, B. D., Paty, P. B. & Weiser, M. R. (2007) L576P KIT mutation in anal melanomas correlates with KIT protein expression and is sensitive to specific kinase inhibition. *Int J Cancer,* **121,** 257-64.

Appelbaum, F. R., Gundacker, H., Head, D. R., Slovak, M. L., Willman, C. L., Godwin, J. E., Anderson, J. E. & Petersdorf, S. H. (2006) Age and acute myeloid leukemia. *Blood,* **107,** 3481-5.

Bacher, U., Haferlach, C., Kern, W., Haferlach, T. & Schnittger, S. (2008) Prognostic relevance of FLT3-TKD mutations in AML: the combination matters--an analysis of 3082 patients. *Blood,* **111,** 2527-37.

Balleisen, S., Kuendgen, A., Hildebrandt, B., Haas, R. & Germing, U. (2009) Prognostic relevance of achieving cytogenetic remission in patients with acute myelogenous leukemia or high-risk myelodysplastic syndrome following induction chemotherapy. *Leukemia Research,* **33,** 1189-1193.

Becker, H., Pfeifer, D., Afonso, J. D., Nimer, S. D., Veelken, H., Schwabe, M. & Lubbert, M. (2008) Two cell lines of t(8;21) acute myeloid leukemia with activating KIT exon 17 mutation: models for the 'second hit' hypothesis. *Leukemia,* **22,** 1792-4.

Beghini, A., Ripamonti, C. B., Cairoli, R., Cazzaniga, G., Colapietro, P., Elice, F., Nadali, G., Grillo, G., Haas, O. A., Biondi, A., Morra, E. & Larizza, L. (2004) KIT activating mutations: incidence in adult and pediatric acute myeloid leukemia, and identification of an internal tandem duplication. *Haematologica,* **89,** 920-5.

Bennett, J. M., Catovsky, D., Daniel, M. T., Flandrin, G., Galton, D. A., Gralnick, H. R. & Sultan, C. (1976) Proposals for the classification of the acute leukaemias. French-American-British (FAB) co-operative group. *Br J Haematol,* **33,** 451-8.

Bennett, J. M., Catovsky, D., Daniel, M. T., Flandrin, G., Galton, D. A., Gralnick, H. R. & Sultan, C. (1985) Proposed revised criteria for the classification of acute myeloid leukemia. A report of the French-American-British Cooperative Group. *Ann Intern Med,* **103,** 620-5.

Beran, M., Luthra, R., Kantarjian, H. & Estey, E. (2004) FLT3 mutation and response to intensive chemotherapy in young adult and elderly patients with normal karyotype. *Leuk Res,* **28,** 547-50.

Billottet, C., Grandage, V. L., Gale, R. E., Quattropani, A., Rommel, C., Vanhaesebroeck, B. & Khwaja, A. (2006) A selective inhibitor of the p110delta isoform of PI 3-kinase inhibits AML cell proliferation and survival and increases the cytotoxic effects of VP16. *Oncogene,* **25,** 6648-59.

Birkenkamp, K. U., Geugien, M., Schepers, H., Westra, J., Lemmink, H. H. & Vellenga, E. (2004) Constitutive NF-kappaB DNA-binding activity in AML is frequently mediated by a Ras/PI3-K/PKB-dependent pathway. *Leukemia,* **18,** 103-12.

Bjerkvig, R., Tysnes, B. B., Aboody, K. S., Najbauer, J. & Terzis, A. J. (2005) Opinion: the origin of the cancer stem cell: current controversies and new insights. *Nat Rev Cancer,* **5,** 899-904.

Boissel, N., Leroy, H., Brethon, B., Philippe, N., De Botton, S., Auvrignon, A., Raffoux, E., Leblanc, T., Thomas, X., Hermine, O., Quesnel, B., Baruchel, A., Leverger, G., Dombret, H. & Preudhomme, C. (2006) Incidence and prognostic impact of c-Kit, FLT3, and Ras gene mutations in core binding factor acute myeloid leukemia (CBF-AML). *Leukemia,* **20,** 965-70.

Bonnet, D. & Dick, J. E. (1997) Human acute myeloid leukemia is organized as a hierarchy that originates from a primitive hematopoietic cell. *Nature Medicine,* **3,** 730-737.

Bowen, D. T., Frew, M. E., Hills, R., Gale, R. E., Wheatley, K., Groves, M. J., Langabeer, S. E., Kottaridis, P. D., Moorman, A. V., Burnett, A. K. & Linch, D. C. (2005) RAS mutation in acute myeloid leukemia is associated with distinct cytogenetic subgroups but does not influence outcome in patients younger than 60 years. *Blood,* **106,** 2113-9.

Brandts, C. H., Sargin, B., Rode, M., Biermann, C., Lindtner, B., Schwäble, J., Buerger, H., Müller-Tidow, C., Choudhary, C., Mcmahon, M., Berdel, W. E. & Serve, H. (2005) Constitutive activation of Akt by Flt3 internal tandem duplications is necessary for increased survival, proliferation, and myeloid transformation. *Cancer Res,* **65,** 9643-50.

Burnett, A. K., Goldstone, A. H., Stevens, R. M., Hann, I. M., Rees, J. K., Gray, R. G. & Wheatley, K. (1998) Randomised comparison of addition of autologous bone-marrow transplantation to intensive chemotherapy for acute myeloid leukaemia in first remission: results of MRC AML 10 trial. UK Medical Research Council Adult and Children's Leukaemia Working Parties. *Lancet,* **351,** 700-8.

Burnett, A. K., Hills, R. K., Milligan, D., Kjeldsen, L., Kell, J., Russell, N. H., Yin, J. A., Hunter, A., Goldstone, A. H. & Wheatley, K. (2011) Identification of patients with acute myeloblastic leukemia who benefit from the addition of gemtuzumab ozogamicin: results of the MRC AML15 trial. *J Clin Oncol,* **29,** 369-77.

Cairoli, R., Beghini, A., Grillo, G., Nadali, G., Elice, F., Ripamonti, C. B., Colapietro, P., Nichelatti, M., Pezzetti, L., Lunghi, M., Cuneo, A., Viola, A., Ferrara, F., Lazzarino, M., Rodeghiero, F., Pizzolo, G., Larizza, L. & Morra, E. (2006) Prognostic impact of

c-KIT mutations in core binding factor leukemias: an Italian retrospective study. *Blood,* **107,** 3463-8.

Care, R. S., Valk, P. J., Goodeve, A. C., Abu-Duhier, F. M., Geertsma-Kleinekoort, W. M., Wilson, G. A., Gari, M. A., Peake, I. R., Lowenberg, B. & Reilly, J. T. (2003) Incidence and prognosis of c-KIT and FLT3 mutations in core binding factor (CBF) acute myeloid leukaemias. *Br J Haematol,* **121,** 775-7.

Carnevale, J., Ross, L., Puissant, A., Banerji, V., Stone, R. M., Deangelo, D. J., Ross, K. N. & Stegmaier, K. (2013) SYK regulates mTOR signaling in AML. *Leukemia,* **27,** 2118-2128.

Carracedo, A., Ma, L., Teruya-Feldstein, J., Rojo, F., Salmena, L., Alimonti, A., Egia, A., Sasaki, A. T., Thomas, G., Kozma, S. C., Papa, A., Nardella, C., Cantley, L. C., Baselga, J. & Pandolfi, P. P. (2008) Inhibition of mTORC1 leads to MAPK pathway activation through a PI3K-dependent feedback loop in human cancer. *Journal of Clinical Investigation,* **118,** 3065-3074.

Cassileth, P. A., Harrington, D. P., Appelbaum, F. R., Lazarus, H. M., Rowe, J. M., Paietta, E., Willman, C., Hurd, D. D., Bennett, J. M., Blume, K. G., Head, D. R. & Wiernik, P. H. (1998) Chemotherapy compared with autologous or allogeneic bone marrow transplantation in the management of acute myeloid leukemia in first remission. *N Engl J Med,* **339,** 1649-56.

Chapuis, N., Tamburini, J., Green, A. S., Vignon, C., Bardet, V., Neyret, A., Pannetier, M., Willems, L., Park, S., Macone, A., Maira, S. M., Ifrah, N., Dreyfus, F., Herault, O., Lacombe, C., Mayeux, P. & Bouscary, D. (2010) Dual Inhibition of PI3K and mTORC1/2 Signaling by NVP-BEZ235 as a New Therapeutic Strategy for Acute Myeloid Leukemia. *Clinical Cancer Research,* **16,** 5424-5435.

Chen, W., Drakos, E., Grammatikakis, I., Schlette, E. J., Li, J., Leventaki, V., Staikou-Drakopoulou, E., Patsouris, E., Panayiotidis, P., Medeiros, L. J. & Rassidakis, G. Z. (2010) mTOR signaling is activated by FLT3 kinase and promotes survival of FLT3-mutated acute myeloid leukemia cells. *Mol Cancer,* **9,** 292.

Chou, T. C. & Talalay, P. (1983) Analysis of Combined Drug Effects - a New Look at a Very Old Problem. *Trends in Pharmacological Sciences,* **4,** 450-454.

Chou, T. C. & Talalay, P. (1984) Quantitative-Analysis of Dose-Effect Relationships - the Combined Effects of Multiple-Drugs or Enzyme-Inhibitors. *Advances in Enzyme Regulation,* **22,** 27-55.

Chou, W. C., Chou, S. C., Liu, C. Y., Chen, C. Y., Hou, H. A., Kuo, Y. Y., Lee, M. C., Ko, B. S., Tang, J. L., Yao, M., Tsay, W., Wu, S. J., Huang, S. Y., Hsu, S. C., Chen, Y. C., Chang, Y. C., Kuo, K. T., Lee, F. Y., Liu, M. C., Liu, C. W., Tseng, M. H., Huang, C. F. & Tien, H. F. (2011) TET2 mutation is an unfavorable prognostic factor in acute myeloid leukemia patients with intermediate-risk cytogenetics. *Blood,* **118,** 3803-10.

Choudhary, C., Schwable, J., Brandts, C., Tickenbrock, L., Sargin, B., Kindler, T., Fischer, T., Berdel, W. E., Muller-Tidow, C. & Serve, H. (2005) AML-associated Flt3 kinase domain mutations show signal transduction differences compared with Flt3 ITD mutations. *Blood,* **106,** 265-273.

Cortes, J., Foran, J., Ghirdaladze, D., Devetten, M. P., Zodelava, M., Holman, P., Levis, M. J., Kantarjian, H. M., Borthakur, G., James, J., Zarringkar, P. P., Gunawardane, R. N., Armstrong, R. C., Padre, N. M., Wierenga, W., Corringham, R. & Trikha, M. (2009) AC220, a Potent, Selective, Second Generation FLT3 Receptor Tyrosine Kinase (RTK) Inhibitor, in a First-in-Human (FIH) Phase 1 AML Study. *Blood,* **114,** 264-264.

Cortes, J., Giles, F., O'brien, S., Thomas, D., Albitar, M., Rios, M. B., Talpaz, M., Garcia-Manero, G., Faderl, S., Letvak, L., Salvado, A. & Kantarjian, H. (2003) Results of imatinib mesylate therapy in patients with refractory or recurrent acute myeloid leukemia, high-risk myelodysplastic syndrome, and myeloproliferative disorders. *Cancer,* **97,** 2760-2766.

Cortes, J. E., Perl, A. E., Dombret, H., Kayser, S., Steffen, B., Rousselot, P., Martinelli, G., Estey, E. H., Burnett, A. K., Gammon, G., Trone, D., Leo, E. & Levis, M. J. (2012) Final Results of a Phase 2 Open-Label, Monotherapy Efficacy and Safety Study of Quizartinib (AC220) in Patients >= 60 Years of Age with FLT3 ITD Positive or Negative Relapsed/Refractory Acute Myeloid Leukemia. *Blood,* **120,** 48.

Crosier, P. S., Ricciardi, S. T., Hall, L. R., Vitas, M. R., Clark, S. C. & Crosier, K. E. (1993) Expression of isoforms of the human receptor tyrosine kinase c-kit in leukemic cell lines and acute myeloid leukemia. *Blood,* **82,** 1151-8.

Crump, M., Hedley, D., Kamel-Reid, S., Leber, B., Wells, R., Brandwein, J., Buckstein, R., Kassis, J., Minden, M., Matthews, J., Robinson, S., Turner, R., Mcintosh, L., Eisenhauer, E. & Seymour, L. (2010) A randomized phase I clinical and biologic study of two schedules of sorafenib in patients with myelodysplastic syndrome or acute myeloid leukemia: a NCIC (National Cancer Institute of Canada) Clinical Trials Group Study. *Leukemia & Lymphoma,* **51,** 252-260.

Davies, B. R., Greenwood, H., Dudley, P., Crafter, C., Yu, D. H., Zhang, J., Li, J., Gao, B., Ji, Q., Maynard, J., Ricketts, S. A., Cross, D., Cosulich, S., Chresta, C. C., Page, K., Yates, J., Lane, C., Watson, R., Luke, R., Ogilvie, D. & Pass, M. (2012) Preclinical pharmacology of AZD5363, an inhibitor of AKT: pharmacodynamics, antitumor activity, and correlation of monotherapy activity with genetic background. *Mol Cancer Ther,* **11,** 873-87.

De Angelo, D. J., Stone, R. M., Heaney, M. L., Nimer, S. D., Paquette, R., Bruner-Klisovic, R., Caligiuri, M. A., Cooper, M. R., Le-Cerf, J. M. & Iyer, G. (2004) Phase II evaluation of the tyrosine kinase inhibitor MLN518 in patients with acute myeloid leukemia (AML) bearing a FLT3 internal tandem duplication (ITD) mutation. *Blood,* **104,** 496a-497a.

De Guzman, C. G., Warren, A. J., Zhang, Z., Gartland, L., Erickson, P., Drabkin, H., Hiebert, S. W. & Klug, C. A. (2002) Hematopoietic stem cell expansion and distinct myeloid developmental abnormalities in a murine model of the AML1-ETO translocation. *Mol Cell Biol,* **22,** 5506-17.

Deangelo, D. J., Stone, R. M., Heaney, M. L., Nimer, S. D., Paquette, R. L., Klisovic, R. B., Caligiuri, M. A., Cooper, M. R., Lecerf, J. M., Karol, M. D., Sheng, S. H., Holford, N., T Curtin, P., Druker, B. J. & Heinrich, M. C. (2006) Phase 1 clinical results with tandutinib (MLN518), a novel FLT3 antagonist, in patients with acute myelogenous leukemia or high-risk myelodysplastic syndrome: safety, pharmacokinetics, and pharmacodynamics. *Blood,* **108,** 3674-3681.

Deschler, B. & Lubbert, M. (2006) Acute myeloid leukemia: Epidemiology and etiology. *Cancer,* **107,** 2099-2107.

Ding, L., Ley, T. J., Larson, D. E., Miller, C. A., Koboldt, D. C., Welch, J. S., Ritchey, J. K., Young, M. A., Lamprecht, T., Mclellan, M. D., Mcmichael, J. F., Wallis, J. W., Lu, C., Shen, D., Harris, C. C., Dooling, D. J., Fulton, R. S., Fulton, L. L., Chen, K., Schmidt, H., Kalicki-Veizer, J., Magrini, V. J., Cook, L., Mcgrath, S. D., Vickery, T.

L., Wendl, M. C., Heath, S., Watson, M. A., Link, D. C., Tomasson, M. H., Shannon, W. D., Payton, J. E., Kulkarni, S., Westervelt, P., Walter, M. J., Graubert, T. A., Mardis, E. R., Wilson, R. K. & Dipersio, J. F. (2012) Clonal evolution in relapsed acute myeloid leukaemia revealed by whole-genome sequencing. *Nature,* **481,** 506-10.

Dinitto, J. P., Deshmukh, G. D., Zhang, Y., Jacques, S. L., Coli, R., Worrall, J. W., Diehl, W., English, J. M. & Wu, J. C. (2010) Function of activation loop tyrosine phosphorylation in the mechanism of c-Kit auto-activation and its implication in sunitinib resistance. *J Biochem,* **147,** 601-9.

Dos Santos, C., Mcdonald, T., Ho, Y. W., Liu, H., Lin, A., Forman, S. J., Kuo, Y. H. & Bhatia, R. (2013) The Src and c-Kit kinase inhibitor dasatinib enhances p53-mediated targeting of human acute myeloid leukemia stem cell by chemotherapeutic agents. *Blood,* **122,** 1900-1913.

Doulatov, S., Notta, F., Laurenti, E. & Dick, J. E. (2012) Hematopoiesis: a human perspective. *Cell Stem Cell,* **10,** 120-36.

Dubreuil, P., Letard, S., Ciufolini, M., Gros, L., Humbert, M., Casteran, N., Borge, L., Hajem, B., Lermet, A., Sippl, W., Voisset, E., Arock, M., Auclair, C., Leventhal, P. S., Mansfield, C. D., Moussy, A. & Hermine, O. (2009) Masitinib (AB1010), a potent and selective tyrosine kinase inhibitor targeting KIT. *PLoS One,* **4,** e7258.

Elagib, K. E. & Goldfarb, A. N. (2007) Oncogenic pathways of AML1-ETO in acute myeloid leukemia: Multifaceted manipulation of marrow maturation. *Cancer Letters,* **251,** 179-186.

Eppert, K., Takenaka, K., Lechman, E. R., Waldron, L., Nilsson, B., Van Galen, P., Metzeler, K. H., Poeppl, A., Ling, V., Beyene, J., Canty, A. J., Danska, J. S., Bohlander, S. K., Buske, C., Minden, M. D., Golub, T. R., Jurisica, I., Ebert, B. L. & Dick, J. E. (2011) Stem cell gene expression programs influence clinical outcome in human leukemia. *Nature Medicine,* **17,** 1086-93.

Erba, H. P. (2007) Prognostic factors in elderly patients with AML and the implications for treatment. *Hematology Am Soc Hematol Educ Program,* **2007,** 420-8.

Farag, S. S., Archer, K. J., Mrozek, K., Ruppert, A. S., Carroll, A. J., Vardiman, J. W., Pettenati, M. J., Baer, M. R., Qumsiyeh, M. B., Koduru, P. R., Ning, Y., Mayer, R. J., Stone, R. M., Larson, R. A. & Bloomfield, C. D. (2006) Pretreatment cytogenetics add to other prognostic factors predicting complete remission and long-term outcome in patients 60 years of age or older with acute myeloid leukemia: results from Cancer and Leukemia Group B 8461. *Blood,* **108,** 63-73.

Fernandez, H. F., Sun, Z., Yao, X., Litzow, M. R., Luger, S. M., Paietta, E. M., Racevskis, J., Dewald, G. W., Ketterling, R. P., Bennett, J. M., Rowe, J. M., Lazarus, H. M. & Tallman, M. S. (2009) Anthracycline dose intensification in acute myeloid leukemia. *N Engl J Med,* **361,** 1249-59.

Fiedler, W., Serve, H., Döhner, H., Schwittay, M., Ottmann, O. G., O'farrell, A. M., Bello, C. L., Allred, R., Manning, W. C., Cherrington, J. M., Louie, S. G., Hong, W., Brega, N. M., Massimini, G., Scigalla, P., Berdel, W. E. & Hossfeld, D. K. (2005) A phase 1 study of SU11248 in the treatment of patients with refractory or resistant acute myeloid leukemia (AML) or not amenable to conventional therapy for the disease. *Blood,* **105,** 986-93.

Fischer, T., Stone, R. M., Deangelo, D. J., Galinsky, I., Estey, E., Lanza, C., Fox, E., Ehninger, G., Feldman, E. J., Schiller, G. J., Klimek, V. M., Nimer, S. D., Gilliland, D. G., Dutreix, C., Huntsman-Labed, A., Virkus, J. & Giles, F. J. (2010) Phase IIB trial of oral Midostaurin (PKC412), the FMS-like tyrosine kinase 3 receptor (FLT3) and multi-targeted kinase inhibitor, in patients with acute myeloid leukemia and high-risk myelodysplastic syndrome with either wild-type or mutated FLT3. *J Clin Oncol,* **28,** 4339-45.

Frohling, S., Schlenk, R. F., Breitruck, J., Benner, A., Kreitmeier, S., Tobis, K., Dohner, H. & Dohner, K. (2002) Prognostic significance of activating FLT3 mutations in younger adults (16 to 60 years) with acute myeloid leukemia and normal cytogenetics: a study of the AML Study Group Ulm. *Blood,* **100,** 4372-80.

Frohling, S., Scholl, C., Gilliland, D. G. & Levine, R. L. (2005) Genetics of myeloid malignancies: pathogenetic and clinical implications. *J Clin Oncol,* **23,** 6285-95.

Frohling, S., Scholl, C., Levine, R. L., Loriaux, M., Boggon, T. J., Bernard, O. A., Berger, R., Dohner, H., Dohner, K., Ebert, B. L., Teckie, S., Golub, T. R., Jiang, J., Schittenhelm, M. M., Lee, B. H., Griffin, J. D., Stone, R. M., Heinrich, M. C., Deininger, M. W., Druker, B. J. & Gilliland, D. G. (2007) Identification of driver

and passenger mutations of FLT3 by high-throughput DNA sequence analysis and functional assessment of candidate alleles. *Cancer Cell,* **12,** 501-13.

Frost, M. J., Ferrao, P. T., Hughes, T. P. & Ashman, L. K. (2002) Juxtamembrane mutant V560GKit is more sensitive to Imatinib (STI571) compared with wild-type c-kit whereas the kinase domain mutant D816VKit is resistant. *Molecular Cancer Therapeutics,* **1,** 1115-1124.

Furitsu, T., Tsujimura, T., Tono, T., Ikeda, H., Kitayama, H., Koshimizu, U., Sugahara, H., Butterfield, J. H., Ashman, L. K., Kanayama, Y. & Et Al. (1993) Identification of mutations in the coding sequence of the proto-oncogene c-kit in a human mast cell leukemia cell line causing ligand-independent activation of c-kit product. *J Clin Invest,* **92,** 1736-44.

Gaidzik, V. I., Paschka, P., Späth, D., Habdank, M., Köhne, C. H., Germing, U., Von Lilienfeld-Toal, M., Held, G., Horst, H. A., Haase, D., Bentz, M., Götze, K., Döhner, H., Schlenk, R. F., Bullinger, L. & Döhner, K. (2012) TET2 mutations in acute myeloid leukemia (AML): results from a comprehensive genetic and clinical analysis of the AML study group. *J Clin Oncol,* **30,** 1350-7.

Gajiwala, K. S., Wu, J. C., Christensen, J., Deshmukh, G. D., Diehl, W., Dinitto, J. P., English, J. M., Greig, M. J., He, Y. A., Jacques, S. L., Lunney, E. A., Mctigue, M., Molina, D., Quenzer, T., Wells, P. A., Yu, X., Zhang, Y., Zou, A. H., Emmett, M. R., Marshall, A. G., Zhang, H. M. & Demetri, G. D. (2009) KIT kinase mutants show unique mechanisms of drug resistance to imatinib and sunitinib in gastrointestinal stromal tumor patients. *Proceedings of the National Academy of Sciences of the United States of America,* **106,** 1542-1547.

Gale, R. E., Green, C., Allen, C., Mead, A. J., Burnett, A. K., Hills, R. K., Linch, D. C. & Party, M. R. C. a. L. W. (2008) The impact of FLT3 internal tandem duplication mutant level, number, size, and interaction with NPM1 mutations in a large cohort of young adult patients with acute myeloid leukemia. *Blood,* **111,** 2776-84.

Gallay, N., Dos Santos, C., Cuzin, L., Bousquet, M., Simmonet Gouy, V., Chaussade, C., Attal, M., Payrastre, B., Demur, C. & Récher, C. (2009) The level of AKT phosphorylation on threonine 308 but not on serine 473 is associated with high-risk cytogenetics and predicts poor overall survival in acute myeloid leukaemia. *Leukemia,* **23,** 1029-38.

Garcia-Echeverria, C. (2009) Protein and lipid kinase inhibitors as targeted anticancer agents of the Ras/Raf/MEK and PI3K/PKB pathways. *Purinergic Signalling,* **5,** 117-125.

Garcia-Montero, A. C. (2006) KIT mutation in mast cells and other bone marrow hematopoietic cell lineages in systemic mast cell disorders: a prospective study of the Spanish Network on Mastocytosis (REMA) in a series of 113 patients. *Blood,* **108,** 2366-2372.

Gilliland, D. G. & Griffin, J. D. (2002) The roles of FLT3 in hematopoiesis and leukemia. *Blood,* **100,** 1532-42.

Goardon, N., Marchi, E., Atzberger, A., Quek, L., Schuh, A., Soneji, S., Woll, P., Mead, A., Alford, K. A., Rout, R., Chaudhury, S., Gilkes, A., Knapper, S., Beldjord, K., Begum, S., Rose, S., Geddes, N., Griffiths, M., Standen, G., Sternberg, A., Cavenagh, J., Hunter, H., Bowen, D., Killick, S., Robinson, L., Price, A., Macintyre, E., Virgo, P., Burnett, A., Craddock, C., Enver, T., Jacobsen, S. E., Porcher, C. & Vyas, P. (2011) Coexistence of LMPP-like and GMP-like leukemia stem cells in acute myeloid leukemia. *Cancer Cell,* **19,** 138-52.

Goemans, B. F., Zwaan, C. M., Cloos, J., De Lange, D., Loonen, A. H., Reinhardt, D., Hahlen, K., Gibson, B. E. S., Creutzig, U. & Kaspers, G. J. L. (2010) FLT3 and KIT mutated pediatric acute myeloid leukemia (AML) samples are sensitive in vitro to the tyrosine kinase inhibitor SU11657. *Leukemia Research,* **34,** 1302-1307.

Goemans, B. F., Zwaan, C. M., Miller, M., Zimmermann, M., Harlow, A., Meshinchi, S., Loonen, A. H., Hahlen, K., Reinhardt, D., Creutzig, U., Kaspers, G. J. & Heinrich, M. C. (2005) Mutations in KIT and RAS are frequent events in pediatric core-binding factor acute myeloid leukemia. *Leukemia,* **19,** 1536-42.

Goodman, V. L., Rock, E. P., Dagher, R., Ramchandani, R. P., Abraham, S., Gobburu, J. V., Booth, B. P., Verbois, S. L., Morse, D. E., Liang, C. Y., Chidambaram, N., Jiang, J. X., Tang, S., Mahjoob, K., Justice, R. & Pazdur, R. (2007) Approval summary: sunitinib for the treatment of imatinib refractory or intolerant gastrointestinal stromal tumors and advanced renal cell carcinoma. *Clin Cancer Res,* **13,** 1367-73.

Gozgit, J. M., Wong, M. J., Wardwell, S., Tyner, J. W., Loriaux, M. M., Mohemmad, Q. K., Narasimhan, N. I., Shakespeare, W. C., Wang, F., Druker, B. J., Clackson, T. & Rivera, V. M. (2011) Potent activity of ponatinib (AP24534) in models of FLT3-

driven acute myeloid leukemia and other hematologic malignancies. *Mol Cancer Ther,* **10,** 1028-35.

Grandage, V. L., Gale, R. E., Linch, D. C. & Khwaja, A. (2005) PI3-kinase/Akt is constitutively active in primary acute myeloid leukaemia cells and regulates survival and chemoresistance via NF-kappaB, Mapkinase and p53 pathways. *Leukemia,* **19,** 586-94.

Green, C. L., Evans, C. M., Hills, R. K., Burnett, A. K., Linch, D. C. & Gale, R. E. (2010a) The prognostic significance of IDH1 mutations in younger adult patients with acute myeloid leukemia is dependent on FLT3/ITD status. *Blood,* **116,** 2779-82.

Green, C. L., Evans, C. M., Zhao, L., Hills, R. K., Burnett, A. K., Linch, D. C. & Gale, R. E. (2011) The prognostic significance of IDH2 mutations in AML depends on the location of the mutation. *Blood,* **118,** 409-12.

Green, C. L., Koo, K. K., Hills, R. K., Burnett, A. K., Linch, D. C. & Gale, R. E. (2010b) Prognostic significance of CEBPA mutations in a large cohort of younger adult patients with acute myeloid leukemia: impact of double CEBPA mutations and the interaction with FLT3 and NPM1 mutations. *J Clin Oncol,* **28,** 2739-47.

Griffith, J., Black, J., Faerman, C., Swenson, L., Wynn, M., Lu, F., Lippke, J. & Saxena, K. (2004) The structural basis for autoinhibition of FLT3 by the juxtamembrane domain. *Mol Cell,* **13,** 169-78.

Grimwade, D., Hills, R. K., Moorman, A. V., Walker, H., Chatters, S., Goldstone, A. H., Wheatley, K., Harrison, C. J. & Burnett, A. K. (2010) Refinement of cytogenetic classification in acute myeloid leukemia: determination of prognostic significance of rare recurring chromosomal abnormalities among 5876 younger adult patients treated in the United Kingdom Medical Research Council trials. *Blood,* **116,** 354-65.

Grimwade, D., Walker, H., Oliver, F., Wheatley, K., Harrison, C., Harrison, G., Rees, J., Hann, I., Stevens, R., Burnett, A. & Goldstone, A. (1998) The importance of diagnostic cytogenetics on outcome in AML: analysis of 1,612 patients entered into the MRC AML 10 trial. The Medical Research Council Adult and Children's Leukaemia Working Parties. *Blood,* **92,** 2322-33.

Growney, J. D., Clark, J. J., Adelsperger, J., Stone, R., Fabbro, D., Griffin, J. D. & Gilliland, D. G. (2005) Activation mutations of human c-KIT resistant to imatinib mesylate are sensitive to the tyrosine kinase inhibitor PKC412. *Blood,* **106,** 721-4.

Grundler, R., Miething, C., Thiede, C., Peschel, C. & Duyster, J. (2005) FLT3-ITD and tyrosine kinase domain mutants induce 2 distinct phenotypes in a murine bone marrow transplantation model. *Blood,* **105,** 4792-9.

Guerrini, F., Galimberti, S., Ciabatti, E., Brizzi, S., Testi, R., Pollastrini, A., Falini, B. & Petrini, M. (2007) Molecular detection of GNNK- and GNNK+ c-kit isoforms: a new tool for risk stratification in adult acute myeloid leukaemia. *Leukemia,* **21,** 2056-8.

Guerrouahen, B. S., Futami, M., Vaklavas, C., Kanerva, J., Whichard, Z. L., Nwawka, K., Blanchard, E. G., Lee, F. Y., Robinson, L. J., Arceci, R., Kornblau, S. M., Wieder, E., Cayre, Y. E. & Corey, S. J. (2010) Dasatinib Inhibits the Growth of Molecularly Heterogeneous Myeloid Leukemias. *Clinical Cancer Research,* **16,** 1149-1158.

Gunawardane, R. N., Nepomuceno, R. R., Rooks, A. M., Hunt, J. P., Ricono, J. M., Belli, B. & Armstrong, R. C. (2013) Transient exposure to quizartinib mediates sustained inhibition of FLT3 signaling while specifically inducing apoptosis in FLT3-activated leukemia cells. *Mol Cancer Ther,* **12,** 438-47.

Han, L., Schuringa, J. J., Mulder, A. & Vellenga, E. (2010) Dasatinib impairs long-term expansion of leukemic progenitors in a subset of acute myeloid leukemia cases. *Annals of Hematology,* **89,** 861-871.

Hayakawa, F., Towatari, M., Kiyoi, H., Tanimoto, M., Kitamura, T., Saito, H. & Naoe, T. (2000) Tandem-duplicated Flt3 constitutively activates STAT5 and MAP kinase and introduces autonomous cell growth in IL-3-dependent cell lines. *Oncogene,* **19,** 624-31.

Higuchi, M., O'brien, D., Kumaravelu, P., Lenny, N., Yeoh, E. J. & Downing, J. R. (2002) Expression of a conditional AML1-ETO oncogene bypasses embryonic lethality and establishes a murine model of human t(8;21) acute myeloid leukemia. *Cancer Cell,* **1,** 63-74.

Hu, S., Niu, H., Minkin, P., Orwick, S., Shimada, A., Inaba, H., Dahl, G. V. H., Rubnitz, J. & Baker, S. D. (2008) Comparison of antitumor effects of multitargeted tyrosine kinase inhibitors in acute myelogenous leukemia. *Molecular Cancer Therapeutics*, **7,** 1110-1120.

Huntly, B. J., Shigematsu, H., Deguchi, K., Lee, B. H., Mizuno, S., Duclos, N., Rowan, R., Amaral, S., Curley, D., Williams, I. R., Akashi, K. & Gilliland, D. G. (2004) MOZ-TIF2, but not BCR-ABL, confers properties of leukemic stem cells to committed murine hematopoietic progenitors. *Cancer Cell,* **6,** 587-96.

Iida, M., Towatari, M., Nakao, A., Iida, H., Kiyoi, H., Nakano, Y., Tanimoto, M., Saito, H. & Naoe, T. (1999) Lack of constitutive activation of MAP kinase pathway in human acute myeloid leukemia cells with N-Ras mutation. *Leukemia,* **13,** 585-589.

Jin, L., Tabe, Y., Lu, H., Borthakur, G., Miida, T., Kantarjian, H., Andreeff, M. & Konopleva, M. (2013) Mechanisms of apoptosis induction by simultaneous inhibition of PI3K and FLT3-ITD in AML cells in the hypoxic bone marrow microenvironment. *Cancer Lett,* **329,** 45-58.

Juliusson, G., Antunovic, P., Derolf, A., Lehmann, S., Mollgard, L., Stockelberg, D., Tidefelt, U., Wahlin, A. & Hoglund, M. (2009) Age and acute myeloid leukemia: real world data on decision to treat and outcomes from the Swedish Acute Leukemia Registry. *Blood,* **113,** 4179-87.

Karakas, B., Bachman, K. E. & Park, B. H. (2006) Mutation of the PIK3CA oncogene in human cancers. *Br J Cancer*, **94,** 455-9.

Kelly, L. M., Liu, Q., Kutok, J. L., Williams, I. R., Boulton, C. L. & Gilliland, D. G. (2002) FLT3 internal tandem duplication mutations associated with human acute myeloid leukemias induce myeloproliferative disease in a murine bone marrow transplant model. *Blood,* **99,** 310-8.

Kerr, A. H., James, J. A., Smith, M. A., Willson, C., Court, E. L. & Smith, J. G. (2003) An investigation of the MEK/ERK inhibitor U0126 in acute myeloid leukemia. *Ann N Y Acad Sci*, **1010,** 86-9.

Kindler, T. (2004) Efficacy and safety of imatinib in adult patients with c-kit-positive acute myeloid leukemia. *Blood,* **103,** 3644-3654.

Kindler, T., Breitenbuecher, F., Kasper, S., Estey, E., Giles, F., Feldman, E., Ehninger, G., Schiller, G., Klimek, V., Nimer, S. D., Gratwohl, A., Choudhary, C. R., Mueller-Tidow, C., Serve, H., Gschaidmeier, H., Cohen, P. S., Huber, C. & Fischer, T. (2005) Identification of a novel activating mutation (Y842C) within the activation loop of FLT3 in patients with acute myeloid leukemia (AML). *Blood,* **105,** 335-40.

Kitamura, Y. & Hirotab, S. (2004) Kit as a human oncogenic tyrosine kinase. *Cellular and Molecular Life Sciences,* **61,** 2924-2931.

Knapper, S., Burnett, A. K., Littlewood, T., Kell, W. J., Agrawal, S., Chopra, R., Clark, R., Levis, M. J. & Small, D. (2006) A phase 2 trial of the FLT3 inhibitor lestaurtinib (CEP701) as first-line treatment for older patients with acute myeloid leukemia not considered fit for intensive chemotherapy. *Blood,* **108,** 3262-70.

Kohl, T. M., Schnittger, S., Ellwart, J. W., Hiddemann, W. & Spiekermann, K. (2005) KIT exon 8 mutations associated with core-binding factor (CBF)-acute myeloid leukemia (AML) cause hyperactivation of the receptor in response to stem cell factor. *Blood,* **105,** 3319-21.

Kong, D. & Yamori, T. (2007) ZSTK474 is an ATP-competitive inhibitor of class I phosphatidylinositol 3 kinase isoforms. *Cancer Sci,* **98,** 1638-42.

Konopleva, M., Konoplev, S., Hu, W., Zaritskey, A. Y., Afanasiev, B. V. & Andreeff, M. (2002) Stromal cells prevent apoptosis of AML cells by up-regulation of anti-apoptotic proteins. *Leukemia,* **16,** 1713-24.

Koreth, J., Schlenk, R., Kopecky, K. J., Honda, S., Sierra, J., Djulbegovic, B. J., Wadleigh, M., Deangelo, D. J., Stone, R. M., Sakamaki, H., Appelbaum, F. R., Dohner, H., Antin, J. H., Soiffer, R. J. & Cutler, C. (2009) Allogeneic stem cell transplantation for acute myeloid leukemia in first complete remission: systematic review and meta-analysis of prospective clinical trials. *JAMA,* **301,** 2349-61.

Kornblau, S. M., Womble, M., Qiu, Y. H., Jackson, C. E., Chen, W., Konopleva, M., Estey, E. H. & Andreeff, M. (2006) Simultaneous activation of multiple signal transduction

pathways confers poor prognosis in acute myelogenous leukemia. *Blood,* **108,** 2358-65.

Kottaridis, P. D., Gale, R. E., Frew, M. E., Harrison, G., Langabeer, S. E., Belton, A. A., Walker, H., Wheatley, K., Bowen, D. T., Burnett, A. K., Goldstone, A. H. & Linch, D. C. (2001) The presence of a FLT3 internal tandem duplication in patients with acute myeloid leukemia (AML) adds important prognostic information to cytogenetic risk group and response to the first cycle of chemotherapy: analysis of 854 patients from the United Kingdom Medical Research Council AML 10 and 12 trials. *Blood,* **98,** 1752-9.

Kottaridis, P. D., Gale, R. E., Langabeer, S. E., Frew, M. E., Bowen, D. T. & Linch, D. C. (2002) Studies of FLT3 mutations in paired presentation and relapse samples from patients with acute myeloid leukemia: implications for the role of FLT3 mutations in leukemogenesis, minimal residual disease detection, and possible therapy with FLT3 inhibitors. *Blood,* **100,** 2393-8.

Kubota, Y., Ohnishi, H., Kitanaka, A., Ishida, T. & Tanaka, T. (2004) Constitutive activation of PI3K is involved in the spontaneous proliferation of primary acute myeloid leukemia cells: direct evidence of PI3K activation. *Leukemia,* **18,** 1438-1440.

Kuo, Y. H., Landrette, S. F., Heilman, S. A., Perrat, P. N., Garrett, L., Liu, P. P., Le Beau, M. M., Kogan, S. C. & Castilla, L. H. (2006) Cbf beta-SMMHC induces distinct abnormal myeloid progenitors able to develop acute myeloid leukemia. *Cancer Cell,* **9,** 57-68.

Kusec, R., Jaksic, O., Ostojic, S., Kardum-Skelin, I., Vrhovac, R. & Jaksic, B. (2006) More on prognostic significance of FLT3/ITD size in acute myeloid leukemia (AML). *Blood,* **108,** 405-406.

Lagadinou, E. D., Sach, A., Callahan, K., Rossi, R. M., Neering, S. J., Minhajuddin, M., Ashton, J. M., Pei, S., Grose, V., O'dwyer, K. M., Liesveld, J. L., Brookes, P. S., Becker, M. W. & Jordan, C. T. (2013) BCL-2 inhibition targets oxidative phosphorylation and selectively eradicates quiescent human leukemia stem cells. *Cell Stem Cell,* **12,** 329-41.

Laine, E., Chauvot De Beauchene, I., Perahia, D., Auclair, C. & Tchertanov, L. (2011) Mutation D816V alters the internal structure and dynamics of c-KIT receptor

cytoplasmic region: implications for dimerization and activation mechanisms. *PLoS Comput Biol,* **7,** e1002068.

Lemmon, M. A. & Schlessinger, J. (2010) Cell signaling by receptor tyrosine kinases. *Cell,* **141,** 1117-34.

Levis, M., Brown, P., Smith, B. D., Stine, A., Pham, R., Stone, R., Deangelo, D., Galinsky, I., Giles, F., Estey, E., Kantarjian, H., Cohen, P., Wang, Y., Roesel, J., Karp, J. E. & Small, D. (2006) Plasma inhibitory activity (PIA): a pharmacodynamic assay reveals insights into the basis for cytotoxic response to FLT3 inhibitors. *Blood,* **108,** 3477-83.

Levis, M., Ravandi, F., Wang, E. S., Baer, M. R., Perl, A., Coutre, S., Erba, H., Stuart, R. K., Baccarani, M., Cripe, L. D., Tallman, M. S., Meloni, G., Godley, L. A., Langston, A. A., Amadori, S., Lewis, I. D., Nagler, A., Stone, R., Yee, K., Advani, A., Douer, D., Wiktor-Jedrzejczak, W., Juliusson, G., Litzow, M. R., Petersdorf, S., Sanz, M., Kantarjian, H. M., Sato, T., Tremmel, L., Bensen-Kennedy, D. M., Small, D. & Smith, B. D. (2011) Results from a randomized trial of salvage chemotherapy followed by lestaurtinib for patients with FLT3 mutant AML in first relapse. *Blood,* **117,** 3294-301.

Levis, M. J., Perl, A. E., Dombret, H., Dohner, H., Steffen, B., Rousselot, P., Martinelli, G., Estey, E. H., Burnett, A. K., Gammon, G., Trone, D., Leo, E. & Cortes, J. E. (2012) Final Results of a Phase 2 Open-Label, Monotherapy Efficacy and Safety Study of Quizartinib (AC220) in Patients with FLT3-ITD Positive or Negative Relapsed/Refractory Acute Myeloid Leukemia After Second-Line Chemotherapy or Hematopoietic Stem Cell Transplantation. *ASH Annual Meeting Abstracts,* **120,** 673.

Levy, D. S., Kahana, J. A. & Kumar, R. (2009) AKT inhibitor, GSK690693, induces growth inhibition and apoptosis in acute lymphoblastic leukemia cell lines. *Blood,* **113,** 1723-1729.

Ley, T. J. (2013) Genomic and Epigenomic Landscapes of Adult De Novo Acute Myeloid Leukemia (vol 368, pg 2059, 2013). *New England Journal of Medicine,* **369,** 98-98.

Ley, T. J., Ding, L., Walter, M. J., Mclellan, M. D., Lamprecht, T., Larson, D. E., Kandoth, C., Payton, J. E., Baty, J., Welch, J., Harris, C. C., Lichti, C. F., Townsend, R. R., Fulton, R. S., Dooling, D. J., Koboldt, D. C., Schmidt, H., Zhang, Q., Osborne, J. R., Lin, L., O'laughlin, M., Mcmichael, J. F., Delehaunty, K. D., Mcgrath, S. D., Fulton,

L. A., Magrini, V. J., Vickery, T. L., Hundal, J., Cook, L. L., Conyers, J. J., Swift, G. W., Reed, J. P., Alldredge, P. A., Wylie, T., Walker, J., Kalicki, J., Watson, M. A., Heath, S., Shannon, W. D., Varghese, N., Nagarajan, R., Westervelt, P., Tomasson, M. H., Link, D. C., Graubert, T. A., Dipersio, J. F., Mardis, E. R. & Wilson, R. K. (2010) DNMT3A mutations in acute myeloid leukemia. *N Engl J Med,* **363,** 2424-33.

Licht, J. D. (2001) AML1 and the AML1-ETO fusion protein in the pathogenesis of t(8;21) AML. *Oncogene,* **20,** 5660-79.

Liu, T. C., Lin, P. M., Chang, J. G., Lee, J. P., Chen, T. P. & Lin, S. F. (2000) Mutation analysis of PTEN/MMAC1 in acute myeloid leukemia. *Am J Hematol,* **63,** 170-5.

Liu, Y. & Gray, N. S. (2006) Rational design of inhibitors that bind to inactive kinase conformations. *Nature Chemical Biology,* **2,** 358-364.

Long, X., Lin, Y., Ortiz-Vega, S., Yonezawa, K. & Avruch, J. (2005) Rheb binds and regulates the mTOR kinase. *Curr Biol,* **15,** 702-13.

Lunghi, P., Tabilio, A., Dall'aglio, P. P., Ridolo, E., Carlo-Stella, C., Pelicci, P. G. & Bonati, A. (2003) Downmodulation of ERK activity inhibits the proliferation and induces the apoptosis of primary acute myelogenous leukemia blasts. *Leukemia,* **17,** 1783-93.

Majeti, R., Chao, M. P., Alizadeh, A. A., Pang, W. W., Jaiswal, S., Gibbs, K. D., Van Rooijen, N. & Weissman, I. L. (2009) CD47 is an adverse prognostic factor and therapeutic antibody target on human acute myeloid leukemia stem cells. *Cell,* **138,** 286-99.

Malaise, M., Steinbach, D. & Corbacioglu, S. (2009) Clinical implications of c-Kit mutations in acute myelogenous leukemia. *Curr Hematol Malig Rep,* **4,** 77-82.

Marcucci, G., Haferlach, T. & Dohner, H. (2011a) Molecular Genetics of Adult Acute Myeloid Leukemia: Prognostic and Therapeutic Implications. *Journal of Clinical Oncology,* **29,** 475-486.

Marcucci, G., Haferlach, T. & Döhner, H. (2011b) Molecular genetics of adult acute myeloid leukemia: prognostic and therapeutic implications. *J Clin Oncol,* **29,** 475-86.

Marcucci, G., Mrozek, K., Ruppert, A. S., Archer, K. J., Pettenati, M. J., Heerema, N. A., Carroll, A. J., Koduru, P. R. K., Kolitz, J. E., Sterling, L. J., Edwards, C. G., Anastasi, J., Larson, R. A. & Bloomfield, C. D. (2004) Abnormal cytogenetics at date of morphologic complete remission predicts short overall and disease-free survival, and higher relapse rate in adult acute myeloid leukemia: Results from cancer and leukemia group B study 8461. *Journal of Clinical Oncology,* **22,** 2410-2418.

Martelli, A. M., Evangelisti, C., Chiarini, F., Grimaldi, C., Manzoli, L. & Mccubrey, J. A. (2009) Targeting the PI3K/AKT/mTOR signaling network in acute myelogenous leukemia. *Expert Opinion on Investigational Drugs,* **18,** 1333-1349.

Martelli, A. M., Evangelisti, C., Chiarini, F. & Mccubrey, J. A. (2010) The phosphatidylinositol 3-kinase/Akt/mTOR signaling network as a therapeutic target in acute myelogenous leukemia patients. *Oncotarget,* **1,** 89-103.

Mead, A. J., Gale, R. E., Kottaridis, P. D., Matsuda, S., Khwaja, A. & Linch, D. C. (2008) Acute myeloid leukaemia blast cells with a tyrosine kinase domain mutation of FLT3 are less sensitive to lestaurtinib than those with a FLT3 internal tandem duplication. *Br J Haematol,* **141,** 454-60.

Mead, A. J., Linch, D. C., Hills, R. K., Wheatley, K., Burnett, A. K. & Gale, R. E. (2007) FLT3 tyrosine kinase domain mutations are biologically distinct from and have a significantly more favorable prognosis than FLT3 internal tandem duplications in patients with acute myeloid leukemia. *Blood,* **110,** 1262-70.

Meshinchi, S., Alonzo, T. A., Stirewalt, D. L., Zwaan, M., Zimmerman, M., Reinhardt, D., Kaspers, G. J., Heerema, N. A., Gerbing, R., Lange, B. J. & Radich, J. P. (2006) Clinical implications of FLT3 mutations in pediatric AML. *Blood,* **108,** 3654-61.

Meshinchi, S. & Appelbaum, F. R. (2009) Structural and functional alterations of FLT3 in acute myeloid leukemia. *Clin Cancer Res,* **15,** 4263-9.

Meshinchi, S., Stirewalt, D. L., Alonzo, T. A., Boggon, T. J., Gerbing, R. B., Rocnik, J. L., Lange, B. J., Gilliland, D. G. & Radich, J. P. (2008) Structural and numerical variation of FLT3/ITD in pediatric AML. *Blood,* **111,** 4930-3.

Meshinchi, S., Woods, W. G., Stirewalt, D. L., Sweetser, D. A., Buckley, J. D., Tjoa, T. K., Bernstein, I. D. & Radich, J. P. (2001) Prevalence and prognostic significance of Flt3 internal tandem duplication in pediatric acute myeloid leukemia. *Blood,* **97,** 89-94.

Milella, M., Konopleva, M., Precupanu, C. M., Tabe, Y., Ricciardi, M. R., Gregorj, C., Collins, S. J., Carter, B. Z., D'angelo, C., Petrucci, M. T., Foà, R., Cognetti, F., Tafuri, A. & Andreeff, M. (2007) MEK blockade converts AML differentiating response to retinoids into extensive apoptosis. *Blood,* **109,** 2121-9.

Min, Y. H., Eom, J. I., Cheong, J. W., Maeng, H. O., Kim, J. Y., Jeung, H. K., Lee, S. T., Lee, M. H., Hahn, J. S. & Ko, Y. W. (2003) Constitutive phosphorylation of Akt/PKB protein in acute myeloid leukemia: its significance as a prognostic variable. *Leukemia,* **17,** 995-7.

Mizuki, M., Fenski, R., Halfter, H., Matsumura, I., Schmidt, R., Muller, C., Gruning, W., Kratz-Albers, K., Serve, S., Steur, C., Buchner, T., Kienast, J., Kanakura, Y., Berdel, W. E. & Serve, H. (2000) Flt3 mutations from patients with acute myeloid leukemia induce transformation of 32D cells mediated by the Ras and STAT5 pathways. *Blood,* **96,** 3907-14.

Mol, C. D., Dougan, D. R., Schneider, T. R., Skene, R. J., Kraus, M. L., Scheibe, D. N., Snell, G. P., Zou, H., Sang, B. C. & Wilson, K. P. (2004) Structural basis for the autoinhibition and STI-571 inhibition of c-Kit tyrosine kinase. *J Biol Chem,* **279,** 31655-63.

Molina, J. R. & Adjei, A. A. (2006) The Ras/Raf/MAPK pathway. *J Thorac Oncol,* **1,** 7-9.

Moreno, I., Martin, G., Bolufer, P., Barragan, E., Rueda, E., Roman, J., Fernandez, P., Leon, P., Mena, A., Cervera, J., Torres, A. & Sanz, M. A. (2003) Incidence and prognostic value of FLT3 internal tandem duplication and D835 mutations in acute myeloid leukemia. *Haematologica,* **88,** 19-24.

Mpakou, V. E., Kontsioti, F., Papageorgiou, S., Spathis, A., Kottaridi, C., Girkas, K., Karakitsos, P., Dimitriadis, G., Dervenoulas, I. & Pappa, V. (2013) Dasatinib inhibits proliferation and induces apoptosis in the KASUMI-1 cell line bearing the t(8;21)(q22;q22) and the N822K c-kit mutation. *Leuk Res,* **37,** 175-82.

Mrozek, K., Heerema, N. A. & Bloomfield, C. D. (2004) Cytogenetics in acute leukemia. *Blood Rev,* **18,** 115-36.

Mrozek, K., Marcucci, G., Paschka, P. & Bloomfield, C. D. (2008) Advances in molecular genetics and treatment of core-binding factor acute myeloid leukemia. *Current Opinion in Oncology,* **20,** 711-718.

Mrozek, K., Marcucci, G., Paschka, P., Whitman, S. P. & Bloomfield, C. D. (2007) Clinical relevance of mutations and gene-expression changes in adult acute myeloid leukemia with normal cytogenetics: are we ready for a prognostically prioritized molecular classification? *Blood,* **109,** 431-48.

Muranyi, A. L., Dedhar, S. & Hogge, D. E. (2009) Combined inhibition of integrin linked kinase and FMS-like tyrosine kinase 3 is cytotoxic to acute myeloid leukemia progenitor cells. *Exp Hematol,* **37,** 450-60.

Nakao, M., Yokota, S., Iwai, T., Kaneko, H., Horiike, S., Kashima, K., Sonoda, Y., Fujimoto, T. & Misawa, S. (1996) Internal tandem duplication of the flt3 gene found in acute myeloid leukemia. *Leukemia,* **10,** 1911-1918.

Naoe, T. & Kiyoi, H. (2013) Gene mutations of acute myeloid leukemia in the genome era. *Int J Hematol,* **97,** 165-74.

Neben, K., Schnittger, S., Brors, B., Tews, B., Kokocinski, F., Haferlach, T., Muller, J., Hahn, M., Hiddemann, W., Eils, R., Lichter, P. & Schoch, C. (2005) Distinct gene expression patterns associated with FLT3- and NRAS-activating mutations in acute myeloid leukemia with normal karyotype. *Oncogene,* **24,** 1580-8.

Nick, H. J., Kim, H. G., Chang, C. W., Harris, K. W., Reddy, V. & Klug, C. A. (2011) Distinct classes of c-Kit activating mutations differ in their ability to promote RUNX1-ETO-associated acute myeloid leukemia. *Blood,* **199,** 1522-1531.

Ning, Z. Q., Li, J., Mcguinness, M. & Arceci, R. J. (2001) STAT3 activation is required for Asp(816) mutant c-Kit induced tumorigenicity. *Oncogene,* **20,** 4528-36.

O'donnell, M. R., Abboud, C. N., Altman, J., Appelbaum, F. R., Arber, D. A., Attar, E., Borate, U., Coutre, S. E., Damon, L. E., Goorha, S., Lancet, J., Maness, L. J., Marcucci, G., Millenson, M. M., Moore, J. O., Ravandi, F., Shami, P. J., Smith, B. D., Stone, R. M., Strickland, S. A., Tallman, M. S., Wang, E. S., Naganuma, M. & Gregory, K. M. (2012) Acute myeloid leukemia. *J Natl Compr Canc Netw,* **10,** 984-1021.

O'farrell, A. M., Foran, J. M., Fiedler, W., Serve, H., Paquette, R. L., Cooper, M. A., Yuen, H. A., Louie, S. G., Kim, H., Nicholas, S., Heinrich, M. C., Berdel, W. E., Bello, C., Jacobs, M., Scigalla, P., Manning, W. C., Kelsey, S. & Cherrington, J. M. (2003) An innovative phase I clinical study demonstrates inhibition of FLT3 phosphorylation by SU11248 in acute myeloid leukemia patients. *Clinical Cancer Research,* **9,** 5465-76.

Orfao, A., Garcia-Montero, A. C., Sanchez, L. & Escribano, L. (2007) Recent advances in the understanding of mastocytosis: the role of KIT mutations. *British Journal of Haematology,* **138,** 12-30.

Orkin, S. H. & Zon, L. I. (2008) Hematopoiesis: an evolving paradigm for stem cell biology. *Cell,* **132,** 631-44.

Ozeki, K., Kiyoi, H., Hirose, Y., Iwai, M., Ninomiya, M., Kodera, Y., Miyawaki, S., Kuriyama, K., Shimazaki, C., Akiyama, H., Nishimura, M., Motoji, T., Shinagawa, K., Takeshita, A., Ueda, R., Ohno, R., Emi, N. & Naoe, T. (2004) Biologic and clinical significance of the FLT3 transcript level in acute myeloid leukemia. *Blood,* **103,** 1901-8.

Pabst, T., Eyholzer, M., Fos, J. & Mueller, B. U. (2009) Heterogeneity within AML with CEBPA mutations; only CEBPA double mutations, but not single CEBPA mutations are associated with favourable prognosis. *Br J Cancer,* **100,** 1343-6.

Pan, J., Quintas-Cardama, A., Kantarjian, H. M., Akin, C., Manshouri, T., Lamb, P., Cortes, J. E., Tefferi, A., Giles, F. J. & Verstovsek, S. (2007) EXEL-0862, a novel tyrosine kinase inhibitor, induces apoptosis in vitro and ex vivo in human mast cells expressing the KIT D816V mutation. *Blood,* **109,** 315-322.

Papa, V., Tazzari, P. L., Chiarini, F., Cappellini, A., Ricci, F., Billi, A. M., Evangelisti, C., Ottaviani, E., Martinelli, G., Testoni, N., Mccubrey, J. A. & Martelli, A. M. (2008)

Proapoptotic activity and chemosensitizing effect of the novel Akt inhibitor perifosine in acute myelogenous leukemia cells. *Leukemia,* **22,** 147-60.

Park, J. H., Hedvat, C. V. & Tallman, M. S. (2011a) Blood consult: acute myeloid leukemia and the t(8;21)(q22;22). *Blood,* **117,** 2775-2777.

Park, S., Chapuis, N., Bardet, V., Tamburini, J., Gallay, N., Willems, L., Knight, Z. A., Shokat, K. M., Azar, N., Viguie, F., Ifrah, N., Dreyfus, F., Mayeux, P., Lacombe, C. & Bouscary, D. (2008) PI-103, a dual inhibitor of Class IA phosphatidylinositide 3-kinase and mTOR, has antileukemic activity in AML. *Leukemia,* **22,** 1698-1706.

Park, S., Chapuis, N., Tamburini, J., Bardet, V., Cornillet-Lefebvre, P., Willems, L., Green, A., Mayeux, P., Lacombe, C. & Bouscary, D. (2010) Role of the PI3K/AKT and mTOR signaling pathways in acute myeloid leukemia. *Haematologica,* **95,** 819-28.

Park, S. H., Chi, H. S., Min, S. K., Park, B. G., Jang, S. & Park, C. J. (2011b) Prognostic impact of c-KIT mutations in core binding factor acute myeloid leukemia. *Leukemia Research,* **35,** 1376-1383.

Paschka, P., Marcucci, G., Ruppert, A. S., Mrozek, K., Chen, H. K., Kittles, R. A., Vukosavljevic, T., Perrotti, D., Vardiman, J. W., Carroll, A. J., Kolitz, J. E., Larson, R. A. & Bloomfield, C. D. (2006) Adverse prognostic significance of KIT mutations in adult acute myeloid leukemia with inv(16) and t(8;21): A Cancer and Leukemia Group B study. *Journal of Clinical Oncology,* **24,** 3904-3911.

Paschka, P., Marcucci, G., Ruppert, A. S., Whitman, S. P., Mrózek, K., Maharry, K., Langer, C., Baldus, C. D., Zhao, W., Powell, B. L., Baer, M. R., Carroll, A. J., Caligiuri, M. A., Kolitz, J. E., Larson, R. A. & Bloomfield, C. D. (2008) Wilms' tumor 1 gene mutations independently predict poor outcome in adults with cytogenetically normal acute myeloid leukemia: a cancer and leukemia group B study. *J Clin Oncol,* **26,** 4595-602.

Pauwels, D., Sweron, B. & Cools, J. (2012) The N676D and G697R mutations in the kinase domain of FLT3 confer resistance to the inhibitor AC220. *Haematologica,* **97,** 1773-4.

Pedersen, M., Ronnstrand, L. & Sun, J. (2009) The c-Kit/D816V mutation eliminates the differences in signal transduction and biological responses between two isoforms of c-Kit. *Cellular Signalling,* **21,** 413-418.

Piao, X., Curtis, J. E., Minkin, S., Minden, M. D. & Bernstein, A. (1994) Expression of the Kit and KitA receptor isoforms in human acute myelogenous leukemia. *Blood,* **83,** 476-81.

Pietschmann, K., Bolck, H. A., Buchwald, M., Spielberg, S., Polzer, H., Spiekermann, K., Bug, G., Heinzel, T., Böhmer, F. D. & Krämer, O. H. (2012) Breakdown of the FLT3-ITD/STAT5 axis and synergistic apoptosis induction by the histone deacetylase inhibitor panobinostat and FLT3-specific inhibitors. *Mol Cancer Ther,* **11,** 2373-83.

Platanias, L. C. (2003) Map kinase signaling pathways and hematologic malignancies. *Blood,* **101,** 4667-79.

Pollard, J. A., Alonzo, T. A., Gerbing, R. B., Ho, P. A., Zeng, R., Ravindranath, Y., Dahl, G., Lacayo, N. J., Becton, D., Chang, M., Weinstein, H. J., Hirsch, B., Raimondi, S. C., Heerema, N. A., Woods, W. G., Lange, B. J., Hurwitz, C., Arceci, R. J., Radich, J. P., Bernstein, I. D., Heinrich, M. C. & Meshinchi, S. (2010) Prevalence and prognostic significance of KIT mutations in pediatric patients with core binding factor AML enrolled on serial pediatric cooperative trials for de novo AML. *Blood,* **115,** 2372-9.

Ponziani, V., Gianfaldoni, G., Mannelli, F., Leoni, F., Ciolli, S., Guglielmelli, P., Antonioli, E., Longo, G., Bosi, A. & Vannucchi, A. M. (2006) The size of duplication does not add to the prognostic significance of FLT3 internal tandem duplication in acute myeloid leukemia patients. *Leukemia,* **20,** 2074-6.

Pratz, K. W., Cortes, J., Roboz, G. J., Rao, N., Arowojolu, O., Stine, A., Shiotsu, Y., Shudo, A., Akinaga, S., Small, D., Karp, J. E. & Levis, M. (2009) A pharmacodynamic study of the FLT3 inhibitor KW-2449 yields insight into the basis for clinical response. *Blood,* **113,** 3938-3946.

Purtill, D., Cooney, J., Sinniah, R., Carnley, B., Cull, G., Augustson, B. & Cannell, P. (2008) Dasatinib therapy for systemic mastocytosis: four cases. *European Journal of Haematology,* **80,** 456-458.

Quentmeier, H., Reinhardt, J., Zaborski, M. & Drexler, H. G. (2003) FLT3 mutations in acute myeloid leukemia cell lines. *Leukemia,* **17,** 120-4.

Ravandi, F., Cortes, J. E., Jones, D., Faderl, S., Garcia-Manero, G., Konopleva, M. Y., O'brien, S., Estrov, Z., Borthakur, G., Thomas, D., Pierce, S. R., Brandt, M., Byrd, A., Bekele, B. N., Pratz, K., Luthra, R., Levis, M., Andreeff, M. & Kantarjian, H. M. (2010) Phase I/II Study of Combination Therapy With Sorafenib, Idarubicin, and Cytarabine in Younger Patients With Acute Myeloid Leukemia. *Journal of Clinical Oncology,* **28,** 1856-1862.

Recher, C., Beyne-Rauzy, O., Demur, C., Chicanne, G., Dos Santos, C., Mansat-De Mas, V., Benzaquen, D., Laurent, G., Huguet, F. & Payrastre, B. (2005) Antileukemic activity of rapamycin in acute myeloid leukemia. *Blood,* **105,** 2527-2534.

Reilly, J. T. (2005) Pathogenesis of acute myeloid leukaemia and inv(16)(p13;q22): a paradigm for understanding leukaemogenesis? *Br J Haematol,* **128,** 18-34.

Reindl, C., Bagrintseva, K., Vempati, S., Schnittger, S., Ellwart, J. W., Wenig, K., Hopfner, K. P., Hiddemann, W. & Spiekermann, K. (2006) Point mutations in the juxtamembrane domain of FLT3 define a new class of activating mutations in AML. *Blood,* **107,** 3700-7.

Ricciardi, M. R., Mcqueen, T., Chism, D., Milella, M., Estey, E., Kaldjian, E., Sebolt-Leopold, J., Konopleva, M. & Andreeff, M. (2005) Quantitative single cell determination of ERK phosphorylation and regulation in relapsed and refractory primary acute myeloid leukemia. *Leukemia,* **19,** 1543-1549.

Ricciardi, M. R., Scerpa, M. C., Bergamo, P., Ciuffreda, L., Petrucci, M. T., Chiaretti, S., Tavolaro, S., Mascolo, M. G., Abrams, S. L., Steelman, L. S., Tsao, T., Marchetti, A., Konopleva, M., Del Bufalo, D., Cognetti, F., Foa, R., Andreeff, M., Mccubrey, J. A., Tafuri, A. & Milella, M. (2012) Therapeutic potential of MEK inhibition in acute myelogenous leukemia: rationale for "vertical" and "lateral" combination strategies. *J Mol Med (Berl),* **90,** 1133-44.

Rinehart, J., Adjei, A. A., Lorusso, P. M., Waterhouse, D., Hecht, J. R., Natale, R. B., Hamid, O., Varterasian, M., Asbury, P., Kaldjian, E. P., Gulyas, S., Mitchell, D. Y., Herrera, R., Sebolt-Leopold, J. S. & Meyer, M. B. (2004) Multicenter phase II study of the

oral MEK inhibitor, CI-1040, in patients with advanced non-small-cell lung, breast, colon, and pancreatic cancer. *J Clin Oncol,* **22,** 4456-62.

Roboz, G. J. (2011) Novel approaches to the treatment of acute myeloid leukemia. *Hematology Am Soc Hematol Educ Program,* **2011,** 43-50.

Rocnik, J. L., Okabe, R., Yu, J. C., Lee, B. H., Giese, N., Schenkein, D. P. & Gilliland, D. G. (2006) Roles of tyrosine 589 and 591 in STAT5 activation and transformation mediated by FLT3-ITD. *Blood,* **108,** 1339-45.

Sallmyr, A., Fan, J., Datta, K., Kim, K. T., Grosu, D., Shapiro, P., Small, D. & Rassool, F. (2008) Internal tandem duplication of FLT3 (FLT3/ITD) induces increased ROS production, DNA damage, and misrepair: implications for poor prognosis in AML. *Blood,* **111,** 3173-82.

Schittenhelm, M. M., Shiraga, S., Schroeder, A., Corbin, A. S., Griffith, D., Lee, F. Y., Bokemeyer, C., Deininger, M. W., Druker, B. J. & Heinrich, M. C. (2006) Dasatinib (BMS-354825), a dual SRC/ABL kinase inhibitor, inhibits the kinase activity of wild-type, juxtamembrane, and activation loop mutant KIT isoforms associated with human malignancies. *Cancer Res,* **66,** 473-81.

Schlenk, R. F., Dohner, K., Krauter, J., Frohling, S., Corbacioglu, A., Bullinger, L., Habdank, M., Spath, D., Morgan, M., Benner, A., Schlegelberger, B., Heil, G., Ganser, A. & Dohner, H. (2008a) Mutations and treatment outcome in cytogenetically normal acute myeloid leukemia. *N Engl J Med,* **358,** 1909-18.

Schlenk, R. F., Pasquini, M. C., Pérez, W. S., Zhang, M. J., Krauter, J., Antin, J. H., Bashey, A., Bolwell, B. J., Büchner, T., Cahn, J. Y., Cairo, M. S., Copelan, E. A., Cutler, C. S., Döhner, H., Gale, R. P., Ilhan, O., Lazarus, H. M., Liesveld, J. L., Litzow, M. R., Marks, D. I., Maziarz, R. T., Mccarthy, P. L., Nimer, S. D., Sierra, J., Tallman, M. S., Weisdorf, D. J., Horowitz, M. M., Ganser, A. & Committee, C. a. L. W. (2008b) HLA-identical sibling allogeneic transplants versus chemotherapy in acute myelogenous leukemia with t(8;21) in first complete remission: collaborative study between the German AML Intergroup and CIBMTR. *Biol Blood Marrow Transplant,* **14,** 187-96.

Schlessinger, J. (2000) Cell signaling by receptor tyrosine kinases. *Cell,* **103,** 211-25.

Schmid, C., Schleuning, M., Tischer, J., Holler, E., Haude, K. H., Braess, J., Haferlach, C., Baurmann, H., Oruzio, D., Hahn, J., Spiekermann, K., Schlimok, G., Schwerdtfeger, R., Buechner, T., Hiddemann, W. & Kolb, H. J. (2012) Early allo-SCT for AML with a complex aberrant karyotype-results from a prospective pilot study. *Bone Marrow Transplantation,* **47,** 46-53.

Schnittger, S., Schoch, C., Kern, W., Mecucci, C., Tschulik, C., Martelli, M. F., Haferlach, T., Hiddemann, W. & Falini, B. (2005) Nucleophosmin gene mutations are predictors of favorable prognosis in acute myelogenous leukemia with a normal karyotype. *Blood,* **106,** 3733-9.

Shah, N. P., Lee, F. Y., Luo, R., Jiang, Y., Donker, M. & Akin, C. (2006) Dasatinib (BMS-354825) inhibits KITD816V, an imatinib-resistant activating mutation that triggers neoplastic growth in most patients with systemic mastocytosis. *Blood,* **108,** 286-91.

Shimada, A., Taki, T., Kubota, C., Itou, T., Tawa, A., Horibe, K., Tsuchida, M., Hanada, R., Tsukimoto, I. & Hayashi, Y. (2007) N822 mutation of KIT gene was frequent in pediatric acute myeloid leukemia patients with t(8;21) in Japan: a study of the Japanese childhood AML cooperative study group. *Leukemia,* **21,** 2218-2219.

Slovak, M. L., Kopecky, K. J., Cassileth, P. A., Harrington, D. H., Theil, K. S., Mohamed, A., Paietta, E., Willman, C. L., Head, D. R., Rowe, J. M., Forman, S. J. & Appelbaum, F. R. (2000) Karyotypic analysis predicts outcome of preremission and postremission therapy in adult acute myeloid leukemia: a Southwest Oncology Group/Eastern Cooperative Oncology Group Study. *Blood,* **96,** 4075-83.

Smith, B. D., Levis, M., Beran, M., Giles, F., Kantarjian, H., Berg, K., Murphy, K. M., Dauses, T., Allebach, J. & Small, D. (2004) Single-agent CEP-701, a novel FLT3 inhibitor, shows biologic and clinical activity in patients with relapsed or refractory acute myeloid leukemia. *Blood,* **103,** 3669-76.

Smith, C. C., Lasater, E. A., Zhu, X., Lin, K. C., Stewart, W. K., Damon, L. E., Salerno, S. & Shah, N. P. (2013) Activity of ponatinib against clinically-relevant AC220-resistant kinase domain mutants of FLT3-ITD. *Blood,* **121,** 3165-3171.

Smith, C. C., Wang, Q., Chin, C. S., Salerno, S., Damon, L. E., Levis, M. J., Perl, A. E., Travers, K. J., Wang, S., Hunt, J. P., Zarrinkar, P. P., Schadt, E. E., Kasarskis, A.,

Kuriyan, J. & Shah, N. P. (2012) Validation of ITD mutations in FLT3 as a therapeutic target in human acute myeloid leukaemia. *Nature,* **485,** 260-U153.

Smith, M. L., Hills, R. K. & Grimwade, D. (2011) Independent prognostic variables in acute myeloid leukaemia. *Blood Rev,* **25,** 39-51.

Smolich, B. D. (2001) The antiangiogenic protein kinase inhibitors SU5416 and SU6668 inhibit the SCF receptor (c-kit) in a human myeloid leukemia cell line and in acute myeloid leukemia blasts. *Blood,* **97,** 1413-1421.

Somervaille, T. C. & Cleary, M. L. (2006) Identification and characterization of leukemia stem cells in murine MLL-AF9 acute myeloid leukemia. *Cancer Cell,* **10,** 257-68.

Spiekermann, K., Dirschinger, R. J., Schwab, R., Bagrintseva, K., Faber, F., Buske, C., Schnittger, S., Kelly, L. M., Gilliland, D. G. & Hiddemann, W. (2003) The protein tyrosine kinase inhibitor SU5614 inhibits FLT3 and induces growth arrest and apoptosis in AML-derived cell lines expressing a constitutively activated FLT3. *Blood,* **101,** 1494-504.

Stone, R. M., Deangelo, D. J., Klimek, V., Galinsky, I., Estey, E., Nimer, S. D., Grandin, W., Lebwohl, D., Wang, Y., Cohen, P., Fox, E. A., Neuberg, D., Clark, J., Gilliland, D. G. & Griffin, J. D. (2005) Patients with acute myeloid leukemia and an activating mutation in FLT3 respond to a small-molecule FLT3 tyrosine kinase inhibitor, PKC412. *Blood,* **105,** 54-60.

Stone, R. M., Fischer, T., Paquette, R., Schiller, G., Schiffer, C. A., Ehninger, G., Cortes, J., Kantarjian, H. M., Deangelo, D. J., Huntsman-Labed, A., Dutreix, C., Rai, S. & Giles, F. (2009) A Phase 1b Study of Midostaurin (PKC412) in Combination with Daunorubicin and Cytarabine Induction and High-Dose Cytarabine Consolidation in Patients Under Age 61 with Newly Diagnosed De Novo Acute Myeloid Leukemia: Overall Survival of Patients Whose Blasts Have FLT3 Mutations Is Similar to Those with Wild-Type FLT3. *ASH Annual Meeting Abstracts,* **114,** 634.

Sujobert, P., Bardet, V., Cornillet-Lefebvre, P., Hayflick, J. S., Prie, N., Verdier, F., Vanhaesebroeck, B., Muller, O., Pesce, F., Ifrah, N., Hunault-Berger, M., Berthou, C., Villemagne, B., Jourdan, E., Audhuy, B., Solary, E., Witz, B., Harousseau, J. L., Himberlin, C., Lamy, T., Lioure, B., Cahn, J. Y., Dreyfus, F., Mayeux, P., Lacombe, C. & Bouscary, D. (2005) Essential role for the p110delta isoform in

phosphoinositide 3-kinase activation and cell proliferation in acute myeloid leukemia. *Blood,* **106,** 1063-6.

Sun, J., Pedersen, M. & Ronnstrand, L. (2009) The D816V mutation of c-Kit circumvents a requirement for Src family kinases in c-Kit signal transduction. *Journal of Biological Chemistry,* **284,** 11039-47.

Tabone-Eglinger, S., Subra, F., El Sayadi, H., Alberti, L., Tabone, E., Michot, J. P., Theou-Anton, N., Lemoine, A., Blay, J. Y. & Emile, J. F. (2008) KIT mutations induce intracellular retention and activation of an immature form of the KIT protein in gastrointestinal stromal tumors. *Clin Cancer Res,* **14,** 2285-94.

Takahashi, S. (2011) Downstream molecular pathways of FLT3 in the pathogenesis of acute myeloid leukemia: biology and therapeutic implications. *J Hematol Oncol,* **4,** 13.

Tallman, M. S. (2005) New strategies for the treatment of acute myeloid leukemia including antibodies and other novel agents. *Hematology Am Soc Hematol Educ Program,* **2005,** 143-50.

Tamburini, J., Chapuis, N., Bardet, V., Park, S., Sujobert, P., Willems, L., Ifrah, N., Dreyfus, F., Mayeux, P., Lacombe, C. & Bouscary, D. (2008) Mammalian target of rapamycin (mTOR) inhibition activates phosphatidylinositol 3-kinase/Akt by up-regulating insulin-like growth factor-1 receptor signaling in acute myeloid leukemia: rationale for therapeutic inhibition of both pathways. *Blood,* **111,** 379-82.

Taussig, D. C., Miraki-Moud, F., Anjos-Afonso, F., Pearce, D. J., Allen, K., Ridler, C., Lillington, D., Oakervee, H., Cavenagh, J., Agrawal, S. G., Lister, T. A., Gribben, J. G. & Bonnet, D. (2008) Anti-CD38 antibody-mediated clearance of human repopulating cells masks the heterogeneity of leukemia-initiating cells. *Blood,* **112,** 568-75.

Tazzari, P. L., Cappellini, A., Ricci, F., Evangelisti, C., Papa, V., Grafone, T., Martinelli, G., Conte, R., Cocco, L., Mccubrey, J. A. & Martelli, A. M. (2007) Multidrug resistance-associated protein 1 expression is under the control of the phosphoinositide 3 kinase/Akt signal transduction network in human acute myelogenous leukemia blasts. *Leukemia,* **21,** 427-38.

Thiede, C., Steudel, C., Mohr, B., Schaich, M., Schakel, U., Platzbecker, U., Wermke, M., Bornhauser, M., Ritter, M., Neubauer, A., Ehninger, G. & Illmer, T. (2002) Analysis of FLT3-activating mutations in 979 patients with acute myelogenous leukemia: association with FAB subtypes and identification of subgroups with poor prognosis. *Blood,* **99,** 4326-35.

Thol, F., Damm, F., Lüdeking, A., Winschel, C., Wagner, K., Morgan, M., Yun, H., Göhring, G., Schlegelberger, B., Hoelzer, D., Lübbert, M., Kanz, L., Fiedler, W., Kirchner, H., Heil, G., Krauter, J., Ganser, A. & Heuser, M. (2011) Incidence and prognostic influence of DNMT3A mutations in acute myeloid leukemia. *J Clin Oncol,* **29,** 2889-96.

Vanhaesebroeck, B., Leevers, S. J., Ahmadi, K., Timms, J., Katso, R., Driscoll, P. C., Woscholski, R., Parker, P. J. & Waterfield, M. D. (2001) Synthesis and function of 3-phosphorylated inositol lipids. *Annual Review of Biochemistry,* **70,** 535-602.

Vardiman, J. W., Harris, N. L. & Brunning, R. D. (2002) The World Health Organization (WHO) classification of the myeloid neoplasms. *Blood,* **100,** 2292-2302.

Vardiman, J. W., Thiele, J., Arber, D. A., Brunning, R. D., Borowitz, M. J., Porwit, A., Harris, N. L., Le Beau, M. M., Hellstrom-Lindberg, E., Tefferi, A. & Bloomfield, C. D. (2009) The 2008 revision of the World Health Organization (WHO) classification of myeloid neoplasms and acute leukemia: rationale and important changes. *Blood,* **114,** 937-951.

Vellenga, E., Van Putten, W., Ossenkoppele, G. J., Verdonck, L. F., Theobald, M., Cornelissen, J. J., Huijgens, P. C., Maertens, J., Gratwohl, A., Schaafsma, R., Schanz, U., Graux, C., Schouten, H. C., Ferrant, A., Bargetzi, M., Fey, M. F., Löwenberg, B., , D.-B. H.-O. C. G. & , S. G. F. C. C. R. C. G. (2011) Autologous peripheral blood stem cell transplantation for acute myeloid leukemia. *Blood,* **118,** 6037-42.

Vendome, J., Letard, S., Martin, F., Svinarchuk, F., Dubreuil, P., Auclair, C. & Le Bret, M. (2005) Molecular modeling of wild-type and D816V c-Kit inhibition based on ATP-competitive binding of ellipticine derivatives to tyrosine kinases. *J Med Chem,* **48,** 6194-201.

Verstovsek, S., Tefferi, A., Cortes, J., O'brien, S., Garcia-Manero, G., Pardanani, A., Akin, C., Faderl, S., Manshouri, T., Thomas, D. & Kantarjian, H. (2008) Phase II study of

dasatinib in Philadelphia chromosome-negative acute and chronic myeloid diseases, including systemic mastocytosis. *Clinical Cancer Research,* **14,** 3906-3915.

Wang, Y. Y. (2005) AML1-ETO and C-KIT mutation/overexpression in t(8;21) leukemia: Implication in stepwise leukemogenesis and response to Gleevec. *Proceedings of the National Academy of Sciences,* **102,** 1104-1109.

Wang, Y. Y., Zhao, L. J., Wu, C. F., Liu, P., Shi, L., Liang, Y., Xiong, S. M., Mi, J. Q., Chen, Z., Ren, R. B. & Chen, S. J. (2011) C-KIT mutation cooperates with full-length AML1-ETO to induce acute myeloid leukemia in mice. *Proceedings of the National Academy of Sciences of the United States of America,* **108,** 2450-2455.

Weisberg, E., Liu, Q., Zhang, X., Nelson, E., Sattler, M., Liu, F., Nicolais, M., Zhang, J., Mitsiades, C., Smith, R. W., Stone, R., Galinsky, I., Nonami, A., Griffin, J. D. & Gray, N. (2013) Selective Akt inhibitors synergize with tyrosine kinase inhibitors and effectively override stroma-associated cytoprotection of mutant FLT3-positive AML cells. *PLoS One,* **8,** e56473.

Wheatley, K., Burnett, A. K., Goldstone, A. H., Gray, R. G., Hann, I. M., Harrison, C. J., Rees, J. K., Stevens, R. F. & Walker, H. (1999) A simple, robust, validated and highly predictive index for the determination of risk-directed therapy in acute myeloid leukaemia derived from the MRC AML 10 trial. United Kingdom Medical Research Council's Adult and Childhood Leukaemia Working Parties. *Br J Haematol,* **107,** 69-79.

Whitman, S. P., Ruppert, A. S., Marcucci, G., Mrózek, K., Paschka, P., Langer, C., Baldus, C. D., Wen, J., Vukosavljevic, T., Powell, B. L., Carroll, A. J., Kolitz, J. E., Larson, R. A., Caligiuri, M. A. & Bloomfield, C. D. (2007) Long-term disease-free survivors with cytogenetically normal acute myeloid leukemia and MLL partial tandem duplication: a Cancer and Leukemia Group B study. *Blood,* **109,** 5164-7.

Whitman, S. P., Ruppert, A. S., Radmacher, M. D., Mrozek, K., Paschka, P., Langer, C., Baldus, C. D., Wen, J., Racke, F., Powell, B. L., Kolitz, J. E., Larson, R. A., Caligiuri, M. A., Marcucci, G. & Bloomfield, C. D. (2008) FLT3 D835/I836 mutations are associated with poor disease-free survival and a distinct gene-expression signature among younger adults with de novo cytogenetically normal acute myeloid leukemia lacking FLT3 internal tandem duplications. *Blood,* **111,** 1552-1559.

Wodicka, L. M., Ciceri, P., Davis, M. I., Hunt, J. P., Floyd, M., Salerno, S., Hua, X. H., Ford, J. M., Armstrong, R. C., Zarrinkar, P. P. & Treiber, D. K. (2010) Activation state-dependent binding of small molecule kinase inhibitors: structural insights from biochemistry. *Chem Biol,* **17,** 1241-9.

Wodnar-Filipowicz, A. (2003) Flt3 ligand: role in control of hematopoietic and immune functions of the bone marrow. *News Physiol Sci,* **18,** 247-51.

Xiang, Z., Kreisel, F., Cain, J., Colson, A. & Tomasson, M. H. (2007) Neoplasia driven by mutant c-KIT is mediated by intracellular, not plasma membrane, receptor signaling. *Molecular and cellular biology,* **27,** 267-82.

Xu, Q., Simpson, S. E., Scialla, T. J., Bagg, A. & Carroll, M. (2003) Survival of acute myeloid leukemia cells requires PI3 kinase activation. *Blood,* **102,** 972-980.

Yanada, M., Matsuo, K., Suzuki, T., Kiyoi, H. & Naoe, T. (2005) Prognostic significance of FLT3 internal tandem duplication and tyrosine kinase domain mutations for acute myeloid leukemia: a meta-analysis. *Leukemia,* **19,** 1345-9.

Yee, K. W. L., Zeng, Z. H., Konopleva, M., Verstovsek, S., Ravandi, F., Ferrajoli, A., Thomas, D., Wierda, W., Apostolidou, E., Albitar, M., O'brien, S., Andreeff, M. & Giles, F. J. (2006) Phase I/II study of the mammalian target of rapamycin inhibitor everolimus (RAD001) in patients with relapsed or refractory hematologic malignancies. *Clinical Cancer Research,* **12,** 5165-5173.

Yoshimoto, G., Miyamoto, T., Jabbarzadeh-Tabrizi, S., Iino, T., Rocnik, J. L., Kikushige, Y., Mori, Y., Shima, T., Iwasaki, H., Takenaka, K., Nagafuji, K., Mizuno, S., Niiro, H., Gilliland, G. D. & Akashi, K. (2009) FLT3-ITD up-regulates MCL-1 to promote survival of stem cells in acute myeloid leukemia via FLT3-ITD-specific STAT5 activation. *Blood,* **114,** 5034-43.

Yu, K., Lucas, J., Zhu, T. M., Zask, A., Gaydos, C., Toral-Barza, L., Gu, J. X., Li, F. B., Chaudhary, I., Cai, P., Lotvin, J., Petersen, R., Ruppen, M., Fawzi, M., Ayral-Kaloustian, S., Skotnicki, J., Mansour, T., Frost, P. & Gibbons, J. (2005) PWT-458, a novel pegylated-17-hydroxywortmannin, inhibits phosphatidylinositol 3-kinase signaling and suppresses growth of solid tumors. *Cancer Biology & Therapy,* **4,** 538-545.

Yu, K., Toral-Barza, L., Shi, C., Zhang, W. G., Lucas, J., Shor, B., Kim, J., Verheijen, J., Curran, K., Malwitz, D. J., Cole, D. C., Ellingboe, J., Ayral-Kaloustian, S., Mansour, T. S., Gibbons, J. J., Abraham, R. T., Nowak, P. & Zask, A. (2009) Biochemical, cellular, and in vivo activity of novel ATP-competitive and selective inhibitors of the mammalian target of rapamycin. *Cancer Res,* **69,** 6232-40.

Yuan, Y., Zhou, L., Miyamoto, T., Iwasaki, H., Harakawa, N., Hetherington, C. J., Burel, S. A., Lagasse, E., Weissman, I. L., Akashi, K. & Zhang, D. E. (2001) AML1-ETO expression is directly involved in the development of acute myeloid leukemia in the presence of additional mutations. *Proc Natl Acad Sci U S A,* **98,** 10398-403.

Zarrinkar, P. P., Gunawardane, R. N., Cramer, M. D., Gardner, M. F., Brigham, D., Belli, B., Karaman, M. W., Pratz, K. W., Pallares, G., Chao, Q., Sprankle, K. G., Patel, H. K., Levis, M., Armstrong, R. C., James, J. & Bhagwat, S. S. (2009) AC220 is a uniquely potent and selective inhibitor of FLT3 for the treatment of acute myeloid leukemia (AML). *Blood,* **114,** 2984-2992.

Zhang, H., Mi, J. Q., Fang, H., Wang, Z., Wang, C., Wu, L., Zhang, B., Minden, M., Yang, W. T., Wang, H. W., Li, J. M., Xi, X. D., Chen, S. J., Zhang, J., Chen, Z. & Wang, K. K. (2013) Preferential eradication of acute myelogenous leukemia stem cells by fenretinide. *Proc Natl Acad Sci U S A,* **110,** 5606-11.

Zhang, W., Konopleva, M., Burks, J. K., Dywer, K. C., Schober, W. D., Yang, J. Y., Mcqueen, T. J., Hung, M. C. & Andreeff, M. (2010) Blockade of mitogen-activated protein kinase/extracellular signal-regulated kinase kinase and murine double minute synergistically induces Apoptosis in acute myeloid leukemia via BH3-only proteins Puma and Bim. *Cancer Res,* **70,** 2424-34.

Zhang, W., Konopleva, M., Ruvolo, V. R., Mcqueen, T., Evans, R. L., Bornmann, W. G., Mccubrey, J., Cortes, J. & Andreeff, M. (2008) Sorafenib induces apoptosis of AML cells via Bim-mediated activation of the intrinsic apoptotic pathway. *Leukemia,* **22,** 808-18.

Zhao, L., Melenhorst, J. J., Alemu, L., Kirby, M., Anderson, S., Kench, M., Hoogstraten-Miller, S., Brinster, L., Kamikubo, Y., Gilliland, D. G. & Liu, P. P. (2012) KIT with D816 mutations cooperates with CBFB-MYH11 for leukemogenesis in mice. *Blood,* **119,** 1511-21.

Zheng, R., Levis, M., Piloto, O., Brown, P., Baldwin, B. R., Gorin, N. C., Beran, M., Zhu, Z. P., Ludwig, D., Hicklin, D., Witte, L., Li, Y. W. & Small, D. (2004) FLT3 ligand causes autocrine signaling in acute myeloid leukemia cells. *Blood,* **103,** 267-274.

Zoncu, R., Efeyan, A. & Sabatini, D. M. (2011) mTOR: from growth signal integration to cancer, diabetes and ageing. *Nature Reviews Molecular Cell Biology,* **12,** 21-35.

Zwaan, C. M., Rizzari, C., Mechinaud, F., Lancaster, D. L., Lehrnbecher, T., Van Der Velden, V. H., Beverloo, B. B., Den Boer, M. L., Pieters, R., Reinhardt, D., Dworzak, M., Rosenberg, J., Manos, G., Agrawal, S., Strauss, L., Baruchel, A. & Kearns, P. R. (2013) Dasatinib in Children and Adolescents With Relapsed or Refractory Leukemia: Results of the CA180-018 Phase I Dose-Escalation Study of the Innovative Therapies for Children With Cancer Consortium. *J Clin Oncol,* **31,** 2460-8.